UNIVERSITÀ
DEGLI STUDI
DI PADOVA

Sede Amministrativa: Università degli Studi di Padova

Dipartimento di Geoscienze

CORSO DI DOTTORATO DI RICERCA IN: Scienze della Terra

CICLO: XXXI

Late-Quaternary incised valleys and tidal inlets
of the northern Adriatic shelf and related alluvial plains

Coordinatore: Prof. Claudia Agnini

Supervisore: Prof. Alessandro Fontana

Co-Supervisore: Dr. Kim M. Cohen

Co-Supervisore: Dr. Annamaria Correggiari

Dottorando: Livio Ronchi

ABSTRACT

The reconstruction of the past sea-level changes and of their effects on the paleoenvironmental evolution are necessary steps for the modelling of the future sea-level rise and for the elaboration of management plans for the safeguard of the coastal systems. Such reconstruction is often hampered by the scarceness of adequate indicators as a consequence of the lack of formation/preservation or due to the low resolution.

This work focuses on the analysis of possible new paleo sea-level indicators. This research is essential in order to provide new data to constrain the marine transgression that took place after the Last Glacial Maximum (LGM) and to understand the consequent environmental evolution. A series of incised landforms that formed and were infilled during this period were therefore analysed. Incised landforms constitute one of the few available archives for the reconstruction of the past and especially for periods of high sea-level rise rate, which are usually characterized by few available paleo sea-level indicators as a consequence of the lack of formation or preservation.

The northern Adriatic shelf and the contiguous Venetian-Friulian Plain were chosen for this research due to their peculiar physiography, notably the low gradient of the continental shelf.

The northern Adriatic shelf was investigated through a series of high-resolution seismic profiles, allowing to document for the first time the presence of almost 100 paleo tidal inlets. Some of these have been investigated in detail, providing new pieces of evidence for the understanding of the evolution of the area during the early Holocene and the relation between the different rates of sea-level rise and the formation and preservation of lagoon environments.

The analysis of a large dataset of cores that sampled the infilling material of an incised valley located in the subsurface of the modern Venetian-Friulian Plain allowed a detailed reconstruction of the environmental evolution in the area since the Late Glacial. In particular, the switch from a fluvial freshwater environment to a brackish lagoon one was recognized and dated to Early Holocene.

Finally, this work presents some considerations and possible future developments for the use of such indicators in the reconstruction of timing and modes of the last marine transgression.

RIASSUNTO

La ricostruzione di modalità e tempistiche associate alle variazioni del livello marino tardo-Quaternarie e alla loro influenza sull'evoluzione paleoambientale è necessaria al fine di modellare il futuro innalzamento del livello marino e per l'elaborazione di piani di gestione degli ambienti costieri. Questo tipo di ricostruzione è però spesso ostacolato dalla scarsità di adeguati indicatori.

Il presente lavoro è focalizzato sull'analisi paleoambientale e sullo studio di possibili nuovi indicatori per lo studio della fase di trasgressione marina che ha avuto luogo a partire dalla fine dell'ultimo massimo glaciale (LGM). In particolare, questa ricerca prende in considerazione alcune morfologie erosive, quali canali tidali e valli incise. Queste forme spesso costituiscono un eccezionale archivio morfologico e stratigrafico per la ricostruzione del passato e dei periodi caratterizzati da un elevato tasso di risalita del livello marino, per i quali gli indicatori paleoambietali disponibili sono solitamente scarsi in seguito alla mancata formazione/limitata preservazione o a causa della bassa risoluzione disponibile.

Le aree scelte per questo lavoro sono la piattaforma nord adriatica e la contigua pianura veneto-friulana. Questa scelta è stata dettata in particolare dalla fisiografia e dal basso gradiente topografico presenti in questa zona.

L'analisi di profili sismici ad alta risoluzione acquisiti sulla piattaforma continentale nord adriatica ha consentito di individuare per la prima volta la presenza di quasi 100 bocche tidali fossili. Alcune di queste sono state studiate in dettaglio per ottenere informazioni sull'evoluzione e la distribuzione degli ambienti lagunari trasgressivi sviluppatisi nell'area all'inizio dell'Olocene.

Lo studio dei depositi di riempimento di una valle incisa individuata nel sottosuolo della moderna pianura veneto-friulana ha permesso la ricostruzione dell'evoluzione dell'area a partire dal Tardiglaciale. È stato inoltre possibile riconoscere e datare la transizione da un ambiente fluviale ad uno lagunare nel corso dell'Olocene iniziale.

Questo lavoro ha permesso di tracciare alcune considerazioni sui possibili sviluppi e potenzialità offerte dall'uso di questo tipo di indicatori per la ricostruzione delle fasi di trasgressione marina.

CONTENTS

LIST OF TABLES

INTRODUCTION

The ongoing global climate change (Nicholls and Cazenave, 2010; Church et al., 2013) and the related relative sea-level (RSL) rise demand for the development of strategies of adaptation and prevention to be adopted in the policy making and in the management of the coastal areas. This topic acquires a dramatic value considering that ca. 10% of the global population lives in areas placed below 10 m MSL (McGranahan et al., 2007) and the RSL rise projections for the end of the 21st century estimate an increase of the mean sea level up to 1 m (IPCC, 2014). A refining of the available models and the improvement in our knowledge on the evolution of natural systems forced by a high rates of RSL rise is therefore crucial, and a necessary step in this direction is the reconstruction of the environmental changes that took place in the past. In other words, the effort in reconstructing the past is a necessary mean to foresight the future. As a matter of fact, the increasing amount of studies concerning the prediction and consequences of the global sea-level rise relies, among other factors, on the past sea-level reconstruction and environmental changes (e.g. Antonioli et al., 2017; Stocchi et al., 2018). The available RSL curves, both for future prediction and past reconstruction, are produced via geophysical models which necessitate a constant improving and widening of the available past relative sea-level indicators, which are fundamental for their calibration of the Glacio-Isostatic Adjustment (GIA) and tectonic displacements (cf. Peltier and Andrews, 1976; Lambeck et al., 2014; Vacchi et al., 2016; Roy and Peltier, 2018; Stocchi et al., 2018). Such indicators must be carefully evaluated in order to understand their relative position in relation to the paleo sea level, the possible occurrence of vertical displacements and the reliability of the dated material. The interest in the paleo sea-level indicators has therefore rapidly increased in the last few decades and a number of research papers, books and reviews addressing the different aspects of this topic have been produced (e.g. Fairnaks, 1989; Dorale et al., 2010; Muhs et al., 2011; Mauz et al., 2015; Rovere et al., 2016; Benjamin et al., 2017).

This work aims to provide new constraints for a detailed reconstruction of the environmental changes that took place during the global eustatic rise that followed the Last Glacial Maximum (LGM). This objective has been pursued by considering a series of incised and infilled features, notably tidal inlets

and incised valleys, for the definition of new stratigraphic and morphologic indicators of past sea levels. In particular, we attempt to understand the behaviour and the evolution of the analysed systems in the context of the sea-level rise that followed the LGM. This may help to better understand the response of shallow-marine and coastal systems so sea-level rise, and provide new constraints on the post-LGM rates of realtive sea-level change.

Given its peculiar characteristics, described in the next paragraphs, the focus area of this work is represented by the northern Adriatic shelf and by the Venetian-Friulian Plain.

1.1 SETTINGS

This research focuses on an area that encompass the northern Adriatic shelf and the Venetian-Friulian Plain (VFP), covering a surface of more than $10\,000$ km^2, extending from north to south for almost 200 km, from the apex of the Tagliamento megafan (ca. 180 m MSL) to the area offshore Ravenna (ca. -40 m MSL). This area is framed by the Apennines on the west, by the Alps on the north and by the Dinaric belt on the east (Fig. 1.1).

The modern northern Adriatic shelf is characterized by an overall low gradient (about 0.4‰; Trincardi et al., 1994, 2014) punctuated by a complex microrelief with metric undulations and local scours that can reach depths of 5 m (Giorgietti and Mosetti, 1969; Gordini et al., 2003; Trincardi et al., 2014). As shown in Fig. 1.1, this area is characterized by the presence of the lowstand alluvial plain sediments deposited during the last glaciation (more details in the next section), and by some patches of transgressive marine deposits.A wedge of highstand deposits buries the older units along the modern coastline.

The main morphological motif of the VFP is constituted by the presence of a series of megafans, which are large fan-shaped landforms that typically occupy the foreland basins of some of the major mountain active belts (Latrubesse, 2015). Megafans have been recognized in the Venetian-Friulian Plain as the product of the glacial outwash of the main river systems, such as the Brenta, Piave and Tagliamento megafans (Fontana et al., 2008). These landforms are characterized by a typical bipartite morphology. The apical portion is characterized by a conic shape and a relatively steep gradient (ca. $7-3$‰), where sediments consist of gravel deposits related to braided channels (Fontana et al., 2008). The distal portions of the megafans are instead characterized by a lower gradient (generally decreasing from 3 to 1‰) and mainly consist of fine
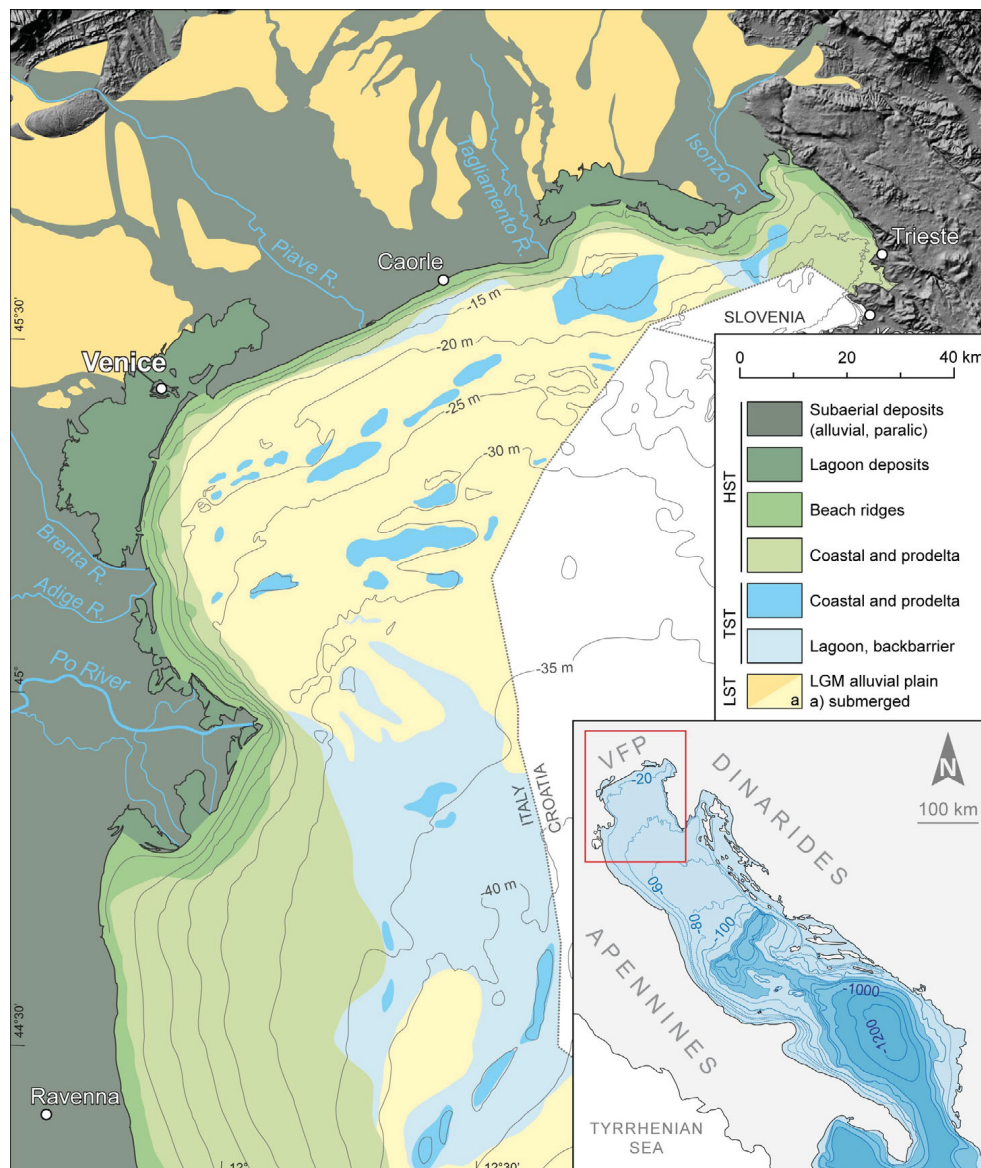
Figure 1.1: Geological map of the study area. Redrawn after Fontana et al. (2014a) and Trincardi et al. (2001, 2011).

dominated sediments with sandy channels. The VFP megafans formed during the Last Glacial Maximum (see section 1.2) and still characterize the modern pandscae of the alluvial plain, especially on its upstream portion, whereas on the coastal area those landforms have been partially buried by younger highstand sediments (Fontana et al., 2010; Fig. 1.1).

Tectonic and subsidence

The area considered in this work lay on the Adria microplate and is part of the foreland basin of the Dinarides, Southern Alps and Northern Apenninens thrust belts (Doglioni, 1993; Patacca and Scandone, 2004; Scisciani and Calamita, 2009). This area is characterized by an overall subsiding trend. Through the comparison between the position of the MIS 5.5 sea-level markers and geophysical models Antonioli et al., (2009) a value of ca. -0.7 mm/a was obtained in the VFP which, moving southward, becomes an interval comprise between -0.3 and -1.0 mm/a. The value proposed for the VFP is well comparable with the one of -0.6 mm/a inferred for the Venice area on the base of borehole stratigraphy (Massari et al., 2004; Maselli et al., 2010). These values have to be considered as averages for the last ca. 125 ka. Vertical movement data recently obtained through GPS measurements on the western coast of the northern Adriatic indicate values up to -4 mm/a (Serpelloni et al., 2013). The long-term subsidence in this area can be explained with the overburden represented by the rapid sedimentation in the area (Picotti and Pazzaglia, 2008) or with a flexural response as a consequence of the north-eastward retreat of the Adriatic subduction (Carminati et al., 2003). The subsidence variability highlighted by the GPS measurements can be induced by the differential compaction of the sediments and, in particular, by anthropogenic factors, such as the exploitation of superficial fluid reservoirs (Carminati and Martinelli, 2002) or short-term natural processes (e.g. glacio-isostatic adjustments; Carminati et al., 2003). A value of ca. -0.3 mm/a has been calculated for the central Adriatic area averaged over the last 340 ka (Maselli et al., 2010).

1.2 THE ONSET OF THE QUATERNARY GLACIAL-INTERGLACIAL CYCLES AND THE SEA-LEVEL FLUCTUATIONS

The beginning of the Quaternary period, ca. 2.6 Ma, marks the onset of an extended reorganization of the Earth climatic pattern, characterized by the beginning of the alternation of glacial and interglacial phases. The reorganization of the climate was characterized by a shift toward a different pace (ca. 23 ka to ca. 41 ka) and shape of the climatic cycles. This modification has been clearly highlighted by the marine oxygen isotope record (δ ^{18}O record), which shows an asymmetrical, sawtooth-shaped alternation of cold and temperate

stages (Lisiecki and Raymo, 2007; Fig. 1.2). Moreover, a further modification of the periodicity, from ca. 41 to ca. 100 ka has been observed around 800 ka BP (Mid Pleistocene Revolution, Maslin and Ridgwell, 2005). The cold-temperate alternation observed through the Quaternary is the consequence of the so-called Milankovitch cycles, which consist of periodic modifications in the eccentricity of the orbit (period of ca. 100 ka) m in the obliquity of the ecliptic (period of ca. 41 ka) and in the precession of the equinoxes (period of ca. 21 ka). As active over a longer time than the Quaternary Period only, these variables cannot explain the onset of the climatic cyclicity themselves, and other parameters must be taken in account. One of the major factors that contributed in the climatic tuning is constituted by the modification of the continental masses, and notably by the closure of the Panama Isthmus, ca. 2.75 Ma BP, which led to a modification in the oceanic circulation (Bartoli et al., 2005; Schneider and Schmittner, 2006). Another possible factor consists in the tectonic activity In the Tibet Plateau, which would have modified the jet stream pattern and led to an intensification of the monsoonal circulation (Raymo and Ruddiman, 1992), finally leading to an overall cooling trend.

Last Glacial Maximum (LGM)

This new global climatic pattern led to the periodic growing and collapse of continental ice sheets, which in turn triggered the onset of extensive environmental changes. In particular, the glacio-isostatic, eustatic and thermosteric effects led to a periodic variation of the sea level, which oscillated between ca. -130 and +10 m MSL (Waelbroeck et al., 2002; Siddall et al., 2003; Antonioli et al., 2009; Lisiecki and Stern, 2016).

After the last interglacial (i.e. MIS 5, $132 − 116$ ka cal BP) the sea level followed a fluctuating downward trajectory that culminated in the Last Glacial Maximum (LGM, $29 − 19$ ka cal BP; Clark et al., 2009) marine lowstand that, in the Adriatic Sea, was characterized by a sea level of ca. -130 m MSL (Correggiari et al., 1996; Maselli et al., 2010 Amorosi et al., 2016). During this period, the northern Adriatic shelf was completely exposed to subaerial conditions and was occupied by an extensive alluvial plain (Amorosi et al., 2016;Pellegrini et al., 2017). It has been hypothesized that most of the rivers from the Alpine, Apennine and Dinaric regions may have drained into a "mega" Po River (De Marchi, 1922; Correggiari et al., 1996; Maselli et al., 2011). The existence of a Mega Po River is corroborated by the presence of a thick
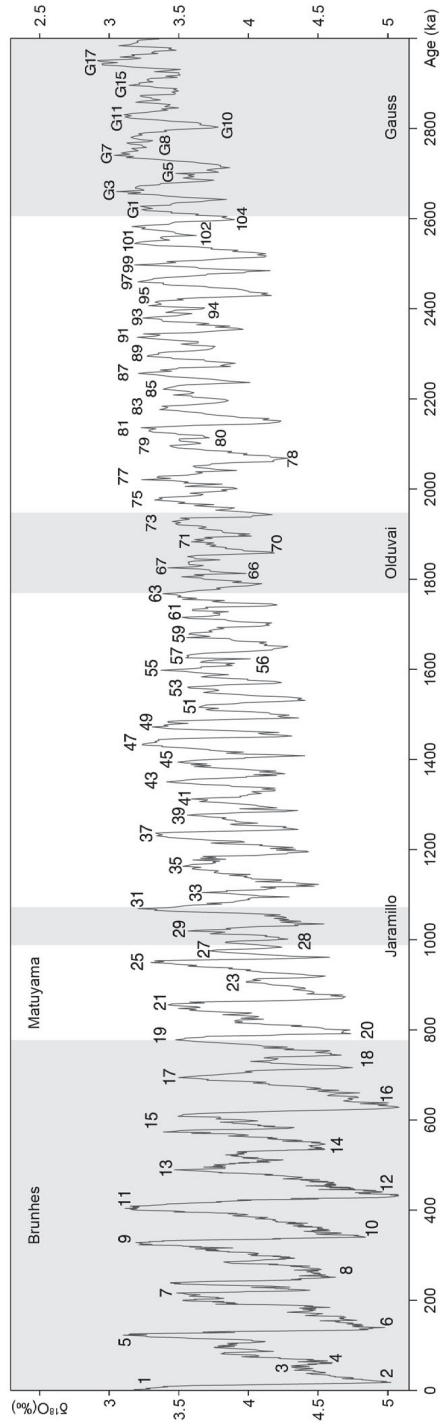
Figure 1.2: Stacked oxygen isotope record for the Quaternary Period, redrawn after Lisiecki and Raymo, (2005). The oscillation of the oxygen isotope can be used as a proxy for the climatic record. Lower values of $\delta^{18}O$ indicate warmer conditions, whereas higher values indicate colder phases.

lowstand wedge system at the shelf break (Pellegrini et al., 2017, 2018). During the entire glacial period, the Adriatic Sea experienced a prolonged phase of fluvial deposition, in contrast with the typical dissection operated by the fluvial systems on the exposed continental shelves as record on a global scale (Catuneanu, 2006; Blum et al., 2013).

While the Adriatic shelf was experiencing only a slight but prolonged aggradation, the Venetian-Friulian Plain, located at the piedmont of the southern Alps (Fig. 1.1), was subjected to strong rate of sedimentation, with an inferred vertical aggradation ranging between 15 and 35 m, even in the distal sector of the modern plain (Fontana et al., 2010, 2014a; Rossato and Mozzi, 2016). This deposition was fed by the high quantity of sediments conveyed by the major alpine glaciers, which during the LGM reached the plain and, in some cases, built extensive terminal moraine systems (e.g. Garda and Tagliamento morainic amphitheatres, Monegato et al., 2007, 2017). The large quantity of sediments delivered to the piedmont fed the outwash streams of the major glaciers leading to the construction of a series of megafans.

Post-LGM marine transgression

After the peak of the last glaciation the relative sea-level started to rose because of the melting of the continental ice-sheets (Bard et al., 1990; Stanford et al., 2011). As highlighted both by the available stable proxies (e.g. Barbados coral reef: Fairnaks, 1989; Bard et al., 1990; Tahiti coral reef: Bard et al., 2010) and by local sea-level indicators (e.g. the Adriatic Sea: Correggiari et al., 1996) the sea level transgression did not follow a monotonous trend, but was punctuated by several periods of RSL rise rate increase and decrease. In particular, the former were driven by phases of rapid ice sheets deterioration and, in a smaller proportion, by the pro-glacial and pluvial lake drainage (Harrison et al., 2018), such as the meltwater pulses (MWP) 1A (14.8 to 13.0 ka BP) and 1B (11.5 to 11.1 ka BP; Alley et al., 2005; Lambeck et al., 2014; Harrison et al., 2018), whereas the latter were caused by temporary cold outbreak, which is the case of the Younger Dryas Stadial (Bard et al., 2010; Pellegrini et al., 2015).

These fluctuations affected the evolution and movements of the coastline, forcing the development of different environments in response to different transgression rates. The relative sea-level rise led to the submersion of the former alluvial plain that occupied the Adriatic shelf, culminating with a maximum

marine ingression which is recorded at ca. 5.5 ka cal BP (e.g. Amorosi et al., 2016 and references therein). The deglaciation process affected also the Alpine glaciers, which experienced a rapid retreat and shrinking. In particular, the end of the LGM for the Tagliamento system is recorded at 19 ka cal BP (Monegato et al., 2007; Fontana et al., 2014b). This rapid decay of the Alpine glaciers interrupted the sediment conveying to the alluvial plain, a phenomenon that is attributed to the presence of several sediment traps (e.g. lakes) within the Alpine catchment (cf. Fontana et al., 2010; Carton et al., 2009). Thus, the dramatic sediment starvation that followed the retreat of the glaciers tongues led to the drastic incision of the apexes of the megafans (Fontana et al., 2014a). Such deep erosive features are still recognizable in the modern landscape of the Venetian-Friulian Plain. More insights are presented in chapter 2.

1.3 THE RECONSTRUCTION OF PAST SEA-LEVEL VARIATIONS

The reconstruction of the evolutionary history of an area through a certain period is necessarily demanded to the availability of relict landforms or deposits formed during the considered time frame. A recently-compiled database of hundreds of post-LGM paleo sea-level indicators from the western Mediterranean Sea (Vacchi et al., 2016) clearly indicates that half of the available control points are roughly concentrated in the last 4 ka, while the other half is unevenly distributed between ca. 4 and 14 ka cal BP. Moreover, the age range between 7 and 14 ka cal BP is particularly depleted, being represented only by the 25% of the entire dataset (Fig. 1.3; see also Bard et al., 2010). This dishomogeneity can be attributed to two main factors: 1) the difficult accessibility of the indicators and 2) a defect of formation or preservation of the indicators. The first problem is intrinsic to the concept of relative sea-level rise, as the older is the deposit the deeper is its position respect to the MSL, unless the indicator has been subjected to some vertical displacements. This is clearly highlighted by the available RSL curves (Fig. 1.3). The second issue is due to the preservation potential and the non-formation of indicators. Among the mid-latitude non-anthropic relative sea-level proxies, the most used and widespread sea-level and paleogeographic indicators are often constituted by landforms and sedimentary features connected to the marine erosive and depositional action, such as beachrocks, marine terraces and lagoon deposits
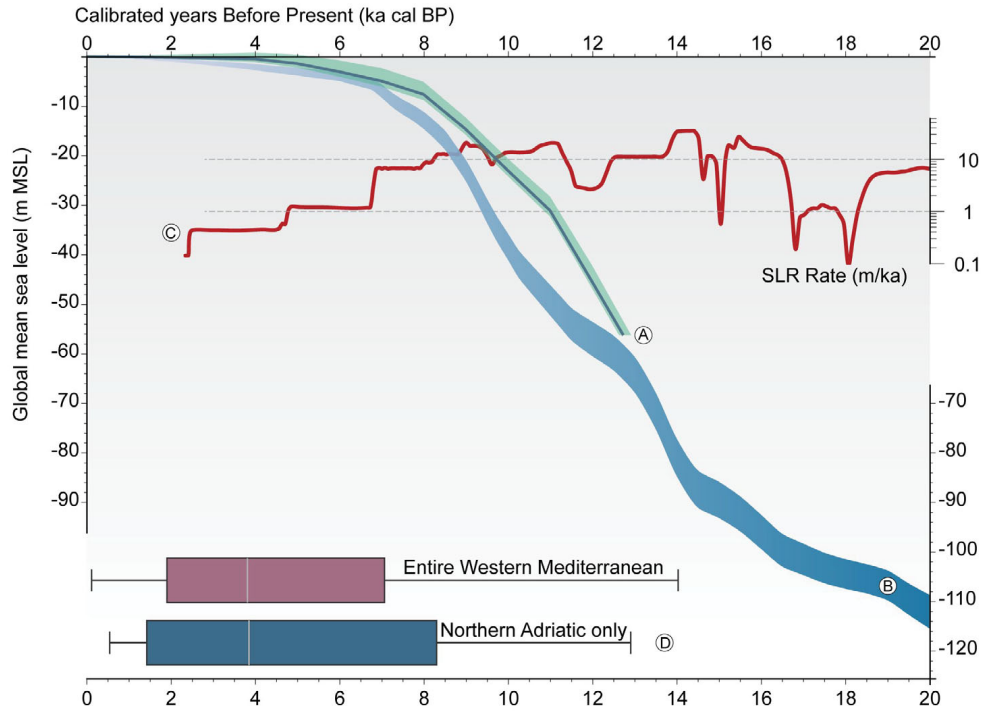
Figure 1.3: A: RSL curve calculated for the northern Adriatic Sea following the ICE-5G (VM2) model from Peltier, (2004); B: RSL stacked curve for the northern Adriatic Sea as published in Lambeck et al., (2011); C: RSL rate as calculated in Lambeck et al., (2014); D: Distribution of the relative sea-level index points from the dataset published in Vacchi et al. (2016). The indicators are subdivided in quartiles.

(Mauz et al., 2015; Vacchi et al., 2016; Rovere et al., 2016). The formation and preservation of such indicators is strongly constrained by the geological, geographical and environmental characteristics of the different sites affected by the marine transgression. In particular, the interplay among different rates of relative sea-level rise, different physiography of the transgressed areas and different patterns of sediment discharge and dispersion would alternatively hamper or foster the formation of morphologies or sediment deposits necessary to the definition of an indicator. The same factors can also strongly affect the preservation of the same features (cf. Cattaneo and Steel, 2003).

It is worth noting that the reconstructed RSL rate (Fig. 1.3) indicates the occurrence of high rates of relative sea-level rise, up to 10 m/ka, for the period between 7 and 11 ka cal BP. On the one hand, this condition would have strongly affected the formation of any indicator, due to the extreme rapidity

of the transgression, while on the other it would have fostered the preservation of lagoon deposits (Storms et al., 2008).

In this perspective, the Adriatic shelf with its peculiar low gradient (ca. 0.4‰) represents a unique setting that heavily influenced the dynamics of the post-LGM transgression, leading to the submersion of wide portions of the former alluvial/coastal plain even for small sea level increments. This induced a rapid retrogradation of the coastline and allowed the formation of discrete sea-level indicators that, on a steeper coastal area, would instead be amalgamated.

During the marine transgression, between the end of the LGM and the maximum marine transgression (ca. $20 - 5$ ka BP; Correggiari et al., 1996), the coastline moved from the shelf break to almost its current position and the whole northern Adriatic shelf (ca. 300 km long) was progressively flooded with an average speed for the coast retrogradation of 20 m/a. This value just represents an overall rough estimation and has been subjected to accelerations and decelerations due to different trends of the eustatic level change (e.g. Melt Water Pulses; Harrison et al., 2018), sediment availability and local geomorphological response of the different coastal areas.

Although the very low gradient of the northern Adriatic only fostered the formation of thin layers of transgressive deposits (Cattaneo and Steel, 2003) and, except for few cases (cf. Storms et al., 2008; Moscon et al., 2015), such deposits were eroded and dismantled by the wave erosive action of the rising sea, the transgressive deposits of this area potentially constitute an ideal proxy for adding new constraints for the post-LGM relative sea-level curve. The preservation potential can be increased by the physiography of the basin or by the presence of sediment-filled erosive features, such channels and scours. An example of the latter can be identified in the paleo tidal inlets that formed at the boundary between ancient barrier-lagoon complexes and the open sea. These landforms are particularly suitable as their depth promoted the almost entire preservation of their morphology and infilling within the stratigraphic record. These structures can be recognized via shallow geophysical surveying. See paragraph 1.4 for more insights.

In a broader perspective, incised valleys are also exceptional witnesses for the reconstruction of the last marine transgression, as their infilling often record the shift to an estuarine environment, which can therefore provide important information on the relative sea-level rise. The presence of some known incised valleys in the area of the Venetian-Friulian Plain (cf. Fontana, 2006; Fontana

et al., 2008, 2010, 2012, 2014a; Carton et al., 2009), provided the ideal springboard for this study.

1.4 INCISED AND INFILLED LANDFORMS: AN OVERVIEW

This work mainly focused on the paleo tidal inlets and incised valleys recognized in the study area. In the next paragraphs a general outline on the formation and evolution of such landforms is presented.

Tidal inlets

Tidal inlets are breaches along a barrier coastline that connects a protected lagoon to the open sea (Fig. 1.4). Due to their strategic value as preferential maritime gateway and for their economic and ecological relevance, tidal inlets have long attracted the attention of scientist, and in particular of hydraulic engineers and geologist, which started their study on such features in the last decades of the 19th century (Stevenson, 1886; Watt, 1905; Brown, 1928; O'Brien, 1931; Escoffier, 1940; Jarret, 1976; Hayes, 1979; Mehta and Joshi, 1988; Tran et al., 2012; Hinwood and McLean, 2018). Studies on tidal inlets and their infilling sequence have been conducted on a worldwide scale on the basis of shallow-seismic data and sediment cores (e.g. Texas Coast; Israel et al., 1987; Siringan and Anderson, 1993; Simms et al., 2006; North and South Carolinas: Moslow and Heron, 1978; Susman and Herron, 1979; Tye and Moslow, 1993; Culver et al., 2006; Virginia-North Carolina Barrier Coast: McBride et al., 1999; French Atlantic coast: Allard et al., 2009; Bay of Biscay: Chaumillon et al., 2008; Northern Adriatic: Zecchin et al., 2009). Tidal inlets deposits have been identified and described also in the rock record (cf. Bridges, 1976; Cheel and Leckie, 1990; Brownridge and Moslow, 1991; Ricketts, 1991; Okazaki and Masuda, 1995). From a morphological point of view a tidal inlet typically consists of three main components: an ebb tidal delta, a flood tidal delta and a tidal channel or inlet throat (Dalrymple et al., 1992; Boyd et al., 2006; FitzGerald et al., 2012; Tran et al., 2012). The inlet throat is the opening that guarantees the exchange of water between the two connected water bodies during the rise and fall of the tide, while the ebb and flood deltas are the accumulation of sediments, transported by the water flux, that can be found respectively at the seaward and landward termination of the inlet (Elias and Van Der Spek, 2006). These landforms exist as a consequence of the tidal

11
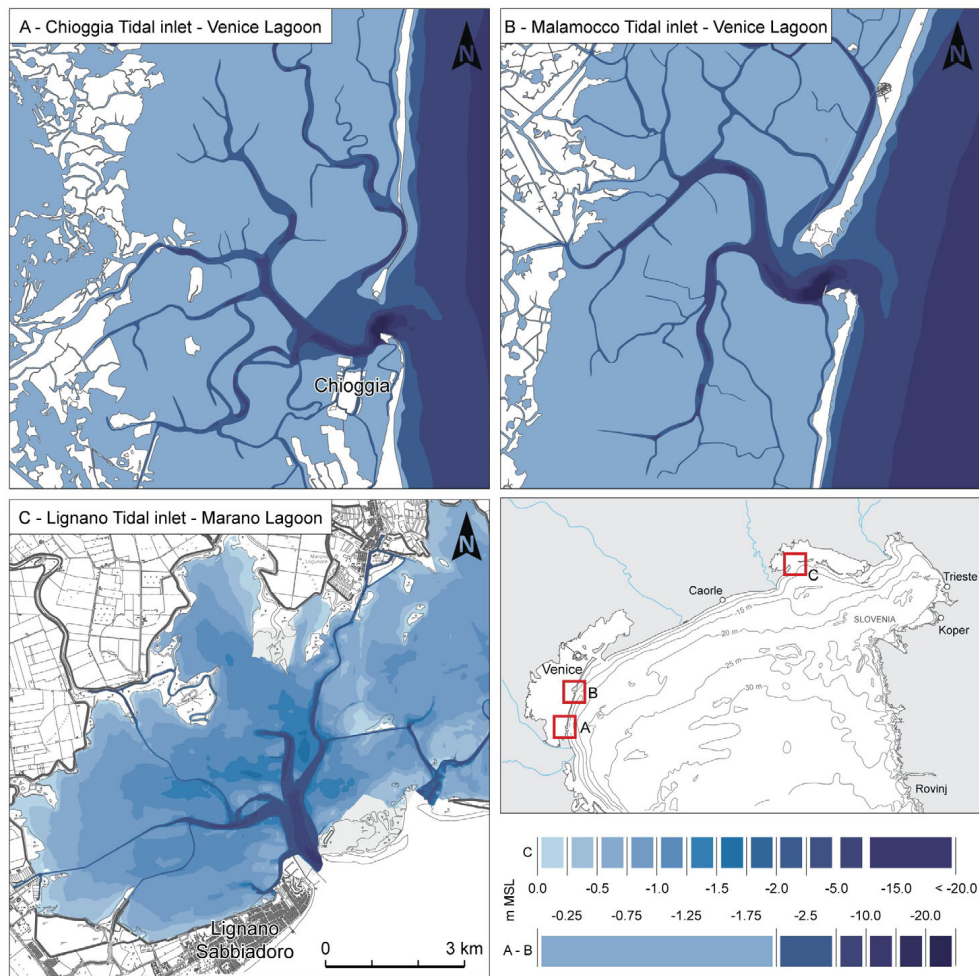
Figure 1.4: Bathymetric maps of three of the main tidal inlets of the northern Adriatic. The bathymetry of the Chioggia and Malamocco inlets (A and B) is taken from the historic map drawn by Augusto Dénaix in 1811. The bathymetry reported for the Lignano inlet (C) correspond to the modern one and it is published in Triches et al., (2011).

currents that convey the marine waters in and out of the lagoon area and are strongly influenced by the hydro-morphodynamics induced by the shape and characteristic of the lagoon, including the inherited physiography of the area, by the tidal range, by the conditions of relative sea-level rise (Van Goor et al., 2003) and by the storm activity (FitzGerald and Miner, 2013). These landforms adjust their shape and morphology through a complex interaction of feedback processes (Lanzoni and Seminara, 2002).
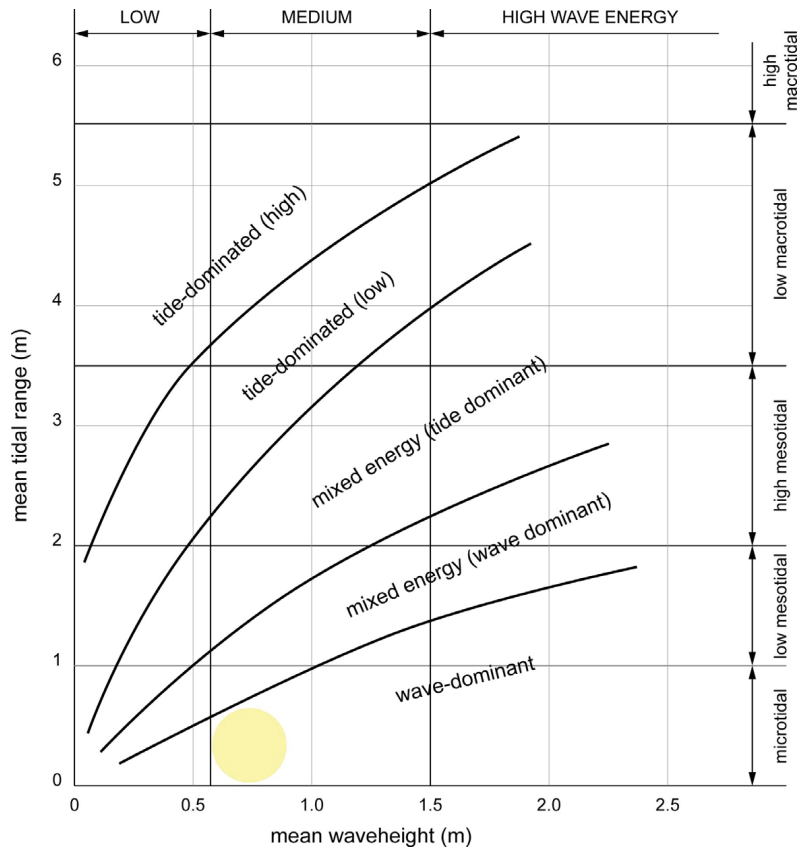
Figure 1.5: Hydrodynamic-based classification of tidal inlets. After Hayes, (1979). The pale-yellow circle indicates the presumed conditions for the Adriatic Sea during the entire Holocene.

A classification of tidal inlets based on the energy of the system (mean tidal range and mean significant wave height) was proposed by Hayes, (1979) and is reported in Fig. 1.5. Considering the paleoenvironmental reconstruction proposed by Storms et al., (2008), the early Holocene tidal inlets of the Adriatic area can be defined as wave-dominated given the microtidal regime (ca. 0.5 m) and the low to medium wave height (< 1 m). It is worth noting that these values can be considered almost constant for the entire Holocene.

Tidal inlets are common features in the modern highstand coastal areas and several works addressing their evolution, stability and morphology are therefore available (e.g. Fontolan et al., 2012; Fraccascia et al., 2016; Harrison et al., 2017; de Haas et al., 2018). On the contrary, the transgressive tidal inlets are underrepresented in the Quaternary geological record (Hine and

Snyder, 1985; Cattaneo and Steel, 2003; FitzGerald et al., 2012). This fact is mainly a consequence of the erosive processes promoted by the rising sea (Cattaneo and Steel, 2003; FitzGerald et al., 2012), but it should also take into account the possibility of a lack of formation of such deposits due to the rapid relative sea-level rise and the rather constant landward migration of the coastline. Moreover, the scarce accessibility of these relict landforms is another factor that affected the quantity of available studies on such features. Some notable studies on transgressive tidal channels and inlets are available for the offshore of the Netherlands (Rieu et al., 2005; Hijma et al., 2010).

Given the importance of the tidal inlets as gateways to safe harbors and sheltered areas, these landforms have been studied since the first half of the last century (e.g. O'Brien, 1931; Escoffier, 1940). These seminal works highlighted some fundamental empirical relations that describe the behavior of the tidal inlets. These relations, which still constitute the base for the interpretation of these geomorphological features, are briefly summarized hereunder. It is worth noting that these empiric lows were extrapolated and tested on highstand tidal inlets, therefore it should be evaluated to which extent they can be considered valid for transgressive settings.

O'BRIEN LAW   The O'Brien law (O'Brien, 1931) is an empirical relationship between the tidal prism of a lagoon (P) and the cross-sectional area of a tidal inlet (A):

$$A = CP^q$$

In which C and q are empirical parameters. This equation has been discussed and reviewed in several papers (Jarret, 1976; Kraus, 1998; Suprijo and Mano, 2004; Van De Kreeke, 2004; D'Alpaos et al., 2009; Tran et al., 2012; FitzGerald and Miner, 2013). In Fig. 1.6 the O'Brien power law curves for different values of C and q are reported.

ESCOFFIER DIAGRAM   The diagram proposed by Escoffier, (1940) consists of a closure curve and an equilibrium velocity curve (Fig. 1.7). The closure curve describes the relation between the characteristic velocity (V_c) of the water through the inlet (which can be assumed to be equal to the cross-sectionally averaged velocity) and the cross-section area of the inlet (A). The equilibrium velocity curve represents instead the velocity of the flow as a function of
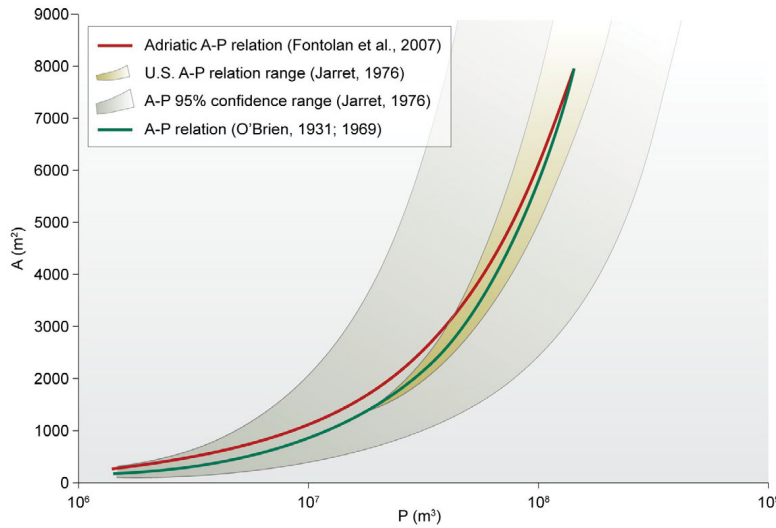
Figure 1.6: Representation of the O'Brien power law for different coefficient of C and q. The parameters used for the red curve were calculated by Fontolan et al., (2007) for the modern tidal inlets of the northern Adriatic.

the cross-sectional area and of the empirical parameter C and q from the O'Brien law (Fig. 1.6). The intersections between the closure curve and the equilibrium velocity curve identify two equilibrium states (stable roots) in which the sediment provided by the littoral drift is equal to the sediment driven out by the ebb currents, meaning that the tidal inlet is in a steady-state. As represented in Fig. 1.7, moving from the equilibrium position, the tidal inlets tend to decrease their section when the characteristic velocity is lower than the equilibrium velocity (i.e. sediment input higher than sediment output), and to increase it when the characteristic velocity is higher (i.e. sediment output higher than sediment input). For more insights the reader is referred to the work of Tran et al., (2012) and references therein.

Incised valleys

Incised valleys (IVs) have been recognized and described since the half of the 20th century (Fisk, 1944) and several examples are known throughout the whole geological record, from the Precambrian to the Quaternary (cf. Dalrymple et al., 1994). In particular, several examples have been individuated in the Late Quaternary record of the marine shelves and coastal plains of the entire world (e.g. Blum and Törnqvist, 2000; Lin et al., 2005; Nordfjord et al., 2005, 2006;
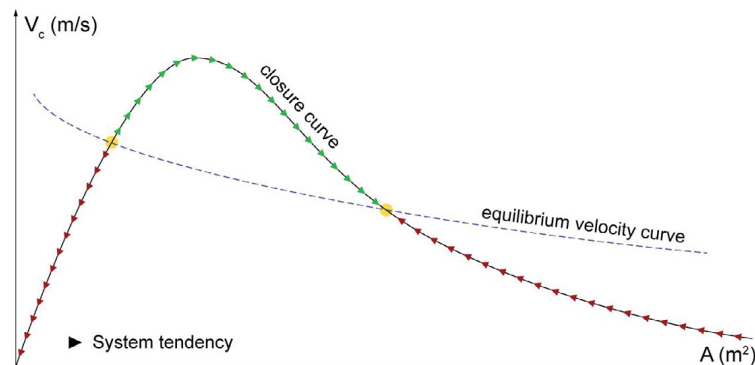
Figure 1.7: Escoffier Diagram. The typical shapes of the closure and equilibrium velocity curves are reported. After Escoffier, (1940).

Mattheus et al., 2007; Ngueutchoua and Giresse, 2010; Tanabe et al., 2010, 2013; Mattheus and Rodrigues, 2011; Green et al., 2013; Blum et al., 2013). From a sequence stratigraphy point of view, the historical importance of IVs is represented by their contribute to the identification of sequence-bounding surfaces over large areas (e.g. Vail et al., 1977; Posamantier and Vail, 1988; Van Wagoner et al., 1988, 1990). Furthermore, incised valley systems can host important hydrocarbon reservoirs (Van Wagoner et al., 1990; Zaitlin et al. 1990; Pulham, 1994). Finally, IVs, especially those formed during the Quaternary, are particularly important for the reconstruction of processes and environment, as they often represent the only available record of marine regressive and lowstand phases (Thomas and Anderson, 1994; Payenberg et al., 2006).

From a sequence stratigraphy point of view incised valleys were originally defined on the basis of (1) the truncation of older strata, (2) the juxtaposition of fluvial-estuarine deposits onto marine ones and (3) the basinward shift of facies due to relative sea-level fall (Van Wagoner et al., 1990; Allen et al., (1993)). These points have been further discussed and expanded by Boyd et al., (2006), up to reach a list of 14 parameters which take into account, among others, the estuarine behavior of the incised valley induced by the sea-level rise (the reader is invited to refer to the publication for the complete description). Nevertheless, the definition of incised valley has been debated, as some authors argue that such parameters do not univocally define the incised valleys, and furthermore proposed to deemphasize the concept of "incision", inherent in the name Incised Valley, in favour of the name Paleovalley (Blum and Törnqvist,
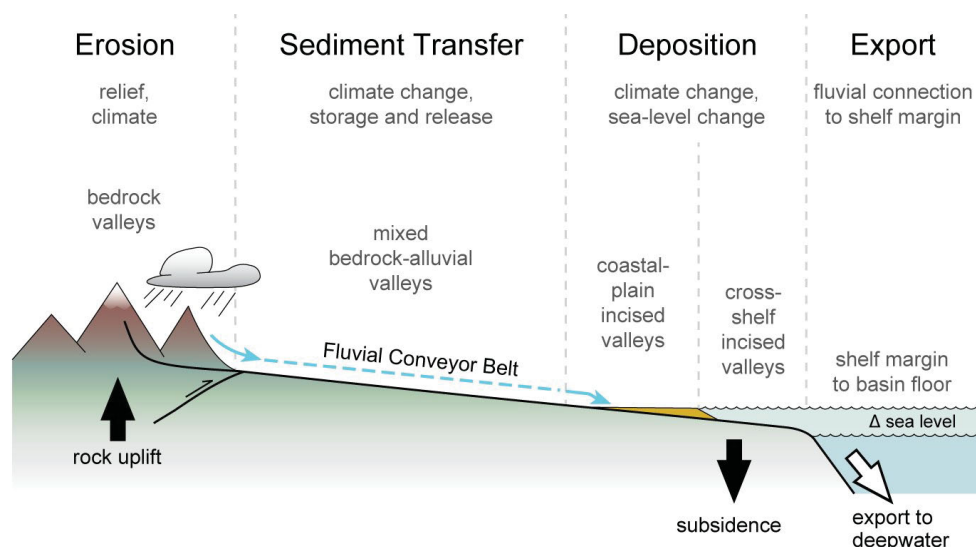
Figure 1.8: Source to sink representation for fluvial systems. Redrawn from Blum and Hattier-Womack, (2009).

2000, Blum et al., 2013). Despite the reasonable argument provided, in this work we decided to abide by the term Incised Valley (IV), as it is used in most of the works on the Adriatic area (e.g. Maselli and Trincardi, 2013; Amorosi et al., 2017) and, more in general, in most of the published works addressing this topic. For the purposes of this work, we generically define an IV as a relict landform produced by river incision during base level fall.

Incised valleys constitute an essential component in the sediment routing and storage and are subjected to a diversity of processes and controls along the entire source to sink path (Fig. 1.8; Blum and Hattier-Womack, 2009, Blum et al., 2013; Bhattacharya et al., 2015).

The incised valley considered in this research (Chapter 3) is currently located in a coastal plain environment.

MECHANISM OF INCISION   The mechanism of formation of an Incised Valley is related to a destabilization of the longitudinal profile and to the subsequent movement toward a new equilibrium state. Typically, incised valleys form as the consequence of the exposure of the continental shelf and the basinward migration and reorganization of the riverine systems (Schumm, 1993; Van Heijst and Postma, 2001; Fagherazzi et al. 2008; Martin et al., 2011). This is associated to a base level fall, which can be the consequence of either an
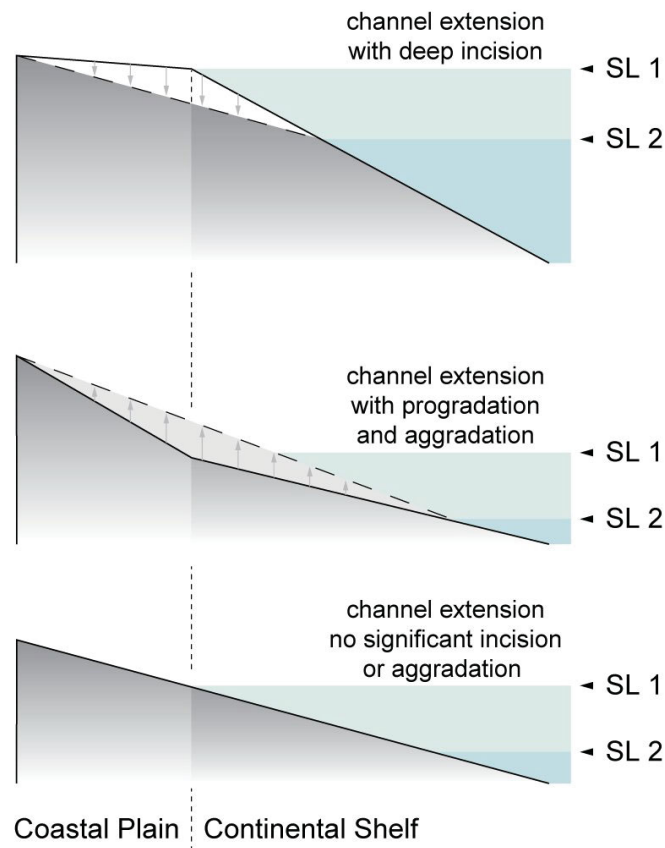
Figure 1.9: Effect of the relative slope of coastal plain and continental shelf on the development of an incised valley after a sea-level fall. Redrawn from Schumm (1993).

eustatic fall or a tectonic uplift (Jervey, 1988). If the sea level fluctuation does not led to the exposure of the shelf break, incised valleys can form on the shelf as piedemont IV systems (Talling, 1998). Another possible mechanism for the destabilization of the longitudinal profile is the variation of the ratio between water and sediment in a river. In a natural environment this is typically induce by climatic fluctuations that can influence the catchment area, such as the increase or drop of precipitations, the quantity and quality of vegetated cover or the formation of sediment traps (Thorne et al., 1997; Fontana et al., 2008). Given these main forcings, the formation and evolution of an incised valley can be still strongly influenced by local factors. For instance, the presence of a low slope shelf can prevent the incision during the marine falling stage and instead induces an aggradation phase, as illustrated in Chapter 2 (Fig. 1.9).

MORPHOLOGY   Incised Valleys have a wide variety of morphologies, depending on their position on the source to sink route and on the driving mechanisms that induce their formation. The lower boundary of an IV is typically composed by the envelope of the erosive unconformity surfaces of a river (Strong and Paola, 2009). The boundary between an IV infilling and the incised deposit is therefore highly diachronic and defined by the wandering of the river in different moments. Therefore, the large majority of IVs have never been totally empty, as it would be in the hypothesis of a perfect bypass mechanism, while they experienced pulses of erosion and deposition driven by lateral migration (Blum and Törnqvist, 2000).

EVOLUTION AND INFILLING   The infilling stage is necessarily a consequence of an alteration in the boundary conditions of the system, which shift from an incising or steady-state condition to aggrading one. In coastal environments, IVs infillings are typically linked to a rise of the RSL. In an ideal case the first infilling phase is linked directly to the riverine deposition arouse by the base level rise and the consequent changing of the hydraulic conditions. As soon as the sea level approaches the floor of the incised valley a gradually move toward an estuarine environment takes place. Eventually the submersion of the valley can lead to the formation of a shallow marine environment (cf. Dalrymple et al., 1992; Allen et al., 1993; Boyd et al., 2006; Vis and Kasse et al., 2009; Maselli and Trincardi, 2013; Clement et al., 2017). This tripartite infilling, which has been described for several IVs, was first explained by Dalrymple et al., (1992) with a model that takes into account the relative influences and the interplay between the fluvial and marine domains (Fig. 1.10).

Two main types of incised valleys fills are recognized in the literature: simple and compound (Boyd et al., 2006; Maselli and Trincardi, 2013). Simple-filled IVs have been characterized by a single depositional phase that lead to their complete infilling. On the contrary compound-filled IVs recorded different cycles of incision and infilling, which are separated by erosive unconformities. Following the principles from Paola et al., (1992) and Blum et al., (2013), the amount of time required by an IV to reach an equilibrium state can be defined as:

$$T_{eq} = \frac{L^2}{V}$$
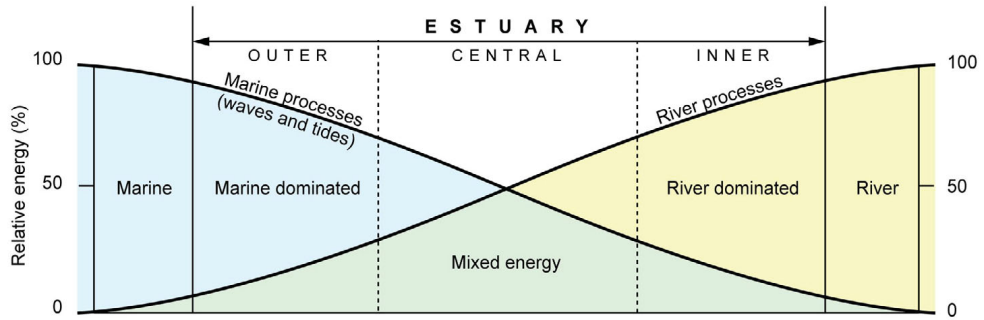
Figure 1.10: Diagram of the relative influences of marine and fluvial processes in an estuarine environment. Redrawn from Dalrymple et al. (1992).

Where L is the characteristic length of a basin and V is a physically-derived sediment-transport coefficient. By imposing a variation in the boundary conditions of the system characterized by a time T it is also possible to define the rapidity of the evolution of the morphology, which is defined as:

$$T^* = \frac{T}{T_{eq}}$$

Slow variations in the system would be characterized by $T^* >> 1$, whereas for a fast variation $T^* << 1$ is expected.

A typical steady-state alluvial plain river normally shows a horizontal evolution, characterized by avulsions, migration of meanders and activation and deactivation of braids. The river wandering affects, during a long period, the entire available surface of an alluvial plain. It is possible to speculate that a deviation from the equilibrium state can follow different paths in response to the rapidity of the destabilization of the longitudinal profile. A rapid variation would lead to a vertical evolution of the system, characterized by the entrenching of the river which would reach a remarkably high deep/width ratio ($T^* << 1$). The persistence of the same boundary conditions after the destabilization would than lead to a horizontal evolution of the river, which would reproduce the condition of the above described alluvial plain within the moving boundaries of the incised valley walls. If the destabilization is followed by another fast change in the environment the evolution of the valley is likely to follow again a vertical trend, characterize in this case by its infilling. Summarizing, the morphology and the infilling stratigraphy of the incised valleys are directly linked to changes in the boundary conditions, therefore

these features constitute unique morphological and sedimentary windows for the paleo environmental reconstruction.

The works presented in the next chapters address the topics here illustrated. In the 2nd chapter a thorough analysis performed on an incised valley buried in the subsurface of the modern Venetia-Friulian Plain is presented. A dataset constituted by more than 2 000 cores allowed a reconstruction of the basal unconformity of the valley and a precise definition of the different infilling units, which recorded the transition from an alluvial to a lagoon environment. In the 3rd chapter the reconstruction performed on a set incised channels recognized via sub-bottom profiling on the northern Adriatic shelf is reported. This work allowed to distinguish the presence of two different generation of features, an older one, which is an incised valley, and a younger one, constituted by tidal inlets and channels. This study was published in the journal *Marine Geology* (Ronchi et al., 2018).

The 4th chapter analyses another example of tidal inlet recognized in the offshore of the Po Delta and allows to discuss the main characteristics of such landforms, providing also a regional view on the area. This work has been submitted to the Journal *Geomorphology* (Ms. Ref. No.: GEOMOR-7998).

In the 5th chapter the data collected on all the recognized tidal inlets of the northern Adriatic shelf are reported, along with an interpretation on their potentiality as paleo environmental indicators.

Finally, in the 6th chapter the conclusion of this research work is presented along with an overview on the evolution of the entire northern Adriatic area. The chapters of this thesis, if not already published or submitted, are being elaborated for the submission to peer-reviewed journals.

REFERENCES

Allard, J., Chaumillon, E., Féniès, H., 2009. A synthesis of morphological evolutions and Holocene stratigraphy of a wave-dominated estuary: the Arcachon lagoon, SW France. Continental Shelf Research, 29, 957-969.

Allen, G.P., Posamentier, H.W., 1993. Sequence stratigraphy and facies model of an incised valley fill: The Gironde Estuary, France. Journal of Sedimentary Petrology, 63, 378-391.

Alley, R.B., Clark, P.U., Huybrechts, P., Joughin, I., 2005. Ice-sheet and sea-level changes. Science, 310, 456-460.

Amorosi, A., Maselli, V., Trincardi, F., 2016. Onshore to offshore anatomy of a late Quaternary source-to-sink system (Po Plain-Adriatic Sea, Italy). Earth-Science Reviews, 153, 212-237.

Amorosi, A., Bruno, L., Cleveland D.M., Morelli, A., Hong, W., 2017b. Paleosols and associated channel-belt sand bodies from a continuously subsiding late Quaternary system (Po Basin, Italy): New insights into continental sequence stratigraphy Geological Society of America Bulletin, 129, 449-463.

Antonioli, F., Ferranti, L., Fontana, A., Amorosi, A., Bondesan, A., Braitenberg, C., Fontolan, G., Furlani, S., Mastronuzzi, G., Monaco, C., Spada, G., Stocchi, P., 2009. Holocene relative sea-level changes and vertical movements along the Italian and Istrian coastlines. Quaternary International, 206, 102-133.

Antonioli, F., Anzidei, M., Amorosi, A., Lo Presti, V., Mastronuzzi, G., Deiana, G., De Falco, G., Fontana, A., Fontolan, G., Lisco, S., Marsico, A., Moretti, M., Orrú, P.E., Sannino, G.M., Serpelloni, E., Vecchio, A., 2017. Sea-level rise and potential drowning of the Italian coastal plains: Flooding risk scenarios for 2100. Quaternary Science Reviews, 158, 29-43.

Bard, E., Hamelin, B., Fairbanks, R.G., 1990. U-Th ages obtained by mass spectrometry in corals from Barbados: Sea level during the past 130,000 years. Nature, 346, 456-458.

Bard, E., Hamelin, B., Delanghe-Sabatier, D., 2010. Deglacial Meltwater Pulse 1B and Younger Dryas Sea Levels Revisited with Boreholes at Tahiti. Science, 327(5970), 1235-1237.

Bartoli, G., Sarnthein, M., Weinelt, M., Erlenkeuser, H., Garbe-Schönberg, C.D., Lea, D.W., 2005. Stable isotope analysis and temperature reconstruction data from DSDP Hole 94-609B and ODP Hole 162-984B. Earth and Planetary Science Letters, 237, 33-44.

Benjamin, J., Rovere, A., Fontana, A., Furlani, S., Vacchi, M., Inglis, R.H., Galili, E., Antonioli, F., Sivan, D., Miko, S., Mourtzas, N., Felja, I., Meredith-Williams, I., Goodman-Tchernov, B., Kolaiti, E., Anzidei, M., Gehrels, R., 2017. Late Quaternary sea-level changes and early human societies in the central and eastern Mediterranean Basin: An interdisciplinary review. Quaternary International, 449, 29-57.

Bhattacharya, J.P., Copeland, P., Lawton, T.F., Holbrook, J., 2015. Estimation of source area, river paleo-discharge, paleoslope and sediment budgets of linked deep-time depositional systems and implications for hydrocarbons. Earth-Science Reviews, 153.

Blum, M., Törnqvist, T.E., 2000. Fluvial responses to climate and sea-level change: a review and look forward. Sedimentology, 47, 2-48.

Blum, M.D., Hattier-Womack, J., 2009. Climate Change, Sea-Level Change, and Fluvial Sediment Supply to Deepwater Depositional Systems. External Controls of Deep-Water Depositional Systems, 92(92), 15-39.

Blum, M., Martin, J., Milliken, K., Garvin, M., 2013. Paleovalley systems: Insights from Quaternary analogs and experiments. Earth-Science Reviews, 116, 128-169.

Boyd, R., Dalrymple, R.W., Zaitlin, B.A., 2006. Estuarine and Incised-Valley Facies Models. In H.W. Posamentier R.G. Walker (eds), Facies Models Revisited. SEPM Special Publication, 84, 171-235.

Bridges, P.H., 1976. Lower Silurian transgressive Barrier islands, southwest Wales. Sedimentology 23, 347-362.

Brown, E.I., 1928. Inlets on sandy coasts. Proc, ASCE, 54, 505-553.

Brownridge, F., Moslow, T.F., 1991. Tidal estuary and marine facies of the Glauconitic Member, Drayton Valley, central Alberta. In: Smith D.G., Reinson G.E., Zaitlin B.A., Rahmani R.A. (eds) Clastic tidal sedimentology, Canadian Society of Petroleum Geologists, Memoir 16. Canadian Society of Petroleum Geologists, Calgary.

Carminati, E., Martinelli, G., 2002. Subsidence rates in the Po Plain, northern Italy: The relative impact of natural and anthropogenic causation. Engineering Geology, 66, 241-255.

Carminati, E., Doglioni, C., Scrocca, D., 2003. Apennines subduction-related subsidence of Venice (Italy). Geophysical Research Letters, 30, 1-4.

Carminati, E., Martinelli, G., Severi, P., 2003. Influence of glacial cycles and tectonics on natural subsidence in the Po Plain (Northern Italy): Insights from ^{14}C ages. Geochemistry, Geophysics, Geosystems, 4.

Carton, A., Bondesan, A., Fontana, A., Meneghel, M., Miola, A., Mozzi, P., Primon, S., Surian, N., 2009. Geomorphological evolution and sediment transfer in the Piave River system (northeastern Italy) since the Last Glacial Maximum. Géomorphologie : relief, processus, environnement, 3, 155-174.

Cattaneo, A., Steel, R.J., 2003. Transgressive deposits: A review of their variability. Earth-Science Reviews, 62, 187-228.

Catuneanu, O., 2006. Principles of Sequence Stratigraphy. Elsevier, Amsterdam, 386

Chaumillon, E., Proust, J.-N.N., Menier, D., Weber, N., 2008. Incised-valley morphologies and sedimentary-fills within the inner shelf of the northern Bay of Biscay. Journal of Marine Systems, 72, 383-396.

Cheel, R.J., Leckie, D.A., 1990. A tidal-inlet complex in the Cretaceous epeiric sea of North America: Virgelle Member, Milk River Formation, southern Alberta, Canada. Sedimentology 37, 67-81.

Church, J.A., Clark, P.U., Cazenave, A., Gregory, J.M., Jevrejeva, S., Levermann, A., Merrifield, M.A., Milne, G.A., Nerem, R.S., Nunn, P.D., Payne, A.J., Pfeffer, W.T., Stammer, D., Unnikrishnan, A.S., 2013. Sea level change. In: Climate Change 2013: the Physical Science Basis. Contribution of

Working Group I to the Fifth Assessment Report of the Intergovernmental Panel on Climate Change. Cambridge University Press, Cambridge, United Kingdom and New York, NY, USA.

Clark, P., Dyke, A., Shakun, J., Carlson, A., Clark, J., Wohlfarth, B., Mitrovica, J., Hostetler, S., McCabe, A., 2009. The Last Glacial Maximum. Science, 325, 710-714.

Clement, A.J.H., Fuller, I.C., Sloss, C.R., 2017. Facies architecture, morphostratigraphy, and sedimentary evolution of a rapidly-infilled Holocene incised-valley estuary: The lower Manawatu valley, North Island New Zealand. Marine Geology, 390, 214-233.

Correggiari, A., Roveri, M. Trincardi, F., 1996b. Late Pleistocene and Holocene Evolution of the North Adriatic Sea. Il Quaternario-Italian Journal of Quaternary Sciences, 9, 697-704.

Culver, S.J., Ames, D.V., Corbett, D.R., Mallinson, D.J., Riggs, S.R., Smith, C.G., Vance, D.J., 2006. Foraminiferal and sedimentary record of late Holocene barrier island evolution, Pea Island, North Carolina: the role of storm overwash, inlet processes, and anthropogenic modification. Journal of Coastal Research, 22, 836-846.

D'Alpaos, A., Lanzoni, S., Marani, M., Rinaldo, A., 2009. On the O'Brien-Jarrett-Marchi law. Rendiconti Lincei, 20(3), 225-236.

Dalrymple, R.W., Zaitlin, B.A., Boyd, R., 1992. Estuarine facies models; conceptual basis and stratigraphic implications. Journal of Sedimentary Research, 62(6), 1130-1146.

Dalrymple, R.W., Boyd, R., Zaitlin, B.A. (eds) 1994. Incised-Valley Systems: Origin and Sedimentary Sequences: SEPM Special Publication, 51, 391.

de Haas, T., Pierik, H.J., van der Spek, A.J.F., Cohen, K.M., van Maanen, B., Kleinhans, M.G., 2018. Holocene evolution of tidal systems in The Netherlands: Effects of rivers, coastal boundary conditions, eco-engineering species, inherited relief and human interference. Earth-Science Reviews, 177, 13-163.

28

De Marchi, L., 1922. Variazioni del livello dell'Adriatico in corrispondenza con le espansioni glaciali, Atti Accademia Scientifica Veneto-Trentino-Istriana 12-13, 1-15.

Doglioni, C., 1993. Some remarks on the origin of foredeeps. Tectonophysics, 228, 1-20.

Dorale, J.A, Onac, B.P., Fornos, J.J., Gines, J., Gines, A., Tuccimei, P., Peate, D.W., 2010. Sea-Level Highstand 81,000 Years Ago in Mallorca. Science, 327(5967), 860-863.

Elias, E.P.L., Van Der Spek, A.J.F., 2006. Long-term morphodynamic evolution of Texel Inlet and its ebb-tidal delta (The Netherlands). Marine Geology, 225, 5-21.

Escoffier, F.F., 1940. The stability of tidal inlets. Shore and Beach 8, 111-114.

Fagherazzi, S., Howard, A.D., Niedoroda, A.W., Wiberg, P.L., 2008. Controls on the degree of fluvial incision of continental shelves. Computers and Geosciences, 34(10), 1381-1393.

Fairbanks, R.G., 1989. A 17,000-year glacio-eustatic sea level record: influence of glacial melting dates on the Younger Dryas event and deep ocean circulation. Nature 342, 637-642.

Fisk, H.N., 1944. Geological investigation of the alluvial valley of the lower Mississippi River: Vicksburg, United States Army Corps of Engineers, Mississippi River Commission, 78.

FitzGerald, D.M., Buynevich, I.V., Hein, C.J., 2012. Morphodynamics and facies architecture of tidal inlets and tidal deltas. In: Davis, R.A., and Dalrymple, R.W. (eds) Principles of tidal sedimentology, Springer, New York. 12, 301-333.

FitzGerald, D.M., Miner, M.D., 2013. Tidal Inlets and Lagoons along Siliciclastic Barrier Coasts. Treatise on Geomorphology (Vol. 10). Elsevier Ltd.

Fontana, A., 2006. Evoluzione geomorfologica della bassa pianura friulana e sue relazioni con le dinamiche insediative antiche. Enclosed Geomorphological Map of the Low Friulian Plain scale 47. Monografie Museo Friulano Storia Naturale, Udine (288).

Fontana, A., Mozzi, P., Bondesan, A., 2008. Alluvial megafans in the Venetian-Friulian Plain (north-eastern Italy): Evidence of sedimentary and erosive phases during Late Pleistocene and Holocene. Quaternary International, 189, 71-90.

Fontana, A., Mozzi, P., Bondesan, A., 2010. Late Pleistocene evolution of the Venetian-Friulian Plain. Rendiconti Lincei, 21, 181-196.

Fontana, A., Mozzi, P., Marchetti, M., 2014a. Alluvial fans and megafans along the southern side of the Alps. Sedimentary Geology, 301, 150-171.

Fontana, A., Monegato, G., Devoto, S., Zavagno, E., Burla, I., Cucchi, F., 2014b. Evolution of an Alpine fluvioglacial system at the LGM decay: The Cormor megafan (NE Italy). Geomorphology, 204, 136-153.

Fontolan, G., Pillon, S., Delli Quadri, F., Bezzi, A., 2007. Sediment storage at tidal inlets in northern Adriatic lagoons: Ebb-tidal delta morphodynamics, conservation and sand use strategies. Estuarine, Coastal and Shelf Science, 75, 261-277.

Fontolan, G., Pillon, S.F., Bezzi, A., Villalta, R., Lipizer, M., Triches, A., D'Aietti, A., 2012. Human impact and the historical transformation of salt-marshes in the Marano and Grado Lagoon, northern Adriatic Sea. Estuarine, Coastal and Shelf Science, 113, 41-56.

Fraccascia, S., Winter, C., Ernstsen, V.B., Hebbeln, D., 2016. Residual currents and bedform migration in a natural tidal inlet (Knudedyb, Danish Wadden Sea). Geomorphology, 271, 74-83.

Giorgetti, G., Mosetti, F., 1969. General morphology of the Adriatic Sea. Bollettino di Geofisica Teorica ed Applicata, 11, 44-56.

Gordini, E., Caressa, S., Marocco, R., 2003. New morpho-sedimentological map of the Trieste Gulf (from Punta Tagliamento to Isonzo mouth). Gortania-Atti Museo Friulano Storia Naturale, 25, 5-29.

Green, A.N., Dladla, N., Garlick, G.L., 2013. Spatial and temporal variations in incised valley systems from the Durban continental shelf, KwaZulu-Natal, South Africa. Marine Geology, 335, 148-161.

Harrison, S.R., Bryan, K.R., Mullarney, J.C., 2017. Observations of morphological change at an ebb-tidal delta. Marine Geology, 385, 131-145.

Harrison, S., Smith, D.E., Glasser, N.F., 2018. Late Quaternary meltwater pulses and sea level change. Journal of Quaternary Science.

Hayes, M.O., 1979. Barrier island morphology as a function of tidal and wave regime. In: Leatherman, S.P. (eds), Barrier Island. Academic Press, New York, 1-28.

Hijma, M. P., van der Spek, A.J.F., van Heteren, S., 2010. Development of a mid-Holocene estuarine basin, Rhine-Meuse mouth area, offshore The Netherlands. Marine Geology, 271,198-211.

Hine, A.C., Snyder, S.W., 1985. Coastal lithosome preservation: evidence from the shoreface and inner continental shelf off Bogue Banks, North Carolina. Marine Geology 63, 307-330.

Hinwood, J.B., McLean, E.J., 2018. Tidal inlets and estuaries: Comparison of Bruun, Escoffier, O'Brien and attractors, Coastal Engineering, 133, 92-105.

IPCC, 2014: Climate Change 2014: Synthesis Report. Contribution of Working Groups I, II and III to the Fifth Assessment Report of the Intergovernmental Panel on Climate Change [Core Writing Team, R.K. Pachauri and L.A. Meyer (eds)]. IPCC, Geneva, Switzerland.

Israel, A.M., Etheridge, F.G., Estes, E.L., 1987. A sedimentological description of a microtidal, flood-tidal delta, San Luis pass, Texas. Journal of Sedimentary Petrology, 57, 288-300.

Kraus, N.C., 1998. Inlet cross-sectional area calculated by process-based model. In: Proceedings of the 26th Coastal Engineering Conference. American Society of Civil Engineers, VA, 3265-3278.

Jarrett, J.T., 1976. Tidal prism-inlet area relationships. US Army Corps of Engineers, Waterways Experiment Station, Vicksburg, MS, GITI Report No. 3, 54.

Jervey, M.T., 1988. Quantitative geological modeling of siliciclastic sequences and their seismic expressions, in Wilgus, C. K., Hastings, B.S., Kendall, C.G.St.C., Posamentier, H.W., Ross, C.A., and Van Wagoner, J.C., (eds)

Sea-level Changes: An Integrated Ap- proach: Tulsa, Society of Economic Paleontologists and Mineralogists Special Publication 42, 47-69.

Lambeck, K., Antonioli, F., Anzidei, M., Ferranti, L., Leoni, G., Scicchitano, G., Silenzi, S., 2011. Sea level change along the Italian coast during the Holocene and projections for the future. Quaternary International, 232, 250-257.

Lambeck, K., Roubya, H., Purcell, A., Sun, Y., Malcolm, S., 2014. Sea level and global ice volumes from the Last Glacial Maximum to the Holocene. PNAS, 111, 15296-15303.

Lanzoni, S., Seminara, G., 2002. Long-term evolution and morphodynamic equilibrium of tidal channels. Journal of Geophysical Research, 107, 3001.

Latrubesse, E.M., 2015. Large rivers, megafans and other Quaternary avulsive fluvial systems: A potential "who's who" in the geological record, Earth-Science Reviews, 146, 1-30.

Lin, C.M., Zhuo, H.C., Gao, S., 2005. Sedimentary facies and evolution in the Qiantang River incised valley, eastern China. Marine Geology, 219(4), 235-259

Lisiecki, L.E., Raymo, M.E., 2005. A Pliocene-Pleistocene stack of 57 globally distributed benthic δ ^{18}O records. Paleoceanography, 20, 1-17.

Lisiecki, L.E., Raymo, M.E., 2007. Plio-Pleistocene climate evolution: trends and transitions in glacial cycle dynamics. Quaternary Science Reviews 26, 56-69.

Lisiecki, L.E., Stern, J.V., 2016. Regional and global benthic δ ^{18}O stacks for the last glacial cycle. Paleoceanography, 31, 1368-1394.

Martin, J., Cantelli, A., Paola, C., Blum, M., Wolinsky, M., 2011. Quantitative modeling of the evolution and geometry of incised valley. Journal of Sedimentary Research, 81, 64-79.

Maselli, V., Trincardi, F., Cattaneo, A., Ridente, D., Asioli, A., 2010. Subsidence pattern in the central Adriatic and its influence on sediment architecture during the last 400 kyr. Journal of Geophysical Research: Solid Earth, 115, 1-23.

Maselli, V., Hutton, E.W., Kettner, A.J., Syvitski, J.P.M., Trincardi, F., 2011. High-frequency sea level and sediment supply fluctuations during Termination I: An integrated sequence-stratigraphy and modeling approach from the Adriatic Sea (Central Mediterranean). Marine Geology, 287, 54-70.

Maselli, V., Trincardi, F., 2013. Large-scale single incised valley from a small catchment basin on the western Adriatic margin (central Mediterranean Sea). Global and Planetary Change, 100, 245-262.

Maslin, M.A., Ridgwell, A.J., 2005. Mid-Pleistocene revolution and the 'eccentricity myth'. Geological Society, London, Special Publications, 247, 19-34.

Massari, F., Rio, D., Serandrei Barbero, R., Asioli, A., Capraro, L., Fornaciari, E., Vergerio, P.P., 2004. The environment of Venice area in the past two million years. Palaeogeography, Palaeoclimatology, Palaeoecology, 202, 273-308.

Mattheus, C.R., Rodriguez, A.B., Greene, D.L., Simms, A.R., Anderson, J.B., 2007. Control of Upstream Variables on Incised-Valley Dimension. Journal of Sedimentary Research, 77, 213-224.

Mattheus, C.R., Rodriguez, A.B., 2011. Controls on late quaternary incised-valley dimension along passive margins evaluated using empirical data. Sedimentology, 58, 1113-1137.

Mauz, B., Vacchi, M., Green, A., Hoffmann, G., Cooper, A., 2015. Beachrock: A tool for reconstructing relative sea level in the far-field. Marine Geology, 362, 1-16.

McBride, R.A., 1999. Spatial and temporal distribution of historical and active tidal inlets: Delmarva Peninsula and New Jersey, USA. In: Coastal Sediments '99 Proceedings, American Society of Civil Engineers, New York.

McGranahan, G., Balk, D., Anderson, B., 2007. Environment and Urbanization, 19, 17.

Mehta, A.J., Joshi, P.B., 1988. Tidal Inlet Hydraulics. Journal of Hydraulic Engineering, 114, 1321-1338.

Monegato, G., Ravazzi, C., Donegana, M., Pini, R., Calderoni, G.,Wick, L., 2007. Evidence of a two-fold glacial advance during the last glacial maximum

in the Tagliamento end moraine system (eastern Alps). Quaternary Research, 68, 284-302.

Monegato, G., Scardia, G., Hajdas, I., Rizzini, F., Piccin, A., 2017. The Alpine LGM in the boreal ice-sheets game. Scientific Reports, 7, 1-8.

Moscon, G., Correggiari, A., Stefani, C., Fontana, A., Remia, A., 2015. Very-high resolution analysis of a transgressive deposit in the Northern Adriatic Sea (Italy). Alpine and Mediterranean Quaternary 28, 121-129.

Moslow, T.F., Heron, S.D., 1978. Relict inlets: preservation and occurrence in the Holocene stratigraphy of southern Core Banks, North Carolina. Journal of Sedimentary Petrology, 48, 1275-1286.

Mozzi, P., Ferrarese, F., Fontana, A., 2013. Integrating Digital Elevation Models and stratigraphic data for the reconstruction of the post-lgm unconformity in the Brenta alluvial megafan (north-eastern Italy). Alpine and Mediterranean Quaternary, 26, 41-54.

Muhs, D.R., Simmons, K.R., Schumann, R.R., Halley, R.B., 2011. Sea-level history of the past two interglacial periods: New evidence from U-series dating of reef corals from south Florida. Quaternary Science Reviews, 30(5-6), 570-590.

Ngueutchoua, G., Giresse, P., 2010. Sand bodies and incised valleys within the Late Quaternary Sanaga-Nyong delta complex on the middle continental shelf of Cameroon. Marine and Petroleum Geology, 27, 2173-2188.

Nicholls, R.J., Cazenave, A., 2010. Sea-Level Rise and Its Impact on Coastal Zones. Science, 328, 1517-1520.

Nordfjord, S., Goff, J.A., Austin, J.A., Sommerfield, C.K., 2005. Seismic geomorphology of buried channel systems on the New Jersey outer shelf: assessing past environmental conditions. Marine Geology, 214, 339-364.

Nordfjord, S., Goff, J.A., Austin, J.A., Gulick, S.P.S., 2006. Seismic Facies of Incised-Valley Fills, New Jersey Continental Shelf: Implications for Erosion and Preservation Processes Acting During Latest Pleistocene-Holocene Transgression. Journal of Sedimentary Research, 76, 1284-1303.

O'Brien, M.P., 1931. Estuary tidal prisms related to entrance areas. Civil Engineering 1, 738-739.

Okazaki, H., Masuda, F., 1995. Sequence stratigraphy of the late Pleistocene Palaeo-Tokyo Bay: barrier islands and associated tidal delta and inlet. In: Flemming B.W., Bartholomä A. (eds) Tidal signatures in modern and ancient sediments, International Association of Sediment Special Publication 24. Blackwell Science, Oxford/Cambridge.

Paola, C., Heller, P.L., Angevine, C.L., 1992. The large-scale dynamics of grain-size variation in alluvial basins, 1: Theory, Basin Res., 4, 73-90.

Patacca, E., Scandone P., 2004, The Plio-Pleistocene thrust belt: Foredeep system in the southern Apennines and Sicily, in Geology of Italy: Special Volume of the Italian Geological Society for the IGC 32 Florence 2004, edited by V. Crescenti et al., 93-129, Societá Geologica Italiana, Rome, Italy.

Payenberg, T.H.D., Boyd, R., Beaudoin, J., Ruming, K., Davies, S., Roberts, J., Lang, S.C., 2006. The filling of an incised valley by shelf dunes-an example from Hervey Bay, east coast of Australia. In: Dalrymple, R.W., Leckie, D.A., Tillman, R.W. (eds) Incised Valleys in Time and Space. SEPM Special Publication, 85, 87-98.

Pellegrini, C., Maselli, V., Gamberi, F., Asioli, A., Bohacs, K.M., Drexler, T.D., Trincardi, F., 2017. How to make a 350-m-thick lowstand systems tract in 17,000 years: The Late Pleistocene Po River (Italy) lowstand wedge. Geology, 45, 327-330.

Pellegrini, C., Asioli, A., Bohacs, K.M., Drexler, T.M., Feldman, H.R., Sweet, M.L., Maselli, V., Rovere, M., Gamberi, F., Dalla Valle, G., Trincardi, F., 2018. The late Pleistocene Po River lowstand wedge in the Adriatic Sea: Controls on architecture variability and sediment partitioning. Marine and Petroleum Geology, 96, 16-50.

Peltier, W.R., Andrews, J.T., 1976. Glacial-Isostatic Adjustment-I. The Forward Problem. Geophysical Journal of the Royal Astronomical Society, 46(3), 605-646.

Peltier, W.R., 2004. Global glacial isostasy and the surface of the ice-age earth: the ice-5G (VM2) model and grace. Annu. Rev. Earth Planet. Sci. 32, 111-149.

Picotti, V., Pazzaglia, F.J., 2008. A new active tectonic model for the construction of the Northern Apennines mountain front near Bologna (Italy). Journal of Geophysical Research: Solid Earth, 113, 1-24.

Posamantier, H.W., Vail, P.R., 1988. Eustatic controls on elastic deposition II- sequence and systems tract models, in Wilgus, C.K., Hastings, B.S., Kendall, C.G.St.C., Posamentier, H.W., Ross, C.A., Van Wagoner, J.C., (eds) Sea-level Changes: An Integrated Approach: Tulsa, Society of Economic Paleontologists and Min- eralogists Special Publication 42, 125-154.

Pulham, A.J., 1994, The Crusiana field, Llanos basin, eastern Colombia: high resolution sequence stratigraphy applied to late Paleocene- early Oligocene, estuarine, coastal plain and alluvial clastic reservoirs, in Johnson, S., (eds), High Resolution Sequence Stratigraphy: Innovations and Applications: University of Liverpool, Liverpool, England, 63-68.

Raymo, M.E., Ruddiman, W.F., 1992. Tectonic forcing of late Cenozoic climate. Nature, 359, 117-122.

Ricketts, B.D., 1991. Lower Paleocene drowned valley and barred estuaries, Canadian Arctic Islands: aspects of their geomorphological and sedimentological evolution. In: Smith D.G., Reinson G.E., Zaitlin B.A., Rahmani R.A. (eds) Clastic tidal sedimentology, Canadian Society of Petroleum Geologists, Memoir 16. Canadian Society of Petroleum Geologists, Calgary.

Rieu, R., van Heteren, S., Van der Spek, A.J.F., De Boer, P.L., 2005. Development and preservation of a Mid-Holocene tidal-channel network offshore the Western Netherlands. Journal of Sedimentary Research, 75, 409-419.

Rovere, A., Raymo, M.E., Vacchi, M., Lorscheid, T., Stocchi, P., Gómez-Pujol, L., Harris, D.L., Casella, E., O'Leary, M.J., Hearty, P.J., 2016. The analysis of Last Interglacial (MIS 5e) relative sea-level indicators: Reconstructing sea-level in a warmer world. Earth-Science Reviews, 159, 404-427.

Rossato, S., Mozzi, P., 2016. Inferring LGM sedimentary and climatic changes in the southern Eastern Alps foreland through the analysis of a 14C ages database (Brenta megafan, Italy). Quaternary Science Reviews 148, 115-127.

Roy, K., Peltier, W.R., 2018. Relative sea level in the Western Mediterranean basin: A regional test of the ICE-7G_NA (VM7) model and a constraint

on late Holocene Antarctic deglaciation. Quaternary Science Reviews, 183, 76-87.

Schneider, B., Schmittner, A., 2006. Simulating the impact of the Panamanian Seaway closure on ocean circulation, marine productivity and nutrient cycling. Earth and Planetary Science Letters. 246. 367-380.

Scisciani, V., Calamita, F., 2009. Active intraplate deformation within Adria: Examples from the Adriatic region. Tectonophysics, 476, 57-72.

Schumm, S.A., 1993. River Response to Baselevel Change: Implications for Sequence Stratigraphy River Response to Baselevel Change: Implications for Sequence Stratigraphy. Source: The Journal of Geology, 101, 279-294.

Serpelloni, E., Faccenna, C., Spada, G., Dong, D., Williams, S.D.P., 2013. Vertical GPS ground motion rates in the Euro-Mediterranean region: New evidence of velocity gradients at different spatial scales along the Nubia-Eurasia plate boundary. Journal of Geophysical Research: Solid Earth, 118, 6003-6024.

Siddall, M., Rohling, E., Almogi-Labin, A., Hemleben, C., Meischner, D., Schmelzer, I., Smeed, D.A., 2003. Sea-level fluctuations during the last glacial cycle. Nature, 423, 853-858.

Simms, A.R., Anderson, J.B., Blum, M., 2006. Barrier-island aggradation via inlet migration: Mustang Island, Texas. Sedimentary Geology, 187, 105-125.

Siringan, F.P., Anderson, J.B., 1993. Seismic facies, architecture, and evolution of the Bolivar Roads tidal inlet/delta complex, East Texas Gulf Coast. Journal of Sedimentary Petrology, 63, 794-808.

Stanford, J.D., Hemingway, R., Rohling, E. J., Challenor, P.G., Medina-Elizalde, M., Lester, A.J., 2011. Sea-level probability for the last deglaciation: A statistical analysis of far-field records. Global and Planetary Change, 79, 193-203.

Stevenson, T., 1886. The design and construction of harbours: a treatise on maritime engineering, 3rd Ed., A & C Black, Edinburgh, U.K.

Stocchi, P., Vacchi, M., Lorscheid, T., de Boer, B., Simms, A. R., van de Wal, R.S.W., Vermeersen, B.L.A., Pappalardo, M., Rovere, A., 2018. MIS 5e

relative sea-level changes in the Mediterranean Sea: Contribution of isostatic disequilibrium. Quaternary Science Reviews, 185, 122-134.

Storms, J.E.A., Weltje, G.J., Terra, G.J., Cattaneo, A., Trincardi, A., 2008. Coastal dynamics under conditions of rapid sea-level rise: Late Pleistocene to Early Holocene evolution of barrier-lagoon systems on the northern Adriatic shelf (Italy). Quaternary Science Reviews 27, 1107-1123.

Strong, N., Paola, C., 2009. Valleys that never were: time surfaces versus stratigraphic surfaces. Journal of Sedimentary Research 78, 579-593.

Suprijo, T., Mano, A., 2004. Dimensionless parameters to describe topographical equilibrium of coastal inlet. Proceedings of the 29th Conference on Coastal Engineering: ASCE, 2531-2543.

Susman, K.R., Herron, S.D., 1979. Evolution of a barrier island-Shackleford Banks, Carteret County, North Carolina. Geological Society of America Bulletin, 90, 205-215.

Talling, P.J., 1998. How and where do incised valleys form if sea level remains above the shelf edge? Geology, 26, 87-90.

Tanabe, S., Nakanishi, T., Yasui, S., 2010. Relative sea-level change in and around the Younger Dryas inferred from late Quaternary incised-valley fills along the Japan Sea. Quaternary Science Reviews, 29, 3956-3971.

Tanabe, S., Nakanishi, T., Matsushima, H., Hong, W., 2013. Sediment accumulation patterns in a tectonically subsiding incised valley: Insight from the Echigo Plain, central Japan. Marine Geology, 336, 33-43.

Thomas, M.A., Anderson, J.B., 1994. Sea-level controls on the facies architecture of the Trinity/Sabine incised-valley system, Texas continental shelf. In: Dalrymple, R.W., Boyd, R., Zaitlin, B.A. (eds) Incised-valley System: Origin and Sedimentary Sequences. SEPM Special Publication, 51, 63-83.

Thorne, C.R., Hey, R.D., Newson, M.D., 1997. Applied Fluvial Geomorphology for River Engineering and Management, Wiley, Chichester.

Tran, T-T.T., van de Kreeke, J., Stive, M.J.F., Walstra, D.-J.J.R., 2012. Cross-sectional stability of tidal inlets: A comparison between numerical and empirical approaches. Coastal Engineering, 60, 21-29.

Triches, A., Pillon, S., Bezzi, A., Lipizer, M., Gordini, E., Villalta, R., Fontolan, G., Menchini, G., 2011. Carta batimetrica della Laguna di Marano e Grado. Arti Grafiche Friulane, Imoco spa (UD), 39, 5 Maps.

Trincardi, F., Correggiari, A., Roveri, M., 1994. Late Quaternary transgressive erosion and deposition in a modern epicontinental shelf: The Adriatic semienclosed basin. Geo-Marine Letters, 14, 41-51.

Trincardi F., Argnani A. (eds), 2001. Note illustrative della Carta Geologica d'Italia alla scala 1:250,000-Foglio NL33-10 "Ravenna". ISPRA-Servizio Geologico d'Italia.

Trincardi, F., Argnani, A., Correggiari, A., 2011. Note illustrative della Carta Geologica d'Italia alla scala 1:250,000-Foglio NL33-7 "Venezia", ISPRA-Servizio Geologico d'Italia.

Trincardi, F., Campiani, E., Correggiari, A., Foglini, F., Maselli, V., Remia, A., 2014. Bathymetry of the Adriatic Sea: The legacy of the last eustatic cycle and the impact of modern sediment dispersal. Journal of Maps, 10, 151-158.

Tye, R.S., Moslow, T.F., 1993. Tidal inlet reservoirs: insights from modern examples. In: Rhodes E.G., Moslow T.F. (eds) Marine clastic reservoirs: examples and analogues. Springer, New York.

Vacchi, M., Marriner, N., Morhange, C., Spada, G., Fontana, A., Rovere, A., 2016. Multiproxy assessment of Holocene relative sea-level changes in the western Mediterranean: variability in the sea-level histories and redefinition of the isostatic signal. Earth Science Reviews, 155, pp, 172-197.

Vail, P.R., Mitchum, R.M., Thompson, S., III, 1977. Seismic stratigraphy and global changes of sea level, part 3: relative changes of sea level from coastal onlap, in Payton, C. W., ed., Seismic Stratigraphy Applications to Hydrocarbon Exploration: Tulsa, American Association of Petroleum Geologists Memoir 26, 63-97.

Van de Kreeke, J., 2004. Equilibrium and cross-sectional stability of tidal inlets: Application to the Frisian Inlet before and after basin reduction. Coastal Engineering, 51, 337-350.

Van Goor, M.A., Zitman, T.J., Wang, Z.B., Stive, M.J.F., 2003. Impact of sea-level rise on the morphological equilibrium state of tidal inlets. Marine Geology, 202, 211-227.

Van Heijst, M.W.I.M., Postma, G., 2001. Fluvial response to sea-level changes: a quantita- tive analogue, experimental approach. Basin Research 13, 269-292.

Van Wagoner, J.C., Posamentier, H.W., Mitchum, R.M., Vail, P.R., Sarg, R., Loutit, T.S., Hardenbol, J., 1988. An overview of sequence stratigraphy and key definitions, in Wilgus, C.K., Hastings, B.S., Kendall, C.G.St.C., Posamentier, H.W., Ross, C.A., Van Wagoner, J.C., (eds) Sea-level Changes: An Integrated Approach: Tulsa, Society of Economic Paleontologists and Min- eralogists Special Publication 42, 125-154.

Van Wagoner, J.C., Mitchum, R.M., Campion, K.M., Rahmanian, V.D., 1990. Siliciclastic sequence stratigraphy in well logs, cores, and outcrops: concepts for high-resolution correlation of time and facies. AAPG Methods Explor, 7, 55.

Vis, G.J., Kasse, C., 2009. Late Quaternary valley-fill succession of the Lower Tagus Valley, Portugal. Sedimentary Geology 221, 19-39.

Waelbroeck, C., Labeyrie, L., Michel, E., Duplessy, J.C., McManus, J.F., Lambeck, K., Balbon, E., Labracherie, M., 2002. Sea-level and deep water temperature changes derived frombenthic foraminifera isotopic records. Quaternary Science Reviews, 21, 295-305.

Watt, D.A., 1905. Notes on the improvement of river and harbor outlets in the United States. Trans., ASCE, LV, Dec, 288-305.

Zaitlin, B.A., Shultz, B.C., 1990. Wave-influenced estuarine sand body, Senlac heavy oil pool, Saskatchewan, Canada, in Barwis, J.H., McPherson, J.G., and Studlick, J.R.J., (eds) Sandstone Petroleum Reservoirs: New York, Springer-Verlag, 363-387.

Zecchin, M., Brancolini, G., Tosi, L., Rizzetto, F., Caffau, M., Baradello, L., 2009. Anatomy of the Holocene succession of the southern Venice lagoon revealed by very high resolution seismic data. Continental Shelf Research, 29, 1343-1359.

BURIED MORPHOLOGY, SEDIMENTARY FACIES AND EVOLUTION OF A POST–LGM INCISED VALLEY OF TAGLIAMENTO RIVER (NE ITALY)

Abstract

A wide dataset of mechanical and hand-made cores collected in the Venetian-Friulian Plain (NE Italy), geotechnical tests and lidar imaging allowed a detailed reconstruction of a post-LGM incised valley, now almost completely filled and with little to absent morphologic expression. The formation of this valley, which is located in the distal portion of the Tagliamento Megafan, has been probably triggered by a low sediment supply coupled to a high water discharge, likely provided by spring-fed rivers. The valley is up to 1.2 km, it reaches a depth of about 20 m below the top of Pleistocene alluvial plain and it can be tracked for a length up to 25 km. Our dataset allowed a detailed characterization of the sedimentary infilling, which can be subdivided in two main phases. The first one is the result of the paleo Tagliamento River activity within the valley. It is constituted by an up to 10 m thick gravelly unit, deposited after 19.5 ka cal BP. This deposit is capped by an organic-rich layer with an age ranging from ca. 9.5 to 6.5 ka cal BP. The second phase can be linked to the Holocene marine transgression, which led to the formation of a lagoon environment within the incised valley and the consequent deposition of an up to 15 m thick unit of lagoon muds. The absence of estuarine facies or evident riverine inputs suggests an upstream diversion of the paleo Tagliamento River. Therefore, the incised valley acted as a tidal-influenced liman characterized by a freshwater supply provided by spring-fed rivers, groundwater seepage and runoff. The presence of some dated peat horizons within the lagoon deposits allowed to precisely reconstruct the timing of the valley infill. This work presents a rare example of a non-estuarine incised-valley fill, providing new data on the paleo environmental and geographic evolution of the Venetian-Friulian Plain area and on the Holocene transgression in the northern Adriatic Sea. Moreover, this study presents a rare example of infilling of an incised-valley in conditions of almost absent upstream sediment discharge, providing interesting information on the facies and architecture of the infilling.

Incised valleys have been thoroughly investigated through a wealth of papers in the last 30 years (e.g. Thomas and Anderson, 1989, 1994; Dalrymple et al., 1992; Zaitlin et al. 1990; Posamentier and Allen, 1993; Allen et al., 1993; Blum and Törnqvist, 2000; Boyd et al., 2006; Blum et al., 2013). Quaternary incised-valley fills can provide important stratigraphic and paleoenvironment information, as they often preserve the only available stratigraphic record of an area (e.g. Vis and Kasse et al., 2009; Bogemans et al., 2016; Simms et al., 2010; Clement and Fuller., 2018). These features gain value also in the light of the source-to-sink studies, especially linked to the evaluation of sediment budgets transported through the bypass zone (e.g. Blum et al., 2013, Mattheus and Rodrigues, 2011; Bhattacharya et al., 2015).

Excluding the formation of localized fluvial incisions as a consequence of the confluence of different river branches (Best and Ashworth, 1997; Gibling et al., 2011) or due to fluctuation in the water or sediment discharge, the most accepted and widespread paradigm for explaining the formation of an incised valleys is the lowering of base level, which is normally associated to tectonics, river capture or eustatism (Schumm, 1993).

This latter condition is common in the Quaternary geological record due to the periodic and ample fluctuations that characterized the sea level. As a matter of fact, several incised valleys are scattered on the marine shelves and coastal plains of the entire world (e.g. Blum and Törnqvist, 2000; Lin et al., 2005; Nordfjord et al., 2005, 2006; Mattheus et al., 2007; Ngueutchoua and Giresse, 2010; Tanabe et al., 2010, 2013; Mattheus and Rodrigues, 2011; Green et al., 2013; Blum et al., 2013) as witnesses of the sea level drop and lowstand associated to the Last Glacial Maximum (LGM). Most of these valleys were then infilled in the interplay between continental and marine processes that took place during the successive post-LGM marine transgression, therefore losing their morphologic expression (e.g. Maselli and Trincardi, 2013, Maselli et al., 2014; Martínez-Carreño and, García-Gil, 2017), or becoming estuaries or rias/limans (e.g. Simms et al., 2010; Traini et al., 2013).

Some notable examples of incised valleys formed as a consequence of the marine lowstand occurred during the LGM can be found along European coasts (e.g. Danish North Sea: Huuse and Lykke-Andersen, 2000; Dutch coast: Peeters et al., 2016; Belgian coast: Bogemans et al., 2016; De Clercq et al., 2018;

French coasts: Lericolais et al. 1998, 2001; Chaumillon et al., 2008, 2011; Labaune et al., 2010; Estournès et al., 2012; Gregoire et al., 2017; English Channel: Lericolais et al., 2003; Chaumillon et al., 2010; Gibbard et al., 2017; Iberian Peninsula: Vis and Kasse et al., 2009) and more specifically along the Italian coasts (Biferno: Amorosi et al., 2016; Lesina: Longhitano et al., 2015; Manfredonia: Maselli and Trincardi, 2013, Maselli et al., 2014; Metaponto: Tropeano et al., 2013; Volturno: Amorosi et al., 2012; Tuscany: Amorosi et al., 2009, 2013a, Breda et al., 2016).

In contrast with this global trend, along the western side of the northern Adriatic Sea, in the distal sector of the modern Venetian-Friulian Plain, important incised fluvial valleys formed only during the post-LGM transgression, between Late Glacial and Early Holocene (Fontana et al., 2008, 2014a). In particular, these fluvial incisions have been documented in the alluvial megafans of Brenta (Mozzi et al., 2013), Piave (Carton et al., 2009), Tagliamento (Fontana, 2006; Fontana et al., 2004, 2010, 2014a) and Isonzo rivers (Arnaud-Fassetta, 2003). Several researches documented the fluvial incisions formed by Tagliamento River, between its present course and Livenza River (Figs. 2.1 and 2.2). Among these features, the most investigated is represented by the so-called incised valley of Concordia, after the name of the important Roman city of *Julia Concordia* that was settled on an isolated terrace in the middle of the valley (Fontana et al., 2004; Fontana, 2006). The evolution of this fluvial incision and its infilling stratigraphy constitute a reference for the entire Venetian-Friulian Plain for detecting major erosive and aggradation phases that occurred on the megafans along southern Alps after the LGM (Fontana et al., 2010, 2014a). Nevertheless, the available reconstructions are based on a single stratigraphic section, perpendicular to the incision in the area of Concordia Sagittaria (cf. section 2.2), while some other scattered subsoil data allowed to follow the main planform of the incised valley (Fontana, 2006; Fontana et al., 2004, 2008, 2012). In this work we used a very large database of about 2 200 new cores in order to describe with a good resolution the buried morphology of the incised fluvial valley and the architecture and sedimentary facies of its infilling. This work aims to recognizing the different phases that characterized the evolution of the valley and the possible connections with regional and global processes.
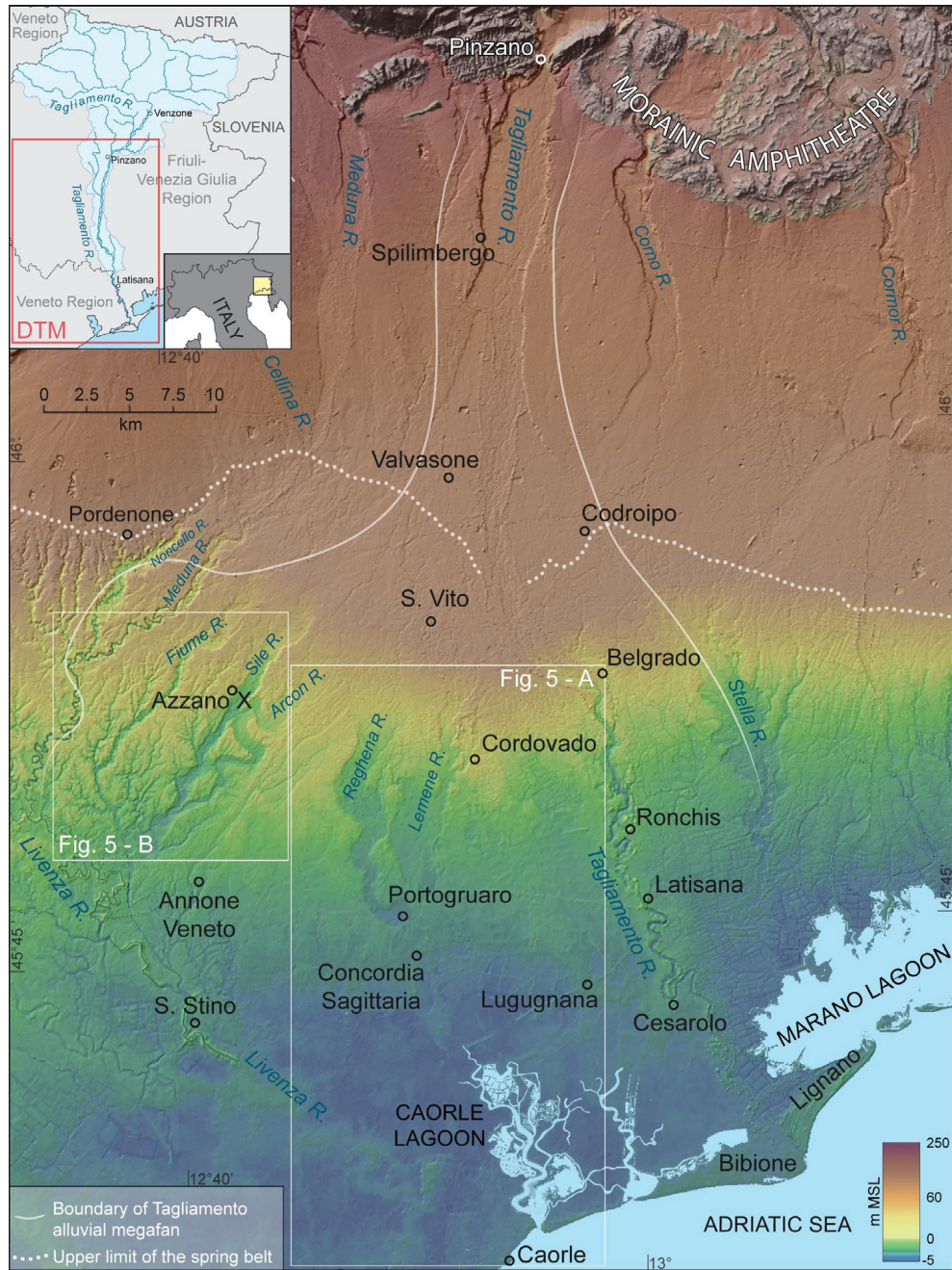
Figure 2.1: DTM of the Tagliamento Megafan and position of the principal localities in the study area. The inset shows the drainage basin of the modern Tagliamento River. Modified from Surian and Fontana, (2017).

This research considers part of the distal portion of the alluvial megafan of Tagliamento River. This geographic region represents the eastern continuation of the Venetian Plain and has been formed by the rivers draining the Carnic and Julian Alps. From a tectonic point of view, this sector of the alluvial plain is characterized by the interplay between the Alpine south-verging thrust and fold belt and the NW-SE thrust belt of the Dinaric Alps (Zanferrari et al., 2008a) The main active tectonic thrust runs along the mountain front and can generate important earthquakes, as the events of 1976, with Mw 6.5 (Burrato et al., 2008). Minor active faults are documented in the apical portion of the plain, where some tectonic terraces deform the late-Quaternary deposits, as near Udine and Pozzuolo (Galadini et al., 2005; Monegato and Poli., 2015). A long-term subsidence is affecting the coastal plain, with an average value of 0.4 mm/a recorded between Tagliamento and Piave rivers (Carminati et al., 2003; Antonioli et al., 2009).

The Tagliamento is the main river of the Friulian Plain and it has a mountain catchment of $2\,700$ km^2 (Fig. 2.1), with an annual average discharge of about 90 m^3/s and a peak flood of $4\,500$ m^3/s for a recurrence time of 100 years (Surian and Fontana, 2017). For most part of its length along the plain, up to Ronchis (Fig. 2.2), the river displays a braided morphology. This reach of the Tagliamento is considered a reference for the dynamics of gravelly-bed streams (Tockner et al., 2003; Surian et al., 2009). Moving downstream, the fluvial style shifts to a classical meandering typology. The gravels of Tagliamento consist of carbonate rocks (limestones and dolostones) for over 70%, but the mountain catchment is also marked by the presence of siliciclastic formations of Paleozoic and Triassic age (Venturini 2003; Carulli et al., 2011). The presence of gravels in the modern bedload gradually decreases moving downstream and it gets null between Latisana and Ronchis. This sector corresponds also to the most landward limit of tide influence, which along the coast has an amplitude of about 1 m (Fontana, 2006). The stratigraphy of the study area is formed by Late-Quaternary alluvial sediments alternated to lagoon, deltaic and marine deposits in the distal sector of the plain (Fontana et al., 2010). Between the depths of -35 and -55 m Mean Sea Level (MSL) the marine-related deposits formed during the last interglacial (i.e. MIS 5.5: $132-116$ ka cal BP; Antonioli et al., 2009) can be found. This ancient coastal unit is covered by $5-10$ m
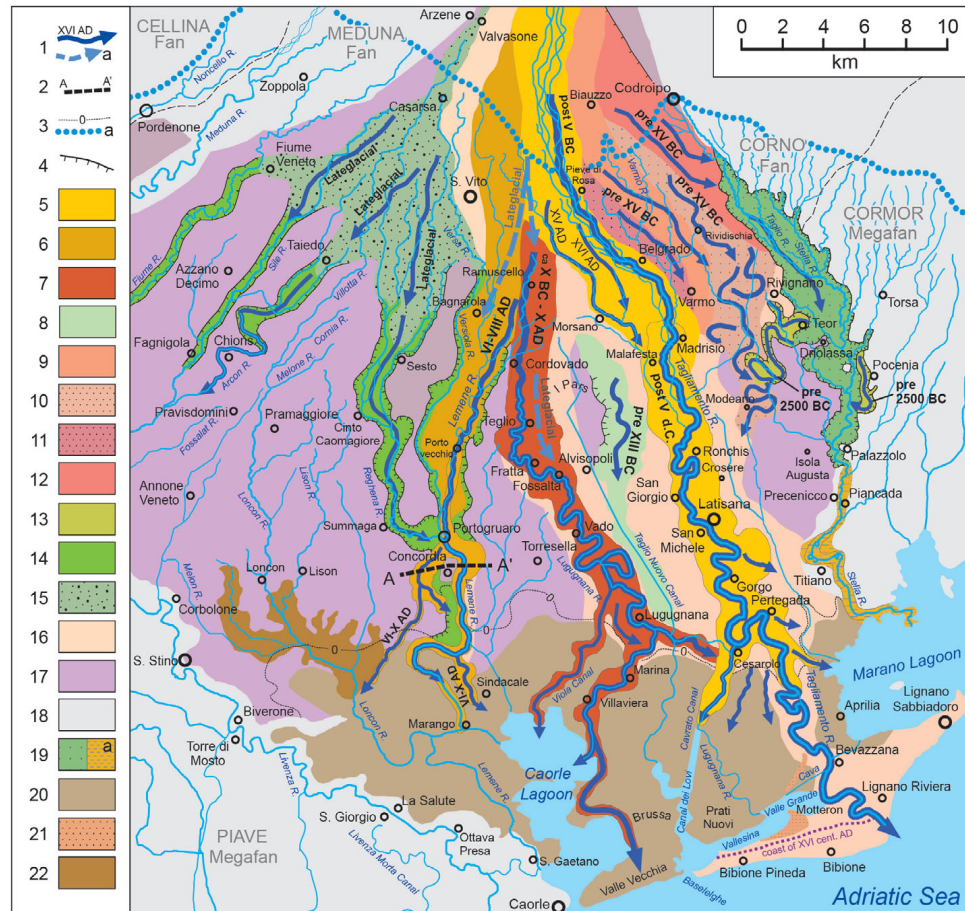
Figure 2.2: Simplified scheme of the Tagliamento River evolution during post-LGM (last 17 ka), modified after Fontana (2006). Legend: (1) channel belt, with indication of the period of activity, (1a) buried channel belt, (2) trace of stratigraphic section in Fig. 2.3, (3) isoline 0 m MSL, (3a) upper limit of the spring belt, (4) fluvial scarp, (5) present Tagliamento unit $< 6^{th}$ century AD, (6) Concordia Sagittaria unit $< 6^{th} - 8^{th}$ century AD, (7) unit of *Tiliaventum Maius* active in Roman period 1st millennium BC$- < 8^{th}$ century AD, (8) Alvisopoli unit > 3.3 ka BP, (9) Glaunicco-Varmo unit > 3.0 ka BP, (10) Rividischia unit > 3.5 ka BP, (11) San Vidotto unit > 3.5 ka BP, (12) Iutizzo unit > 3.5 ka BP, (13) Campomolle and Pocenia units > 4.5 ka BP, (14) Lateglacial units, (15) Lateglacial valleys now reoccupied by groundwater-fed streams, (16) undifferentiated post-LGM deposits, (17) LGM deposits, (18) deposits of other fluvial systems, (19) incision of Stella River, remodeled by Tagliamento between $4.5 - 2.8$ ka BP, (19a) deposits of Stella River with input from Tagliamento River < 4.5 ka BP, (20) Holocene lagoon deposits, (21) pre-Roman coastal sand ridges, (22) swamp of Loncon.

of alluvial silts and sands, mainly deposited during MIS 4 and part of MIS 3, that are often capped by a thick layer of peat (from 1 to 3 m), which top has an age of about 30 ka cal BP (Fontana et al., 2010; Hippe et al., 2018). The main unit recognizable in the upper stratigraphy of the Friulian plain consists of 20 to 35 m of alluvial deposits related to the alluvial megafans and fans that still characterize the landscape of large portion of the area (Fontana et al., 2008). These large alluvial landforms mainly formed during the Last Glacial Maximum (LGM, $29 - 19$ ka cal BP; Clark et al., 2009), when the glaciers hosted in the Alps reached the plain (Castiglioni, 2004) and the level of Adriatic was over 120 m lower than the present (Moscon, 2016; Pellegrini et al., 2017). The megafan of Tagliamento extends from the valley outlet, near Pinzano, to the coastal plain (Fig. 2.1), where it has been later drowned by the Adriatic and partly buried by post-LGM deposits. This megafan formed when the Tagliamento was one of the major outwashes of the glacier host in the mountain catchment (Monegato et al., 2007). At that time the river used to transport the gravels up to $15 - 25$ km from the glacial front, while only silts, clays and sands reached the distal sector of the megafan. This lithological distinction generated the important difference between the apical portion, that is gravelly, and the distal one, that is dominated by fine sediments (Fontana et al., 2008). In particular, the boundary between coarse (permeable) and fine sediments (impermeable) corresponds to the upper limit of the spring line (Fig. 2.2), where part of the groundwater is forced to the surface and feeds a dense network of minor streams. These are called groundwater-fed rivers, which are characterized by a rather stable water discharge along the year and almost no sedimentary load, as they originate in the middle of the plain by spring waters (Feruglio, 1925; Comel, 1950; Minelli et al., 2001; Fontana et al., 2014a). The peak of LGM was reached at $24 - 22.5$ ka BP Monegato et al., 2017) while, soon after, between 22.0 and 19.5 ka cal BP, the glacier of Tagliamento started to withdraw, abandoning its terminal morainic amphitheater (Fontana et al., 2014b). At that time, the Tagliamento River started to incise the apical portion of its megafan, entrenching for about 15 m from the top of LGM deposits (Monegato et al., 2007). The fluvial incision is limited by scarps that are up to 70 m high near Pinzano, but this value gradually decreases downstream and eventually becomes null near Codroipo (Fig. 2.1). While dissecting the megafan apex, the river was still aggrading on the distal sector of the megafan along some narrow fluvial ridges, which were characterized by

gravelly sandy channels and sandy loamy natural levees (Fontana et al., 2014b). The sedimentary unit deposited during this phase can be easily distinguished in the distal portion of the megafan from the older fine-grained deposits of the LGM peak. These two units correspond respectively to the *Remanzacco* subsynthem and the *Canodusso* synthem described in the recent geological maps of the area (Zanferrari et al., 2008a,b; Fontana et al., 2012). Where preserved, the surface of the LGM plain is marked by a rather well-developed and overconsolidated soil, locally named *caranto*, which is characterized by the occurrence of a calcic horizon (Bk/Ck) with centimetric carbonate concretions and widespread mottling (e.g. Mozzi et al., 2003; Fontana et al., 2014b and reference therein).

The surface of the distal sector of the megafan is characterized by the presence of several fluvial scarps starting from the lower limit of the spring line and arranged into a divergent pattern (#15 and 14 in Fig. 2.2; inset B in Fig. 2.4). These scarps coincide with the major groundwater-fed streams of the area (Stella, Lemene, Reghena, Sile, Arcon and Fiume Rivers; cf. Comel, 1950, 1958; Fontana, 2006; Fontana et al., 2014a). The investigation of the area allowed to recognize some incised valleys that are now completely filled and buried below the subsurface of the Friulian Plain. In particular, one of these paleo valleys has been recognized below the I millennium BC - early Middle Age course of the Tagliamento River (*Tiliaventum Maius*, # 7 in Fig. 2.2), another one is buried below the present course of Tagliamento, downstream of Morsano (#5 in Fig. 2.2) and finally a third valley, the Concordia incised valley (cf. Section 2.1), has a north-south direction and its position coincides with the present course of Lemene River (#6 in Fig. 2.2). This latter valley, already described in Fontana, (2006) and Fontana et al., (2008), was carved by the Tagliamento River within the LGM alluvial plain after 19.5 ka cal BP (Fig. 2.3). A sandy-gravelly channel unit was partly filling the bottom of the valley already during the Late Glacial and its deposition has been active until Early Holocene. Avulsion processes probably led to the deactivation of the Concordia and Reghena incisions in favour of an eastern branch of the Tagliamento River (#7 in Fig. 2.2; Fig. 2.3). The valley of Concordia was rapidly waterlogged and occupied by swampy environments that led the accumulation of up to 1.5 m of peat and organic sediments. Between 7.0 and 6.5 ka cal BP the valley was drowned by brackish waters, which occupied the entrenched areas up to Portogruaro and deposited a greenish-gray muddy unit
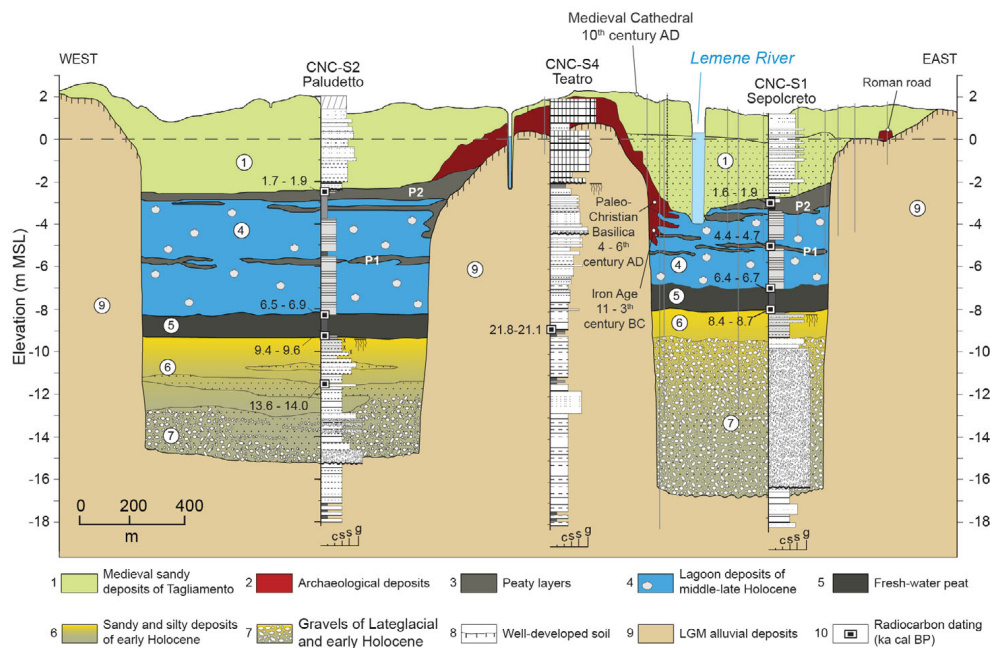
Figure 2.3: Reference cross section of the stratigraphic setting near Concordia Sagittaria (modified after Fontana, 2006, 2015). The location of the section is reported in Fig. 2.2.

characterized by the common occurrence of lagoon fossils and some lenses of peat (Fig. 2.3). This phase was triggered by the post-LGM marine transgression, which reached the present coast of north-western Adriatic around $8.5 - 7.5$ ka cal BP, when relative sea level was between -15 and -5 m MSL (Vacchi et al., 2016; Fontana et al., 2017), and led the lagoon to expand along the pre-existing low-lying areas (Amorosi et al., 2008). In the Venetian-Friulian Plain this process led to the formation of some lagoon branches that arrived from 10 to 20 km landwards than the inner limit of the lagoons and generated a landscape that partly reminds the liman coast of the Black Sea (Fontana, 2006).

The brackish and swampy environment characterized the valley of Concordia until the early Medieval, when an important avulsion phase led the Tagliamento to abandon the direction of the *Tiliaventum Maius* in favour of its present path. During this phase, between 6th and 8th century AD, the river used a temporary branch along the present Lemene River and sedimented a huge quantity of sediment that buried large sectors of the ancient city of *Julia Concordia* (Comel, 1958; Valle and Vercesi, 1996) and formed a remarkable

fluvial ridge which is visible from the highway A4 almost to the present lagoon (#5 in Fig. 2.2; Bondesan et al., 2005). The Lemene spring river is currently flowing along the residual channel that was abandoned by Tagliamento.

In the study area the human presence is documented since the phase between the end of Neolithic and the ancient Bronze Age (ca. $6.0 - 4.0$ ka cal BP) by some small sites located along the terraces of the incised valley south of Concordia (Fontana, 2006; Rossignoli et al., 2015; Fontana et al., 2018). An important phase of settlement started with the recent Bronze Age, when a major site was already existing on the terrace of Concordia and another was near S. Gaetano of Caorle (Fig. 2.2; Balista and Bianchin Citton, 1994; Bianchin Citton, 1996; Fontana et al., 2017). During the Iron Age Concordia flourished as an important city within the cultural group of the Veneti and since 42 BC it become a Roman Municipium. The city was strongly affected by the collapse of the Roman Empire and the Medieval floods of Tagliamento, which caused the migration of most part of the people to Caorle. But Concordia maintained a relative importance because its cathedral was the seat of the Bishop (Croce Da Villa and Di Filippo, 2003). A new developing period started in the area since the beginning of the 20th century, when large sectors of the Caorle Lagoon had been reclaimed and new villages were founded. Nowadays, between Tagliamento and Livenza rivers about 100 km^2 of agricultural land are placed below the sea-level and are drained thanks to the lagoon dykes and a complex network of ditches, canals and pumping stations (Bondesan et al., 2005; Fontana et al., 2004).

2.3 MATERIAL AND METHODS

Lidar DTM

The surface morphology of the study area was investigated analysing the Digital Terrain Model (DTM) obtained by airborne Laser altimetry (LiDAR: Fig. 2.4). For the Veneto Region, these topographic data have been acquired by the Italian Ministry of the Environment (*Extraordinary Plan of Environmental Remote Sensing*, PST-A; PST-A Extension 2008), with a cell size of 1 m^2 and a vertical accuracy of ± 0.10 m (http://wms.pcn.minambiente.it/). In the Regione Autonoma Friuli Venezia Giulia the LiDAR data were collected in 2006 by the regional department of Civil Protection. The final DTM is characterized by a cell size of 1 m^2 and a vertical accuracy of ± 0.15 m (www.irdat.fvg.it). The

DTM presented in this work was obtained not considering the vegetation cover and by filtering the data to eliminate the buildings, while several anthropogenic topographic break lines, as roads and dykes, are still visible (Fig. 2.4).

Stratigraphic data

This work is based on the analysis of two wide datasets of stratigraphic cores (Fig. 2.5). A first database of ca. 500 cores and ca. 70 geotechnical in-situ tests was provided by the Cittá Metropolitana di Venezia (Servizio Geologia, Difesa del Suolo e Tutela del Territorio). This dataset is constituted by the log description of all the cores and by the CPT results collected in the area during the last 40 years. All these data were acquired mostly for geotechnical purposes, and they are usually randomly scattered all over the area. The cores of this dataset reached an investigation depth ranging from 6 to 70 m. The available logs are not always accurate, and the descriptions are sometimes too generic to be used, but they nevertheless proved to be useful in discriminating among the major sedimentary units identified in the subsurface through more accurate stratigraphic logs. A second database was acquired by the Physical Geography Department of the Utrecht University (The Netherlands) in collaboration with the University of Padova (Italy). This dataset has been collected between 2013 and 2018, during a series of didactic fieldworks held in the area of the Venetian-Friulian Plain (Fig. 2.5). These cores were collected and described by different generations of students under the supervision of teaching staff. The coring equipment consisted of Edelman and gouge hand augers, respectively for sampling above and below groundwater, and Van der Staay suction corers for coring through sand deposits (Vis et al., 2015). This equipment allowed to reach a mean investigation depth of ca. 5 m, with a maximum reached depth of 19 m. Unlike the previous dataset, these cores are thoroughly described every ten centimetres for the texture of the deposit, the colour, the carbonate content (tested via reaction to 1 M HCl), the fossil content (brackish/fresh water species, with sometimes the precise indication of the genus), the plant remains (e.g. phragmites, wood) and the type of organic deposit (peat, gyttja). The texture of the sediments was determined in the field according with the USDA classification (cf. Thien, 1979; FAO-ISRIC, 2006), which allows to assess the content of clay, silt and sand by feeling the flexibility, stickiness and roughness of the wet sediments. The grain size of sands (size $>63~\mu$m) was directly measured through the comparison with a sand ruler.

#	Lab code	Core	Lat N	Lon E	Stratigraphic position	Height (m)	Sample depth (m)	^{14}C age (a BP)	Calibrated 2σ age (a BP)	Mediane (a BP)	Source
0	Beta-173013	CNC-S1	45.757	12.853	P2*	1.1	4.00	1800 ± 70	1563 - 1875	1727	Fontana (2006)
1	Beta-184247	CNC-S1	45.757	12.853	P1*	1.1	6.18	4080 ± 70	4424 - 4729	4601	Fontana (2006)
2	Beta-184248	CNC-S1	45.757	12.853	U2*/U3	1.1	8.10	5700 ± 70	6390 - 6656	6494	Fontana (2006)
3	Ua-24872	CNC-S1	45.757	12.853	U1/*U2	1.1	9.26	7785 ± 65	8415 - 8727	8563	Fontana (2006)
4	Beta-184249	CNC-S2	45.756	12.829	P2*	1.6	5.54	1920 ± 60	1717 - 1992	1864	Fontana (2006)
5	Beta-184250	CNC-S2	45.756	12.829	U2*/U3	1.6	10.38	5910 ± 70	6553 - 6913	6736	Fontana (2006)
6	Ua-24054	CNC-S2	45.756	12.829	U1*	1.6	13.54	11960 ± 95	13567 - 14049	13810	Fontana (2006)
7	Ua-24055	CNC-S2	45.756	12.829	U1/*U2	1.6	11.13	8515 ± 65	9405 - 9604	9507	Fontana (2006)
8	Beta-184251	CNC-S3	45.652	12.894	U2*/U3	-1.4	7.19	6080 ± 80	6747 - 7164	6952	Fontana (2006)
9	Ua-24053	CNC-S4	45.756	12.451	LGM*	2.2	11.07	18055 ± 175	21420 - 22343	21878	Fontana (2006)
10	Ua-24052	CNC-S4	45.756	12.451	LGM*	2.2	29.31	24275 ± 375	27663 - 29046	28321	Fontana (2006)
11	Beta-184395	CNC6493400	45.763	12.849	P2*	1	4.00	1910 ± 80	1690 - 2041	1851	Fontana (2006)
12	LTL4967A	CNC-Alte	45.759	12.834	P1*	1.7	4.30	3998 ± 45	4382 - 4581	4477	Fontana (2006)
13	Ua-24876	Rocca2	45.647	12.928	LGM/*U2	0.3	5.45	5730 ± 45	6432 - 6638	6527	Fontana (2006)
14	Ua-24056	SUM1	45.794	12.797	LGM*	5.2	1.85	15565 ± 175	18445 - 19234	18825	Fontana (2006)
15	ETH-87035	UU-170624	45.706	12.851	U2*/U3	-0.2	14.80	7006 ± 30	7784 - 7934	7850	This work
16	ETH-87036	UU-170624	45.706	12.851	U1/*U2	-0.2	15.50	8064 ± 28	8972 - 9032	9003	This work

Table 2.1: Radiocarbon dates available in the area. The location of the samples is provided in Fig. 2.5. All the dates were obtained from peat samples. THe stratigraphic position should be interpreted as follows: * represents the position of the sample, / represent the stratigraphic contact between two units (if it is missing the sample was not close to a boundary), the name of the units are the same of section 2.4; for instance, U2*/U3 represents a sample from the basal peat near the boundary with the overlying lagoon deposits.

In particular about 1 500 cores, collected with a pace of ca. 100 m or less, are available in the study area. These cores were realized along transects accurately planned in order to acquire the stratigraphy of key points for the reconstruction of the subsurface. Therefore, most of the work here presented is based on this latter dataset. All the available data were stored and analysed in a GIS environment.

A series of 16 radiocarbon dates were used for constraining the evolution of the reconstructed features (Tab. 2.1). All the values are calibrated with IntCal 13 calibration curve by Reimer et al. (2013).

Subsurface reconstruction

The reconstruction of the stratigraphy of the subsurface was operated through the realization and interpretation of a series of transects (cf. section 2.4) performed by manually correlating the different deposits described in the logs.
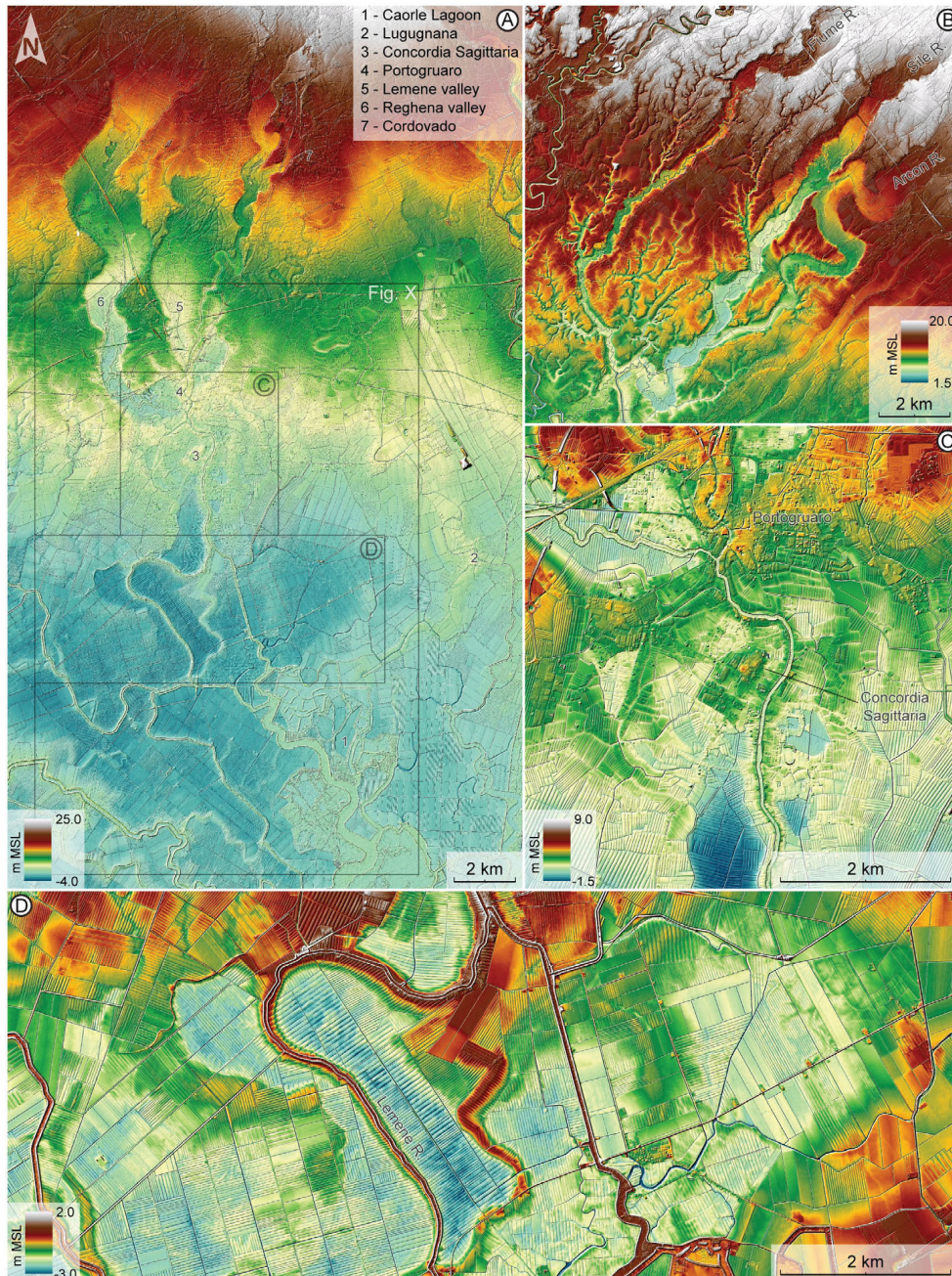
Figure 2.4: Lidar DTM of the study area
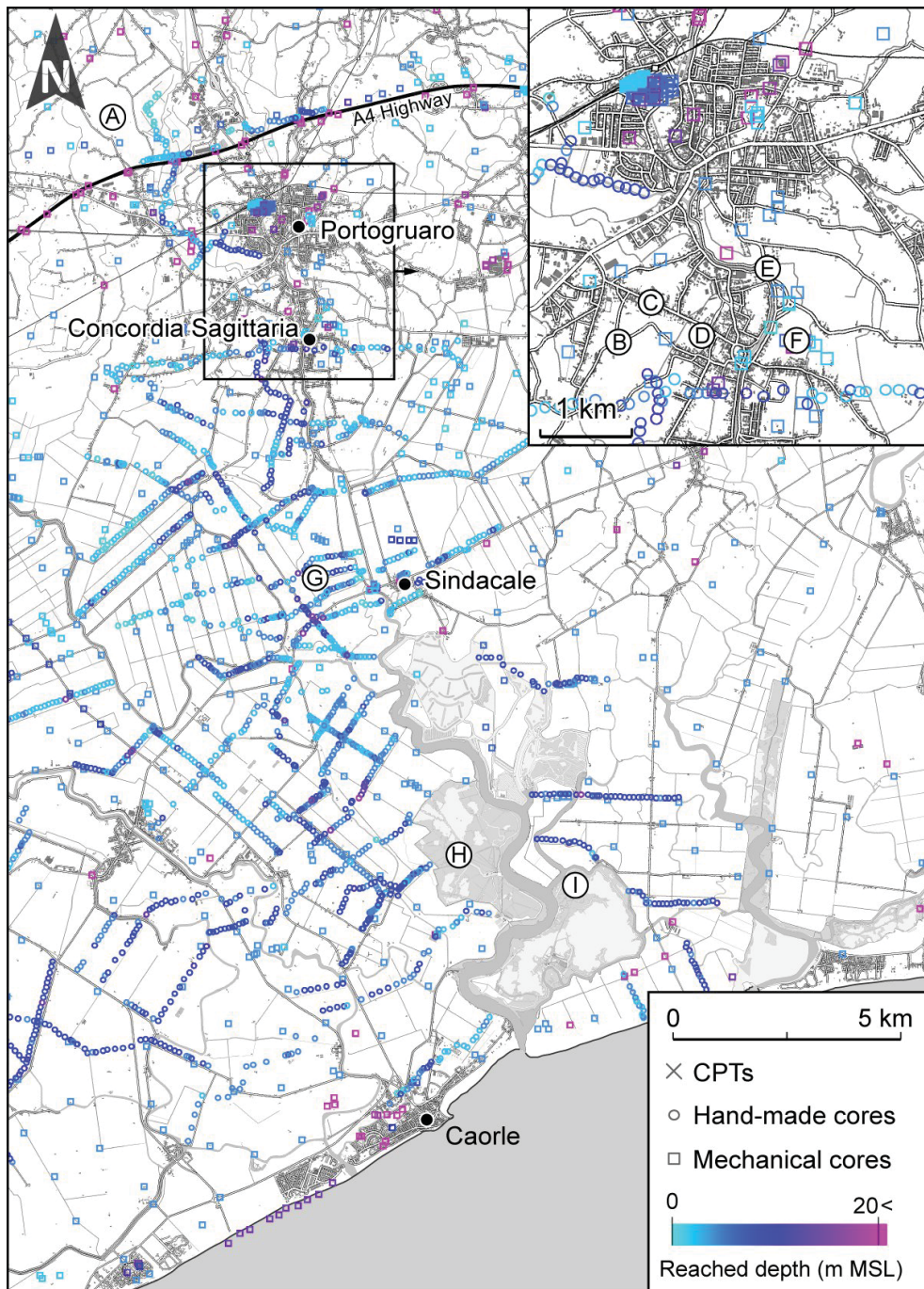
Figure 2.5: Location of the cores, CPT tests considered in this work. Location of the cores with dated samples: (A) SUM1; (B) CNC-S2; (C) CNC-Alte; (D) CNC-S4; (E) CNC6493400; (F) CNC-S1; (G) UU-170624 ; (H) CNC-S3; (I) Rocca2. The location of the area is reported in Fig. 2.1.

Furthermore, a 3D reconstruction of the main discontinuity recognizable in the subsurface (i.e. the top of the Pleistocene megafan) was operated in a GIS environment. A thorough revision of all the available stratigraphic logs and CPT results, along with the available surveys published in the literature (e.g. Fontana, 2006, Fontana et al., 2012), has been necessary for the estimation of the depth of the Pleistocene deposits. The data gather through this preliminary work was then stored into a GIS database. In particular, the spatial distribution and the relationships among the different recognized sedimentary units were considered in order to validate our interpretation. Only the information provided by trusted cores were used in this work, in order to obtain the highest possible reliability. Cores with uncertain interpretation due to an imprecise or ambiguous logging were therefore avoided in the reconstruction. The lengths of the cores that did not reach the top of the Pleistocene deposits have been used as limiting points. All the collected Pleistocene elevation data, which were originally measured from the ground level, were then converted into absolute MSL values using the LiDAR DTM of the area. Furthermore, a series of contour lines were manually drawn following all the depths and limiting points collected for this work, thus allowing to constrain the interpolating algorithm through a geologically-reasoned framework.

The interpolation has been performed with the *Topo to Raster* tool provided by ArcGIS software. Given the amount of available data this tool was set for not considering any sinks and not trying to build any runoff pattern, in order to avoid artifacts and produce a reconstruction based only on real data.

2.4 RESULTS

Facies and geometries of the main stratigraphic units

In this paragraph we illustrate the stratigraphic units that constitute the flanks of the incised valley of Concordia and those forming its infill. The units are here reported from the older to the younger, in agreement with the stratigraphy of the area described in the recent technical literature and reported in the previous section (Bondesan et al., 2008; Fontana et al., 2008, 2012, 2014a).

LGM ALLUVIAL PLAIN (LGM) The valley of Concordia was carved in pre-existing deposits that are mainly constituted by decimetric layers of silt and clayey silt, sometimes alternated with lenses of fine sands and silty sands,

that can be characterized by planar or cross lamination. Organic and peaty horizons, up to 30 cm thick, can be occasionally found and they often show a large lateral continuity. The pollen analysis of some of these layers documented a cold steppe-like environment characterized by the formation of large peat fens due to the occurrence of waterlogged soils (cf. Miola et al., 2006; Fontana et al., 2008, 2012). The paleontological content of this unit is scarce and constituted by continental gastropods, for instance the genera *Planorbis* and *Cingolum* (Fontana et al., 2012). The sediments have gley colours and they are generally grey/bluish grey. Where preserved, the top portion of the unit is characterized by a well-developed stiff soil (*caranto*) with brownish colours spanning from 2.5Y to 10YR. This soil is marked also by the occurrence of carbonate-rich horizons with pluricentimetric concretions.

The mechanical core CNC-S4 (Fig. 2.5 for location) sampled at a depth of ca. 11 m a peat horizon of 20 cm of thickness, whose top was radiocarbon dated to $21.4 - 22.3$ ka cal BP (#9 in Tab. 2.1). In the same core, the organic layer found at a depth between 36 and 39 m below surface is dated at 30 ka cal BP and dates the base of the LGM unit (#10 in Tab. 2.1; Fontana et al., 2012). In the area of the A4 highway (Fig. 2.5) the LGM alluvial plain is cropping out and a peat sample collected at 1.85 m from surface has a radiocarbon age of $18.4 - 19.2$ ka cal BP (#15 in Tab. 2.1; Fontana, 2006, Fontana et al., 2012).

LATE GLACIAL FLUVIAL CHANNEL DEPOSITS (U1)   The lowermost unit recognizable within the incised valley is constituted by sandy-gravels and gravelly-sands, with rare sandy and silty horizons (Fig. 2.6-F) that are separated by the LGM alluvial plain by an erosive unconformity. The gravels are well-rounded and characterized by a maximum diametre that spans between 7 cm north of Portogruaro down to $2 - 3$ cm near the city of Concordia. The petrographic composition is typical of the Tagliamento catchment and is dominated by carbonate lithologies.

The fluvial gravels are generally capped by a subunit, represented by fine-grained deposits with a sandy to silty grain size, which can have a thickness from 1 to over 3 m and is often characterized at the top by the presence of rare centimetric carbonate concretions (#6 in Fig. 2.3). Due to its stiffness, most of the manual cores could not sample more than few decimetres of this unit, therefore most part of the information about the sedimentology is provided

56
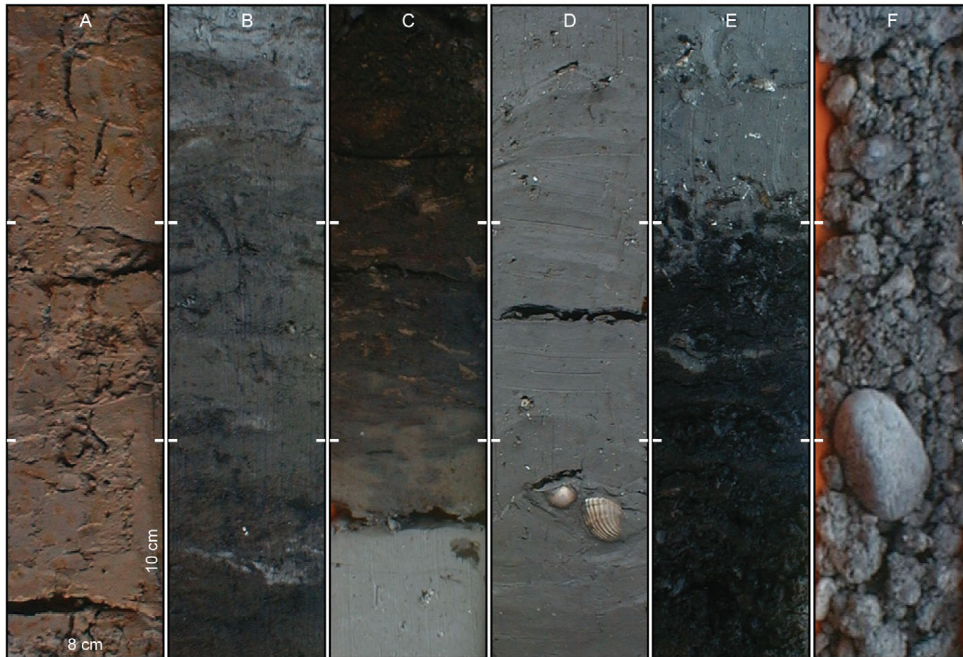
Figure 2.6: Core samples of the main units described in section 2.4. (A) Early Medieval sandy silts; (B) Top of the organic horizon P2; (C) Base of the peat horizon P1 and contact with lagoon deposits; (D) Lagoon deposits; (E) Contact between the top of the basal peat and the lagoon deposits; (F) Sandy gravels of the channel deposits dating to Late Glacial and Early Holocene in core CNC1.

by scattered deep mechanical cores. The samples available for this unit are barren of paleontological remains. The Late Glacial geochronological age of this sample is corroborated also by its pollen analysis, which recognized the strong domination of Pinus and the secondary occurrence of *Betula, Juniperus, Salix* and *Artemisia*, documenting the presence in the surrounding plain of a coniferous forest (Favaretto and Sostizzo, 2006). In the Friulian Plain this was typical in the period between the end of the LGM and the beginning of the Holocene (cf. Donegana et al., 2005; Pini et al., 2010). In core CNC-S2 (location in Fig. 2.5), west of the center of Concordia Sagittaria, a date obtained on an organic sample recovered from the contact between the gravel deposits and the overlying fine-grained plug deposits gave an age of $13.5 - 14.0$ a cal BP (#6 in Tab. 2.1).

The Late Glacial gravelly deposits outcrop slightly north of the A4 highway (Fig. 2.5), while they gradually deepens downstream and are covered by younger units. In the area of Concordia, the top of this unit can be found

between -8.5 and -9.5 m MSL. Further downstream this unit was intercepted at ca. -18 m MSL (cf. paragraph 4.2). This body has a thickness of $4-6$ m north of Portogruaro and reaches a thickness of ca. 10 m in the area of Concordia. In the southern portion of the study area the stratigraphic data only reached the top of the gravelly deposits, while there are no available data to constrain the thickness of this unit. The gradient of the top of this deposit, as inferred from the available depth values, can be estimated to vary from 1.5 to 0.3‰. It is worth noting that the gravels which constitute this unit are markedly coarser than the gravels that can be found on the LGM surface (*Remanzacco* subynthem), thus, allowing to clearly distinguish the two units.

BASAL PEAT - (U2)   The deposits of unit 1 are covered by an organic-rich layer that has been documented along the whole extent of the valley. This layer is characterized by a variable thickness and can reach a maximum value of ca. 1.5 m (#5 in Fig. 2.3). This organic layer is mainly constituted by black peaty deposits that are very stiff and are often characterized by millimetric evident laminations and the presence of plant macroremains as pieces of wood and roots (Fig. 2.6-E).

The top of this unit has been intercepted at different depths, from the ca. -9 m MSL, near Concordia, to more than -18 m MSL moving southward (cf. paragraph 4.2). The pollen content of BP was analysed in detail in core CNC-S2, documenting the progressive increase of *Quercus, Corylus, Tilia, Ulmus, Vitis, Rosaceae, Alnus, Salix* and *Fraxinus excelsior*, with the related decrease of *Pinus* and *Juniperus* (Favaretto and Sostizzo, 2006). The plant macroremains documents a local swampy environments waterlogged by freshwaters and only in the upper centimetre of the BP some influences of brackish waters are suggested (Favaretto and Sostizzo, 2006). The geochronology of this unit is constrained by eight radiocarbon dates spanning from ca. 9.5 to ca. 8.0 ka cal BP at the bottom (#3, 7, 17 in Tab. 2.1) and between cq. 7.5 and 6.5 ka cal BP at the top (#2, 5, 8, 14, 16 in Tab. 2.1). In some areas south of Concordia, this layer occasionally shows a detritus gyttja facies, characterized by typical laminations and pinkish/reddish colour (Fontana et al., 2017).

LAGOON DEPOSITS (U3)   A very-soft silty and clayey deposit, usually characterized by a rather homogeneous light grey and greenish colour (2.5Y 6/1-4/2; Fig. 2.6-D), lay on top of U2. A typical lagoon fossil assemblage, mainly consisting of fragments and preserved shells of *Cerastoderma glaucum, Loripes*

lacteus, Bittium scabrum, Gibbula sp., Abra sp., Hydrobia sp. and, more rarely, by specimens of *Rissoa sp., Scobricularia plana, Cerithium sp., Nassarius sp.* and *Theodoxus fluviatilis*, commonly characterizes these sediments. This assemblage is typical of subtidal environments (cf. Pérès and Picard, 1964; Vacchi et al., 2016). The qualitative analyses carried out on foraminifera from core CNC-S1 (Figs. 2.3 and 2.5) documented the common presence of *Ammonia beccari tepida* in all the layers of the unit, while also *Ammonia perlucida, Elphidium gunteri, Haynesina germanica* can be present. Spiral fragments of agglutinans forams with organic cement are also rather diffused. These micropaleontologic evidence suggest a hyposaline lagoon environment (Bondesan et al., 2005; Asioli, pers. communication).

Plant remains can be rather common and they mainly correspond to fragments and parts of reeds (*Phragmites*), sometimes buried in vertical position and sometimes accumulated in organic horizons with decimetric thickness. Two horizons, P1 and P2, can be recognized in almost the entire valley infill. Sedimentary structures are usually not recognizable within this unit due to the intensive and pervasive bioturbation, sometimes recognizable by the clear presence of burrow marks. Only in few cases some sandy laminations can be found. In the pollen spectra recorded in core CNC2 (Fig. 2.3), this unit is strongly characterized by aquatic plants, but if this local component is excluded, the pollen spectra are dominated by *Quercus, Corylus, Tilia, Ulmus, Vitis, Rosaceae, Alnus, Fraxinus* and *Salix*, while other species as *Acer* and *Fagus* are also documented but they were absent in the previous units (Favaretto and Sostizzo, 2006).

According to the available stratigraphic data, the lagoon deposits are documented from the present coastal zone up to the center of Portogruaro, but they do not reach the A4 highway(2.5). In some areas, south of the city of Concordia, the unit 3 is cropping out at surface and was still in formation until the reclamation of the area performed in the 20 [th] century (Fontana et al., 2004). In this zone the surface has an elevation between 0 and -3 m MSL and the colour of the plowing horizon is light brownish (2.5Y 6/1-4/2), that gradually shift toward a homogeneous light gray in the lower part (Fig. 2.6-D). Where the unit 3 has been buried by younger units the top has elevations between -1.0 to -3.0 m MSL. The bottom of the unit is found at a depth ranging from 2 to 6 m of depth from surface (from -2 to -8 m MSL) in the area north of Concordia, and from 6 to 17 m of depth (from -8 to -19 m MSL)

south of it.

A series of radiocarbon dates obtained from organic samples collected in the basal and intercalated peat layers (previous and next paragraphs) provides several temporal constraints for the reconstruction of the depositional history of the infilling. The dates obtained from the top of the U2 layer suggests that the lagoon environment occupied the incised valley starting from ca. 7.8 ka cal BP in the southern portion of the valley (#16 in Tab. 2.1) and about 6.5 ka cal BP in the northern one (#2, 5 in Tab. 2.1). The cores highlighted the presence of extended bodies of relatively coarse-grained sediments within the muddy lagoon deposits. These bodies can be tracked in all the stratigraphic transects south of Concordia (cf. paragraph 4.2), thus suggesting a longitudinal continuity within the incised valley. In particular, this unit can be followed up to a minimum length of ca. 8 km. A variable depth, ranging from -1 to -5 m MSL, has been observed for the top of these deposits, whereas the lowest sample was recovered from a depth of ca. -11 m MSL. These deposits are mainly constituted by grey sands, but the percentage of mud increases northward. A fining upward trend (in some cases from ca. 400 to ca. 150 μm) and an overall fining trend moving landward (from ca. 300 to ca. 50 μm) are recognizable. This unit is typically characterized by the presence of a pervasive lamination, which can be constituted both by silty and clayey sediments or by thin layers of organic material deposited at regular intervals. The layering of the unit is marked also be the occasional occurrence of clay chips, sometimes clustered in centimetric horizons. The presence of fossils is rare and only sparse shell fragments of brackish water species can be recovered (e.g. *Abra sp., C. glaucum, L. lacteus*). Besides the main body, smaller and isolated patches characterized by the same sandy laminated facies can be found.

INTERCALATED PEAT LAYERS (HORIZONS P1 AND P2)   Some peaty layers can be identified within the lagoon deposits of unit 3. While most of them have only a local extension, two layers can be recognized almost along the entire length of the incised valleys. The older one, named P1 (Fig. 2.6-C), is intercalated to the lagoon deposits of unit 3, has a thickness between 0.10 and 0.7 m and its top is typically found at depths ranging between 2 to 4 m from surface (from -3 to -5 m MSL). The age of P1 is constrained by the radiocarbon analysis of the top of this horizon, which gave results between 4.8 and 4.3 ka cal BP (#1, 13 in Tab. 2.1). The upper widespread organic horizon,

named P2, lies on top of the lagoon deposits of unit 3 in the northern part of the valley of Concordia, almost up to the latitude of the village of Sindacale (location in Fig. 2.2). The top of this horizon has been radiocarbon dated in some places around the city of Concordia and the age is ca. 1.9 ka cal BP (#4, 12 in Tab. 2.1; Fig. 2.6-B).

A layer dating to late Bronze Age (#0, 4, 11 in Tab. 2.1) was detected below the P2 layer and it is covered by the Medieval alluvial deposits of Unit 4 (Bianchin Citton, 1996). A Roman necropolis found along the via Annia, used between 2th century BC and 5th century AD, rests on its top and it is partly intercalated to P2 (Fontana, 2015). Other archaeological remains dug in the LGM alluvial plain and dating between late Neolithic and early Bronze Age are sealed by P2 and in one location some pottery fragments of this chronological period have been documented where the horizon P1 is overlapping the western flank of the valley.

Besides these two main organic layers, several others similar horizons were recognized, but they are usually confined in small areas with no apparent longitudinal continuity. These layers have variable thicknesses, with some of them exceeding 1 m and other with a thickness of just few centimetre. This variability can be noticed also within the same layer.

MEDIEVAL FLUVIAL DEPOSITS (U4)   The younger organic horizon described in the previous paragraph (P2) is covered by silty and sandy sediments with a greyish-yellowish colour (2.5Y 4/2). In the northern part of the valley, these deposits generally form the present topographic surface and they constitute the typical convex landforms characterizing the area: natural levees, crevasse-splays and fluvial ridges (Figs. 2.2 and 2.4). In the area of Concordia Sagittaria, the deposits are rather coarser, with the occurrence of medium to fine sands often characterized by cross to planar bedding. The fossil remains are generally rare or absent and they consist of typical paludal assemblages of *Viviparus viviparus, Planorbis sp.* and *Helix pomatia*. The thickness of unit 4 is variable, up to 5 m near Concordia and less than 1 m out of the incised valley, where it onlapped and aggraded over the LGM alluvial plain. The soil formed on top of this unit is weakly developed (entisol, cf. Soil Survey Staff, 1999) and the diagnostic feature is the presence of common carbonate concretions with dimension of 1 to 5 mm (Fontana, 2006). In the study area the radiocarbon age of the top of unit 3 constrains the deposition of this unit after about 1.9 ka cal BP. The

chronology of this unit is furthermore confirmed by a series of archaeological layers, dating up to the second half of the 5th century AD (Valle and Vercesi, 1996; Fontana et al., 2004; Fontana, 2006), which are intercalated to these deposits. In the area of Cordovado (Fig. 2.2) some trunks included in the gravels of the paleochannel of the Tagliamento branch downstream passing through Concordia have been dated between $560 - 610$ AD, exactly matching with the flood reported in the chronicle of Paolo the Deacon (Frassine et al., 2014). The new data are in agreement with the previous hypothesis that the alluvial sediments were transported by the paleo Tagliamento River, which had one of his main channels active in this area between the 6th and 8th century A.D. (Fig. 2.2).

Cross sections descriptions

SECTION A - REGHENA RIVER VALLEY   This cross section is roughly oriented in a W-E direction and runs along the A4 Highway for about 1 km, perpendicular to the Reghena River (Fig. 2.7). The stratigraphic profile was reconstructed through 18 new hand-made cores, integrating these data with the information collected by mechanical cores and CPTs drilled along the highway and the major electric lines located 700 m north of the road (Fontana, 2006). The top of the Late Glacial fluvial gravels unit, which apparently has a maximum thickness of 3 m, displays a concave morphology, which may suggests a major deepening action of the river in the central sector of the valley. Considering the top of the LGM alluvial plain, the valley reaches a maximum depth of about 8 m (ca. -5.5 m MSL) and the Late Glacial gravels have a thickness up to $3 - 4$ m and a maximum diametre of 7 cm. Over the coarse basal unit filling the valley bottom, only silty and clayey deposits are present, with a thick peat deposit in the central portion of the infilling that is almost cropping out at surface. The occurrence of fresh-water fossils, mainly of the genus *Planorbis* and *Viviparus* can be from rare to rather common, while lagoon shells are completely absent, documenting the presence of alluvial and paludal facies.

SECTION B - LEMENE RIVER VALLEY   This section has a length of almost 2 km, is parallel to the Highway A4 and is perpendicular to the valley currently occupied by the Lemene River (Fig. 2.7). The stratigraphic profile has been reconstructed by the interpretation of 21 new hand-made cores and other 5 mechanical cores, which passed the lower erosive boundary of the valley
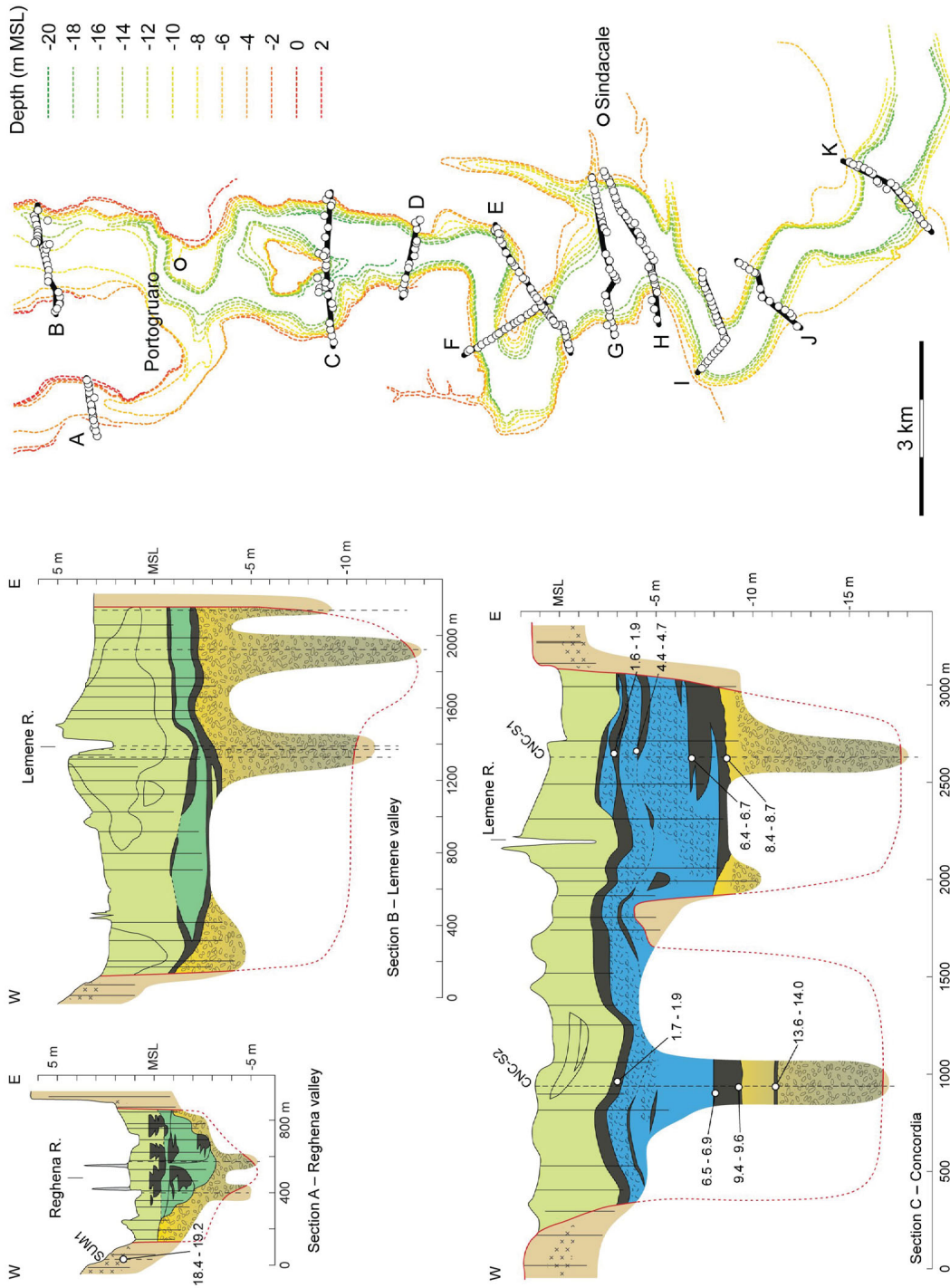
Figure 2.7: Compilation of cross sections available for the Concordia incised valley. Legend in Fig. 2.9. The descriptions are reported in section 2.4.

63
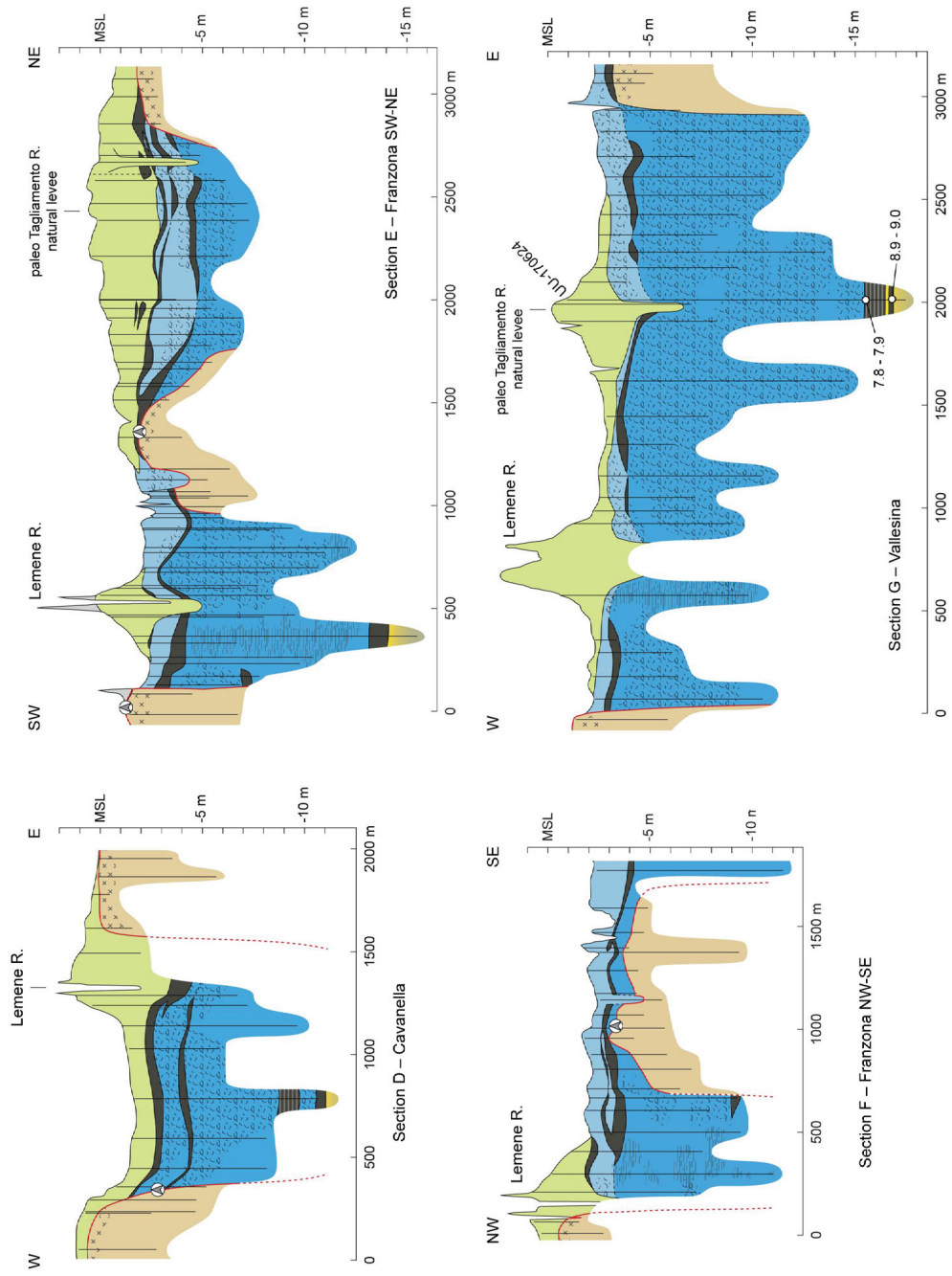
Figure 2.8: Compilation of cross sections available for the Concordia incised valley. Location in Fig. 2.7; Legend in Fig. 2.9. The descriptions are reported in section 2.4.

64
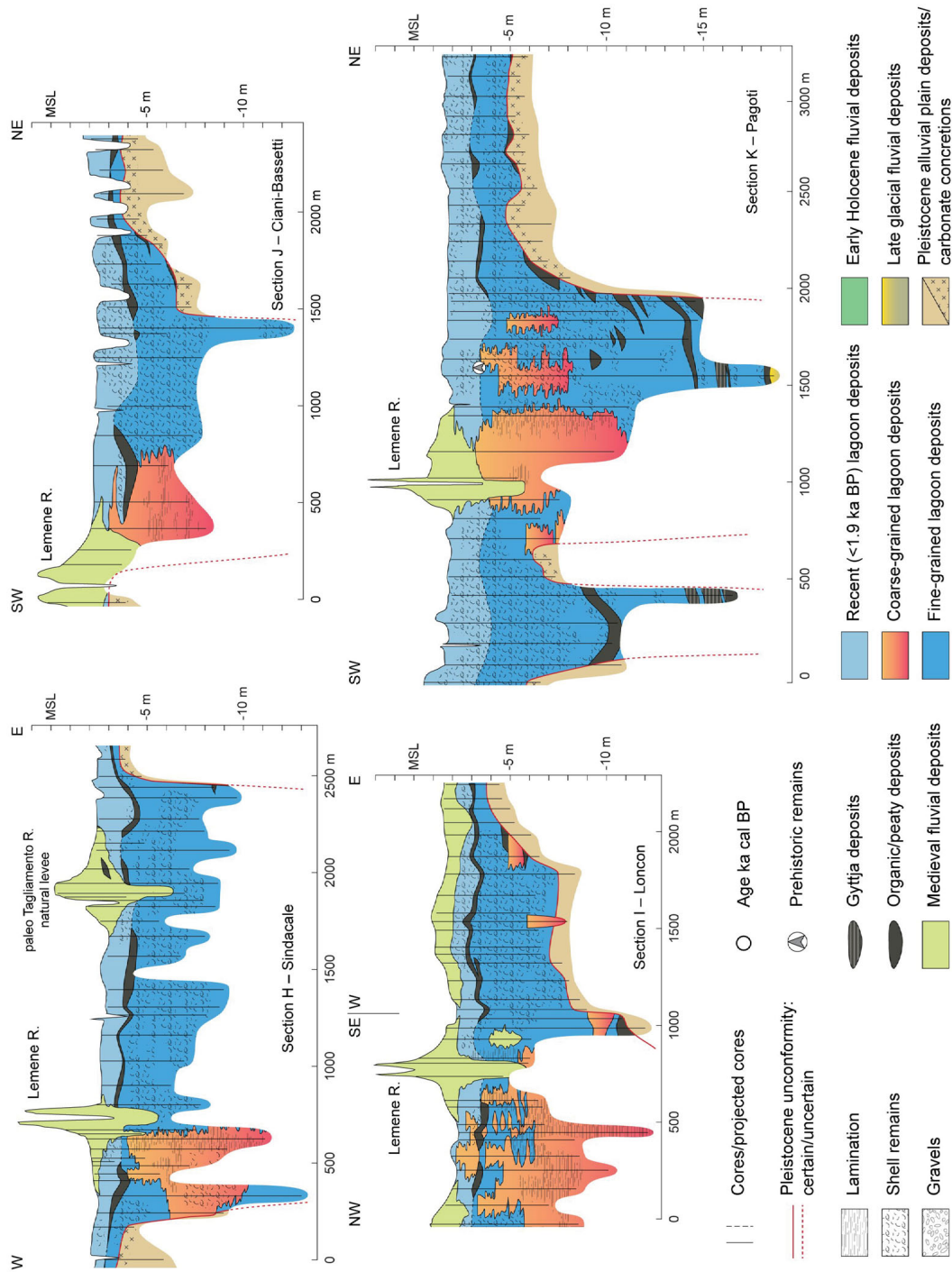
Figure 2.9: From page 63, compilation of all the cross sections available for the Concordia incised valley. Location in Fig. 2.7. The descriptions are reported in section 2.4.

65

and reached a depth of 40 m below the topography. A gravelly unit with a thickness up to 10 m and a diameter of the clasts reaching 6 cm characterises this section. Two widespread peat layers are found almost along the whole profile at depths ranging between $3 - 4$ m (from -0.5 to -1 m MSL) and $5 - 6$ m (from -2 and -3 m MSL), respectively. These organic horizons are clearly separated along the profile by alluvial silty deposits, while they merge in the western sector of the valley. In several cores the lower horizon corresponds to a silty-loamy organic layer displaying mottled features in the lower part, which covers a very stiff decimetric horizon characterized by centimetric carbonate concretions that directly covers the basal gravels. The upper organic horizon is covered by the sandy and silty deposits forming the fluvial ridge which is recognizable in the present topography south of Gruaro (Fig. 2.4-A) and which has been described as the Medieval branch of Tagliamento River that flooded Concordia Sagittaria (cf. Fontana, 2006; Fontana et al., 2004, 2014a). About 2 km north of this section, the shallower organic horizon was found in a core at 5.8 m of depth and radiocarbon dated to $4.4 - 4.1$ ka cal BP. According to geochronological and stratigraphic evidence, the upper organic horizon in section 2 can be tentatively correlated to the P2 layer described in the southern sections, while horizon P1 is probably not present. It is worth noting that the convex topography of the Medieval fluvial ridge of Tagliamento is coupled in the subsoil by a concave trend of the shallower organic horizon, probably induced by differential compaction.

SECTION C - CONCORDIA   Section C (Fig. 2.7) is a ca. 4 km long transect with a W-E direction that is located at the southern limit of the isolated terrace of Concordia Sagittaria and is based on the interpretation of 29 new hand cores and other 5 mechanical cores which reached depths over 20 m. This transect is only 700 m south of the reference section available for the area where the stratigraphic units filling the valley have been originally identified (Fig. 2.3). The entire section is sealed by the alluvial sediments of Medieval Tagliamento, which have a maximum thickness of 5 m inside the valley and onlap over the LGM surface for $1 - 2$ m, where archaeological structures of Roman and Late Antiquity age are also buried. The peat layer P1 is found at a depth between 5 and 3 m (i.e. -2 and -4 m MSL) and it has a constant thickness of 1 m in the western side of the profile, while in the eastern one it splits in two horizons, separated by a lens of fine-grain sediments. The age of

P1 is here further constrained by the Iron Age and Roman structures that are intercalated within the horizon (Fontana, 2006; Fontana, 2015). A second peaty layer can be found roughly between 6 and 5 m of depth (i.e. -4 and -5 m MSL), but it is less continuous of P1 and has a thickness of $0.2 - 0.7$ m. The eastern sector of the valley is characterized by a thick peaty layer, that has been documented between 9 and 11.5 m of depth (i.e. -7 to -10 m MSL). The basal portion of this peat correlates with the basal peat found in the rest of the valley and cover the Late Glacial gravels and sands deposited by paleo Tagliamento River. In this section no data are available for the description of the sedimentology and the thickness of this unit, which has been inferred from the data of the reference section (Fig. 2.3).

SECTION D - CAVANELLA   This 1.5 km W-E cross-section was reconstructed using 17 new hand-made cores, but only one of them passed the whole thickness of the BP and reached the top of the Late Glacial gravels (Fig. 2.8). Nevertheless, none was able to reach the bottom of the incised valley filling. The organic horizons P1 and P2 can be clearly differentiated and they both display a wavy trend, which is amplified in the eastern sector, where the thicker portions of the Medieval alluvial deposits match with the troughs of P1 and P2. In the central portion of the valley, roughly between -9 and -10 m MSL, a gyttja layer was intercepted.

SECTION E - FRANZONA NW-SE   This section covers a length of about 1.8 km and was reconstructed with the data of 21 new hand cores (Fig. 2.8). This profile is characterized in its central portion by the presence of the LGM alluvial plain, that is almost cropping out at surface and is characterized by evidence of Prehistoric occupation dating between 6 and 4 ka cal BP (Fontana et al., 2018). In this sector of the profile, the LGM top is sealed by organic sediments that are in turn covered by a thin layer of Medieval Tagliamento deposits. In the eastern and western sector of the profile the infilling of the valley is almost completely constituted by lagoon sediments, covered by the Medieval Tagliamento fluvial ridge. In the NW cores the lagoon deposits are characterized by a clear millimetric lamination formed by alternations of silt, sandy silt and organic mud. In the eastern portions a main bipartite peat layer, probably P1, can be found between 2 and 3 m of depth (i.e. -3 and -4 m MSL), while P2 can be tentatively identified in the thin layer placed below the

ridge of the Lemene River and partly documented in the western side of the incision. The basal peat was not reached.

SECTION F - FRANZONA SW-NE   The profile is 3 km long and was obtained by the interpretation of 49 new hand cores (Fig. 2.8). This section intercepts perpendicularly the previous Section E (Franzona NW-SE) and is characterized as well by the occurrence of the top of LGM deposits at a shallow depth in its central sector. The P1 layer is widespread and can be found between the depths of 3 and 5 m (i.e. -3, -5 m MSL). The P2 layer is also recognizable in several cores and lays at the boundary between the Medieval Tagliamento deposits and the underlying lagoon sediments, around -2 m MSL. It is worth noting how the deformation of these organic layers are mostly concentrated in the central sectors of the valley, where they are arranged in a large concave shape, while near the stiff LGM deposits the deformation is generally limited or even absent. In the eastern sector a third peat layer can be observed between P1 and P2. The basal peat was intercepted in the western sector at 14 m of depth (i.e. ca. -13 m MSL), where it shows a thickness of about 1 m and it rests on top of the silty deposits of the Late Glacial channel sediments. The lagoon infilling is characterized by the widespread presence of mollusc shells (e.g. *Abra sp., C. glaucum*) and by the presence of a pervasive sandy lamination identified in the SW sector of the cross-section.

SECTION G - VALLESINA   This section is perpendicular to the incised valley, has a length of about 3 km and was reconstructed basing on 27 new hand-made cores (Fig. 2.8). The infilling material in this section is mainly constituted by fine lagoon sediments rich in fossils. A series of sandy laminations were found in the western side of the lagoon infilling. The only recognized and widespread peat layer is found between 1 and 3 m of depth (i.e. -3 and -5 m MSL) and by correlation it can be associated to P1. The Medieval alluvial deposits of Tagliamento seem to directly cover the lagoon unit and they form fluvial ridges along two different branches. The basal peat was also reached by one core at the depth of -15.5 m MSL.

SECTION H - SINDACALE   This cross-section is 2.5 km long and is placed between 500 and 1 000 m south of section G. It has a WSW-ENE direction (Fig. 2.9) and was reconstructed basing on 37 new hand cores. The fine-grained lagoon infilling is again dominant. In the western sector of the incised valley it

is possible to recognize a sandy/loamy body which is found at a depth between 2 and 9 m (i.e. -4 and -11 m MSL) and is characterized by a fine-grained lamination. Within this deposit sparse lagoon fossils can be present. One single organic layer (P1) was found within the upper portion of the infilling, between the depths of 1 and 3 m (i.e. -3 and -5 m MSL). The organic horizon P2 was not documented in this cross-section and the Medieval alluvial units are present only along the fluvial ridges of paleo Tagliamento River.

SECTION I - LONCON   This ca. 2.5 km long profile was reconstructed with 33 new hand-made cores and it crosses the valley in a NW-SE direction, while in the eastern sector it partially follows one of its flanks in a SSW-NNE direction (Fig. 2.9). The cross-cutting sector of this profile intercepted an extended jagged sandy unit characterized by the presence of a pervasive fine-grained lamination. This sedimentary body, which depth spans between 1 and 10 m (i.e. -2 m to -12 m MSL), is enclosed within the muddy lagoon deposits, which are typically found in the upper portion of the valley infilling. Only one widespread peat layer is present along the whole section. According to its depth ($1 - 2$ m, i.e. between -3 and -4 m MSL) and its stratigraphic position, it is interpreted as P1. In the eastern side of the section the profile is almost parallel to the eastern branch of Medieval Tagliamento and the related alluvial deposits, directly resting on the lagoon sediments, have a rather constant thickness of $1 - 2$ m.

SECTION J - CIANI-BASSETTI   This section was reconstructed using the data of 21 new hand-made cores and it crosses the incised valley in a SW-NE direction for ca. 2 km (Fig. 2.9). As in the previous two cross-sections, also in this profile it was possible to recognize a coarse-grained and laminated unit within the lagoon deposits. The top of this body is located almost at surface, just below the Medieval ridge of Tagliamento (ca. -1.5 m MSL), whereas its maximum depth is unknown. P1 layer is still recognizable in this section between 1 and 2 m depth (-3 to -4 m MSL), although it appears to be less continuous if compared to the other upstream sections. The Lemene River is flowing in the middle of the ridge of Medieval Tagliamento and, west of this feature, the top of LGM surface is only between 1.5 and 3 m depth.

SECTION K - PAGOTI   This section is the southernmost, it follows a SW-NE path for ca. 3 km and was reconstructed through 34 new hand-made cores

(Fig. 2.9). In this profile the dominant facies is constituted by the fine-grained lagoon deposits, which enclose some sandy and partially laminated bodies which are located between 1 and 10 m of depth (i.e. -2 and -11 m MSL). An organic layer with a limited continuity, roughly found at 2 m of depth (-3 m MSL), can be associated to the P1 horizon. In the central-eastern sector, at a depth between 1 and 2 m some pot shards dating to the late Bronze Age (1.4 − 1.1 ka cal BP) have been found, thus providing a reliable constrain for the age of the embedding deposits. Several other peaty layers and isolated bodies were intercepted between -6 and -16 m MSL. In particular, one core reached the basal peat at -18 m MSL and sampled the underlying Late Glacial riverine deposits of the paleo Tagliamento River. A small isolated terrace of LGM deposits was intercepted in the southern portion of the cross section.

2.5 DISCUSSION

Morphology of the Concordia incised valley

In the study area, the combined use of DTM analysis and stratigraphic data led to reconstruct the DEM of the unconformity separating the LGM megafan deposits from the post-LGM units, allowing to recognize the buried morphology of the valley of Concordia (Fig. 2.10). Considering the buried portion of the valley and the northern tract where it still has some topographic evidence, the fluvial incision of Concordia can be followed for over 25 km. In particular, according to the DTM of the present topography and the geological surveys available in the northern part (Bondesan and Meneghel, 2004; Bondesan et al., 2008; Zanferrari et al., 2008c; Fontana et al., 2012), it is possible to follow the valley since its origin, in the area of San Vito al Tagliamento (Fig. 2.4-A). This area almost coincides with the spring belt and in this zone the paleochannels of Tagliamento were flowing almost at the level of the pre-existing LGM alluvial plain, as the bottom of the Late Glacial channel is generally between 1.5 and 3 m deeper than the LGM surface.

Few kilometres downstream, towards the town of Cordovado (Fig. 2.2), the channel belt of the paleo Tagliamento is confined by fluvial scarps of 2-3 m, but the ancient erosive morphology has been partly deleted and/or remodelled by the Medieval deposits, which affected large sectors of the former valley of Concordia. Differently, the ancient valley incised by Tagliamento along the present course of Reghena River was not affected by the Medieval deposition

and the present landscape is still characterised by the erosive features carved during Late Glacial or early Holocene. North of Portogruaro the valleys of Reghena and Lemene are almost merging and the morphology of the LGM plain is characterized by a remnant isthmus separating the two fluvial incisions. This stripe of LGM deposits has a width of less than 200 m, thus suggesting the active action of lateral migration and the possible occurrence of river captures on the surface of the Tagliamento megafan. A similar process, characterized by an actual river capture, probably occurred near Portograuro, where the valley of the Reghena River joins with the valley currently occupied by Lemene. It is likely that the two valleys merged also south of Concordia, isolating the terrace where the ancient city was settled.

South of Portograuro the buried portion of the incised valley can be tracked for a total length of about 12 km and it has a roughly north-south direction, with a marked deviation toward east in its downstream portion (2.10). The buried tract of the valley is characterized by the presence of sharp bends, resembling a meandering pattern, with a curvature radius spanning from 800 to 1 500 m, while the overall width of the valley spans between 400 and 1 200 m. The dataset does not allow to assess the depth of the incision along its entire path, but the available cores suggest that the erosive unconformity at the base of the incised valley is characterized by a rough topography, probably marked by localized deeper scours, as it was recognized for the Lemene valley branch (Fig. 2.10). In the northern portion of the valley a series of cores intercepted a flight of terraces placed along the borders of the incision between the depths of -12 and -11 m MSL (Fig. 2.10). A mean longitudinal slope of ca. 4‰ can be estimated, but it must be noticed that the incised valley rapidly gets deeper in the downstream sector, whereas for most of the reconstructed course the valley floor appears to have an almost constant low gradient, probably close to a value of 2‰ (Fig. 2.10). The inclination of the flanks is variable as well, ranging roughly from 35° to 75°. The maximum depth reached by the tract of the incised valley now used by Lemene was assessed between ca. -14 and -16 m MSL (Figs. 2.7 and 2.8), whereas it is much shallower along the valley now occupied by Reghena, where the top of the LGM deposits was intercepted by mechanical cores at depths of ca -6 m MSL or even less (Figs. 2.7 and 2.8). The depth of this latter branch dramatically increases right downstream of the merging point, where a value of about -14 m MSL was recovered by a mechanical core. Thus, the incised valley now occupied by Reghena is a sort
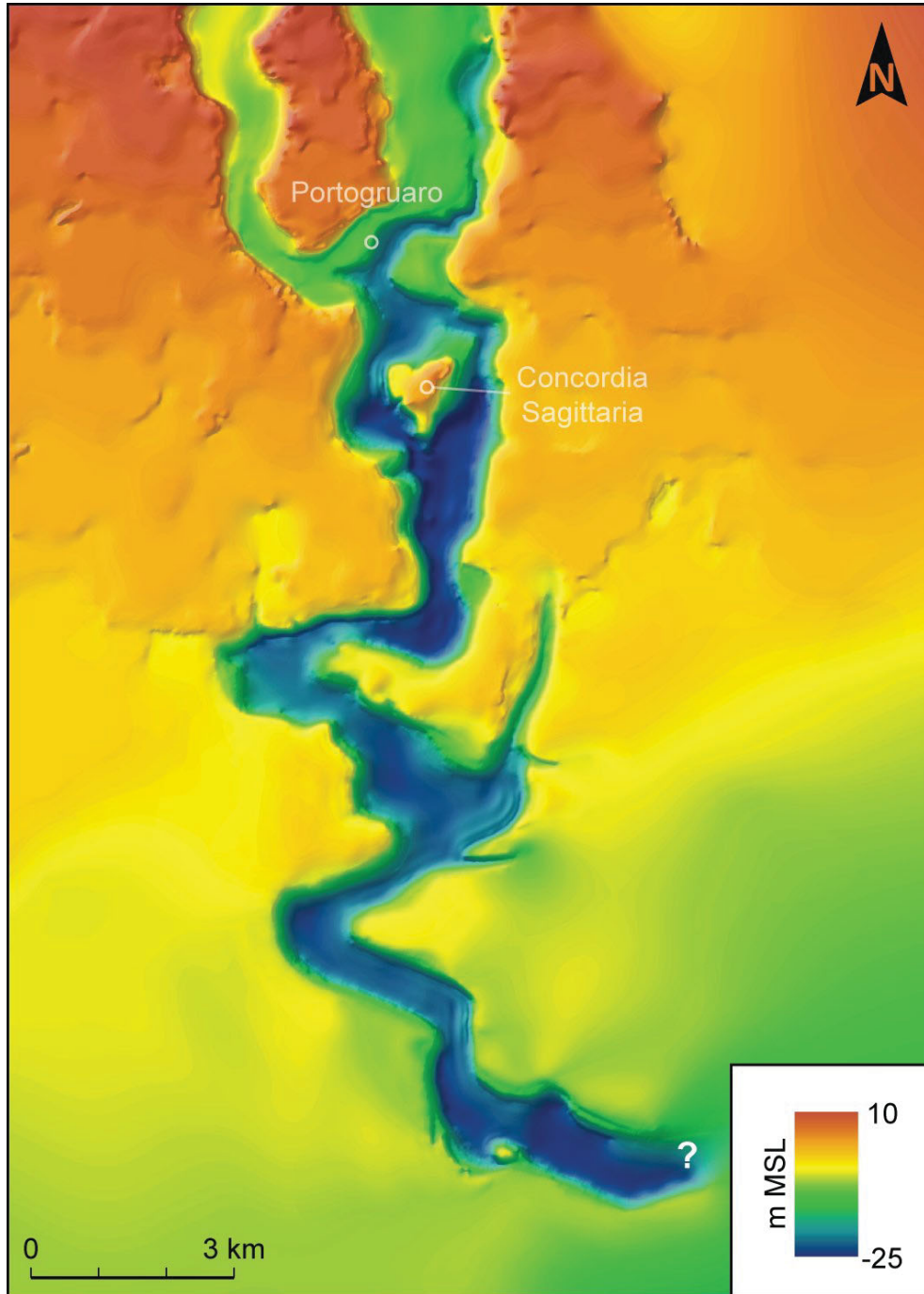
Figure 2.10: Reconstructed DTM of the erosive unconformity at the base of the Concordia incised valley. The location of area is reported in Fig. 2.5.

of hanging valley and this setting suggests that the branch now occupied by Lemene was existing before and it probably captured the other branch. Some minor faintly-incised tributary channels join the main trunk of the valley. The most remarkable example is represented by a 400 m wide channel merging to the main valley from east (Sections G in Fig. 2.8 and H in Fig. 2.9) The presence of this particular channel appears to have strongly influenced the morphology of the Concordia incised valley, as at the merging point the width of the valley suddenly increases. The reconstructed surface of the top of the LGM alluvial plain shows the presence of some other smaller incised tributaries, thus suggesting that the surface of the megafan was probably characterized by an extensive network of minor courses joining the valley, as documented in other case studies (cf. Boyd et al., 2006). However, our research brought only to the partial reconstruction of this network, as the LGM surface in the area is largely covered by younger deposits. Thus, the recognition of the tributaries is based on the stratigraphic cores, but these are spaced between them of ca. 100 m and this length is largely biasing the dimension of the local streams, which normally have a width of $5-20$ m.

An example of the network of tributaries characterizing the top of the LGM surface is visible in Fig. 2.4-B, which shows the DEM of the area near the incisions eroded by other branches of paleo Tagliamento, that now are occupied by Fiume, Sile and Arcon rivers (Figs. 2.1, 2.2 and 2.4-B). In that area the two sites where the valley of Arcon has been captured by Sile are also visible. These cases of fluvial capture had been already highlighted by Comel, (1950, 1958) and, as discussed below, this process was probably a very important mechanism in triggering the formation of some of the incised valleys of Tagliamento.

At the moment the available data do not allow to directly follow the continuation of the valley of Concordia downstream of section K "Pagoti" (Fig. 2.9). Nevertheless, the detailed geophysical surveys performed along the coast between Tagliamento and Piave from bathymetric line -10 m MSL and below did not find any evidence of large incised filled valleys (cf. Trincardi et al., 2011). This situation suggests that the valley of Concordia is progressively shallowing in seaward direction. It is also likely that the valley analysed in this research was joining to another deep incised valley recognized in the subsurface along the so-called *Tiliaventum Maius* (Fig. 2.2; Fontana, 2006; Fontana et al., 2012).

Even if the other incised valleys formed by Alpine rivers in the distal portion

of Venetian-Friulian Plain have been reconstructed with a far lower detail (cf. Arnaud-Fassetta, 2003; Carton et al., 2009; Mozzi et al., 2013; Fontana et al., 2014a), their average and maximum dimensions (depth, width) is rather comparable. This similarity is probably related to the magnitude of the water discharge and to the characteristics of the distal sectors of the alluvial megafans, where the topographic slope of the LGM surface is between 3 and 1 % and the deposits are fine dominated. On the contrary, very different measures characterize the only known example of incised fluvial valley detected in the northern Adriatic, north of Po River (Ronchi et al., 2018). In that case the fluvial incision had been formed during the LGM by a very minor stream, not connected to a major Alpine river and the maximum width is only 400 m. Moreover, the cross section of this valley has a "V" shape, while the incised valleys of the Alpine rivers generally have a "box" profile.

Evolutionary history

TIMING AND TRIGGERS OF THE INCISING PHASE   At the moment, the timing of formation of the incised valley of Concordia can only be estimated considering the age of the depositional units eroded by the fluvial incision and the age of the sediments which sealed the coarse channel body at the bottom of the valley (Fig. 2.11-A). In particular, in the study area the last phase of LGM aggradation is dated between 19 and 18 ka cal BP (Fontana et al., 2014b) and, therefore, this age provides a *terminus post quem* for the beginning of the erosive phase. On the contrary, the base of the basal peat at the top of the coarse channel constrains the end of the fluvial phase which shaped the valley and transported the gravels along it. The basal peat is dated to ca. 9.5, west of Concordia, and 8.5 ka cal BP, in the eastern side, while it is $8.9 - 9.0$ ka BP near Sindacale (#3, 7 and 16 in Tab. 2.1). Thus, the period of activation of the valley of Concordia could have had a maximum time span of almost 9 ka, from 19 to 9 ka BP. This erosive landform was already existing and partly infilled before 14 ka BP, as documented in core CNC-S2 by the age of the organic layer intercalated to the Late Glacial channel deposits (#6 in Tab. 2.1). It is likely that the erosive process occurred very rapidly, as much as the dramatic changes that occurred in the Prealpine area immediately after that the downwasting of the Tagliamento glacier started (cf. Monegato et al., 2007, 2017; Fontana et al., 2014b).

In our opinion, the presence of the Concordia incised valley in the distal portion

of the Tagliamento megafan can be attributed to the interplay of climatic-related processes which would have induced a change in the hydrodynamic conditions, such as the climatic amelioration that followed the LGM period, the variations of annual rainfall and the expansion of braodleaf forests (Monegato et al., 2011). A tectonic trigger can be excluded, as the presence of multiple Late Glacial fluvial incisions is documented in the distal sector of almost all the alluvial megafans along the southern Alps (Fontana et al., 2014a). Moreover, no topographic indications of surface or shallow deformations are present in the distal sector of the Tagliamento megafan (Fig. 2.1).

The presence of large incised valleys formed in the Late Glacial downstream of the spring belt in the Tagliamento megafan suggests a possible relation with the network of secondary spring-fed streams described in the previous paragraph (cf. Fig. 2.4-B). It is in our opinion that they probably played an important role in conditioning the formation of these multiple fluvial valleys of Tagliamento. In particular, as visible in Figs. 2.1 and 2.4-B, the groundwater-fed rivers are generally entrenched in the LGM surface and they form a divergent pattern both in the distal portion of the megafans of Tagliamento and Cellina. Because of their rather constant fluid discharge along the year and the scarce sediment transport, these minor streams have been characterized by headcut erosion during the entire Holocene up to the 20th century (Comel, 1934, 1940; Fontana, 2006). In this perspective, the divergent pattern of the incised valleys attributed to Tagliamento (Figs. 2.1 and 2.2) can be interpreted as partly induced by the activity of minor streams. Two slightly different mechanisms can be therefore suggested: 1) the headcut retreat could have led the spring-fed streams to intercept and capture the Tagliamento River; 2) the avulsion of the Tagliamento could led to its trapping within the former slightly-incised valleys of the spring-fed rivers. After the capture the former spring-river trench would have been reshaped, widened and deepened. In particular, it is likely that the over-deepening caused by the Tagliamento increased the discharge of the groundwater inside the fluvial incision promoting a positive feedback in the erosive power of the river. The merging of different streams would have furthermore increased the water discharge, i.e. the erosive power of the river (cf. Best and Ashworth, 1997). The presence of two merging slightly-incised branches at the head of the reconstructed incised valley (Lemene and Reghena valleys, Fig. 2.10) may support our hypothesis. It is worth noting that the silty and clayey composition of the distal sector of the Tagliamento megafan

would have promoted an avulsive fluvial style rather than a lateral migration, thus fostering the river capture processes and the formation of incised valleys.

LATE GLACIAL AND EARLY HOLOCENE FLUVIAL INFILLING   The boreholes drilled with hand augers could not pass through the coarse deposits forming the basal valley fill, thus the available information are mainly constituted by the position and the characteristics of the top of this unit. Therefore, it is not possible to assess the fluvial style of the Tagliamento during this first depositional stage. Nevertheless, the homogeneous gravelly nature of this deposit and the remarkable diametre of the clasts (up to 3 cm near Concordia) documented in sections A, B and in the reference section (Figs. 2.3 and 2.7), suggests a braided channel typology, which probably led to the formation of a multistorey braided channel deposit (Blum et al., 2013). The fine-grained deposits documented in several sections above the gravelly unit probably corresponds to the deactivation phase of the Tagliamento in the Concordia incised valley, likely induced by an avulsion process in the upstream sector. The pedogenesis of this fine-grained deposit indicates a relatively prolonged period of subaerial exposure. The elevation of the coarse sediments gradually decreases along the valley, shifting from the area of San Vito area, where it is at the same elevation of the LGM surface (ca. 17 m MSL), to section C, where it is about 9 m below it (-8 m MSL), to section G, where it is at about 15 m below it (-19 m MSL). In section K the top of the channel deposits is still about 15 m below the LGM surface (i.e. -19 m MSL), suggesting that the maximum depth of the valley of Concordia is reached in between these two sections. As discussed in the previous paragraph, it is likely that the valley is progressively shallowing downstream section K, as no evidence of incised valleys are documented in the northern Adriatic shelf between the present mouths of Tagliamento and Piave rivers.

It is likely that downstream of Concordia the channel deposits shift from gravels to gravelly sands and sands, promoting the onset of a different fluvial style, but no direct data are available to test this hypothesis. Moreover, south of Concordia no data are available for constraining the thickness of this unit. Along the valley of *Tiliaventum Maius*, the mechanical cores demonstrated that near Marina of Lugugnana (Figs. 2.1 and 2.2) sandy gravels up to 2 cm are presents between 18 and 24.5 m of depth (i.e. -17 and -23.5 m MSL; Fontana et al., 2012).

Considering that the erosive phase of Tagliamento was triggered at the end of LGM by the dramatic contraction of the sedimentary flux supplied by the mountain catchment (cf. Fontana et al., 2008, 2014a; Carton et al., 2009), probably a significant portion of the coarse deposits recorded at the base of the valley of Concordia were removed from the apical sector of the megafan.

FRESH MARSH/LACUSTRINE ENVIRONMENT   The occurrence of a thick layer of peat on top of the Late Glacial Tagliamento deposits clearly points toward the formation of a freshwater marsh within the valley. These waterlogged environments were fed by the spring and runoff waters and by the aquifers intercepted by the flanks of the valley, formed above the fine-grained sediments that cap the late glacial fluvial sediments (Fig. 2.11-B and -C). The pollen data available for these organic deposits (Favaretto and Sostizzo, 2006) shows a progressive decrease of the *Pinus* in favour of more thermophilous species. The presence of the hygrophilous species *Salix, Fraxinus* and *Alnus* strengthen the hypothesis of a lacustrine/freshwater marsh environment.

In order to obtain the age of this unit, three different sites were analysed. In each site the age of two samples were measured, one at the bottom of the organic layer, i.e. at the boundary with the underlying fluvial deposits (#3, 7 and 16 in Tab. 2.1), and one at the top of the organic layer, i.e. at the boundary with the overlying lagoon deposits (#2, 5 and 15 in Tab. 2.1). The ages of the bottom deposits cover a time span of a millennium, roughly from 9.5 to 8.5 ka cal BP. These period is indicative for the onset of the widespread presence of a freshwater environment within the incised valley. The ages of the top of the basal peat range between 6.7 and 7.8 ka cal BP. The waterlogged environment at the bottom of the Concordia incised valley lasted therefore for ca. two millennia.

The paludification of the valley was triggered by a rising of the water table in the area coupled to a reduced sediment discharge. These conditions would have been the result of the alteration of the hydraulic equilibrium of the Tagliamento, probably caused by a rise of the base level, which possibly induced an upstream avulsion. This speculation is supported by the age of such deposits (ca. 9.0 ka cal BP) which is perfectly matching with an increase of the relative sea-level (RSL) rise rate recorded in the northern Adriatic area (cf. Covelli et al., 2006; Ronchi et al., 2018). An abrupt increase of the sea-level has been recorded on a Mediterranean scale, as in the Rhône Delta area (Amorosi et al., 2013b)

and in the Pego-Oliva basin in Spain (Brisset et al., 2018), where similar ages for marked marine transgression were recorded. Moreover, a global RSL rise around 9.0 ka BP has been pointed out by several authors, as reported by Harrison et al. (2018).

The presence of deposits of detritus gyttja intercalated to the basal peat indicates the development of some small eutrophic lakes. The formation of such sub-environments would have been fostered by the presence of small sink areas and depressions delimited by the superficial roughness of the underlying deposits, such as small natural levees or localized slides of the flanks of the valley. This is the first time that a lacustrine environment is documented in the coastal plains of the northern Italy.

After this period the incised valley experienced a progressive salinization in landward direction as a consequence of the post-LGM sea-level rise.

LAGOON DEVELOPMENT   With the progressive sea-level rise, the freshwater marsh existing at the bottom of the incised valley of Concordia has been converted into a brackish marsh/lagoon environment (Fig. 2.12). This process was not synchronous throughout the entire valley, but the onset of the lagoon deposition followed an upstream migrating path, controlled by the steepness of the valley floor and the rate of sea-level rise (Fig. 2.11-C). The dominance of the lagoon processes within the incision are clearly indicated by the typical brackish faunal associations (cf. section 2.4). Moreover, some typical sedimentary structures can be recognized within the deposit, such as the laminations of the sediments and the tidal bundling.

The presence of an elongated body of coarser sediments within the fine-grained lagoon deposits was associated to a tidal channel (cf. section 2.4). This feature, characterized by a pervasive lamination and by the limited presence of a brackish fauna, is distinguishable in the seaward sector of the valley infilling. The thickness of these deposits indicates a relatively steady position throughout the evolution of the lagoon environment, whereas its apparent width (up to 500 m) is the result of the lateral migration of the tidal channels. The landward fining trend that characterizes this body suggests an energy decrease in the inner portion of the incised valley, in good accordance with the expected trend for an incised valley/estuary (cf. Dalrymple et al., 1992). It is worth to notice that the classic tripartite subdivision for a tide-dominated estuarine environment (marine-dominated, mixed-energy, river-dominated; sensu Dalrymple and Choi,
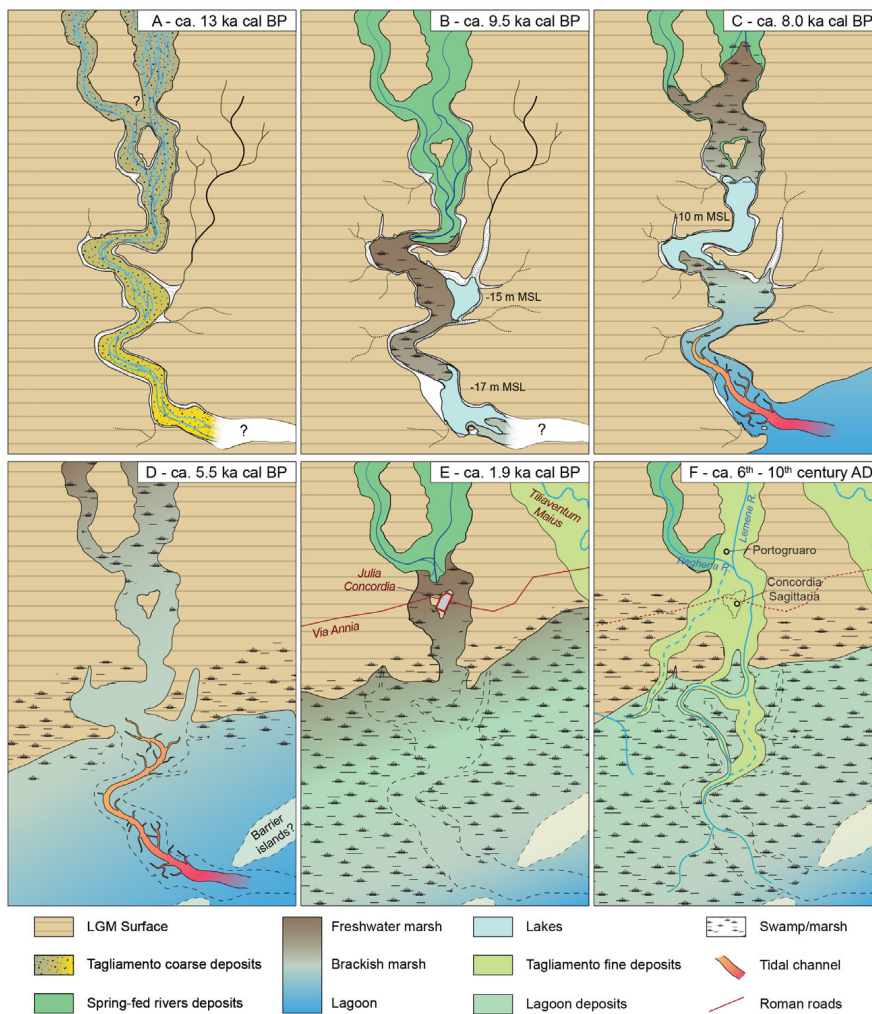
Figure 2.11: Graphic overview of the evolution of the Concordia incised valley.

2007) does not entirely apply to the case of the Concordia incised valley as the riverine input, provided only by spring-fed rivers, is strongly sediment-depleted and, thus, almost absent in the sedimentary record.

The generalized fining-upward trend highlighted in some cores may be the result of an overall progressive abandonment of the lagoon as a consequence of a relative sea-level stability. It must be noticed that, like most of the deposits investigated in this work, the vertical position reported for these bodies has been subjected to subsidence processes promoted by the compaction of the underlying lagoon muds.

The progressive landward shift of the upper limit of the lagoon environment

within the valley matched with the gradual deactivation of the pre-existent freshwater marshes. The radiocarbon dates obtained from the top portion of the basal peat layer allowed therefore to reconstruct the timing of the marine ingression between ca. 7.9 and 6.5 ka cal BP (Figs. 2.11 and 2.12; #2, 5 and 15 in Tab. 2.1). Two more dates (#8 and 13 in Tab. 2.1) were obtained from samples placed outside of the valley infill and directly lying on the Pleistocene surface (Fontana et al., 2017). The analyzed peat samples gave ages which are coherent with those measured within the incised valley at comparable depths. The available pollen analysis shows the continuous presence of hygrophilous species also during the development of the lagoon environment. The vegetation outside the incised valley was dominated by the association of *Quercus* and *Carpinus*, but within the peat layer P2 the percentage of forest cover clearly decreases and this trend has been related to the human impact, which strongly affected the area Iron Age and especially the Roman period (Favaretto and Sostizzo, 2006).

FRESHWATER MARSHES   The only widespread indicators of environmental changes within the valley are represented by a series of peaty layers interspersed within the lagoon deposits. The presence of such layers suggests a recurrent freshening of the salt marsh and can be useful in the reconstruct the evolution of the lagoon environment (Fig.2.11-C and -D).
While the less extended organic layers recognized in only one or few transects are the result of local conditions, (e.g. formation of temporary sills, localized freshwater inputs) the widespread horizons, notably P1 and P2, may provide information on a larger scale, as they are the result of more pervasive forcings. In particular, two main processes can be associated to the formation of such organic deposits: 1) an enhanced period of fluvial discharge or 2) a relative slowdown of the sea-level rise.
In the first case, the freshening of the salt marsh is controlled by upstream factors, which can span from the temporary draining of a stream into the valley to a more climatic-driven forcing related to the precipitations in the area. The new input can promote a temporary shift from a lagoon to a brackish/freshwater swamp environment by temporarily rising the topography of the area with its sediments and by providing a higher freshwater discharge. The P1 peat layer, dated at ca. 4.5 ka cal BP, falls exactly in a period of enhanced flooding activity recorded in Europe and, more specifically, in the
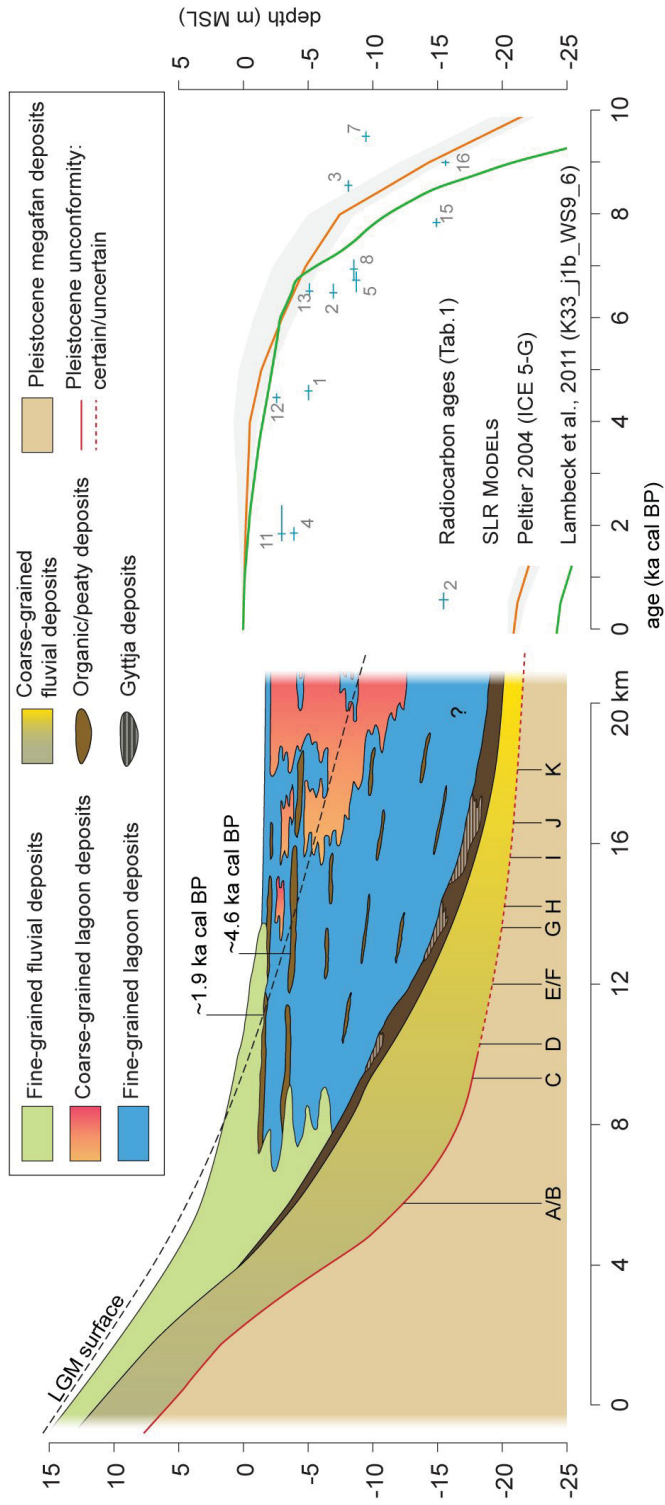
Figure 2.12: Schematic longitudinal section of the Concordia incised valley. On the right two RSL models for the northern Adriatic are reported (Peltier, 2004; Lambeck et al., 2011).

study area (Benito et al., 2008; Macklin et al., 2010; Rossato et al., 2015), thus supporting the hypothesis of an upstream control. Around 4.5 ka cal BP the Tagliamento experienced an important avulsion phase (Fontana, 2006) which led the river to temporarily follow also the direction of Lemene River (Zanferrari et al., 2008a).

The second case implies a regional signal given by a decrease in the rate of the sea-level rise in favour of the groundwater and the runoff/spring water discharge. As this process would be entirely climatic-controlled, other pieces of evidence should be expected, such as a clear signal on the marine record and the presence of indicators in the filling successions of the other incised features of the northern Adriatic Sea (e.g. Istrian Rias). The rate of the sea-level rise may be also modulated by local factors, such as the presence of sandy spits or barriers that temporarily disconnect the lagoon from the open sea. It must be notice that the presence of several bottlenecks along the incised valley may have facilitated the formation of such barriers. A similar mechanism could also have been triggered by an ancient human intervention for the reclamation of the area. It is worth noting that the Romans reclaimed large sectors of the alluvial plain, altering the surface hydrography and probably affecting also the water circulation in the valley bottom, especially near Concordia (cf. Marcello and Comel, 1963; Fontana, 2006, 2015). Thus, it is possible that the extent of the fresh-water peat of horizon P2 and the southern boundary with the brackish environment have been partly conditioned by anthropogenic factors. Unfortunately, at the moment no robust data are available to support this hypothesis.

Given these considerations it is possible to assume that these peaty layers formed almost at the same elevation, or just slightly above, the paleo sea-level. In Fig. 2.12 it is possible to notice that the position of the dated peat layers is lower than the value provided by the reconstructed RSL curves. Such discrepancy can be attributed to the compaction expereinced by the lagoon deposits. Moreover, while the accumulation of organic material in waterlogged environments can be assumed to take place in almost-horizontal conditions, the peaty and organic layers here reconstructed exhibit a markedly-undulated pattern (cf. Figs. 2.7 to 2.9). This peculiarity can be explained with by the different subsidence pattern induced by the overburdens and by the differential compaction of the underlying deposits. A dislocation of up to 2 m has been observed for some of these layers (Fig. 2.8-F). The thickness of these peat

layers has been affected as well by the compaction induced by the overlying sediments. While the peat layers resting on highly-compressible lagoon deposits are strongly deformed and cannot be used as paleo sea-level indicators, the ages obtained from samples directly laying on non-compressible units (e.g. the LGM alluvial deposits of the megafan) can be used as index points. In particular, the dates #6 and #8 (Tab. 2.1) are suitable for such reconstruction, whereas #9, #11 and #13 probably experienced only a minor vertical displacement, as they were obtained from samples of the basal peat, which is directly lying on the non-compressible post-LGM gravels (Fig. 2.12).

MEDIEVAL FLUVIAL ACTIVITY   The present landscape of the study area has been strongly imprinted by the Medieval floods of Tagliamento and the related alluvial deposits, which sealed large sectors of the valley of Concordia and definitely transformed it in a fossil landform. In particular, along the valley the sedimentation was almost continuous until 2 km south of Concordia (D in Fig. 2.10) while, downstream, it fringed along several fluvial ridges (Fig.2.9). The main ridge built by Medieval Tagliamento has been parasitically occupied by Lemene River, which still flows along it, using the last residual channel abandoned by Tagliamento after an upstream avulsion (Fontana, 2006). The new data allow to document that the paleochannel deposits had a thickness between 3 and 5 m and are generally sandy, but characterized at the bottom by coarse sands and sometimes clasts of fine gravels. North of section B the occurrence of gravels and gravelly sands is documented (cf. Fontana, 2006; Zanferrari et al., 2008b). With its convex morphology, the large fluvial ridge formed along the top of the valley of Lemene, partly blocked the out flow of the valley now used by Reghena River. This difficult drainage situation led the valley of Reghena to experience stagnating conditions, favouring the accumulation of plant remains, as documented in section A, where the thickness of peat deposits is much significant than in the other valley. The Medieval deposition sealed the former surface at the base of the valley, where formerly was accumulating the peat horizon P2. Between sections C and H (Figs. 2.7 to 2.9) the different fluvial ridges isolated several sub-basins that have been prone to submersion by brackish waters until the 20th century, when the reclamation completely drained the area. South of Sindacale (section G) the Medieval deposits can be recognized only along the fluvial ridges, which have a width that is progressively narrowing from almost 1 000 to less than 500 m (see

sections in Fig. 2.9). The Medieval deposits reach a maximum thickness (up to 6 m) between Portogruaro and Concordia, where they almost completely buried the Roman city, even onlapping over the top of the LGM surface.

2.6 CONCLUSIONS

This work allowed to recognize and reconstruct the planform and buried morphology of a 25 km-long incised valley carved by the Tagliamento River in the Friulian Plain after the end of the LGM. In particular, this study provided precise data on the evolution of the entire area as recorded by the infilling of the Concordia incised valley:

- The entrenching of the river started after 19.5 ka cal BP and lasted at least until 14 ka cal BP. The incising phase was not characterized by a complete bypass of the sediments that, on the contrary, started to accumulate already during the erosive phase that shaped the valley.

- The deactivation of the incising phase is recorded by a peaty layer resting on top of the lower coarse fluvial sediments that was dated between 9.6 and 8.4 ka cal BP. The presence of detritus gyttja deposits intercalated to the peat suggests the temporary presence of some lacustrine sub-environments within the valley. This is the first time that such environments are documented in the distal sector of the alluvial plains of Northern Italy.

- The formation of this extensive peat layer, which marks the end of the erosive phase in the area, was probably induced by the rising of the base level which would have induced a decrease of the river gradient. The age recorded for such event perfectly matches with an increase in the sea-level rise rate recorded in the northern Adriatic Sea.

- The marine transgression that followed the LGM led to the submersion of the valley and to the formation of a lagoon environment. This process was gradual and followed the trend of the sea-level rise. The available radiocarbon dates indicate an age of ca. 7.8 ka cal BP in seaward position decreasing to 6.5 ka cal BP moving landward. It is likely that the first ingression of the lagoon waters in the more distal sector of the valley was rather rapid and probably occurred soon after the fast sea-level rise

documented in the Adriatic shelf between 9.5 and 9.0 ka cal. BP. The lagoon lasted for several millennia within the valley, with some occasional interruptions marked by the formation of some freshwater peat layers, notably at 4.5 ka cal BP, and between the 1st millennium BC and the 6th century AD.

- A temporary reactivation of a branch of Tagliamento River in the area during the Medieval period led to the almost complete burying of the incised valley. The load represented by this sedimentary unit, which in some areas of the valley reached a thickness of $4-6$ m in less than 200 years, led the pre-existing infill units to be deformed by post-depositional processes.

Even if the dynamics which led the formation of the incised valley are not yet completely clear, this work highlighted the possible interplay between Tagliamento (an Alpine river) and the complex network of groundwater-fed rivers. It is likely that the system of multiple incised valleys documented in the distal sector of Tagliamento megafan was partly induced by the fluvial piracy carried out by these minor streams. Given the similar characteristics of the Venetian-Friulian Plain megafans, we speculate that this hypothesis can be spread to the entire area.

Besides the reconstruction of the environmental evolution proposed in this work, the detailed map of the subsurface morphologies and the characterization of the infilling of the buried valley of Concordia can support a wiser territorial planning of the study area. In particular, the map can help in choosing the best sites for building new large constructions and infrastructures and support the selection of the proper subsoil foundations.

REFERENCES

Allen, G.P., Posamentier, H.W., 1993. Sequence stratigraphy and facies model of an incised valley fill: The Gironde Estuary, France. Journal of Sedimentary Petrology, 63, 378-391.

Amorosi, A., Fontana, A., Antonioli, F., Primon, S., Bondesan, A., 2008. Post-LGM sedimentation and Holocene shoreline evolution in the NW Adriatic coastal area. GeoActa, 7, 41-67.

Amorosi, A., Ricci Lucchi, M., Rossi, V., Sarti, G., 2009. Climate change signature of small-scale parasequences from Lateglacial-Holocene transgressive deposits of the Arno valley fill. Palaeogeography, Palaeoclimatology, Palaeoecology, 273, 142-152.

Amorosi, A., Pacifico, A., Rossi, V., Ruberti, D., 2012. Late Quaternary incision and deposition in an active volcanic setting: The Volturno valley fill, southern Italy. Sedimentary Geology, 282, 307-320.

Amorosi, A., Rossi, V., Sarti, G., Mattei, R., 2013. Coalescent valley fills from the late Quaternary record of Tuscany (Italy). Quaternary International, 288, 129-138.

Amorosi, A., Rossi, V., Vella, C., 2013. Stepwise post-glacial transgression in the Rhône Delta area as revealed by high-resolution core data. Palaeogeography, Palaeoclimatology, Palaeoecology, 374, 314-326.

Amorosi, A., Maselli, V., Trincardi, F., 2016. Onshore to offshore anatomy of a late Quaternary source-to-sink system (Po Plain-Adriatic Sea, Italy). Earth-Science Reviews, 153, 212-237.

Amorosi, A., Bruno, L., Cleveland D.M., Morelli, A., Hong, W., 2017b. Paleosols and associated channel-belt sand bodies from a continuously subsiding late Quaternary system (Po Basin, Italy): New insights into continental sequence stratigraphy Geological Society of America Bulletin, 129, B31575.1.

Antonioli, F., Ferranti, L., Fontana, A., Amorosi, A., Bondesan, A., Braitenberg, C., Fontolan, G., Furlani, S., Mastronuzzi, G., Monaco, C., Spada,

G., Stocchi, P., 2009. Holocene relative sea-level changes and vertical movements along the Italian and Istrian coastlines. Quaternary International, 206, 102-133.

Arnaud-Fassetta, G., 2003. River channel changes in the Rhone Delta (France) since the end of the Little Ice Age: geomorphological adjustment to hydroclimatic change and natural resource management. Catena 51, 141-172.

Balista, C., Bianchin Citton, E., 1994. Indagine archeologica e geosedimentologica in localitá Case Zucca di S. Gaetano (Venezia). Quad. Archeol. del Veneto 10, 161-178.

Benito, G., Thorndycraft, V.R., Rico, M., 2008. Palaeoflood and floodplain records from Spain: evidence for long-term climate variability and environmental changes. Geomorphology 101, 68-77.

Best, J.L., Ashworth, P.J., 1997. Scour in large braided rivers and the recognition of sequence stratigraphic boundaries. Nature, 387, 275-277.

Bhattacharya, J.P., Copeland, P., Lawton, T.F., Holbrook, J., 2015. Estimation of source area, river paleo-discharge, paleoslope and sediment budgets of linked deep-time depositional systems and implications for hydrocarbons. Earth-Science Reviews, 153, 77-110.

Bianchin Citton, E., 1996. Il sito umido di S. Gaetano e Casa Zucca. In: La proto- storia tra Sile e Tagliamento. Antiche genti tra Veneto e Friuli, Catalogo della mostra, Concordia, 14, Esedra, Padova, 175-184.

Blum, M., Törnqvist, T.E., 2000. Fluvial responses to climate and sea-level change: a review and look forward. Sedimentology, 47, 2-48.

Blum, M., Martin, J., Milliken, K., Garvin, M., 2013. Paleovalley systems: Insights from Quaternary analogs and experiments. Earth-Science Reviews, 116, 128-169.

Bogemans, F., Roe, H.M., Baeteman, C., 2016. Incised Pleistocene valleys in the Western Belgium coastal plain: Age, origins and implications for the evolution of the Southern North Sea Basin. Palaeogeography, Palaeoclimatology, Palaeoecology, 456, 46-59.

Bondesan, A., Meneghel, M., 2004. Geomorfologia della provincia di Venezia. Esedra. Padova, 516.

Bondesan A., Asioli A., Favaretto S., Fontana A., Gobbato D., Lubiani A., Miola A., Sostizzo I., Toffoletto F., Valentini G., 2005). "Paleoambienti tardo quaternari nella bassa pianura friulana: ricerche multidisciplinari nell'area di Concordia Sagittaria (VE)", Atti del Convegno Nazionale A.I.Geo. Montagne e Pianure. Padova (15-17 febbraio 2005), Materiali del Dipartimento di Geografia, Università di Padova, n. 28, 44-46.

Bondesan, A., Primon, S., Bassan, V., Vitturi, A., 2008. Le unitá geologiche della provincia di Venezia. Cierre. Verona, 184.

Breda, A., Amorosi, A., Rossi, V., Fusco, F., 2016. Late-glacial to Holocene depositional architecture of the Ombrone palaeovalley system (Southern Tuscany, Italy): Sea-level, climate and local control in valley-fill variability. Sedimentology, 63, 1124-1148.

Brisset, E., Burjachs, F., Ballesteros Navarro, B. J., Fernández-López de Pablo, J., 2018. Socio-ecological adaptation to Early-Holocene sea-level rise in the western Mediterranean. Global and Planetary Change, 169, 156-167.

Burrato, P., Poli, M.E., Vannoli, P., Zanferrari, A., Basili, R., Galadini, F., 2008. Sources of Mw 5+ earthquakes in northeastern Italy and western Slovenia: an updated view based on geological and seismological evidence. Tectonophysics 453, 157-176.

Carminati, E., Doglioni, C., Scrocca, D., 2003. Apennines subduction-related subsidence of Venice (Italy). Geophysical Research Letters, 30, 1-4.

Carton, A., Bondesan, A., Fontana, A., Meneghel, M., Miola, A., Mozzi, P., Primon, S., Surian, N., 2009. Geomorphological evolution and sediment transfer in the Piave River system (northeastern Italy) since the Last Glacial Maximum. Géomorphologie: relief, processus, environnement, 3, 155-174.

Carulli, G.B., 2011. Structural model of the Trieste Gulf: a proposal. J. Geodyn. 51, 156-165.

Castiglioni, G.B., 2004. Quaternary glaciations in the eastern sector of the Italian Alps. Developments in Quaternary Science (Vol. 2). Elsevier B.V.

Chaumillon, E., Tessier, B., Reynaud, J.-Y., 2011. Variability of Incised Valleys and Estuaries Along French Coasts: An Analog to Oil Reservoirs Where Topography Influence Preservation Potential?. CSPG CSEG CWLS Convention.

Chaumillon, E., Proust, J.-N., Ménier, D., Weber, N., 2008. Incised-valley morphologies and sedimentary-fills within the inner shelf of the northern Bay of Biscay. Journal of Marine Systems, 72, 383-396.

Chaumillon, E., Tessier, B., Reynaud, J.Y., 2010. Stratigraphic records and variability of Incised valleys and estuaries along French coasts. Bulletin de La Societe Geologique de France, 181, 75-85.

Clark, P., Dyke, A., Shakun, J., Carlson, A., Clark, J., Wohlfarth, B., Mitrovica, J., Hostetler, S., McCabe, A., 2009. The Last Glacial Maximum. Science, 325, 710-714.

Clement, A.J.H., Fuller, I.C., 2018. Influence of system controls on the Late Quaternary geomorphic evolution of a rapidly-infilled incised-valley system: The lower Manawatu valley, North Island New Zealand. Geomorphology, 303, 13-29.

Comel, A., 1934. L'alta e media pianura del Friuli Occidentale tra Tagliamento e Livenza. Annali Staz. Chim. Agr. Sperim. Udine, 3, 4, 188 pp.

Comel, A., 1940. Carta Geoagronomica della zona del Basso Friuli Occidentale e territori contermini, scala 1:100.000. Stazione per la Sperimentazione Chimico Agraria di Udine.

Comel A., 1950. La bassa pianura del Friuli occidentale tra Tagliamento e Livenza. Annali Stazione chimico-agraria sperimentale di Udine, 3 (7), Udine.

Comel A., 1958. I terreni della zona inferiore della Bassa Pianura Friulana. Udine, Arti Grafiche Friulane, 81.

Covelli, S., Fontolan, G., Faganeli, J., Ogrinc, N., 2006. Anthropogenic markers in the Holocene stratigraphic sequence of the Gulf of Trieste (northern Adriatic Sea). Marine Geology, 230(1-2), 29-51.

Croce Da Villa, P., Di Filippo Balestrazzi, E., (eds), 2003. Concordia. Tremila anni di storia. Esedra, Padova, 393.

Dalrymple, R.W., Zaitlin, B.A., Boyd, R., 1992. Estuarine facies models; conceptual basis and stratigraphic implications. Journal of Sedimentary Research, 62(6), 1130-1146.

Dalrymple, R.W., Choi, K., 2007. Morphologic and facies trends through the fluvial-marine transition in tide-dominated depositional systems: A schematic framework for environmental and sequence-stratigraphic interpretation. Earth-Science Reviews, 81(3-4), 135-174.

De Clercq, M., Missiaen, T., Wallinga, J., Zurita Hurtado, O., Versendaal, A., Mathys, M., De Batist, M., 2018. A well-preserved Eemian incised-valley fill in the southern North Sea Basin, Belgian Continental Shelf-Coastal Plain: Implications for northwest European landscape evolution. Earth Surface Processes and Landforms, 43, 1913-1942.

Donegana, M., Fontana, A., Paiero, G., Ravazzi, G., 2005. Aspetti geomorfologici dell'area di Bannia-Palazzine di Sopra. In: Visentini P., (eds), Bannia-Palazzine di Sotto (PN), una comunitá preistorica del V millennio a.C. Quaderni del Museo Archeologico del Friuli Occidentale, 5. Pordenone, 9-16.

Estournòs, G., Menier, D., Guillocheau, F., Le Roy, P., Paquet, F. and Goubert, E., 2012. The paleo-Etel River incised valley on the Southern Brittany inner shelf (Atlantic coast, France): Preservation of Holocene transgression within the remnant of a middle Pleistocene incision? Marine Geology, 329-331, 75-92.

FAO-ISRIC, 2006. Guidelines for Soil Description, fourth ed. International Soil Reference Information Centre, Rome. 97 pp.

Favaretto S., Sostizzo, I., 2006. Vegetazione e ambienti del passato nell'area di Concordia Sagittaria (VE). Quaderni del Dottorato 1, Dipartimento di Geografia Universitá di Padova, 57-69.

Feruglio, E., 1925. Carta geologica delle Tre Venezie. Foglio 25 "Udine". Ufficio Idrografico Regio Magistrato Acque di Venezia.

Fontana, A., Mozzi, P., Bondesan, A., 2004. L'evoluzione geomorfologica della Pianura Veneto-Friulana. In: Bondesan, A., Meneghel, M., (eds), 113-136.

Fontana, A., 2006. Evoluzione geomorfologica della bassa pianura friulana e sue relazioni con le dinamiche insediative antiche. Enclosed Geomorphological

Map of the Low Friulian Plain scale 47. Monografie Museo Friulano Storia Naturale, Udine, 288 pp.

Fontana, A., Mozzi, P., Bondesan, A., 2008. Alluvial megafans in the Venetian-Friulian Plain (north-eastern Italy): Evidence of sedimentary and erosive phases during Late Pleistocene and Holocene. Quaternary International, 189, 71-90.

Fontana, A., Mozzi, P., Bondesan, A., 2010. Late Pleistocene evolution of the Venetian-Friulian Plain. Rendiconti Lincei, 21(SUPPL. 1), 181-196.

Fontana A., Bondesan A., Meneghel M., Toffoletto F., Vitturi A., Bassan V., (eds), 2012. Note illustrative della Carta Geologica d'Italia alla scala 1:50.000-Foglio 107 "Portogruaro". Regione Veneto, Infocartografica, Piacenza, 196 pp.

Fontana, A., Mozzi, P., Marchetti, M., 2014a. Alluvial fans and megafans along the southern side of the Alps. Sedimentary Geology, 301, 150-171.

Fontana, A., Monegato, G., Devoto, S., Zavagno, E., Burla, I., Cucchi, F., 2014b. Evolution of an Alpine fluvioglacial system at the LGM decay: The Cormor megafan (NE Italy). Geomorphology, 204, 136-153.

Fontana, A., 2015. Il contesto paleoambientale. In: Rinaldi F., Vigoni A., (eds), Le necropoli della media e tarda etá imperiale (III-IV secolo d.C.) a Iulia Concordia e nell'arco alto adriatico-organizzazione spaziale, aspetti monumentali e strutture sociali atti del convegno di studio, Concordia Sagittaria, 5-6 giugno 2014. Gr. A.V.O., Album, 20, 21-32.

Fontana, A., Vinci, G., Tasca, G., Mozzi, P., Vacchi, M., Bivi, G., Salvador, S., Rossato, S., Antonioli, F., Asioli, A., Bresolin, M., Di Mario, F., Hajdas, I., 2017. Lagoonal settlements and relative sea level during Bronze Age in Northern Adriatic: Geoarchaeological evidence and paleogeographic constraints. Quaternary International, 439, 17-36.

Fontana, A., Ronchi, L., Rossato, S., Mozzi, P., 2018. Lidar-derived dems for geoarchaeological investigations in alluvial and coastal plains. Alpine and Mediterranean Quaternary, 31, 13-14.

Frassine, M., Fontana, A., Bezzi, A., 2014. Viabilitá romana nel territorio di Morsano al Tagliamento (PN): la direttrice Concordia-Norico dal telerilevamento allo scavo archeologico. Journal of Ancient Topography 23, 107-128.

Galadini, F., Poli, M.E., Zanferrari, A., 2005. Seismogenic sources potentially responsible for earthquakes with M ≥ 6 in the eastern southern Alps (Thiene-Udine sector, NE Italy). Geophysical Journal International 161, 739-762.

Gibbard, P.L., Hughes, P.D., Rolfe, C.J., 2017. New insights into the Quaternary evolution of the Bristol Channel, UK. Journal of Quaternary Science, 32, 564-578.

Gibling, M.R., Fielding, C.R., Sinha, R., 2011. Alluvial Valleys and Alluvial Sequences: Towards a Geomorphic Assessment. In From River to Rock Record. SEPM Special Publication, 97, 423-447.

Gregoire, G., Le Roy, P., Ehrhold, A., Jouet, G., Garlan, T., 2017. Control factors of Holocene sedimentary infilling in a semi-closed tidal estuarine-like system: the bay of Brest (France). Marine Geology, 385, 84-100.

Green, A.N., Dladla, N., Garlick, G.L., 2013. Spatial and temporal variations in incised valley systems from the Durban continental shelf, KwaZulu-Natal, South Africa. Marine Geology, 335, 148-161.

Harrison, S., Smith, D.E., Glasser, N.F., 2018. Late Quaternary meltwater pulses and sea level change. Journal of Quaternary Science.

Hippe, K., Fontana, A., Hajdas, I., et al., 2018. A high-resolution 14C chronology tracks pulses of aggradation of glaciofluvial sediment on the Cormor megafan between 45 and 20 ka BP. Radiocarbon, 60, 857-874.

Huuse, M., Lykke-Andersen, H., 2000. Overdeepened Quaternary valleys in the eastern Danish North Sea: Morphology and origin. Quaternary Science Reviews, 19, 1233-1253.

Labaune, C., Tesson, M., Gensous, B., Parize, O., Imbert, P., Delhaye-Prat, V., 2010. Detailed architecture of a compound incised valley system and correlation with forced regressive wedges: Example of Late Quaternary Têt and Agly rivers, western Gulf of Lions, Mediterranean Sea, France. Sedimentary Geology, 223, 360-379.

Lambeck, K., Antonioli, F., Anzidei, M., Ferranti, L., Leoni, G., Scicchitano, G., Silenzi, S., 2011. Sea level change along the Italian coast during the Holocene and projections for the future. Quaternary International, 232, 250-257.

Lericolais, G., Féniés, H., Tastet, J.-P., Berné, S., 1998. High resolution seismic stratigraphy of the Gironde paleovalley on the continental shelf. Marine Geology, 326, 701-708.

Lericolais, G., Berné, S., Féniés, H., 2001. Seaward pinching out and internal stratigraphy of the gironde incised valley on the shelf (bay of biscay). Marine Geology, 175, 183-197.

Lericolais, G., Auffret, J.P., Bourillet, J.F., 2003. The Quaternary Channel River: Seismic stratigraphy of its palaeo-valleys and deeps. Journal of Quaternary Science, 18, 245-260.

Lin, C.M., Zhuo, H.C., Gao, S., 2005. Sedimentary facies and evolution in the Qiantang River incised valley, eastern China. Marine Geology, 219, 235-259.

Longhitano, S.G., Della Luna, R., Milone, A.L., Cilumbriello, A., Caffau, M., Spilotro, G., 2015. The 20,000-years-long sedimentary record of the Lesina coastal system (southern Italy): From alluvial, to tidal, to wave process regime change. The Holocene, 26, 678-698.

Marcello, A., Comel, A., 1963. L'alluvione che seppellí Julia Concordia. Memorie Biogeografia Adriatica, Istituto Studi Adriatici 5, 139-145.

Martínez-Carreño, N., García-Gil, S., 2017. Reinterpretation of the Quaternary sedimentary infill of the Ría de Vigo, NW Iberian Peninsula, as a compound incised valley. Quaternary Science Reviews, 173, 124-144.

Macklin, M.G., Jones, A.F., Lewin, J., 2010. River response to rapid Holocene environmental change: evidence and explanation in British catchments. Quat. Sci. Rev. 29, 1555-1576.

Maselli, V., Trincardi, F., 2013. Large-scale single incised valley from a small catchment basin on the western Adriatic margin (central Mediterranean Sea). Global and Planetary Change, 100, 245-262.

Maselli, V., Trincardi, F., Asioli, A., Ceregato, A., Rizzetto, F., Taviani, M., 2014. Delta growth and river valleys: The influence of climate and sea level changes on the South Adriatic shelf (Mediterranean Sea). Quaternary Science Reviews, 99, 146-163.

Mattheus, C.R., Rodriguez, A.B., Greene, D.L., Simms, A.R., Anderson, J.B., 2007. Control of Upstream Variables on Incised-Valley Dimension. Journal of Sedimentary Research, 77, 213-224.

Mattheus, C.R., Rodriguez, A.B., 2011. Controls on late quaternary incised-valley dimension along passive margins evaluated using empirical data. Sedimentology, 58, 1113-1137.

Miola, A., Bondesan, A., Corain, L., Favaretto, S., Mozzi, P., Piovan, S., Sostizzo, I., 2006. Wetlands in the Venetian Po Plain (northeastern Italy) during the Last Glacial Maximum: Interplay between vegetation, hydrology and sedimentary environment. Review of Palaeobotany and Palynology, 141, 53-81.

Minelli, A., (eds), 2001. Risorgive e fontanili, Acque sorgenti di pianura dell'Italia Settentrionale, Quaderni Habitat 2. Ministero dell'Ambiente, Museo Friulano Storia Naturale, Udine (154 pp.).

Monegato, G., Ravazzi, C., Donegana, M., Pini, R., Calderoni, G.,Wick, L., 2007. Evidence of a two-fold glacial advance during the last glacial maximum in the Tagliamento end moraine system (eastern Alps). Quaternary Research, 68, 284-302.

Monegato, G., Pini, R., Ravazzi, C., Reimer, P. J., Wick, L., 2011. Correlating Alpine glaciation with Adriatic sea-level changes through lake and alluvial stratigraphy. Journal of Quaternary Science, 26, 791-804.

Monegato, G., Poli, M.E., 2015. Tectonic and climatic inferences from the terrace staircase in the Meduna valley, eastern Southern Alps, NE Italy. Quaternary Research, 83, 229-242.

Monegato, G., Scardia, G., Hajdas, I., Rizzini, F., Piccin, A., 2017. The Alpine LGM in the boreal ice-sheets game. Scientific Reports, 7, 1-8.

Mozzi, P., Bini, C., Zilocchi, L., Becattini, R., Mariotti Lippi, M., 2003. Stratigraphy, palaeopedology and palynology of Late Pleistocene and Holocene

deposits in the landward sector of the lagoon of Venice (Italy), in relation to the Caranto level. Il Quaternario, 16, 193-210.

Mozzi, P., Ferrarese, F., Fontana, A., 2013. Integrating Digital Elevation Models and stratigraphic data for the reconstruction of the post-lgm unconformity in the Brenta alluvial megafan (north-eastern Italy). Alpine and Mediterranean Quaternary, 26, 41-54.

Ngueutchoua, G., Giresse, P., 2010. Sand bodies and incised valleys within the Late Quaternary Sanaga-Nyong delta complex on the middle continental shelf of Cameroon. Marine and Petroleum Geology, 27, 2173-2188.

Nordfjord, S., Goff, J.A., Austin, J.A., Sommerfield, C. K., 2005. Seismic geomorphology of buried channel systems on the New Jersey outer shelf: assessing past environmental conditions. Marine Geology, 214, 339-364.

Nordfjord, S., Goff, J.A., Austin, J.A., Gulick, S.P.S., 2006. Seismic Facies of Incised-Valley Fills, New Jersey Continental Shelf: Implications for Erosion and Preservation Processes Acting During Latest Pleistocene-Holocene Transgression. Journal of Sedimentary Research, 76, 1284-1303.

Peeters, J., Busschers, F.S., Stouthamer, E., Bosch, J.H.A., Van den Berg, M W., Wallinga, J., Versendaal, A.J., Bunnik, F.P., Middelkoop, H.,2016. Sedimentary architecture and chronostratigraphy of a late Quaternary incised-valley fill: A case study of the late Middle and Late Pleistocene Rhine system in the Netherlands. Quaternary Science Reviews, 131, 211-236.

Pellegrini, C., Maselli, V., Gamberi, F., Asioli, A., Bohacs, K.M., Drexler, T.D., Trincardi, F., 2017. How to make a 350-m-thick lowstand systems tract in 17,000 years: The Late Pleistocene Po River (Italy) lowstand wedge. Geology, 45, 327-330.

Peltier, W.R., 2004. Global glacial isostasy and the surface of the ice-age earth: the ice-5G (VM2) model and grace. Annu. Rev. Earth Planet. Sci. 32, 111-149.

Pérès, J.M., Picard, J., 1964. Nouveau manuel de bionomie benthique de la mer Méditerranée. Rech. Trav. Stat. Marit. Endoume 31, 1-137.

Pini, R., Ravazzi, C., Reimer, P.J., 2010. The vegetation and climate history of the last glacial cycle in a new pollen record from Lake Fimon (southern Alpine foreland, N-Italy). Quaternary Science Reviews, 29(23-24), 3115-3137.

Posamentier, H.W., Allen, G.P., 1993. Variability of the sequence stratigraphic model: effects of local basin factors. Sedimentary Geology, 86, 91-109.

Reimer, P.J., Bard, E., Bayliss, A., Beck, J.W., Blackwell, P.G., Bronk Ramsey, C., Grootes, P.M., Guilderson, T.P., Haflidason, H., Hajdas, I., Hatté, C., Heaton, T.J., Hoffmann, D.L., Hogg, A.G., Hughen, K.A., Kaiser, K.F., Kromer, B., Manning, S.W., Niu, M., Reimer, R.W., Richards, D.A., Scott, E.M., Southon, J.R., Staff, R.A., Turney, C.S.M., van der Plicht, J., 2013. IntCal13 and Marine13 Radiocarbon Age Calibration Curves 0-50,000 Years cal BP. Radiocarbon 55, 1869-1887.

Ronchi, L., Fontana, A., Correggiari, A., Asioli, A., 2018. Late Quaternary incised and infilled landforms in the shelf of the northern Adriatic Sea (Italy). Marine Geology, 405, 47-67.

Rossato, S., Fontana, A., Mozzi, P., 2015. Meta-analysis of a Holocene ^{14}C database for the detection of paleohydrological crisis in the Venetian-Friulian Plain (NE Italy). Catena, 130, 34-45.

Rossignoli, C., Pujatti, E., Vicenzutto, D., Reggiani, P., De Angeli, G., Groppo, V., 2014. Concordia Sagittaria localitá Loncon. Scavo di un sito multifase di etá preistorica. Notiziario Archeologia del Veneto, 1, 37-48.

Schumm, S.A., 1993. River Response to Baselevel Change: Implications for Sequence Stratigraphy River Response to Baselevel Change: Implications for Sequence Stratigraphy. Source: The Journal of Geology, 101, 279-294.

Simms, A.R., Aryal, N., Miller, L., Yokoyama, Y., 2010. The incised valley of Baffin Bay, Texas: a tale of two climates. Sedimentology 57, 642-669.

Soil Survey Staff, 1999. Soil Taxonomy: A Basic System of Soil Classification for Making and Interpreting Soil Surveys. second ed. USDA-SCS Agric. Handb. 436. US Gov. Print. Office, Washington, DC.

Surian, N., Ziliani, L., Comiti, F., Lenzi, A.M., Mao, L., 2009. Channel adjustments and alter- ations of sediment fluxes in gravel-bed rivers of north-

eastern Italy: potentials and limitations for channel recovery. River Res. Appl. 25, 551-567.

Surian, N., Fontana, A., 2017. The Tagliamento River: The Fluvial Landscape and Long-Term Evolution of a Large Alpine Braided River. In: Soldati M., Marchetti M., (eds) Landscapes and Landforms of Italy. World Geomorphological Landscapes. Springer, Cham.

Tanabe, S., Nakanishi, T., Yasui, S., 2010. Relative sea-level change in and around the Younger Dryas inferred from late Quaternary incised-valley fills along the Japan Sea. Quaternary Science Reviews, 29, 3956-3971.

Tanabe, S., Nakanishi, T., Matsushima, H., Hong, W., 2013. Sediment accumulation patterns in a tectonically subsiding incised valley: Insight from the Echigo Plain, central Japan. Marine Geology, 336, 33-43.

Thien, S.J., 1979. A flow diagram for teaching texture by feel analysis. Journal of Agronomic Education, 8, 54-55.

Thomas, M.A., Anderson, J.B., 1989. Glacial eustatic controls on seismic sequences and parasequences of the Trinity/Sabine incised valley, Texas Continental Shelf: Gulf Coast. Association of Geological Societies Transactions 39, 563-570.

Thomas, M.A., Anderson, J.B., 1994. Sea-level controls on the facies architecture of the Trinity/Sabine incised-valley system, Texas continental shelf. In: Dalrymple, R.W., Boyd, R., Zaitlin, B.A., (eds) Incised-Valley Systems: Origin and Sedimentary Sequences: SEPM Special Publications, 51, 63-82.

Tockner, K., Ward, J.V., Arscott, D.B., Edwards, P.J., Kollmann, J., Gurnell, A.M., Petts, G.E., Maiolini, B., 2003. The Tagliamento River: a model ecosystem of European importance. Aquat. Sci. 65, 239-253.

Traini, C., Menier, D., Proust, J.N., Sorrel, P., 2013. Transgressive systems tract of a ria-type estuary: The late holocene vilaine river drowned valley (France). Marine Geology, 337, 140-155.

Trincardi, F., Argnani, A., Correggiari, A., 2011. Note illustrative della Carta Geologica d'Italia alla scala 1:250,000-Foglio NL33-7 "Venezia", ISPRA-Servizio Geologico d'Italia.

Tropeano, M., Cilumbriello, A., Sabato, L., Gallicchio, S., Grippa, A., Longhitano, S.G., Bianca, M., Gallipoli, M.R., Mucciarelli, M., Spilotro, G., 2013. Surface and subsurface of the Metaponto Coastal Plain (Gulf of Taranto-southern Italy): Present-day- vs LGM-landscape. Geomorphology, 203, 115-131

Vacchi, M., Marriner, N., Morhange, C., Spada, G., Fontana, A., Rovere, A., 2016. Multiproxy assessment of Holocene relative sea-level changes in the western Mediterranean: variability in the sea-level histories and redefinition of the isostatic signal. Earth Science Reviews, 155, 172-197.

Valle, G., Vercesi, P.L., 1996. Concordia Sagittaria, Sintesi della situazione paleoambientale. In: Bianchin Citton E., Vitri S., (eds), La Protostoria tra Sile e Tagliamento, catalogo della mostra, Esedra, Padova, 188-195.

Venturini, C., 2003. Il Friuli nel Quaternario: evoluzione del territorio. In Muscio G., (eds), Glacies, l'età dei ghiacci in Friuli, ambienti climi e vita negli ultimi 100 000 anni, catalogo della mostra, Museo Friul. St. Nat., Udine, 23-106.

Vis, G.J., Kasse, C., 2009. Late Quaternary valley-fill succession of the Lower Tagus Valley, Portugal. Sedimentary Geology 221, 19-39.

Vis, G.J., Cohen, K.M., Westerhoff, W.E., Ten Veen, J.H., Hijma, M.P., van der Spek, J.K., Vos, P.C., 2015. Paleogeography. In: Shennan J., Long A.J., Horton B.P., (eds), Handbook of Sea-Level Research. Wiley, 514-535.

Zaitlin, B.A., Shultz, B.C., 1990, Wave-influenced estuarine sand body, Senlac heavy oil pool, Saskatchewan, Canada, in Barwis, J.H., McPherson, J.G., and Studlick, J.R.J., eds, Sandstone Petroleum Reservoirs: New York, Springer-Verlag, 363-387.

Zanferrari, A., Avigliano, R., Monegato, G., Paiero, G., Poli, M.E., (eds), 2008a. Note illustrative della Carta Geologica d'Italia alla scala 1:50.000-Foglio 066 Udine. APAT-Regione Friuli Venezia Giulia, Graphic Line sas, Tavagnacco (UD), 176 pp.

Zanferrari, A., Avigliano R., Grandesso, P., Monegato, G., Paiero, G., Poli, M.E., Stefani, C., (eds), 2008b. Note illustrative della Carta Geologica

d'Italia alla scala 1:50.000-Foglio 065 Maniago. APAT-Regione Friuli Venezia Giulia, Graphic Line sas, Tavagnacco (UD), 224 pp.

Zanferrari, A., Avigliano, R., Fontana, A., Paiero, G., (eds), 2008c. Note illustrative della Carta Geologica d'Italia alla scala 1:50.000-Foglio 086 San Vito al Tagliamento. APAT-Regione Friuli Venezia Giulia, Graphic Line sas, Tavagnacco (UD), 190 pp.

LATE QUATERNARY INCISED AND INFILLED LANDFORMS IN THE SHELF OF THE NORTHERN ADRIATIC SEA (ITALY)

Abstract

The northern Adriatic shelf is punctuated by the presence of several incised and filled features that have been revealed by the offshore seismic and stratigraphic surveys carried out in the last decades. In this study we analyzed an area located in the northern Adriatic shelf, 30 km offshore of the Venice Lagoon and between 29 and 34 m below the mean sea level, where the most impressive examples were identified. By integrating the interpretation of about 3 000 km of high-resolution seismic profiles (CHIRP) with sediment cores, paleontological analyses and radiocarbon dates, it was possible to distinguish between two generations of incised features. The older generation (Nadia) is represented by a fluvial incised valley that reaches a depth of up to 30 m and was formed and infilled during the LGM marine lowstand, probably between ca. 26 and 24 ka cal BP. The peculiar horizontal layering displayed by the infilling is characteristic of a low-energy environment. This suggest that, after its formation, the valley was first occupied by a swampy environment, which was then gradually filled-up with sediments received from nearby riverine systems. Differently, the younger generation (Attila) consists of a set of tidal inlets and channels with a maximum depth of 20 m, which are the legacy of a transgressive lagoon environment. The tidal nature of these features is confirmed by the geometry and paleontological content of their infilling and by their overall morphological and morphometric characteristics. The transgressive lagoon where these channels developed probably existed for just few centuries in the Early Holocene (ca. $10 - 9$ ka cal BP). This period likely coincides with a temporary deceleration or stasis of the sea-level rise rate. This work presents new results for the paleogeographic and paleoenvironmental reconstruction of the northern Adriatic area, covering a period that spans from the middle LGM to the beginning of the Holocene.

101

The marine fluctuations that occurred during the last glacial-eustatic cycle led the coastal zones and continental shelves to experience strong environmental variations. These changes are associated to the progressive subaerial exposure of vast areas during the marine forced regression and lowstand phases, while the subsequent transgression induced their drowning (Fairnaks, 1989; Fleming et al., 1998; Blum and Törnqvist, 2000; Cattaneo et al., 2003; Lambeck et al., 2014). As generally observed on a global scale, these dramatic changes mainly affected the continental shelves, while along the present coastal belt only the last phase of transgression and the marine highstand (i.e. last 8 000 years), left traces within the incised valleys infillings (e.g. Allen et al., 1993; Vis and Kasse et al., 2009; Breda et al., 2016; Clement et al., 2017) and in the highstand stratigraphy and landforms (cf. Vacchi et al., 2016).

Apart from few areas, in the Mediterranean Basin the first steps of the post-glacial transgression are generally almost completely lacking because of the absence of the continental shelf or its very steep gradient (Benjamin et al., 2017 and reference therein). A peculiar situation characterizes the northern Adriatic Sea, where the shelf has a very low gradient (ca. 0.4‰) and the distance from the present coastline to the shelf edge reaches 300 km (Fig. 3.1). This setting allowed to record part of the environmental changes that occurred during the Late Pleistocene and Holocene in the sedimentary structures and in the depositional geometries preserved beneath the seafloor. These features can provide valuable information on the sea-level rise history (e.g. Storms et al., 2008; Trincardi et al., 2011; Vacchi et al., 2016) and on the morphological response of the alluvial and coastal systems to climate changes and marine transgression (Maselli et al., 2011; Fontana et al. 2014).

The presence in the northern Adriatic of subtle and elongated sandy ridge-like features (Fig. 2), is interpreted as the legacy of barrier-island systems formed during pulsations of the postglacial sea-level rise (Cattaneo and Steel, 2003; Trincardi et al., 2001, 2014). These morphologies were strongly eroded and reshaped after being drowned (Correggiari et al., 1996; Storms et al., 2008; Trincardi et al., 2014).

Another group of important sea floor features located north of the Po Delta consists of infilled incised channels/valleys that currently have almost no bathymetric expression, but have been recognized through geophysical soundings and

sediment cores since the early 90's (Trincardi et al., 1994, 2011; Correggiari et al., 1996; Zecchin et al., 2008). These features have been generically described as "incised valleys" and their average characteristics (width: $150 - 500$ m, maximum depth up to $25 - 30$ m, fine-grain infill) make them rather similar to the late-Pleistocene fluvial incisions recognized in the distal sector of the Venetian-Friulian Plain (e.g. Carton et al., 2009; Mozzi et al., 2013; Fontana et al. 2014).

With the outbreak of the sequence stratigraphy the relation between incised valleys and relative sea-level change became a major research topic. The concepts related to the incised valleys formation, already described in the first seminal works (e.g. Van Wagoner et al., 1990; Hunt and Tucker, 1992; Dalrymple et al., 1994), have been revisited, refined and integrated during the last two decades (e.g. Blum and Törnqvist, 2000, Dalrymple et al., 2006; Boyd et al., 2006; Blum et al., 2013). Incised valleys constitute a major element in hydrocarbon exploration and paleoenvironmental reconstruction (Simms et al., 2010; Maselli and Trincardi, 2013; Bhattacharya et al., 2015). In particular, the fillings of Late Quaternary incised valleys often constitute the only available sedimentary records of the lowstand and transgressive phases on the shelf, which were generally erased by the marine transgression on the rest of the surface, especially on low-gradient shelves (Li et al., 2006; Nordfjord et al., 2006; Simms et al., 2010; Blum et al., 2013; Weschenfelder et al., 2014; Bogemans et al., 2016; De Clerq et al., 2018). We analyzed one of the most impressive group of these incised and filled features, that are currently located about 30 km offshore of the southern part of the Venice Lagoon (Fig. 2), in a sector where the depth of the present seafloor is about 30 m below present mean sea level (MSL). Through the analysis of a large dataset of seismic lines and cores retrieved during several oceanographic cruises, we reconstruct the planform and morphology of two different generations of channelized incisions and characterize their sediment infill, with the aim of understanding how the local and regional factors forced the evolution of these features. In particular, the stratigraphic sequence recorded by the infill of these incised landforms has been preserved from the erosive processes connected to the marine transgression. It therefore represents one of the few available archives that allow to investigate the processes and environmental changes occurred in the Adriatic shelf since the end of the last glaciation and to constrain the sea-level fluctuations that took place at the beginning of the Holocene, when the rate of transgression
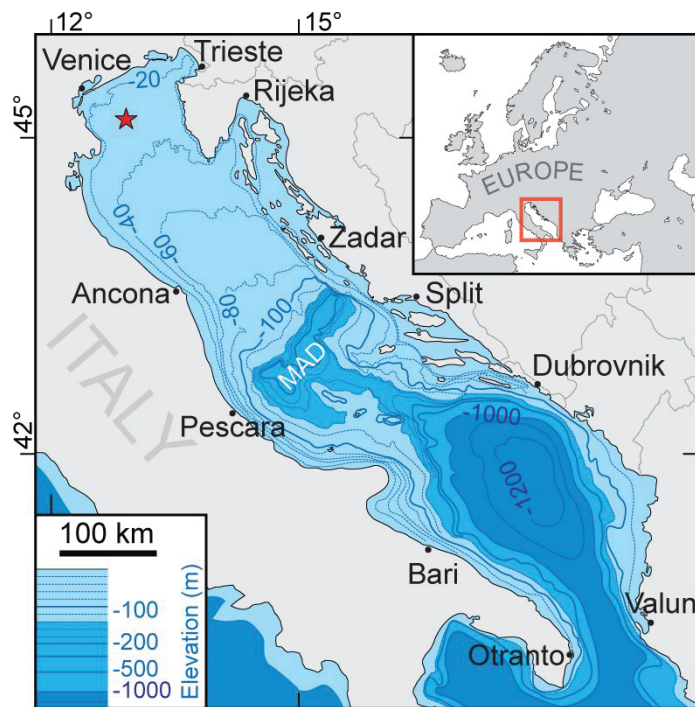
Figure 3.1: Geographical location and bathymetry of the Adriatic Sea. The area analyzed in this study is indicated with a star.

was high.

3.2 REGIONAL SETTINGS

The Adriatic, a narrow and elongated epicontinental sea that separates the Italian Peninsula from the Dinaric-Balcanic mainland (Fig. 1), is located in the foreland basin existing between the Apennines, the Alps and the Dinarids. This structural setting is related to the convergence of Africa and Europe, which caused the subduction of the Adria microplate both under the Apennines and the Dinarids (Doglioni, 1993; Ghielmi et al., 2010). According to its structural, morphological and oceanographic characteristics, the Adriatic basin can be divided in three sectors from North to South. The northern Adriatic consists of a long shelf that is extending with a gentle slope (about 0.4‰) for more than 300 km. A complex microrelief with metric undulations and local scours that can reach depths of 5 m characterizes the seafloor of this area (Giorgietti and Mosetti, 1969; Gordini et al., 2003; Trincardi et al., 2014; Trobec et al., 2017). The Mid Adriatic Deep (MAD) reaches a maximum depth of -260
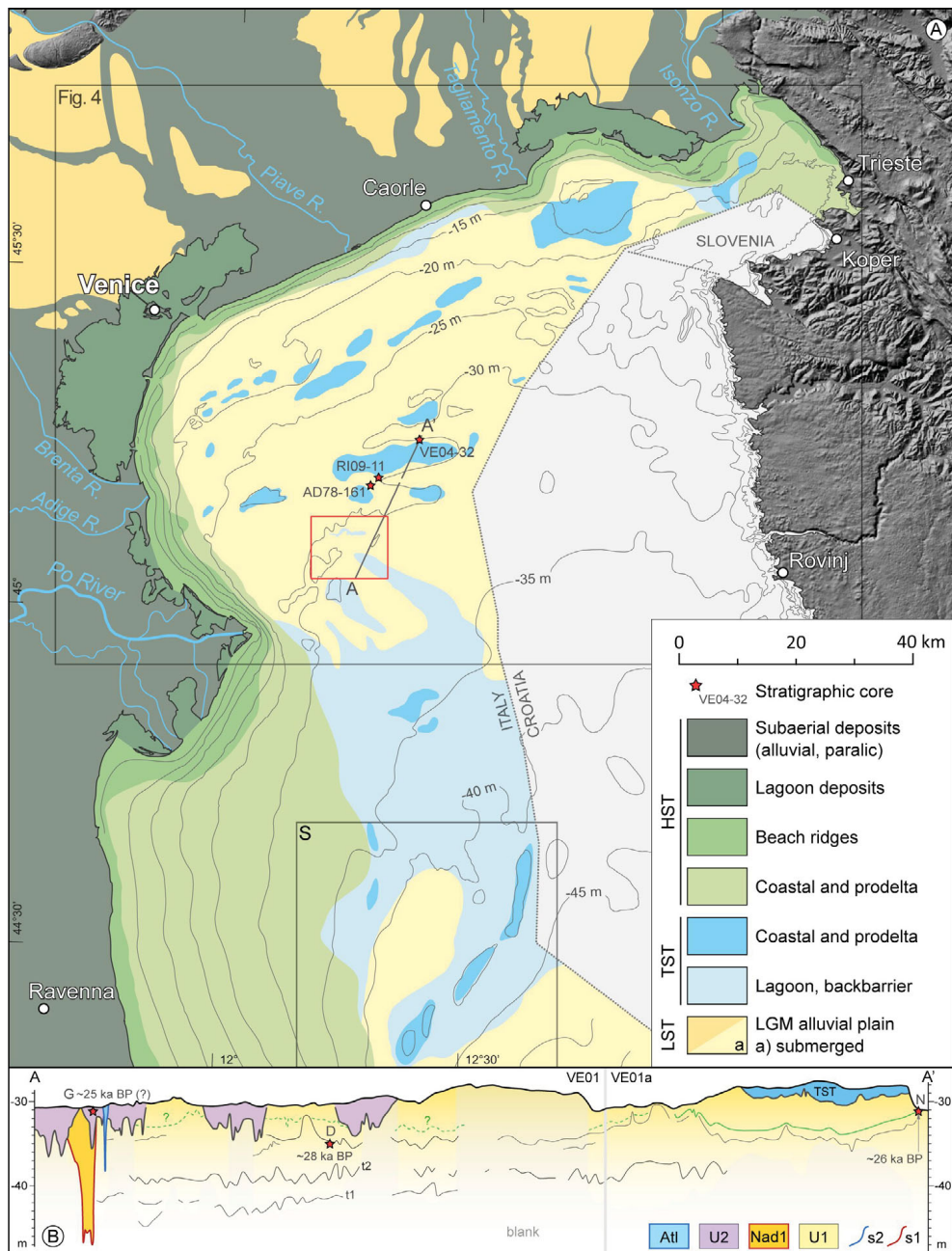
Figure 3.2: (A) Geological map of the northern Adriatic Sea. The upper frame indicates the location of the area represented in Fig. 3.4. The lower frame, marked with an S, identifies a portion of the area addressed in Storms et al., (2008). (B) Line drawing of a regional CHIRP profile that shows the stratigraphic relations among the different units described in this work. Some dates and cores location are reported.

.

m and extends from the shelf break (ca. -120 m MSL) to the structural high of Tremiti Islands. The Southern Adriatic have a maximum depth of about -1200 m MSL and it is separated from the Ionian Sea by the Otranto Strait (Trincardi et al., 2014). The subsurface of the northern Adriatic, in its western side and in the adjacent coastal regions (i.e. Po and Venetian-Friulian plains), consists of Quaternary deposits, with a thickness spanning from few hundreds to some thousands of meters (Ghielmi et al., 2010; Amorosi et al., 2017b). These deposits are characterized by the alternation of shallow-marine and continental sediments that constitutes the transgressive-regressive sequences related to the late Quaternary glacial-eustatic cycles (Amorosi et al., 2003; Massari et al., 2004; Fontana et al., 2010; Zecchin et al., 2017).

After the last interglacial highstand (i.e. MIS 5.5, $132 - 116$ ka cal BP), when the sea reached a height of 6 ± 3 m above present MSL (Antonioli et al., 2009), the marine level dropped with a fluctuating trajectory, but it was already below -60 m since MIS 4 (i.e. after 75 ka; Waelbroeck et al., 2002; Lambeck et al., 2014; Benjamin et al., 2017 and reference therein). This processes turned the Adriatic shelf into an alluvial plain that reached its maximum extent during the marine lowstand of the Last Glacial Maximum (LGM, $29 - 19$ ka cal BP; Clark et al., 2009), when the sea level was below -120 m MSL (Correggiari et al., 1996; Amorosi et al., 2016). At that time the Po River was probably collecting the contributes of the rivers from the Venetian-Friulian Plain, Istria and northern Dalmatia (De Marchi, 1922; Correggiari et al., 1996; Maselli et al., 2011). Between 32 and 15 ka cal BP the "mega Po" alluvial system built a lowstand wedge that prograded in the MAD for over 40 km with a thickness of 350 m (Trincardi and Correggiari, 2000; Pellegrini et al., 2017). The exposed shelf represented also a refugium region for several botanical and faunal species, as well as a resource area for groups of humans (cf. Vai and Cantelli, 2004; Benjamin et al., 2017). Fluvial systems generally dissected the continental shelf during the LGM marine lowstand, as diffusely documented in several shelves around the World (e.g. Blum and Törnqvist, 2000), and especially in the area of the English Channel (e.g. Lericolais et al., 2003; Chaumillon et al., 2010; Gibbard et al., 2017). This phenomenon has been recognized also in the Mediterranean area (e.g. Jouet et al., 2006; Tropeano et al., 2013) and even in the Southern Adriatic (e.g. Maselli and Trincardi, 2013; Longhitano et al., 2015; Pellegrini et al., 2015. On the contrary, in the shelf of the northern Adriatic the incised features are rare and generally younger

than LGM (Fontana et al., 2008, Fontana et al. 2014; Amorosi et al., 2008, 2017b; Zecchin et al., 2008). This situation, which deviates from the classic sequence stratigraphy paradigm (e.g.Catuneanu, 2006; Blum et al., 2013), was favored by the very gentle slope of the shelf and by the high sedimentary load provided by the main glaciers of the southern Alps, which in some cases reached the plain with their fronts (Castiglioni, 1940; Monegato et al., 2007, 2017). The alluvial plain at the foot of the southern Alps experienced a strong sedimentation during the LGM, with the formation of several alluvial megafans. In the Venetian-Friulian Plain these landforms were characterized by a vertical aggradation ranging between 15 and 35 m, even in the distal sector of the plain (Fontana et al., 2010, Fontana et al. 2014; Rossato and Mozzi, 2016). The area of the Po Plain, from the present delta up to 100 km upstream, was characterized by a system of channels, faintly incised for $5-10$ m below the floodplain level, which originated a huge multistorey sand body with a total thickness of almost 30 m (Stefani and Vincenzi, 2005; Amorosi et al., 2017a). After the LGM the sea rose from the lowstand minimum to almost the present level in about 14 ka (i.e. $19-5.5$ ka cal BP; Bard et al., 1990; Stanford et al., 2011; Lambeck et al., 2014), causing the submersion of the shelf and the impressive widening of the basin in the northern Adriatic (Correggiari et al., 1996; Cattaneo and Trincardi, 1999). This process generated a sequence of backstepping barrier-lagoon systems that have been progressively drowned in place and reworked by the wave action. These transgressive bodies (Fig. 3.3) have been recognized at the depths of -90 m ($15-14.3$ ka cal BP, Storms et al., 2008), -65 m ($12.9-11.5$ ka cal BP, Pellegrini et al., 2015), -42 m ($11-10$ ka cal BP, Storms et al., 2008), -34 m ($10-9.5$ ka cal BP, Moscon et al., 2015), $-22--18$ m ($9-8$ ka cal BP, Trincardi et al., 2011; Correggiari et al., 1996) and $-15--12$ m MSL (before 7.5 ka cal BP, Zecchin et al., 2015). As discussed in the just mentioned papers, a major role in the formation of these bodies was played by the marine transgression, which was punctuated by phases of higher (e.g. meltwater pulses 1A, ca. 14.3 ka cal BP; Alley et al., 2005; Lambeck et al., 2014) and lower, or even null (e.g. in the Younger Dryas; Pellegrini et al., 2015), rates of sea-level rise. It is worth noting that, as demonstrated by numerical models, during the Holocene the tidal range in the northern Adriatic has been steadily set at $0.8-1$ m (Storms et al., 2008). Since the end of the LGM, the presence of sediment traps within the Alpine catchment induced a dramatic decrease in the sedimentary load exported to

the alluvial plain along the southern Alps (cf. Fontana et al., 2008; Carton et al., 2009). This strong sediment starvation triggered a phase of fluvial entrenchment which led to the formation of some incised valleys even in the distal portion of the present Venetian-Friulian Plain (Fontana et al., 2008). The alluvial systems fed by northern Apennines experienced a small depositional phase also during the Late Glacial, but a major stop occurred during the Younger Dryas, when the main rivers slightly entrenched and a characteristic soil formed on the surface of the alluvial plain (Amorosi et al., 2017a,b). This surface was then buried during the last phase of the transgression and is clearly recognizable in the subsurface of the Po Delta. Between ca. 10 and 6.8 ka cal BP, with a short interruption dated ca. $7.8 - 8.3$ ka cal BP, the Adriatic Sea, along with the whole eastern Mediterranean, experienced anoxic bottom water conditions that lead to the formation of the most recent sapropel (S1; Tesi et al., 2017). As illustrated in Fig. 2, the modern Adriatic seafloor mainly consists of lowstand units (i.e. remains of the previous alluvial plain), with patches of transgressive-phase lagoon, paralic and barrier complex deposits. These deposits are overlapped by the highstand sedimentary wedge along the modern coast. The maximum extent of the basin was reached around $5.5 - 4.5$ ka cal BP during a period of relative sea-level stability. A major role in this last relative sea-level rise was played by local factors as tectonic and compaction subsidence (Amorosi et al., 2008, 2017b; Vacchi et al., 2016).

3.3 MATERIALS AND METHODS

The study area is located about 30 km offshore of the modern Venetian coastline (Fig. 2) and this research aims at characterizing the two generations of incised features recognized in this zone. These features have been named "Attila" and "Nadia" after the name of two gas exploration wells that were settled in the area in the 70's.
We analyzed the bathymetric, seismic and stratigraphic data collected in the area during the oceanographic surveys CM92, CM95, VE04, VE05, RI09, NAD12 and AS14, which have been carried out on board of RV Urania and organized by the CNR-ISMAR institute of Bologna (Fig. 3.4). The morphology of the seabed was reconstructed according to the bathymetric surveys carried out through the interpolation of Single Beam sonar data (Trincardi et al., 2014).
Most part of the research is based on the interpretation of geophysical high-
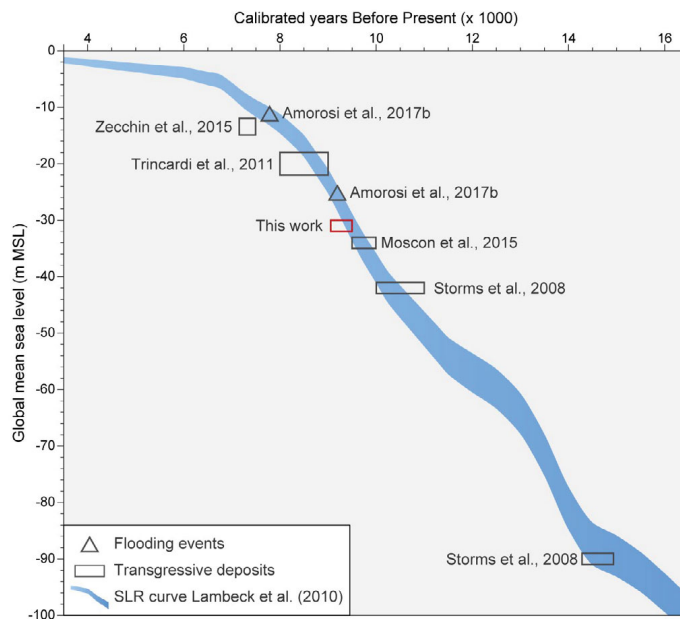
Figure 3.3: Stacking of the RSL curves of the northern Adriatic Sea as reconstructed in Lambeck et al., (2014). The depth and age ranges of the main recognized transgressive deposits are reported along with the relative references. Two major flooding events recorded in the stratigraphy of the Po Delta area are also indicated.

resolution CHIRP (Compressed High Intensity Radar Pulse) profiles, which were acquired with a Teledyne Benthos Chirp-III SBP. This system is composed by a 16 hull-mounted transducer array and uses a $2 - 7$ kHz sweep modulated bandwidth, which allows a vertical resolution in the order of ca. 50 cm. All the collected lines were tracked with a D-GPS in order to obtain the position of the seismic profiles with a decimetric accuracy. The analyzed lines, which extend for more than $3\,000$ km, are evenly distributed over an area of about 400 km^2. Most part of the data was produced interpreting the lines acquired in the missions RI09 and NAD12, that were partly focused on the investigations of the incised features of Nadia and Attila generations (Fig. 3.4). The CHIRP data were acquired with SwanPro v.2.00 software as XTFs and then converted to the open format SEGY. In order to visualize and process the seismic data, SeisPrho v.2.0 software was used (Gasperini and Stanghellini, 2009).

The CHIRP profiles, acquired in water depths of $25 - 35$ m, show a good penetration for the first 8 m, which in some sectors can reach more than 20 m, especially in the case of the filled channels. Under this depth the seismic

response gradually loses definition due to signal dispersion. Some portions of the CHIRP profiles are characterized by little or no seismic response. This blanketing effect can be attributed to the presence of thick sand bodies or gas-bearing deposits that shielded the signal (Orange et al., 2005). In accordance with the literature dealing with the late-Quaternary sea bed and first subsoil of the Adriatic, we used a sound velocity of 1.5 m/ms both for water and sediments in order to migrate the profiles from time to depth domain (e.g. Correggiari et al., 1996; Maselli and Trincardi, 2013; Goff et al., 2006; Nordfjord et al., 2005). All the measurements for each incision (e.g. width, depth, infilling style, see paragraphs 4.2 and 4.3) have been stored into a GIS database (ArcMap ESRI software), and further represented into continuous maps. The plan view reconstruction of the described features has been performed with a manual interpolation of all the available pieces of evidence. An iterative approach has been used for the map drawing, with a preliminary analysis of the seismic facies and cross-cutting relationships among the incised features, which was then refined by checking the consistency of the spatial position of every incision evidence from the seismic profiles.

With the aim of tuning the geophysical interpretation with ground truths and to directly investigate the deposits at the sea floor, ten sediment cores were analyzed. The macropaleontological content of five of them (CM95-01, CM95-02, CM95-03, CM95-04, CM95-05;) is already published (Trincardi et al., 2011), while the others are presented in this work for the first time (RI09-01 and RI09-02 from cruise RISA09; NAD12-14, NAD12-15 and NAD12-16 from NAD12 survey). Part of the cores were collected through a 1.2 tons gravity corer and part with a vibrocorer. Both were equipped with a 6-m long steel barrel. The cores have been splitted in two parts, described and documented with photography. They are currently stored at 4° C in a refrigerated stow room at the CNR-ISMAR in Bologna. Whole-core magnetic susceptibility (χ) for preliminary correlations was measured before splitting using a Bartington MS2 susceptibility meter. The magnetic susceptibility has been provided for comparison with other published works from the Adriatic area (e.g. Cattaneo et al., 2003; Maselli et al., 2011, 2014; Pellegrini et al., 2015). The micropaleontological analysis of the foraminifer assemblages was performed on sediment sampled from cores CM95-01, CM95-02, CM95-03, CM95-04, CM95-05, RI09-01 and NAD12-16. The sediment was dried in oven at 50° C, washed through a 0.063 mm sieve and dried again at 50°

Lab code	Core	Lat N	Lon E	Seafloor (m MSL)	Depth (m)	Material	^{14}C age (a BP)	Calibrated 2σ age (a BP)	Mediane (a BP)	Unit	Fig. 3.15	Source
-	CM95-2	45.123	12.745	-31.0	0.83	C. Glaucum shell	8660 ± 60	9026 - 9446	9249	Atl	A	Trincardi et al. (2011)
-	CM95-3	45.121	12.745	-35.6	3.54	C. Glaucum shell	8730 ± 60	9115 - 9517	9334	Atl	B	Trincardi et al. (2011)
LTL12396A	RI09-1	45.124	12.745	-31.0	4.68	Wood fragment	11007 ± 75	12728 - 13039	12878	Atl	C	This work
LTL12398A	RI09-2	45.119	12.746	-31.3	3.68	Wood fragment	23638 ± 95	27563 - 27918	27742	U1	D	This work
LTL12399A	RI09-11	45.196	12.805	-30.0	2.90	Peat	22384 ± 100	26323 - 27070	26678	U1	E	This work
LTL12400A	RI09-11	45.196	12.805	-30.0	4.55	Wood fragment	25194 ± 100	28934 - 29541	29239	U1	-	This work
ETH-87031	NAD12-14	45.066	12.810	-33.1	1.21	Shell terrestrial	21200 ± 49	25333 - 25730	25558	U2	G	This work
ETH-87032	NAD12-16	45.069	12.810	-33.3	4.92	Shell marine	9045 ± 27	9124 - 9459	9315	Atl	H	This work
-	AD78-161	45.187	12.789	-27.4	1.14	Peat	12210 ± 165	13731 - 14921	14181	-	J	Trincardi et al. (2011)
-	AD78-161	45.187	12.789	-27.4	1.85	Peat	19125 ± 150	22622 - 23463	23040	U1*	K	Trincardi et al. (2011)
-	AD78-161	45.187	12.789	-27.4	2.05	Peat	20110 ± 450	23109 - 25335	24221	U1*	L	Trincardi et al. (2011)
-	VE04-32	45.259	12.889	-31.8	0.41	Peat	21600 ± 110	25678 - 26071	25879	U1	M	Trincardi et al. (2011)
-	VE04-32	45.259	12.889	-31.8	0.67	Peat	22400 ± 110	26329 - 27095	26702	U1	N	Trincardi et al. (2011)
-	VE04-32	45.259	12.889	-31.8	1.22	Peat	23300 ± 130	27321 - 27751	27539	U1	O	Trincardi et al. (2011)

Table 3.1: Radiocarbon dates used in this study. See text for calibration details. Asterisks in the seismic unit column indicate difficulty of attribution due to scarce seismic cover or reworked samples. The reader is referred to the text for more insights. The position of the cores is indicated in Figs. 3.2 and 3.10. The dates for cores CM95 and VE04 are published in Trincardi et al. (2011).

C. The fraction > 0.063 mm was examined for the foraminiferal content (semiquantitative analysis). The paleoenvironmental interpretation followed the models illustrated by D'Onofrio, (1969), Jorissen, (1987, 1988), Hoenegger et al., (1989), Van Der Zwaan and Jorissen, (1991), Barmawidjaja et al., (1992), Jorissen et al., (1992), Langer et al., (1998), Scott et al., (2001), Donnici and Serandrei-Barbero, (2002), Serandrei-Barbero et al., (2004), Mateu-Vicens et al., (2010).

With the aim of constraining the geochronology of the stratigraphic sequence, 14 AMS ^{14}C dates were used in this work (Tab. 3.1). Six dates were carried out on RI09 and NAD12 cores specifically for this work, whereas the remaining eight dates were obtained from literature (Trincardi et al., 2011). All the dates were calibrated with Calib 7.1 software (Stuiver et al., 2017) using the "IntCal13" calibration curve (Reimer et al., 2013). The ages of marine shells were corrected for the marine reservoir effect with a value of 396 ± 61 years according to Reimer and McCormac, (2002). Calendar ages presented hereafter correspond to the 2σ confidence level (Tab. 3.1).

3.4 RESULTS

In this section we describe the information collected in the study area starting from the seismic analyses and then reporting the sedimentological, paleontological and geochronological data collected through the sediment cores.
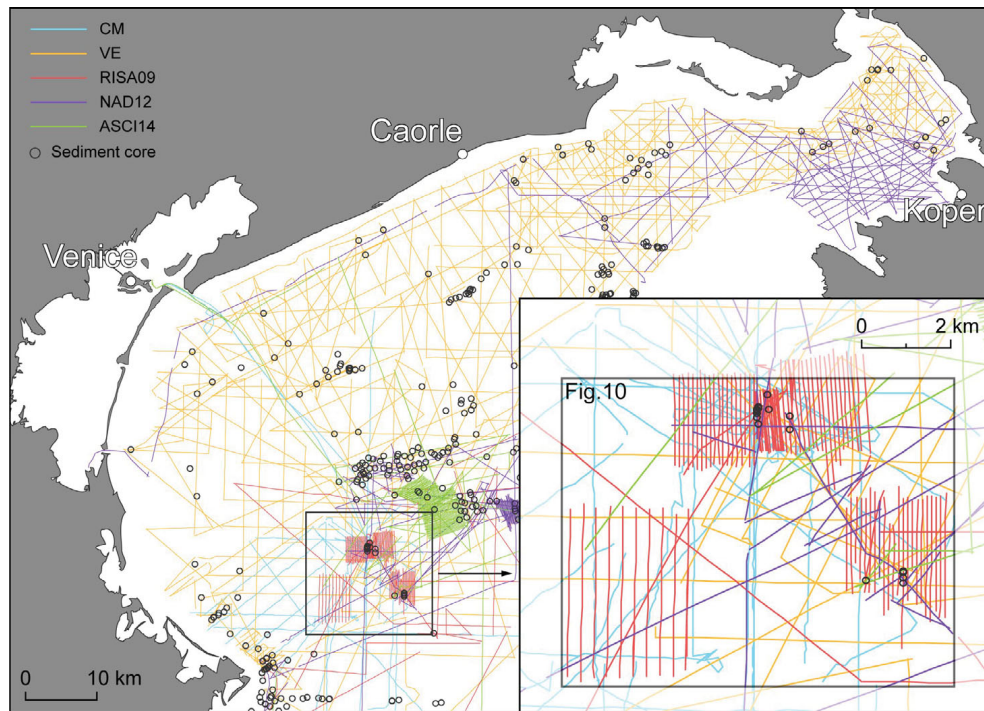
Figure 3.4: Location of the CHIRP profiles and sediment cores (database CNR-ISMAR Bologna). An insight of the analyzed area is provided.

Seismic analysis

In the study area it is possible to distinguish four main seismic units (Figs. 3.5, 3.6 and 3.7), that we named Unit 1, Unit Nad (Nadia), Unit 2 and Unit Atl (Attila). This study mostly focuses on the two generations of incised and infilled features, i.e. Nadia and Attila units. These features are usually easily recognizable as constituted by stratified sedimentary bodies marked at the bottom by an evident erosive unconformity (surface s1 for Nadia, surface s2 for Attila). In several seismic profiles the distinction between the two generations is evident on simple cross-cutting relationship principles, since the Attila features directly intersect those of Nadia (cf. Fig. 3.7). Both the two generations are cut through a unit of regional extent, i.e. Unit 1 (Figs. 3.5, 3.7, 3.8 and 3.9). Moreover, the younger generation (Attila) cuts also another unit (Unit 2), which caps the older generation (Nadia). The present seabed of the whole study area coincides with the wave-ravinement surface (RS), generated by the wave action after the sea transgression (Trincardi et al., 2001, 2011; Catuneanu, 2006). The RS truncates the top of most of the analyzed units.
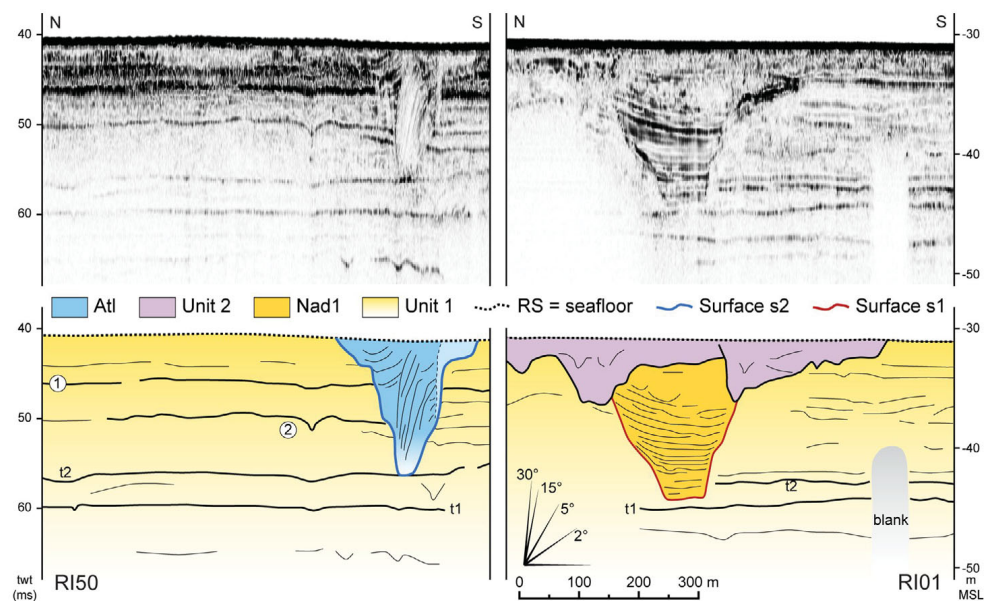
Figure 3.5: Examples of raw CHIRP profiles with line drawing (For location see Fig. 3.10). The interpretation of the units and numbers shown in the figure are provided in the text.

Only the infilling of the older incision was left almost untouched by this process, as the top of this unit has been previously partly reworked and sealed by Unit 2 (Figs. 3.5 and 3.7). The seismic units are here described in accordance with their stratigraphic position, from the older to the younger.

UNIT 1 (U1)   U1 is here defined as the oldest stratigraphic deposit recognized in the entire study area. This unit is mostly characterized by horizontal reflections with scarce lateral continuity and medium to low amplitude (Fig. 3.5). Nevertheless, some rare high-amplitude reflections with a thickness of 10 - 50 cm are recognizable and traceable over surfaces of several tens of squared kilometers (e.g. #1 in Fig. 3.5). In particular, two of these horizons, generally placed at elevations ranging between -35 and -45 m MSL, are easily recognizable in most of the CHIRP profiles of the studied area and were here named t1 and t2 (Figs. 3.5, 3.7 and 3.9). Some reflectors highlight the presence of convex-up features, hundreds of meters wide and slightly elevated $(1 - 2$ m) above the reference surface (#2 in Fig. 3.5). Generally, U1 is still traceable in the CHIRP profiles down to a depth of about $10 - 15$ m below seafloor, while, at greater depths, the seismic signal becomes too weak due to absorption and dispersion

effects. The upper boundary of U1 is represented by an unconformity, as it has been eroded during the processes that led to the formation of the younger units or during the formation of the RS after the marine drowning of the area.

UNIT NADIA (NAD1)   In the CHIRP profiles this unit is clearly bounded at the base by an erosive surface (s1) cut through U1. The seismic facies that characterizes Nad1 is mostly constituted by horizontal reflectors onlapping on s1 and with a high lateral continuity (e.g. line RI110 in Figs. 3.6 and 3.7). As visible in profiles NAD123-S and RI86 (Fig. 3.6, Fig. 3.7 for interpretation), Nad1 is characterized by a rather regular and repetitive pattern of reflections with similar thickness and amplitude. In Nad1 the layers are generally concave-upward and dipping towards the center of the valley, mainly reflecting the geometry of s1 (e.g. # 3, Fig. 3.7). This condition has been probably emphasized by the postdepositional compaction of the sediments, which was more effective in the thicker part of the infill. In some sectors, the upper part of Nad1 is characterized by inclined or slightly convex-upward reflectors, which constitute the subunit Nad1a (e.g. # 4 - 5, Fig. 3.7). In particular, in the profile NAD123-N a set of inclined layers seems to prograde from SE to NW, i.e. upstream along the valley, with a maximum inclination of about 1° (#4, Fig. 3.7). In the north portion of profile NAD123-S some reflectors are arcuate and convex upward (#6, Fig. 3.7) while, in the perpendicular profile (RI86), the same set of layers is dipping northward, i.e. upstream (#7, Fig. 3.8). This geometry reveals the presence of a small lobe within Nad1a that influenced the deposition of the younger sediments. A similar setting is also visible in profile RI79 (#7, Fig. 3.7). The top of Unit Nad1 is sometimes marked by an erosive boundary related to Unit 2 (e.g. #8 in Fig. 3.8).

UNIT 2 (U2)   This unit typically rest on top of Unit Nad1, but in some areas it also lays directly on the top of U1 (cf. Figs. 3.6 and 3.8;Figs. 3.7 and 3.9 for interpretation). U2 is often underlined by an erosive boundary and it is represented by a chaotic seismic facies, characterized by a granular aspect of the signal and a low amplitude seismic response. Nevertheless, in some sectors, rare inclined layers can be recognized (#9 in Fig. 3.7). The internal geometry indicates the presence of channel-like structures with a depth of 1 - 2 m. These geometries are also depicted by the basal erosional surface of this unit (e.g. #10, 11, Fig. 3.7). The average thickness of U2 is 4 m, with peaks of about 7

114

m. The top of this unit was strongly eroded during the formation of the RS (Fig. 3.7).

UNIT ATTILA (ATL)   In the study area several different sedimentary bodies intersect U1, U2 and Nad1. They are marked at the base by a sharp erosive boundary (s2) and are all constituted by the same seismic facies. Thus, these deposits were described as belonging to the seismic unit Atl (Attila-A, -B and -C; cf.; Fig. 3.10). Similarly to Nad1, Unit Atl consists of a thick alternation of dark and light horizons, which is related to the different acoustic impedance of the layers (Figs. 3.5, 3.8 and 3.9). The geometry of the reflectors highlights the presence of draping to lateral-accreting layers (e.g. lines VE148, RI16 in Figs. 3.8 and 3.9) that are often characterized by a low seismic response (e.g. #12, Fig. 3.9). This effect can be attributed to the steepness of these reflectors. In some cases, the geometries depicted by the seismic imaging are complex, with different groups of differently oriented inclined reflectors. This is, for instance, the case of profile VE148 (Fig. 3.9) where the reflectors of #13 are draped on a surface (#14) that truncates the lower reflectors of #15. The upper boundary of Unit Attila is represented by the seafloor, i.e. the ravinement surface.

Core analysis

A series of cores allow the sedimentary and paleontological characterization of the seismic units described above, along with the radiocarbon dating of some organic samples. The detailed description of the identified biofacies is provided in section 3.4. None of the available cores reached this unit because of the depth of Nad1 sediments and the toughness of the younger unit (Unit 2) which is burying them.

UNIT 1 (U1)   The available cores that intercepted U1 (Figs. 3.11 and 3.12) show an alternation of sandy silts, fine sands and clayey silts, punctuated by organic-rich or peaty layers (#1 in Fig. 3.5). The analyzed samples from the upper portion of U1 lack of any micropaleontological content and were attributed to Biofacies C (Paragraph 4.3.3), which is characteristic for a terrestrial environment (Fig. 3.11). The analysis of the cores on a macroscale revealed remains of continental mollusks (e.g. pulmonata gastropods like planorbids) and the presence of carbonate concretions with a diameter of 5 to 15 mm. These features were produced by pedogenetic processes and confirm

the subaerial genesis of this unit. An organic sample collected at a depth of 3.68 m in core RI09-02 was dated to $23\,468 \pm 95\,^{14}C$ a BP ($27.6 - 27.9$ ka cal BP; D, Tab. 3.1), documenting one of the last depositional phases of Unit1 in the study area. Between 5 and 20 km NE of the investigated zone some other samples of U1 were collected by cores AD78-161, VE04-02 and RI09-11 and their ages testify that the formation of the top portion occurred between 29.2 and 23 ka cal BP (Tab. 3.1).

UNIT 2 (U2)   Unit 2 was sampled by two cores (NAD12-14, -15), which reached only a maximum length of 2 m within the upper part of the unit (Fig. 3.11, line RI110). These cores documented the presence of silt, sandy silt and fine sand layers in decimetric alternations. Rare remains of continental gastropods of the genus Planorbis were found in some layers. The traces of mottling processes are evident on the entire length of the analyzed cores and concretions of calcium carbonate with diameters up to 10 mm are present in some intervals. According to these data, U2 represents a continental unit constituted by floodplain and fluvial channel sediments. These deposits were affected by pedogenetic processes which led to the formation of calcic horizons (Bk/Ck). A radiocarbon date performed on a shell of a terrestrial gastropod gave to this unit an age of $21.2\,^{14}C$ ka BP, (G; Tab. 3.1). For considerations on the calibration and interpretation of these dates refer to paragraph 6.1.2.

UNIT ATTILA (ATL)   A wealth of cores sampled Atl, thus allowing a detailed description of this unit (Figs. 3.11 and 3.12). The infilling of the channel consists of alternations of silt and very fine sand layers. In some intervals a centimetric to millimetric lamination is visible, sometimes clearly marked by the occurrence of organic-rich laminae. The micro and macro paleontological analysis indicated the presence of a clear brackish/lagoon faunal association within Atl (Biofacies B, paragraph 4.3.2). This unit is capped by a lag deposit attribute to the wave erosional processes that lead to the formation of the RS. This ravinement lag deposit has a variable thickness ($25 - 50$ cm) and is formed by sandy sediments with abundant remains of mollusks indicative for a shallow marine environment (Biofacies A, paragraph 4.3.1). Unit Atl is typically characterized by almost constant values of the magnetic susceptibility (χ), which ranges between values of 20 and 30 (Fig. 3.11). Radiocarbon dates were carried out on selected samples from cores CM95-2, CM95-3, RI09-1, RI09-2 and NAD12-16 (Tab. 3.1) in order to investigate the geochronology of

the Atl deposits. The results range between $9.5 - 9.0$ ka cal BP, except for the wood fragment recovered by core RI09-1, which has an age of $11\,007 \pm 75^{14}C$ a BP ($13.0 - 12.7$ ka cal BP). A detailed discussion about the geochronology interpretation is provided in paragraph 6.1.3.

Biofacies description

The foraminiferal content of the analyzed cores allowed the distinction of three biofacies, here below described (Fig. 3.11).

BIOFACIES A   The samples contain abundant fine sand along with shell remains (mollusks, bryozoans, ostracods) and bioclasts. Only benthonic foraminifers are present and, in some cases, they are broken or blackened. The assemblage is composed by *Ammonia beccarii tepida* (common), followed in abundance by *Elphidium crispum, Ammonia beccarii, Ammonia papillosa*, and *Elphidium granosum*. Although not common, also the following species are present: Q*uinqueloculina seminulum, Adelosina longirostra, Lobatula lobatula, Asterigerinata mamilla, Buccella granulata, Neoconorbina terquemi, Bigenerina nodosaria, Elphidium advenum, Triloculina trigonula, Eggerella scabra, Triloculina tricarinata, Rosalina globularis, Ammoscalaria pseduospiralis, Planulina ariminensis, Hanzawaia boueana, Adelosina pulchella, Guttulina communis*, and very rare *Nonionella turgida*. This biofacies represents a very shallow marine environment (near-shore area, $< 20 - 25$ m water depth) with probable presence of a vegetal prairie, as suggested by the epiphytic species (i.e. *L. lobatula, A. mamilla, B. granulata, N. terquemi, R. globularis*). However, the concurrent presence of taxa with different preservation state as well of species preferring different environmental characteristics (e.g. epiphytic vs clay-belt taxa) point out the possibility of some reworking. This interpretation is coherent with the one provided by the literature for the malacofaunal content (Trincardi et al., 2011). The same samples examined for the micropaleontological content reveal biosomes and bioclasts of taxa typical of prodelta (the infaunal and detritivorous *Turritella communis, Corbula gibba*) mixed with species of litoral (*Chamaelea gallina*) and transitional (e.g. *Hydrobia ventrosa, Cerastoderma glaucum, Abra ovata*) environment.

BIOFACIES B   The samples contain very-fine micaceous sand and plant fragments. Shell remains (mollusks, ostracods) are present and only benthonic
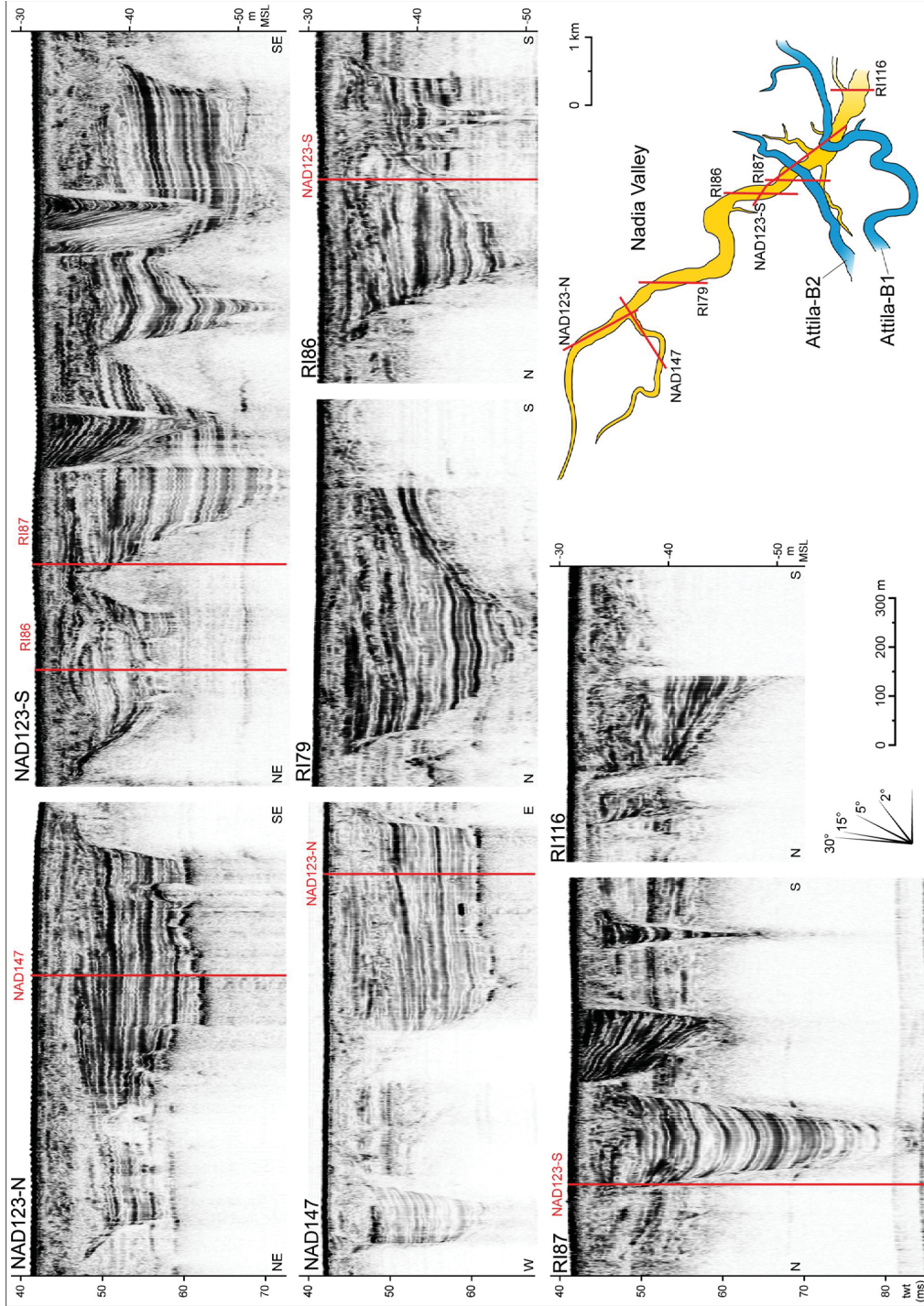
Figure 3.6: Selection of CHIRP profiles of the Nadia valley. The line drawing is provided in Fig. 3.7. See also Fig. 3.10 for location.
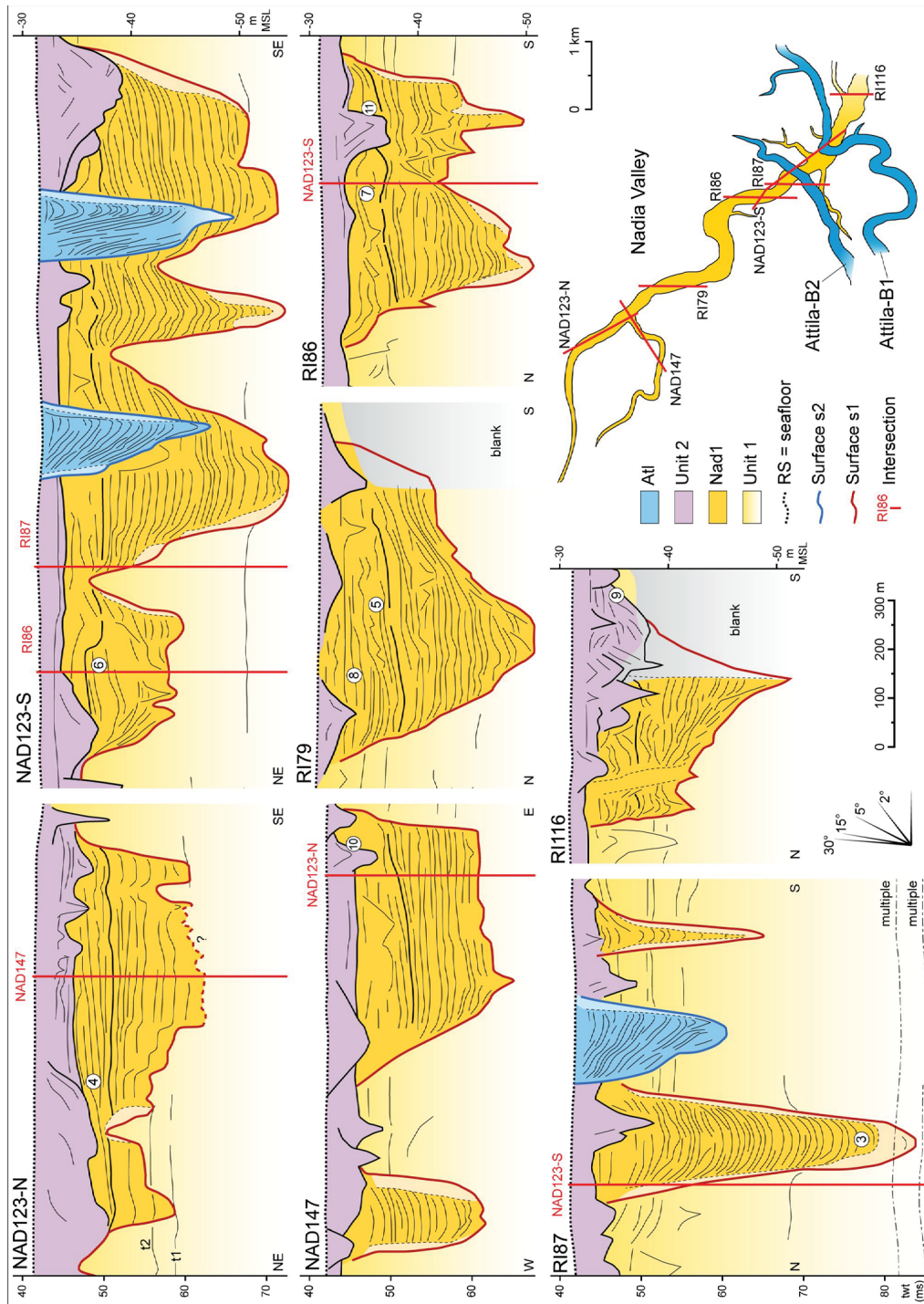
Figure 3.7: Line drawing of the CHIRP profiles shown in Fig. 3.6. The interpretation of the profile and the explanation of the numbers are provided in the text. See also Fig. 3.10 for location.
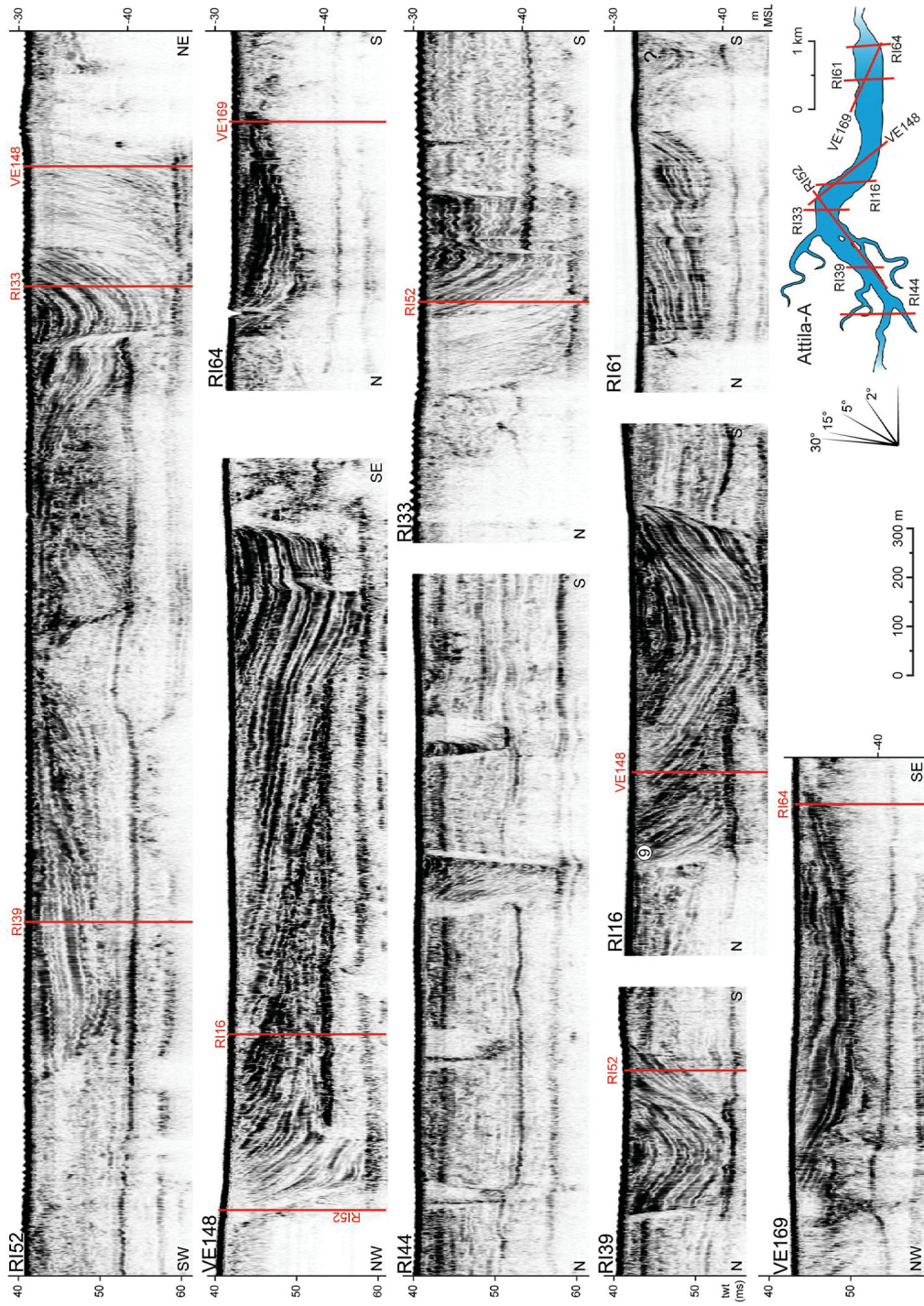
Figure 3.8: Selection of CHIRP profiles of the Attila-A tidal inlet. The line drawing is provided in Fig. 3.9. See also Fig. 3.10 for positioning.
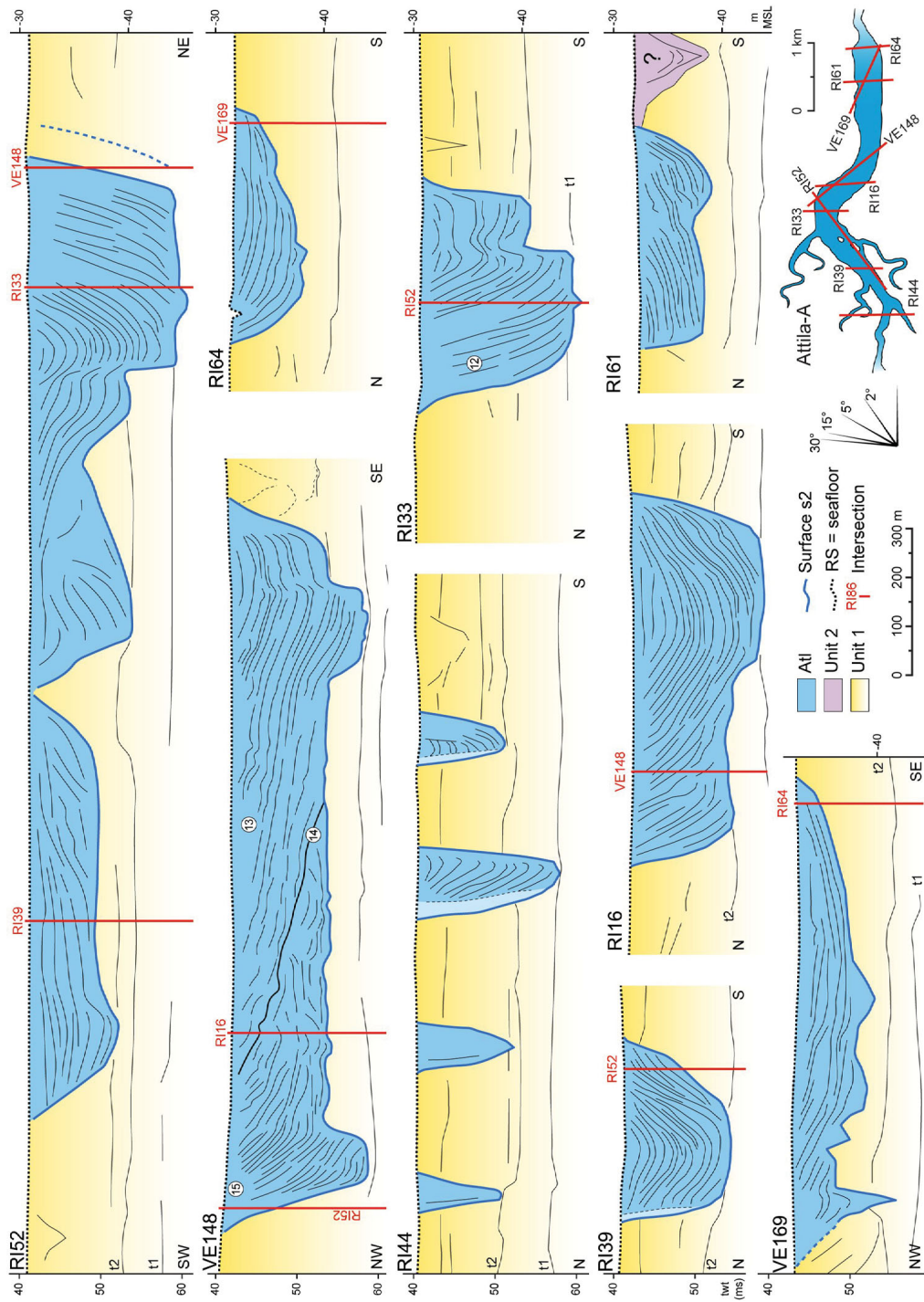
Figure 3.9: Line drawing of the CHIRP profiles shown in Fig. 3.8. The interpretation of the profile and the explanation of the numbers are provided in the text. See also Fig. 3.10 for positioning.

foraminifers are documented with *A. beccarii tepida* (common to abundant) and, less frequent, *Elphidium decipiens-granosum, Ammonia perlucida, Haynesina germanica, Elphidium gunteri, Q. seminulum, Nonion pauciloculu*m. This biofacies indicates a transitional environment/lagoon.Trincardi et al., (2011) report for the same samples the presence of transitional environment taxa, such as *C. glaucum* and *H. ventrosa.*

BIOFACIES C   Samples barren with scarce amount of micaceous very-fine sand and very rare vegetal remains. The absence of fossil remains may suggest a continental environment.

3.5   PLANIMETRIC PATTERN AND MORPHOMETRY

The large number of cross sections provided by the CHIRP profiles allows a good morphological interpretation and characterization of the incised features. Combining the results obtained from the seismic analysis and the data collected through the analysis of the cores it was possible to reconstruct the genesis and evolution of the analyzed features. A characteristic shared by both generations of scours is the steepness of the flanks, which can reach a value of 30°.

Nadia incised valley

Nadia valley is characterized by a main channel that can be tracked for a length of about 10 km in SE direction (Fig. 3.10). The width presents some variability, but it generally spans from 200 m to 300 m and it stays roughly constant along the entire reach. The valley is rather straight, with a sinuosity index of 1.0, and is characterized by a single meander with a curvature radius of about 350 m (Figs. 3.10 and 3.13-A). The valley reaches a maximum depth of 35 m from the present sea floor (ca. -65 m MSL) but, in the upstream direction, it is characterized by a gradual shallowing (Fig. 3.13-A) and by the bifurcation in two minor branches that seem to represent the head of the catchment. Some smaller and shallower tributaries are joining the main trunk in the downstream sector. As detected in several incised valleys (cf. Boyd et al., 2006), the presence of this pattern suggests an entrenched drainage network for the runoff waters. Nadia valley cannot be followed further downstream as its recognition is hampered by the lack of data. In particular, between the study area and the midline separating Italian and Croatian territorial water,

there is a strong blanking of the CHIRP signal (Figs. 2 and 10). As described in some other sectors of the northern Adriatic, this phenomenon is probably related to the presence of superficial hardened deposits or coarse sediments (Trincardi et al., 2001). Thus, it is likely that Nadia valley extends further eastward. Another incised feature with comparable stratigraphic position and a sedimentological infill occurs 5 km west of Nadia valley (line RI01 in Fig. 3.5). Unfortunately, this incised channel has been recognized only in few CHIRP profiles, thus, it is not possible to reconstruct its planform pattern. According to their similarities, it is hypothesized that also this second incised feature formed and evolved at the same time as Nadia valley, thus belonging to the same generation. Further discussions about times and modes of formation of Nadia valley are provided in section 3.6.

Attila incised channels

Attila unit constitute the youngest feature still recognizable in the stratigraphic record. The upper portion of Atl, along with any other younger morphologies or deposits, was erased by the marine erosive processes that lead to the formation of the RS, which roughly matches with the modern seafloor. The shape of the flanks and bottom of Attila incised channels testifies that the erosive action was guided by the differential stiffness of the incised units, as they often match with strata boundaries, likely paleosols or organic horizons (e.g. Figs. 3.8 and 3.9, lines VE148, RI16). The larges feature of this generation (named Attila-A Fig. 3.10) is located in the northern sector of the study area, whereas a smaller channel (Attila-C) was detected in the south-western sector and other two channelized incisions (Attila-B1 and Attila-B2, Fig. 3.10) show a more complex pattern and cut the eastern part of Nadia valley.
Attila-A can be traced for 7 km in a west-east direction, and it is characterized by a single large meander with a curvature radius of 600 m. The width is variable, as it is about $100 - 150$ m in the western tract and it widens progressively for 2 km up to 400 m. This value is almost constant in the eastward direction until the very end of Attila-A, where a funneling of this landform is clearly observable. Several smaller meandering channels join Attila-A, defining a dendritic pattern. These minor branches have a width between 50 and 100 m and a maximum length of about 1 km. They display a sinuosity spanning from 1.2 to 1.4 and join the main trunk with variable inclinations, between 40° and 80° (Figs. 3.10 and 3.13-B). A moderately dendritic pattern

is shown also by Attila-C, while Attila-B1 and Attila-B2 are almost parallel and their planform suggests that these two incisions merge slightly westward of the reconstructed path.

The maximum depth reached by these features is 20 m below the modern sea floor (ca. -50 m MSL), whereas the minimum recognizable thickness of the smaller channels of Atl is about 5 m (Fig. 3.13-B). The peaty horizons of U1, especially t1 and t2, clearly conditioned the development of the erosive base of channel Attila-A, limiting the maximum depth reached by the scour (cf. Figs. 3.8 and 3.9, lines RI16, RI33). The maximum depth values are typically encountered in the middle reaches of the traceable features. A gradual decreasing of the depth is observable both in landward and in seaward direction (Fig. 3.13-B). This characteristic strongly differs from the channels of fluvial origin, where the gradient of the thalweg has a clear downstream trend (e.g. Leopold et al., 1964; Bridge, 2009; Blum et al., 2013). Given the peculiar morphology and morphometry, the paleontological content of the infilling (cf. section 3.4) and its depth and age, these features can be interpreted as tidal inlets (Attila A) and main tidal channels. More insights are presented in paragraph 6.1.3.

3.6 DISCUSSION

Paleogeographic evolution

LOWSTAND ALLUVIAL PLAIN (U1) During the last glaciation the northern Adriatic shelf was the continuation of the Po and Venetian-Friulian plains (Fig. 3.14 - 1). At that time, the study area probably occupied a marginal position between these two main alluvial systems, as it was located $15 - 30$ km downstream of the morphological boundary of the megafans fed by the south-eastern Alpine rivers (Fontana et al. 2014), but it was also out of the reach of the direct influence of the Po River system Stefani and Vincenzi, 2005; Amorosi et al., 2017b). The analysis of the CHIRP profiles documents an alluvial plain (U1) built during a progressive trend of aggradation, formed by the stacking of sedimentary units with a thickness of $3 - 6$ m (line RI50 in Fig. 3.5). These silty to sandy deposits show a clear planar layering, sometimes interrupted by the presence of gentle ridges revealing the action of fluvial channels (#2 in Fig. 3.5). It seems that the area was rarely influenced by the direct activity of the rivers as the geometry of the reflectors suggests that

124

the deposition occurred in a floodplain environment, likely influenced only by major floods. The depositional phases that built-up the alluvial plain have been interspersed by few periods of relatively-long sedimentary stasis, during which weakly-developed soils (entisols, Soil Survey Staff, 1999), or even peaty layers, formed (#1 in Fig. 3.5). These layers are comparable to the peaty horizons that are diffused in the LGM stratigraphy of the Venetian-Friulian Plain (Miola et al., 2006; Fontana et al., 2010, Fontana et al. 2014). These latter have sometimes a regional extent and are partly related to climatic fluctuations occurred during the last glaciation (Rossato and Mozzi, 2016). Several entisols formed during MIS 3 and LGM are present also in the subsoil of the Po Plain, and some of them are spread over a very large area, from the Apennine margin to the modern Po Delta (Amorosi et al., 2014; Bruno et al., 2015). The formation of these soils can be related to the Dansgaard-Oeschger events (Amorosi et al., 2014, 2017b). Nevertheless, some of these organic horizons may have an autocyclic origin linked to river switching and the consequent activation/deactivation of localized depositional lobes (cf. Miola et al., 2006). In the study area the age of the upper portion of U1 is constrained by a radiocarbon measurement to about $28.9 - 28.2$ ka cal BP (D, Tab. 3.1). This result is very similar to the one obtained between 5 and 20 km north (cores RI09-11 and VE04-32, Tab. 3.1, Fig. 2), while the dates of core AD78-161 testify that the alluvial aggradation of U1 was still active between $25.4 - 23.1$ and $23.4 - 22.6$ ka cal BP (K, L; Tab. 3.1), thus during the second part of the LGM (see Fig. 3.2 for cores location). The age range here reported must therefore be considered only as indicative (Fig. 3.15). The base of the LGM deposits is not clearly recognizable in the seismic profiles due to its correlative conformity nature. In the nearby Po Plain, the Sequence Boundary (SB) associated with the onset of the LGM was individuated by Amorosi et al., (2017b) in a soil buried by alluvial deposits and with an age variable between 29 and 24 ka cal BP. In the Mid Adriatic Depression (MAD) and in the southern Adriatic, where the shelf is steeper and the alluvial input influence was less pronounced, the base of the LGM deposits is a key horizon clearly identified by an unconformity, which also corresponds to a SB (sensu Hunt and Tucker, 1992) in the sequence stratigraphy of the basin (Cattaneo and Trincardi, 1999; Maselli and Trincardi, 2013; Amorosi et al., 2017b; Pellegrini et al., 2017). In the MAD, the SB was precisely dated at 31.8 ka cal BP (Pellegrini et al., 2017). The peaty/organic-rich horizons t1 and t2, currently positioned at an
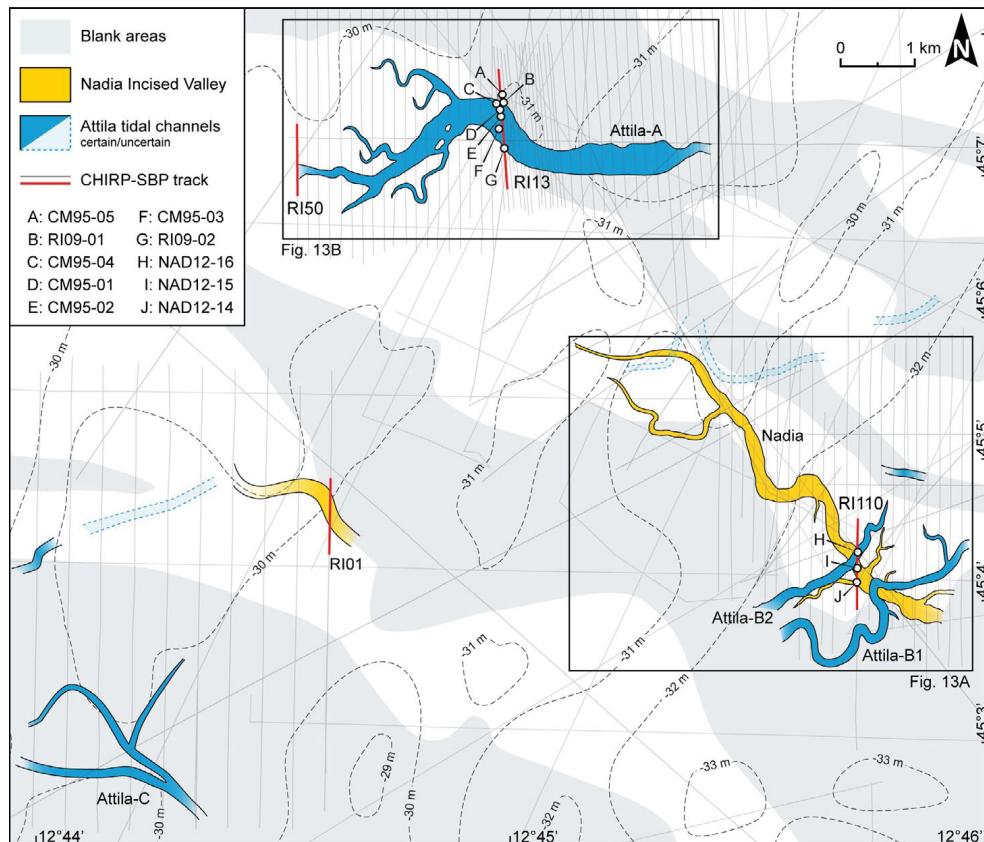
Figure 3.10: Map of the incised features reconstructed through the seismic interpretation. The position of the cores and of the CHIRP profiles addressed in the text is here reported. The gray surface identified with the name "Blank areas" indicates the occurrence of blanking of the deep seismic response. This blanking mainly affects the recognition of Nadia unit, while Attila is unaffected (cf. Figs. 3.6 and 3.7, line NAD147; Figs. 3.8 and 3.9, line RI61).

elevation between -35 and -40 m MSL, may correspond to some of the soils recognized in the Po Plain probably formed during MIS 3 (cf. Amorosi et al., 2017b). In the study area the passage between MIS 3 and MIS 2 is not marked by a clear unconformity and, according to the regional setting, U1 corresponds to the alluvial lowstand unit mapped in the Geological Map of the Adriatic, which includes also continental deposits of MIS 4 (Trincardi et al., 2001, 2011).

FORMATION AND INFILL OF NADIA VALLEY   As testified by the radiocarbon dating carried out on sample from core RI09-1, the incision of Nadia valley
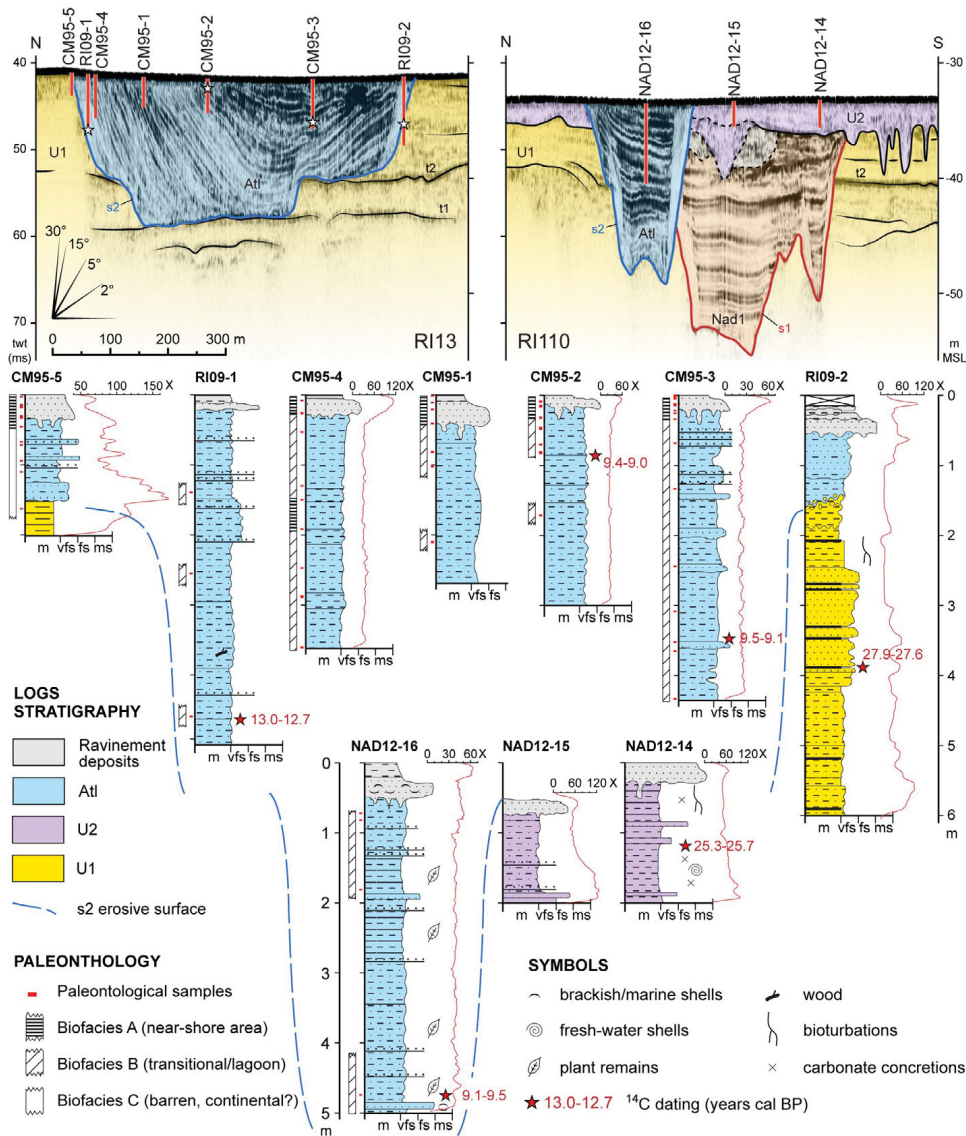
Figure 3.11: RI13: Cross section of Attila-A channel with the location of the available cores. RI110: Evidence of the stratigraphic relations among U1, Nad1, Atl and U2 with the location of the available cores. The position of the profiles is reported in Fig. 3.10. In the lower portion of the image the core logs with magnetic susceptibility, the biofacies and the radiocarbon dates addressed in the text are displayed.
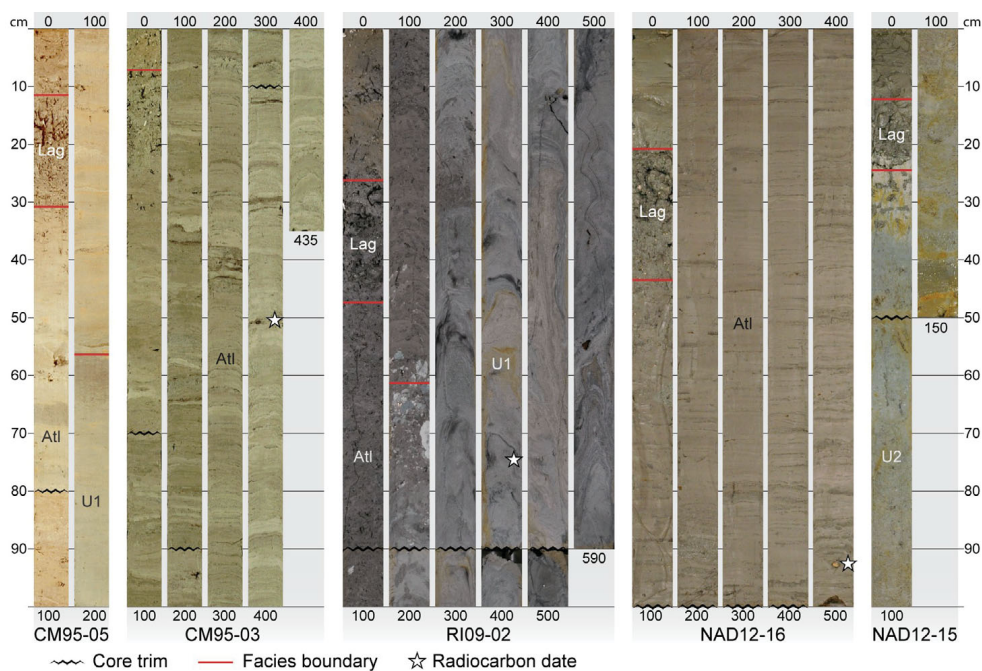
Figure 3.12: Core photo displaying the major units described in the text.

occurred after 28 ka cal BP, but before the formation of U2, which deposited over the whole study area and sealed the top portion of the valley. The shell of a terrestrial gastropod sampled from U2 indicates an age of $21\,200 \pm 49\,^{14}C$ a BP (G, Tab.1), that is calibrated to $25.7 - 25.3$ ka cal BP. Nevertheless, because of the terrestrial origin of the shell and the possible effect induced by older non-organic carbon, the age of the sample can be significantly overestimated (Pigati, 2013). According with literature (Goodfriend and Hood, 1983; Goodfriend et al., 1999; Quarta et al., 2007; Pigati et al., 2010), the real age of the snail, and thus of U2, can be younger than the calibrated results from few centuries up to 3 ka. This situation suggests that U2 formed in an interval before ca. 23 to 25 ka cal BP and, obviously, this applies also to Nad1. It follows that the formation and infill of Nadia valley occurred when U1 was still aggrading slightly north of the study area (samples from cores AD78-161, VE04-32). In a regional perspective, the units Nad1 and U2 can be even considered as just different facies of U1, which in the rest of the plain was still aggrading over the pre-existing surface, while in the study area was infilling Nadia valley. The planform pattern of the western sector of Nadia suggests that this portion of the valley acted as the head of a catchment

basin, while the valley developed in the SE direction, probably well beyond the investigated zone. Furthermore, the seismic data highlighted the absence of any direct connection of Nadia valley with other major river systems, thus strengthening the hypothesis of a local catchment. It follows that the only sediment potentially transported during the valley formation was the material eroded along the bed and the flanks of the valley, which was then delivered east of the recognized reach.

The dense network of the CHIRP profiles robustly supports the evidence that fluvial incision was not a typical process during the LGM in the Adriatic shelf north of the present Po Delta. The main Alpine rivers formed some incised valleys during the Late Glacial in the distal sector of the Venetian-Friulian Plain, but the depth of these valleys gradually decreased downstream and eventually they completely disappear few kilometers away of the present coast, leaving apparently no trace in the shelf (Fontana et al., 2010). The stratigraphic record of the eastern Po Plain revealed that the Po River used to flow in a slightly-incised valley $(5 - 10$ m$)$ during the LGM (Amorosi et al., 2017b), but the CHIRP profiles analyzed in this work show no evidences of links with the Nadia valley.

Nadia valley represents a peculiar situation, not related to the evolutionary trend of the major fluvial systems flowing on the NW Adriatic shelf during the LGM. In this perspective, the river that formed Nadia valley was originally a slightly-incised local stream draining the runoff water and/or fed by groundwater seepage which has been captured by a river system flowing in the lower topographic area located between the Istrian coast and the present Italian-Croatian boundary (Fig. 2). The higher topographic gradient established by this capture would have triggered an upstream propagation of the erosion, creating a valley incised up to $25 - 30$ m from the former surface. The infilling material was provided by the flood deposits of distal riverine systems, as Nadia valley represented a sedimentary trap located in the plain. The parallel layering of the basal portion of Nad1, together with the apparent lack of coarse deposits at the base of the valley fill and the absence of any tractive depositional structure (e.g. channel bars), suggests that the sedimentation took place under low-energy conditions. Indeed, the base of the valley was probably characterized by the presence of a waterlogged environment (e.g. marsh/swamp) fed by the surface runoff and by the intercepted aquifers. Even if U2 was not sampled by sediment cores, the good penetration of the CHIRP

signal suggests a fine grain composition for the infilling material. In particular, by comparing the seismic facies of Nad1 to other seismic data available in the Adriatic area (e.g. Cattaneo and Trincardi, 1999; Maselli and Trincardi, 2013; Brunović et al., 2017) it is reasonable to suggest an alternation of clay/silt and very fine sand for this unit.

In contrast with the lower portion, the upper part of Nadia infilling (Nad1a) formed under slightly different conditions, as the feeder fluvial system progressively approached the area. This hypothesis is supported by the different depositional geometries within the infilling, such as the slightly inclined layers of Nad1a, which highlight the presence of small sediment lobes evenly distributed within the valley (cf. section 3.4). These lobes are attributed to the presence of preferential inlets, most likely represented by the incise network of tributary channels draining into Nadia valley. The progressive approach of the fluvial system recorded by Nad1a finally led to the direct arrival of the river on top of Nadia valley, with the consequent deposition of U2. This phase was followed by a prolonged period of sedimentary starvation, as testified by the presence of a well-developed soil on top of U2. This suggests that the fluvial system which led to the infilling of Nadia incised valley and the formation of U2 shifted to a different position, outside of the study area. The infilling phase of Nadia valley, which occurred between ca. 26 and 24 ka cal BP, can be correlated to one of the main glacial advances of the southern Alps (i.e. $26 - 24$ ka cal BP; Monegato et al., 2007, 2017; Rossato and Mozzi, 2016) as well as to a high sediment discharge event recorded by the prograding clinoforms at the Adriatic shelf-edge between 25 and 24 ka cal BP (Pellegrini et al., 2017; Fig. 3.15). The infilling of Nadia valley would therefore constitute an interesting environmental record for the LGM and could integrate the information provided by other continental sequences of the northern Italy (e.g. Pini et al., 2010; Monegato et al., 2011), as well as those obtained from the lowstand wedge of the MAD (Piva et al., 2008).

FORMATION OF ATTILA TIDAL CHANNELS   The temporal interval intercurred between the deposition of U2 and the formation of Attila is not well constrained. In particular, the formation of the ravinement surface led to the complete erosion of the top of U2 and Atl units, preventing the investigations of the stratigraphic relations existing between them. After the formation of U2, the study area experienced a sedimentary stasis that lasted until the rising of the

sea-level started to affect this zone. With the ongoing transgression the study area first shifted to a brackish environment and then gradually turned into a lagoon, allowing the formation of the Attila inlet/channels (Fig. 3.14). The radiocarbon dates and the paleontological analyses carried out on the infill of channel Attila-A and Attila-B2 allow reconstructing the history of these features. In particular, the ages of the C. glaucum shells sampled in cores CM95-2 and CM95-3 ($9.4 - 9.0$ and $9.5 - 9.1$ ka cal BP, respectively; A, B, Tab. 3.1) dated the same set of layers, which lies almost at the top of the preserved channel infilling. The real top of the channel has been erased by the ravinement surface but, as suggested by the rather gentle slope of the top layers of the infilling, the eroded portion was probably rather limited. Thus, the measured ages are representative for the late phase of activity of the tidal inlet Attila-A, which was probably active until ca. 9.0 ka cal BP. This age range is also further confirmed by the age of $9.5 - 9.1$ ka cal BP (H, Tab. 3.1) obtained at a depth of 4.92 m for Attila-B2. The core RI09-1 was collected through a steep point bar that represents the first phase of the channel infill (Fig. 3.11). The sedimentary facies and the micropaleontological association sampled along core RI09-1 are very similar to the ones described in cores CM95-2 and CM95-3, and document an open lagoon/estuarine environment. These data, interpreted at the light of the homogeneous seismic facies, suggest that no major changes occurred in the depositional environment during the sedimentation of the channel deposits of Attila-A, which occurred in a subtidal environment, likely between 1 and 5 m below the sea level of that period (cf. Vacchi et al., 2016). In core RI09-1 a wood fragment found at a depth of 4.7 m from sea bed was dated to $13.0 - 12.7$ ka cal BP (C, 3.1). This age corresponds to the Younger Dryas climatic period, when the relative sea level in the Adriatic was about -65 m MSL (Storms et al., 2008; Lambeck et al., 2011; Pellegrini et al., 2015) and estuarine condition in the study area were not possible. Our interpretation is that the dated wood fragment was embedded as a clast within the point bar, therefore its age is not representative for the infilling of Attila-A channel. The comparison between the dates from cores CM95-1, CM95-2 and NAD12-16 and the curves of sea-level rise, both from geophysical modeling and observed paleo-sea level indicators (e.g. Lambeck et al., 2011, 2014; Moscon et al., 2015), confirms that the infilling of Attila-A and B took place when the coastline was placed in the area, approximately between $9.5 - 9.0$ ka cal BP. The remarkable depths reached by these scours are related to the strong tidal

currents occurring in the tidal inlet and along the channels directly connected to it. Similar landforms, characterized by a comparable morphometry, with depth values up to 20 m, are present in the modern and pre-anthropized lagoons of the northern Adriatic Sea (cf.Madricardo et al., 2007; Fontolan et al., 2007, 2012; Triches et al., 2011; Zecchin et al., 2009; Madricardo and Donnici, 2014). Filled incised features with similar planforms, dimensions and infilling seismic facies, interpreted as tidal inlets and main tidal channels, were also described by Rieu et al., (2005), Hijma et al., (2010) and Elias and Van Der Spek, (2006) off the coast of The Netherlands, by Fraccascia et al., (2016) in the Danish Wadden Sea, by Allard et al., (2009) in the Arcachon Lagoon (SW France), by Menier et al., (2010) and Traini et al. (2013) in the Vilaine River ria, by Billeaud et al., (2009) in the Mont-Saint-Michel Bay and by Cooper et al., (2016) in the Tijucas Bay in Brazil.

Even if Attila and Nadia generations insist in the same area, apparently there are no relations between the two set if incised features. Notwithstanding, the investigation about this aspect is strongly limited because the topography that existed when the lagoon started to form has been completely eroded during the marine transgression.

Paleogeographic meaning of Attila channels

The considerable thickness of the infillings of the channels of Attila generation allowed their preservation in the sedimentary record, while the shallow landforms and deposits of the related lagoon were completely eroded after their submersion. In particular, the formation of the ravinement surface erased not only the landforms with a convex topography (e.g. barrier islands), but also the lagoon tidal flats, along with the shallow tidal channels and creeks with depth not greater than $1-2$ m. The main tidal channels, which are usually directly connected to the tidal inlets, can reach a depth of 6 - 8 m, as documented in the pre-modern landscape of the lagoons of Venice (Zecchin et al., 2008, 2009; D'Alpaos, 2010) and Grado-Marano (Marocco and Pessina, 1995; Triches et al., 2011; Fontolan et al., 2012) in the northern Adriatic Sea. The preservation of a dendritic pattern of tidal channels connected to the inlets, especially in the area of Attila-A, suggests that the erosion induced by the marine transgression over the former lagoon probably did not removed more than $1-2$ m of the pre-existing stratigraphy, as the thickness of the tidal channels directly draining into the Attila-A inlet reach values up to 7 m (e.g.

132
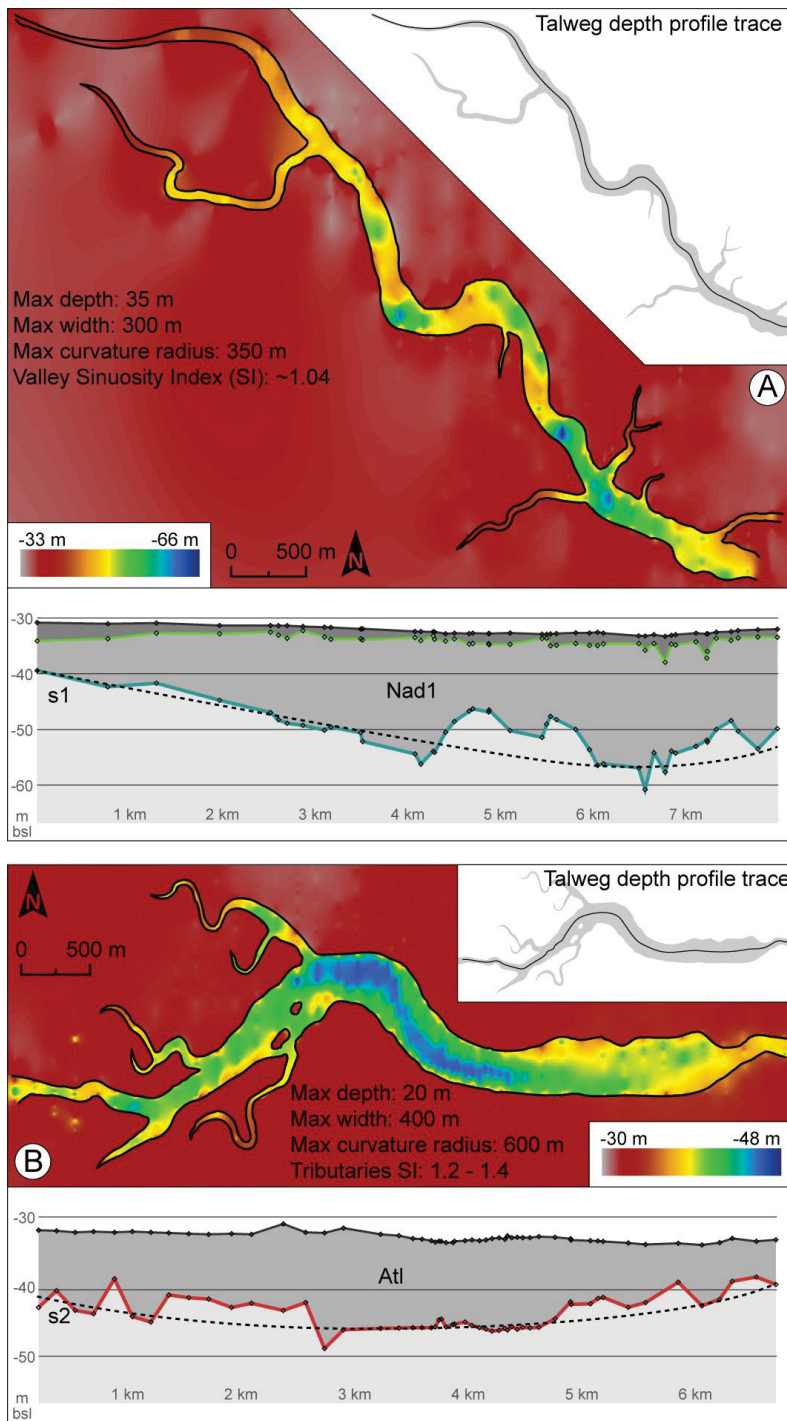
Figure 3.13: Reconstruction of Nadia valley and Attila-A tidal inlet lower boundaries based on the picking of s1 and s2 surfaces. The interpolation was performed with the *Topo to Raster* tool provided in ArcGIS.
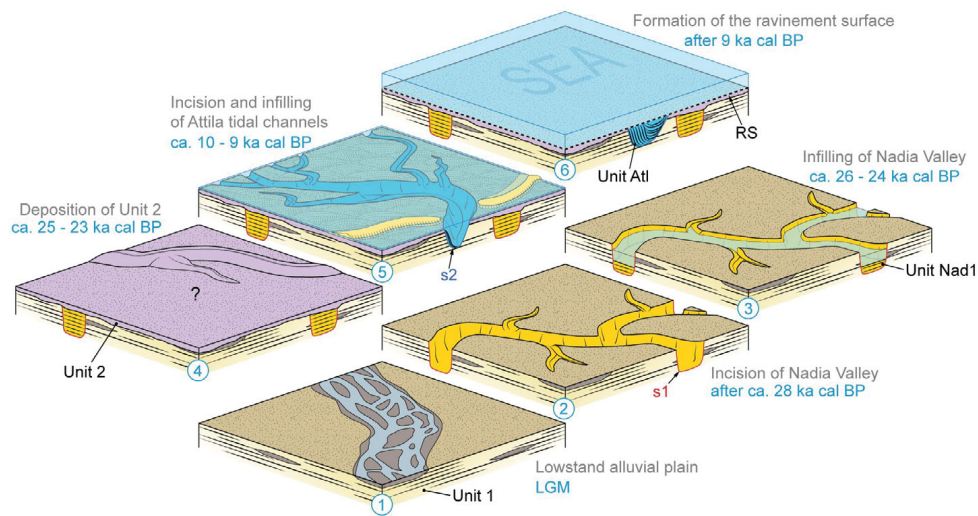
Figure 3.14: Simplified sketch of the geological evolution of the area from the deposition of U1 to the formation of the ravinement surface.

Fig. 3.9, line RI44). Rieu et al., (2005) describes a nice example of truncation of a tidal inlet and the consequent erasing of all the related tidal channels in the coast of the Netherlands. Another important paleogeographic information supported by the tidal inlet of Attila-A is the position of the barrier-island that was protecting the lagoon, which was probably located in proximity of the funneled tract of the channel. The absence of evidence of other tidal inlets in landward direction suggests that, after the period of relative sea-level stasis that led to the formation of the lagoon, the deactivation and submersion of the system was produced by a sudden marine transgression rather than a gradual shift. It is likely that a barrier overstepping occurred around 9 ka cal BP, with a consequent marine submersion of the area. In the subsoil of Po Delta, the core analyses allowed to recognize an important flooding surface of regional extent, which started to form ca. 9.2 ka cal BP (Amorosi et al., 2017a). According to the available reconstruction of the post-LGM sea level curve for the northern Adriatic (Correggiari et al., 1996; Lambeck et al., 2011; Moscon et al., 2015; Vacchi et al., 2016) the depth of ca. -30 m MSL (i.e. the depth of the top of Atl1) has been reached around 9 ka cal BP, so the age-depth model is in good agreement with the radiocarbon dates from the top of Attila infilling (cores CM95-2 and CM95-3). Thus, the dataset analyzed in this work seems to indicate the occurrence of a period of stasis in the rate of the relative sea-level rise that apparently was followed by a sudden increase.

This hypothesis fits with the increase of the sea-level rise that is evidenced by global and local calculated sea-level curve between 9.5 and 8.7 ka cal BP (Lambeck et al., 2011, 2014). Moreover, it fits also with some reconstructions of relative sea level based on core analysis carried out in several Mediterranean and extra-Mediterranean regions (Liu et al., 2005; Carlson and Clark, 2012; Tanabe et al., 2015; Amorosi et al., 2017a and reference therein). According to sedimentary models (Catuneanu, 2006), the lagoon formation in the area could be also related to an increase of the sediment supplied by the fluvial systems, but the available data allow to discard this hypothesis as the Po River, along with the other major rivers fed by SE Alps, were not flowing in the area during the analyzed timeframe (Correggiari et al., 2005; Stefani and Vincenzi, 2005; Piovan et al., 2012; Amorosi et al., 2017a). An overstepping evolution was noticed also for two older lagoon systems positioned in the central and southern Adriatic shelf, which took place respectively around 14.3 and 10.5 ka cal BP (Storms et al., 2008).

3.7 CONCLUSIONS

In this work we thoroughly analyzed two generations of incised and filled features that have been documented in the Late Quaternary of the Adriatic Sea, north of Po Delta, roughly 30 km offshore of the Venice Lagoon.

- The oldest generation (Nadia valley) is a river incised valley with a preserved length of almost 10 km, a width between $200-300$ m and a maximum depth up to 25 m The erosive period that led to the formation of this valley occurred after ca. 28 ka cal BP, whereas the infilling phase was probably already completed between 24 and 23 ka cal BP. Thus, the valley was eroded and filled entirely during the LGM. The formation of Nadia valley was not related to the direct activity of major Alpine rivers, as suggest by its geographic position and by the absence of any recognizable evidence in the seismic profiles. The fluvial incision was probably related to the activity of a minor stream that was captured by a river flowing east of the investigated zone, in the area west of Istria Peninsula.

- After the incision, the bottom of Nadia valley was characterized by a marshy or swampy environment that was reached only by the sediments of distal Alpine rivers, which probably arrived in the area during some
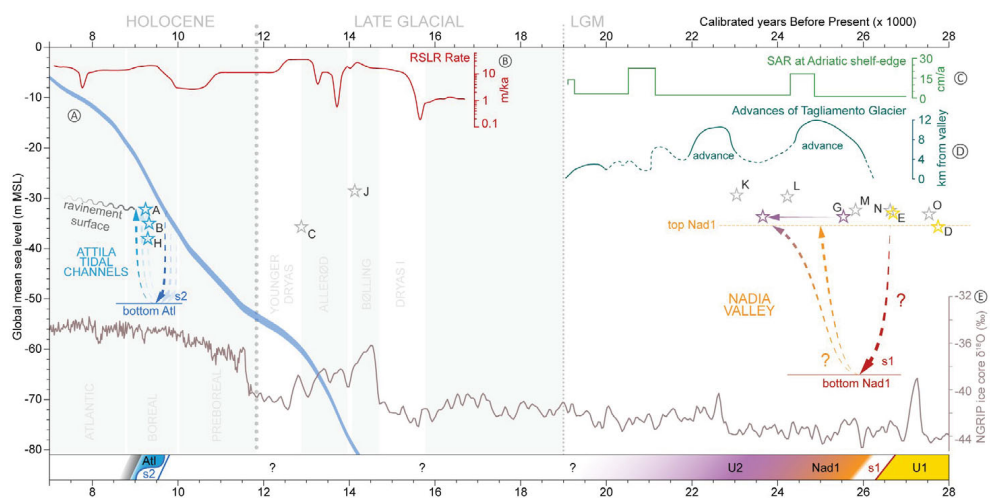
Figure 3.15: Schematic diagram of the evolution of the Nadia and Attila systems. (A) Sea-level rise curve for the northern Adriatic, after Lambeck et al. (2011). (B) Global sea-level rise rate calculated in Lambeck et al. (2014). (C) Sediment Accumulation Rate calculated in Pellegrini et al. (2017) for the clinothems at the Adriatic shelf- edge. (D) Advances of the front of Tagliamento glacier as proposed in Monegato et al. (2007, 2017). (E) $\delta^{18}O$ oscillations from NGRIP ice core (North Greenland Ice Core Project Members, 2004; Kindler et al., 2014). The arrows describe the cycles of scouring (downward arrows) and infilling (upward arrows) of the two generations. The radiocarbon dates are represented with stars (see also Table 1). The reader is referred to the text for more insights.

> major flood events (Unit Nad1). Between 25 and 23 ka cal BP a river system progressively approached the study area up to fill completely Nadia valley with its channel deposits (U2). After this phase, the area was abandoned and a well-developed soil formed on the exposed surface.

- The post-LGM marine transgression started to directly affect the investigated area since ca. 10 ka cal BP, causing the formation of a lagoon system, that was characterized by a complex pattern of channels (Attila generation). The major one (Attila-A) corresponds to a tidal inlet, with a preserved length of about 7 km, a width of 150 m and a maximum depth of almost 20 m below the present seafloor. The barrier island that protected the lagoon was located near the eastern end of Attila-A, where this channel suddenly shallows and narrows, up to disappear.

- The channels of Attila generation probably formed during a relative

still stand of the sea level or during an interval of relatively low rate of marine transgression, which led enough time to the lagoon systems to generate a complex pattern of lagoon channels. The infill of the channels of Attila generation is dated between 9.5 and 9.0 ka cal BP and, in our reconstruction, the sea overstepped the barrier island at the end of that interval, when relative sea level was around -30 m MSL. The consequent marine submersion led to the formation of the ravinement surface, with the erosion of the first $1-2$ m of sediments. Thus, only the deepest lagoon channels were preserved. This work provides new insights on the evolution of a low gradient shelf during the LGM lowstand and the following phase of marine transgression. In particular, this research highlights the importance of recognizing and characterizing the paleo tidal inlets which can be documented in a low-gradient shelf. These incised and filled features sometimes are the only record of lagoon systems that formed during the marine transgression. Their detailed investigation provides essential information for the paleogeographic reconstructions and produces important data for disentangling the history of sea-level variations.

REFERENCES

Allard, J., Chaumillon, E., Féniès, H., 2009. A synthesis of morphological evolutions and Holocene stratigraphy of a wave-dominated estuary: the Arcachon lagoon, SW France. Continental Shelf Research, 29, 957-969.

Allen, G.P., Posamentier, H.W., 1993. Sequence stratigraphy and facies model of an incised valley fill: The Gironde Estuary, France. Journal of Sedimentary Petrology, 63, 378-391.

Alley, R.B., Clark, P.U., Huybrechts, P., Joughin, I., 2005. Ice-sheet and sea-level changes. Science, 310, 456-460.

Amorosi, A., Centineo, M.C., Colalongo, M.L., Pasini, G., Sarti, G., Vaiani, S.C., 2003. Facies Architecture and Latest Pleistocene-Holocene Depositional History of the Po Delta (Comacchio Area), Italy. The Journal of Geology, 111, 39-56.

Amorosi, A., Fontana, A., Antonioli, F., Primon, S., Bondesan, A., 2008. Post-LGM sedimentation and Holocene shoreline evolution in the NW Adriatic coastal area. GeoActa, 7, 41-67.

Amorosi, A., Bruno, L., Rossi, V., Severi, P., Hajdas, I., 2014. Paleosol architecture of a late Quaternary basin margin sequence and its implications for high resolution, non-marine sequence stratigraphy. Glob. Planet. Change 112, 12-25.

Amorosi, A., Maselli, V., Trincardi, F., 2016. Onshore to offshore anatomy of a late Quaternary source-to-sink system (Po Plain-Adriatic Sea, Italy). Earth-Science Reviews, 153, 212-237.

Amorosi, A., Bruno, L., Campo, B., Morelli, A., Rossi, V., Scarponi, D., Drexler, T.M., 2017a. Global sea-level control on local parasequence architecture from the Holocene record of the Po Plain, Italy. Marine and Petroleum Geology, 87, 99-111.

Amorosi, A., Bruno, L., Cleveland D.M., Morelli, A., Hong, W., 2017b. Paleosols and associated channel-belt sand bodies from a continuously subsiding late Quaternary system (Po Basin, Italy): New insights into continental sequence stratigraphy Geological Society of America Bulletin, 129, B31575.1.

Antonioli, F., Ferranti, L., Fontana, A., Amorosi, A., Bondesan, A., Braitenberg, C., Fontolan, G., Furlani, S., Mastronuzzi, G., Monaco, C., Spada, G., Stocchi, P., 2009. Holocene relative sea-level changes and vertical movements along the Italian and Istrian coastlines. Quaternary International, 206, 102-133.

Bard, E., Hamelin, B., Fairbanks, R.G., 1990. U-Th ages obtained by mass spectrometry in corals from Barbados: Sea level during the past 130,000 years. Nature, 346, 456-458.

Barmawidjaja, D.M., Jorissen, F.J., Puskaric, S., van der Zwaan, G.J., 1992. Microhabitat selection by benthic foraminifera in the Northern Adriatic Sea. Journal of Foraminifera Research, 22, 297-317.

Benjamin, J., Rovere, A., Fontana, A., Furlani, S., Vacchi, M., Inglis, R.H., Galili, E., Antonioli, F., Sivan, D., Miko, S., Mourtzas, N., Felja, I., Meredith-Williams, I., Goodman-Tchernov, B., Kolaiti, E., Anzidei, M., Gehrels, R., 2017. Late Quaternary sea-level changes and early human societies in the central and eastern Mediterranean Basin: An interdisciplinary review. Quaternary International, 449, 29-57.

Bhattacharya, J.P., Copeland, P., Lawton, T.F., Holbrook, J., 2015. Estimation of source area, river paleo-discharge, paleoslope and sediment budgets of linked deep-time depositional systems and implications for hydrocarbons. Earth-Science Reviews, 153.

Billeaud, I., Tessier, B., Lesueur, P., 2009. Impacts of late Holocene rapid climate changes as recorded in a macrotidal coastal setting (Mont-Saint-Michel Bay, France). Geology, 37, 1031-1034.

Blum, M., Martin, J., Milliken, K., Garvin, M., 2013. Paleovalley systems: Insights from Quaternary analogs and experiments. Earth-Science Reviews, 116, 128-169.

Blum, M., Törnqvist, T. E., 2000. Fluvial responses to climate and sea-level change: a review and look forward. Sedimentology, 47, 2-48.

Bogemans, F., Roe, H.M., Baeteman, C., 2016. Incised Pleistocene valleys in the Western Belgium coastal plain: Age, origins and implications for the evolution of the Southern North Sea Basin. Palaeogeography, Palaeoclimatology, Palaeoecology, 456, 46-59.

140

Boyd, R., Dalrymple, R.W., Zaitlin, B.A., 2006. Estuarine and Incised-Valley Facies Models. In H.W. Posamentier R.G. Walker (eds), Facies Models Revisited. SEPM Special Publication, 84, 171-235.

Breda, A., Amorosi, A., Rossi, V., Fusco, F., (2016). Late-glacial to Holocene depositional architecture of the Ombrone palaeovalley system (Southern Tuscany, Italy): Sea-level, climate and local control in valley-fill variability. Sedimentology, 1124-1148.

Bridge, J.S., 2009. Rivers and Floodplains: Forms, Processes, and Sedimentary Record, 504. John Wiley Sons.

Bruno, L., Amorosi, A., Severi, P., Bartolomei, P., 2015. High-frequency depositional cycles within the late Quaternary alluvial succession of Reno River (Northern Italy). Italian Journal of Geosciences, 134, 339-354.

Brunović, D., Miko, S., Hasan, O., Ilijanić, N., Papatheodorou, G., Christodoulou, D., Geraga, M., Dumbir, A-M., Razum, I., Hajek Tadesse, V., Bakrač, K., Šparica Miko, M., 2017. The Late Quaternary palaeoenvironmental development of Lošinj Channel, Adriatic Sea. 5th Reg. Mtg. Quaternary Geology dedicated to Geohazards Final Conf. LoLADRIA project, Starigrad-Paklenica, 2017

Carlson, A.E., P.U., Clark, 2012. Ice sheet sources of sea level rise and freshwater discharge during the last deglaciation, Rev. Geophys., 50, RG4007.

Carton, A., Bondesan, A., Fontana, A., Meneghel, M., Miola, A., Mozzi, P., Primon, S., Surian, N., 2009. Geomorphological evolution and sediment transfer in the Piave River system (northeastern Italy) since the Last Glacial Maximum. Géomorphologie : relief, processus, environnement, 3, 155-174.

Castiglioni, B., 1940. L'Italia nell'età quaternaria. In: Dainelli G. (eds), Atlante fisico economico d'Italia, Milano, Consociazione Turistica Italiana, tav. 3.

Cattaneo, A., Correggiari, A., Langone, L., Trincardi, F., 2003. The late-Holocene Gargano subaqueous delta, Adriatic shelf: Sediment pathways and supply fluctuations. Marine Geology, 193, 61-91.

Cattaneo, A., Steel, R.J., 2003. Transgressive deposits: A review of their variability. Earth-Science Reviews, 62, 187-228.

Cattaneo, A., Trincardi, F., 1999. The late Quaternary transgressive record in the Adriatic epicontinental sea: basin widening and facies partitioning. In K.M. Bergman J.W. Snedden, (eds), Isolated Shallow Marine Sand Bodies: Sequence Stratigraphic Analysis and sedimentologic Interpretation. Sequence Stratigraphic Analysis and Sedimentologic Interpretation. SEPM Special Publication, 64, 127-146.

Catuneanu, O., 2006. Principles of Sequence Stratigraphy. Elsevier, Amsterdam, 386 pp.

Chaumillon, E., Proust, J.-N., Ménier, D., Weber, N., 2008. Incised-valley morphologies and sedimentary-fills within the inner shelf of the northern Bay of Biscay. Journal of Marine Systems, 72, 383-396.

Chaumillon, E., Tessier, B., Reynaud, J.Y., 2010. Stratigraphic records and variability of Incised valleys and estuaries along French coasts. Bulletin de La Societe Geologique de France, 181, 75-85.

Clark, P., Dyke, A., Shakun, J., Carlson, A., Clark, J., Wohlfarth, B., Mitrovica, J., Hostetler, S., McCabe, A., 2009. The Last Glacial Maximum. Science, 325, 710-714.

Clement, A. J. H., Fuller, I. C., Sloss, C. R., . (2017). Facies architecture, morphostratigraphy, and sedimentary evolution of a rapidly-infilled Holocene incised-valley estuary: The lower Manawatu valley, North Island New Zealand. Marine Geology, 390(April), 214-233.

Cooper, J.A.G., Green, A.N., Meireles, R.P., Klein, A.H.F., Souza, J., Toldo, E.E., 2016. Sandy barrier overstepping and preservation linked to rapid sea level rise and geological setting. Marine Geology, 382, 80-91.

Correggiari, A., Cattaneo, A., Trincardi, F., 2005. The modern Po Delta system: Lobe switching and asymmetric prodelta growth. Marine Geology, 222-223, pp.49-74.

Correggiari, A., Roveri, M. Trincardi, F., 1996b. Late Pleistocene and Holocene Evolution of the North Adriatic Sea. Il Quaternario-Italian Journal of Quaternary Sciences, 9, 697-704.

Correggiari, A.M., Field, M.E., Trincardi, F., 1996a. Late Quaternary transgressive large dunes on the sediment-starved Adriatic shelf. In: M. DE

BATIST P. JACOBS (eds), Geology of Siliciclastic Shelf Seas. Geol. Soc., spec. publ., 117, 155-169.

D'Alpaos, L., 2010. Fatti e misfatti di idraulica lagunare: la laguna di Venezia dalla diversione dei fiumi alle nuove opere alle bocche di porto. Memorie Istit. Veneto Lettere Scienze Arti 44, Venezia, 329

D'Onofrio, S., 1969. Ricerche sui foraminiferi nei fondali antistanti il delta del Po. G. Geol. Ser. 2, 36, 189-310.

Dalrymple, R.W., Boyd, R., Zaitlin, B.A. (eds), 1994. Incised-Valley Systems: Origin and Sedimentary Sequences: SEPM Special Publication, 51, 391.

Dalrymple, R.W., Leckie, D.A., Tillman, R.W. (eds), 2006. Incised Valleys in Time and Space: SEPM Special Publication, 85, 350.

De Clercq, M., Missiaen, T., Wallinga, J., Zurita Hurtado, O., Versendaal, A., Mathys, M., De Batist, M., 2018. A well-preserved Eemian incised-valley fill in the southern North Sea Basin, Belgian Continental Shelf-Coastal Plain: implications for northwest European landscape evolution. Earth Surface Processes and Landforms.

De Marchi, L., 1922. Variazioni del livello dell'Adriatico in corrispondenza con le espansioni glaciali, Atti Accademia Scientifica Veneto-Trentino-Istriana 12-13, 1-15.

Doglioni, C., 1993. Some remarks on the origin of foredeeps. Tectonophysics, 228, 1-20.

Donnici, S., Serandrei-Barbero, R., 2002. The benthic foraminiferal communities of the North Adriatic continental shelf. Marine Micropaleontology, 44, 93-123.

Elias, E.P.L., Van Der Spek, A.J.F., 2006. Long-term morphodynamic evolution of Texel Inlet and its ebb-tidal delta (The Netherlands). Marine Geology, 225, 5-21.

Fairbanks, R.G., 1989. A 17,000-year glacio-eustatic sea level record: influence of glacial melting dates on the Younger Dryas event and deep ocean circulation. Nature 342, 637-642.

Fleming, K., Johnston, P., Zwartz, D., Yokoyama, Y., Lambeck, K., Chappell, J. (1998). Refining the eustatic sea-level curve since the Last Glacial Maximum using far- and intermediate-field sites. Earth and Planetary Science Letters, 163(1-4).

Fontana, A., Mozzi, P., Bondesan, A., 2008. Alluvial megafans in the Venetian-Friulian Plain (north-eastern Italy): Evidence of sedimentary and erosive phases during Late Pleistocene and Holocene. Quaternary International, 189, 71-90.

Fontana, A., Mozzi, P., Bondesan, A., 2010. Late Pleistocene evolution of the Venetian-Friulian Plain. Rendiconti Lincei, 21, 181-196.

Fontana, A., Monegato, G., Devoto, S., Zavagno, E., Burla, I., Cucchi, F., 2014. Evolution of an Alpine fluvioglacial system at the LGM decay: The Cormor megafan (NE Italy). Geomorphology, 204, 136-153.

Fontolan, G., Pillon, S., Delli Quadri, F., Bezzi, A., 2007. Sediment storage at tidal inlets in northern Adriatic lagoons: Ebb-tidal delta morphodynamics, conservation and sand use strategies. Estuarine, Coastal and Shelf Science, 75, 261-277.

Fontolan, G., Pillon, S.F., Bezzi, A., Villalta, R., Lipizer, M., Triches, A., D'Aietti, A., 2012. Human impact and the historical transformation of salt-marshes in the Marano and Grado Lagoon, northern Adriatic Sea. Estuarine, Coastal and Shelf Science, 113, 41-56.

Fowler, A.J., Gillespie, R., Hedges, R.E.M., 1986. Radiocarbon Dating of Sediments. Radiocarbon, 28, 441-450.

Fraccascia, S., Winter, C., Ernstsen, V. B., Hebbeln, D., 2016. Residual currents and bedform migration in a natural tidal inlet (Knudedyb, Danish Wadden Sea). Geomorphology, 271, 74-83.

Gasperini, L., Stanghellini, G., 2009. SeisPrho: An interactive computer program for processing and interpretation of high-resolution seismic reflection profiles. Computers and Geosciences, 35, 1497-1507.

Ghielmi, M., Minervini, M., Nini, C., Rogledi, S., Rossi, M., Vignolo, A., 2010. Sedimentary and tectonic evolution in the eastern Po-Plain and northern

adriatic sea area from messinian to middle Pleistocene (Italy). Rendiconti Fis. Accad. dei Lincei, 21, 131-166.

Gibbard, P.L., Hughes, P.D., Rolfe, C.J., 2017. New insights into the Quaternary evolution of the Bristol Channel, UK. Journal of Quaternary Science, 32, 564-578.

Giorgetti, G., Mosetti, F., 1969. General morphology of the Adriatic Sea. Bollettino di Geofisica Teorica ed Applicata, 11, 44-56.

Goff, J.A., Austin, J.A., Gulick, S., Nordfjord, S., Christensen, B., Sommerfield, C., Alexander, C., 2005. Recent and modern marine erosion on the New Jersey outer shelf. Marine Geology, 216, 275-296.

Goodfriend, G.A., Hood, D.G., 1983. Carbon isotope analysis of land snail shells: implications for carbon sources and radiocarbon dating. Radiocarbon, 25, 810-830.

Goodfriend, G.A., Ellis, G.L., and Toolin, L.J., 1999. Radiocarbon age anomalies in land snail shells from Texas: ontogenetic, individual, and geographic patterns of variation. Radiocarbon, 41, 149-156.

Gordini, E., Caressa, S., Marocco, R., 2003. New morpho-sedimentological map of the Trieste Gulf (from Punta Tagliamento to Isonzo mouth). Gortania-Atti Museo Friulano Storia Naturale, 25, 5-29.

Hijma, M.P., van der Spek, A.J.F., van Heteren, S., 2010. Development of a mid-Holocene estuarine basin, Rhine-Meuse mouth area, offshore The Netherlands. Marine Geology, 271, pp.198-211.

Hoenegger, J., Piller, W and Baal, C., 1989. Reasons for spatial microdistribution of Foraminifers in a intertidal pool (Northern Adriatic sea). Mar. Ecol., 10, 43-78.

Hunt, D., Tucker, M.E., 1992. Stranded Parasequences and the forced regressive wedge Systems Tract: deposition during base-level fall. Sedimentary Geology, 81, 1-9.

Jorissen, F.J., 1987. The distribution of benthic foraminifera in the Adriatic Sea. Marine Micropaleontology, 12, 21-48.

Jorissen, F.J., 1988. Benthic Foraminifera from the Adriatic Sea; principles of phenotypic variation. Utrecht Micropal. Bulletin, 37, 176 pp.

Jorissen, F.J., Barmawidjaja, D.M., Puskaric, S., Van der Zwaan, G.J., 1992. Vertical distribution of benthic foraminifera in the northern Adriatic Sea: the relation with the organic flux. Marine Micropaleontology, 19, 131-146.

Jouet, G., Berné, S., Rabineau, M., Bassetti, M.A., Bernier, P., Dennielou, B., Taviani, M., 2006. Shoreface migrations at the shelf edge and sea-level changes around the Last Glacial Maximum (Gulf of Lions, NW Mediterranean). Marine Geology, 234, 21-42.

Kindler, P., Guillevic, M., Baumgartner, M., Schwander, J., Landais, A., Leuenberger, M., 2014. Temperature reconstruction from 10 to 120 kyr b2k from the NGRIP ice core. Clim. Environ. Phys., 10, 887-902.

Lambeck, K., Antonioli, F., Anzidei, M., Ferranti, L., Leoni, G., Scicchitano, G., Silenzi, S., 2011. Sea level change along the Italian coast during the Holocene and projections for the future. Quaternary International, 232, 250-257.

Lambeck, K., Antonioli, F., Purcell, A., Silenzi, S., 2004. Sea-level change along the Italian coast for the past 10,000yr. Quaternary Science Reviews, 23, 1567-1598.

Lambeck, K., Roubya, H., Purcell, A., Sun, Y., Malcolm, S., 2014. Sea level and global ice volumes from the Last Glacial Maximum to the Holocene. PNAS, 111, 15296-15303.

Langer, M.R., Frick, H., Silk, M.T., 1998. Photophile and sciaphil foraminiferal assemblages from marine plant communities of Lavezzi Islands (Corsica, Mediterranean Sea). Revue Paleobiol., Geneve 17, 525-530.

Leopold, L.B., Wolman, M.G., Miller, J.P., 1964. Fluvial processes in Geomorphology, 544. Freeman, San Francisco.

Lericolais, G., Auffret, J.P., Bourillet, J.F., 2003. The Quaternary Channel River: Seismic stratigraphy of its palaeo-valleys and deeps. Journal of Quaternary Science, 18, 245-260.

Li, C., Wang, P., Fan, D., Yang, S., 2006. Characteristics and formation of Late Quaternary incised-valley-fill sequences in sediment-rich deltas and estuaries: Case studies from China. Incised Valleys: SEPM Special Publication, 85, 1-20.

Longhitano, S.G., Della Luna, R., Milone, A.L., Cilumbriello, A., Caffau, M., Spilotro, G., 2015. The 20,000-years-long sedimentary record of the Lesina coastal system (southern Italy): From alluvial, to tidal, to wave process regime change. The Holocene, 26, 678-698.

Madricardo, F., Donnici, S., 2014. Mapping past and recent landscape modifications in the Lagoon of Venice through geophysical surveys and historical maps. Anthropocene, 6, 86-96.

Madricardo, F., Donnici, S., Buogo, S., Calicchia, P., Lezziero, A., De Carli, F., Boccardi, E., 2007. Palaeoenvironment reconstruction in the Lagoon of Venice through wide-area acoustic surveys and core sampling. Estuarine, Coastal and Shelf Science, 75, 205-213.

Marocco, R., Pessina, M., 1995. II rischio litorale nell'area circumlagunare del Friuli-Venezia Giulia/Coastal risk in the surrounding area of Marano and Grado lagoon (Friuli-Venezia Giulia, Italy). Gortania, 17, 5-35.

Maselli, V., Hutton, E.W., Kettner, A.J., Syvitski, J.P.M., Trincardi, F., 2011. High-frequency sea level and sediment supply fluctuations during Termination I: An integrated sequence-stratigraphy and modeling approach from the Adriatic Sea (Central Mediterranean). Marine Geology, 287, 54-70.

Maselli, V., Trincardi, F., 2013. Large-scale single incised valley from a small catchment basin on the western Adriatic margin (central Mediterranean Sea). Global and Planetary Change, 100, 245-262.

Maselli, V., Trincardi, F., Asioli, A., Ceregato, A., Rizzetto, F., Taviani, M., 2014. Delta growth and river valleys: The influence of climate and sea level changes on the South Adriatic shelf (Mediterranean Sea). Quaternary Science Reviews, 99, 146-163.

Massari, F., Rio, D., Serandrei Barbero, R., Asioli, A., Capraro, L., Fornaciari, E., Vergerio, P.P., 2004. The environment of Venice area in the past two

million years. Palaeogeography, Palaeoclimatology, Palaeoecology, 202, 273-308.

Mateu-Vicens, G., Box, A., Deudero, S., Rodriguez, B., 2010. Comparative analysis of epiphytic foraminifera in sediments colonized by seagrass Posidonia oceanica S. Caulerpa sJournal of Foraminiferal Research, 40, 134-147.

Menier, D., Tessier, B., Proust, J.N., Baltzer, A., Sorrel, P., Traini, C., 2010. The Holocene transgression as recorded by incised-valley infilling in a rocky coast context with low sediment supply (southern Brittany, western france). Bulletin de La Societe Geologique de France, 181, 115-128.

Miola, A., Bondesan, A., Corain, L., Favaretto, S., Mozzi, P., Piovan, S., Sostizzo, I., 2006. Wetlands in the Venetian Po Plain (northeastern Italy) during the Last Glacial Maximum: Interplay between vegetation, hydrology and sedimentary environment. Review of Palaeobotany and Palynology, 141, 53-81.

Monegato, G., Pini, R., Ravazzi, C., Reimer, P.J., Wick, L., 2011. Correlating Alpine glaciation with Adriatic sea-level changes through lake and alluvial stratigraphy. Journal of Quaternary Science, 26, 791-804.

Monegato, G., Ravazzi, C., Donegana, M., Pini, R., Calderoni, G.,Wick, L., 2007. Evidence of a two-fold glacial advance during the last glacial maximum in the Tagliamento end moraine system (eastern Alps). Quaternary Research, 68, 284-302.

Monegato, G., Scardia, G., Hajdas, I., Rizzini, F., Piccin, A., 2017. The Alpine LGM in the boreal ice-sheets game. Scientific Reports, 7, 1-8.

Moscon, G., Correggiari, A., Stefani, C., Fontana, A., Remia, A., 2015. Very-high resolution analysis of a transgressive deposit in the Northern Adriatic Sea (Italy). Alpine and Mediterranean Quaternary 28, 121-129.

Mozzi, P., Ferrarese, F., Fontana, A., 2013. Integrating digital elevation models and stratigraphic data for the reconstruction of the post-LGM unconformity in the Brenta alluvial megafan (North-Eastern Italy). Alpine and Mediterranean Quaternary 26, 41-54.

148

Nordfjord, S., Goff, J.A., Austin, J.A., Gulick, S.P.S., 2006. Seismic Facies of Incised-Valley Fills, New Jersey Continental Shelf: Implications for Erosion and Preservation Processes Acting During Latest Pleistocene-Holocene Transgression. Journal of Sedimentary Research, 76, 1284-1303.

Nordfjord, S., Goff, J.A., Austin, J.A., Sommerfield, C.K., 2005. Seismic geomorphology of buried channel systems on the New Jersey outer shelf: assessing past environmental conditions. Marine Geology, 214, 339-364.

North Greenland Ice Core Project Members, 2004. High-resolution record of Northern Hemisphere climate extending into the last interglacial period. Nature, 431, 147-151.

Orange, D., García-García, A., Lorenson, T., Nittrouer, C., Milligan, T., Miserocchi, S., Trincardi, F., 2005. Shallow gas and flood deposition on the Po Delta. Marine Geology, 222-223, 159-177.

Pellegrini, C., Maselli, V., Cattaneo, A., Piva, A., Ceregato, A., Trincardi, F., 2015. Anatomy of a compound delta from the post-glacial transgressive record in the Adriatic Sea. Marine Geology, 362, 43-59.

Pellegrini, C., Maselli, V., Gamberi, F., Asioli, A., Bohacs, K.M., Drexler, T.D., Trincardi, F., 2017. How to make a 350-m-thick lowstand systems tract in 17,000 years: The Late Pleistocene Po River (Italy) lowstand wedge. Geology, 45, 327-330.

Pigati J.S., 2013 Radiocarbon Dating of Terrestrial Carbonates. In: Rink W., Thompson J. (eds) Encyclopedia of Scientific Dating Methods. Springer, Dordrecht

Pigati, J.S., Rech, J.A., and Nekola, J.C., 2010. Radiocarbon dating of small terrestrial gastropods in North America. Quaternary Geochronology, 5, 519-532.

Pini, R., Ravazzi, C., Reimer, P.J., 2010. The vegetation and climate history of the last glacial cycle in a new pollen record from Lake Fimon (southern Alpine foreland, N-Italy). Quaternary Science Reviews, 29, 3115-3137.

Piovan, S., Mozzi, P., Zecchin, M., 2012. The interplay between adjacent Adige and Po alluvial systems and deltas in the late Holocene (Northern Italy). Geomorphologie 18, 427-440.

Piva, A., Asioli, A., Schneider, R.R., Trincardi, F., Andersen, N., Colmenero-Hidalgo, E., Dennielou, B., Flores, J.-A., Vigliotti, L., 2008. Climatic cycles as expressed in sediments of the PROMESS1 borehole PRAD1-2, central Adriatic, for the last 370 ka: 1. Integrated stratigraphy. Geochem. Geophys. Geosyst., 9, Q01R01.

Quarta, G., Romaniello, L., D'Elia, M., Mastronuzzi, G., Calcagnile, L., 2007. Radiocarbon age anomalies in pre- and post-bomb land snails from the coastal Mediterranean basin. Radiocarbon 49, 817-826.

Reimer, P.J., McCormac, F.G., 2002. Marine radiocarbon reservoir corrections for the Mediterranean and Aegean Seas. Radiocarbon 44, 159-166.

Reimer, P.J., Bard, E., Bayliss, A., Beck, J.W., Blackwell, P.G., Bronk Ramsey, C., Grootes, P.M., Guilderson, T.P., Haflidason, H., Hajdas, I., Hatté, C., Heaton, T.J., Hoffmann, D.L., Hogg, A.G., Hughen, K.A., Kaiser, K.F., Kromer, B., Manning, S.W., Niu, M., Reimer, R.W., Richards, D.A., Scott, E.M., Southon, J.R., Staff, R.A., Turney, C.S.M., van der Plicht, J., 2013. IntCal13 and Marine13 Radiocarbon Age Calibration Curves 0-50,000 Years cal BP. Radiocarbon 55, 1869-1887.

Rieu, R., van Heteren, S., Van der Spek, A.J.F., De Boer, P.L., 2005. Development and preservation of a Mid-Holocene tidal-channel network offshore the Western Netherlands. Journal of Sedimentary Research, 75, 409-419.

Rossato, S., Mozzi, P., 2016. Inferring LGM sedimentary and climatic changes in the southern Eastern Alps foreland through the analysis of a 14C ages database (Brenta megafan, Italy). Quaternary Science Reviews 148, 115-127.

Scott D.B., Medioli, F.S. and Schafer C., 2001. Monitoring in Coastal Environments using Foraminifera and Thecamoebians Indicators. Cambridge University Press, 177 pp.

Serandrei-Barbero, R., Albani, A., Bonardi, M., 2004. Ancient and modern salt marshes in the Lagoon of Venice. Palaeogeography, Palaeoclimatology, Palaeoecology 202, 229-244.

Shotton, F.W., 1972. An example of hard-water error in radiocarbon dating of vegetable matter. Nature, 240, 460-461.

Simms, A.R., Aryal, N., Miller, L., Yokoyama, Y., 2010. The incised valley of Baffin Bay, Texas: a tale of two climates. Sedimentology 57, 642-669.

Soil Survey Staff, 1999. Soil Taxonomy: A Basic System of Soil Classification for Making and Interpreting Soil Surveys. second ed USDA-SCS Agric. Handb. 436. US Gov. Print. Office,Washington, DC

Stanford, J.D., Hemingway, R., Rohling, E.J., Challenor, P G., Medina-Elizalde, M., Lester, A.J., 2011. Sea-level probability for the last deglaciation: A statistical analysis of far-field records. Global and Planetary Change, 79, 193-203.

Stefani, M., Vincenzi, S., 2005. The interplay of eustasy, climate and human activity in the late Quaternary depositional evolution and sedimentary architecture of the Po Delta system. Marine Geology, 222-223, 19-48.

Stoker, M.S., Pheasant, J.B., Josenhans, H., 1997. Seismic Methods and Interpretation. In: Davies T.A. et al. (eds), Glaciated Continental Margins. Springer, Dordrecht.

Storms, J.E.A., Weltje, G.J., Terra, G.J., Cattaneo, A., Trincardi, A., 2008. Coastal dynamics under conditions of rapid sea-level rise: Late Pleistocene to Early Holocene evolution of barrier-lagoon systems on the northern Adriatic shelf (Italy). Quaternary Science Reviews 27, 1107-1123.

Stuiver, M., Reimer, P.J., and Reimer, R.W., 2017, CALIB 7.1 [WWW program] at http://calib.org, accessed 2017-2-5

Tanabe, S., Nakanishi, T., Ishihara, Y., Nakashima, R., 2015. Millennial-scale stratigraphy of a tide-dominated incised valley during the last 14 kyr: spatial and quantitative reconstruction in the Tokyo Lowland, central Japan. Sedimentology 62, 1837-1872.

Tesi, T., Asioli, A., Minisini, D., Maselli, V., Dalla Valle, G., Gamberi, F., Trincardi, F., 2017. Large-scale response of the Eastern Mediterranean thermohaline circulation to African monsoon intensification during sapropel S1 formation. Quaternary Science Reviews, 159, 139-154.

Triches, A., Pillon, S., Bezzi, A., Lipizer, M., Gordini, E., Villalta, R., Fontolan, G., Menchini, G., 2011. Carta batimetrica della Laguna di Marano e Grado. Arti Grafiche Friulane, Imoco spa (UD), 39.

Trincardi, F., Correggiari, A., Roveri, M., 1994. Late Quaternary transgressive erosion and deposition in a modern epicontinental shelf: The Adriatic semienclosed basin. Geo-Marine Letters, 14, 41-51.

Trincardi, F., Correggiari, A., 2000, Quaternary forced regression deposits in the Adriatic basin and the record of composite sea-level cycles: Geological Society of London Special Publications, 172, 245-269.

Trincardi F., Argnani A. (eds), 2001. Note illustrative della Carta Geologica d'Italia alla scala 1:250,000-Foglio NL33-10 "Ravenna". ISPRA-Servizio Geologico d'Italia.

Trincardi, F., Argnani, A., Correggiari, A., 2011. Note illustrative della Carta Geologica d'Italia alla scala 1:250,000-Foglio NL33-7 "Venezia", ISPRA-Servizio Geologico d'Italia.

Trincardi, F., Campiani, E., Correggiari, A., Foglini, F., Maselli, V., Remia, A., 2014. Bathymetry of the Adriatic Sea: The legacy of the last eustatic cycle and the impact of modern sediment dispersal. Journal of Maps, 10, 151-158.

Trobec, A., Andrej, Š., Sašo, P., Marko, V., 2017. Submerged and Buried Pleistocene River Channels in the Gulf of Trieste (Northern Adriatic Sea): Geomorphic, Stratigraphic and Tectonic Inferences. Geomorphology, 286, 110-20.

Tropeano, M., Cilumbriello, A., Sabato, L., Gallicchio, S., Grippa, A., Longhi-tano, S.G., Bianca, M., Gallipoli, M.R., Mucciarelli, M., Spilotro, G., 2013. Surface and subsurface of the Metaponto Coastal Plain (Gulf of Taranto-southern Italy): Present-day- vs LGM-landscape. Geomorphology, 203, 115-131.

Vacchi, M., Marriner, N., Morhange, C., Spada, G., Fontana, A., Rovere, A., 2016. Multiproxy assessment of Holocene relative sea-level changes in the western Mediterranean: variability in the sea-level histories and redefinition of the isostatic signal. Earth Science Reviews, 155, pp, 172-197.

Vai, G.B., Cantelli, L., (eds), 2004. Litho-Palaeoenvironmental Maps of Italy During the Last Two Climatic Extremes Two Maps 1:1,000,000. Explanatory Notes Edited by Antonioli, F., Vai, G.B., 32 IGC publications.

Van der Zwaan G.J., Jorissen F.J., 1991. Biofacial patterns in river-induced shelf anoxia. In: R.V. Tyson and T.H. Pearson (eds): "Modern and Ancient Continental Shelf Anoxia". Geological Society, Spec. Publ., 58, 65-82.

Van Wagoner, J.C., Mitchum, R.M., Campion, K.M., Rahmanian, V.D., 1990. Siliciclastic sequence stratigraphy in well logs, cores, and outcrops: concepts for high-resolution correlation of time and facies. AAPG Methods Explor, 7, 55.

Vis, G.J., Kasse, C., 2009. Late Quaternary valley-fill succession of the Lower Tagus Valley, Portugal. Sedimentary Geology 221, 19-39.

Waelbroeck, C., Labeyrie, L., Michel, E., Duplessy, J.C., McManus, J.F., Lambeck, K., Balbon, E., Labracherie, M., 2002. Sea-level and deep water temperature changes derived frombenthic foraminifera isotopic records. Quaternary Science Reviews, 21, 295-305.

Weschenfelder, J., Baitelli, R., Corrêa, I.C.S., Bortolin, E.C., dos Santos, C.B., 2014. Quaternary incised valleys in southern Brazil coastal zone. Journal of South American Earth Sciences, 55, 83-93.

Zecchin, M., Baradello, L., Brancolini, G., Donda, F., Rizzetto, F., Tosi, L., 2008. Sequence stratigraphy based on high-resolution seismic profiles in the late Pleistocene and Holocene deposits of the Venice area. Marine Geology, 253, 185-198.

Zecchin, M., Brancolini, G., Tosi, L., Rizzetto, F., Caffau, M., Baradello, L., 2009. Anatomy of the Holocene succession of the southern Venice lagoon revealed by very high resolution seismic data. Continental Shelf Research, 29, 1343-1359.

Zecchin, M., Gordini, E., Ramella, R., 2015. Recognition of a drowned delta in the northern Adriatic Sea, Italy: Stratigraphic characteristics and its significance in the frame of the early Holocene sea-level rise. The Holocene, 25, pp, 1027-1038.

Zecchin, M., Donda, F., Forlin, E., 2017. Genesis of the Northern Adriatic Sea (Northern Italy) since early Pliocene. Marine and Petroleum Geology, 79, 108-130.

ANATOMY OF A TRANSGRESSIVE TIDAL INLET RECONSTRUCTED THROUGH HIGH-RESOLUTION SEISMIC PROFILING

Abstract

Although the morphology and morphodynamics of modern highstand tidal inlets have been analyzed in a wealth of studies, little is known about the characteristics and evolution of their transgressive equivalents. Through the analysis of high-resolution CHIRP profiles, this work investigates a rare example of a preserved infilled tidal inlet formed during the early Holocene on the continental shelf of the northern Adriatic Sea. The quantity and quality of the available data allowed a detailed reconstruction of the morphology and internal architecture of this feature. This 1.2 km long channelized scour is characterized by a maximum thickness of ca. 17 m in its central sector. This value decreases rapidly in both landward and seaward directions up to become null. The internal geometry of the infilling material suggests that this landform underwent a rapid evolution, as no evidence of lateral migration is recognizable.This research highlight the possible use of paleo tidal inlets as paleoenvironmental and paleogeographical proxies, and in particular their role in defining the position of paleo coastlines and paleo sea levels.

4.1 INTRODUCTION

By providing the connection between open sea and sheltered lagoons areas, tidal inlets stand as gateways to different hydrodynamic conditions, morphological settings and ecological environments (Mehta and Joshi, 1988; FitzGerald et al., 2012). In many areas worldwide, they have played an essential role for the maritime transport, allowing the access to important harbors and economic productive poles. As a matter of fact, many tidal inlets are now highly-anthropized landforms due to the construction of jetties and breakwaters and the periodic dredging activity. Because of their importance, their morphology, morphodynamic and evolutionary trends have been investigated in detail since the beginning of the last century (e.g. O'Brien, 1931; Escoffier, 1940; Price, 1947; Kumar and Sanders, 1974; Boothroyd, 1985; Fontolan et

---

al., 2007; FitzGerald et al., 2001; FitzGerald and Miner, 2013). Tidal inlets are extremely dynamic landforms, prone to expand, migrate or shrink and disappear following the variations in the equilibrium between sediment supply, local hydrodynamic conditions and relative sea-level variations (FitzGerald and Miner, 2013). Several empiric laws describing the relationship between the morphometry of the tidal inlets and the hydraulic forcing of the environment have been proposed (cf. O'Brien, 1931; Walton and Adams, 1976; D'Alpaos, 2010; FitzGerald and Miner, 2013). The rate of deposition within a tidal inlet is controlled as well by several variables, such as the tidal range and prism, the basin area, the rate of sediment supply and the grain size (cf. Van Goor et al., 2003, Chang et al., 2006; Tran et al., 2012). All these parameters reflect the geometry of the area and the interplay between basin and source controls. Nevertheless, it is worth noting that all the notions inferred from the modern tidal inlets are representative for highstand lagoon environments.

The long-term preservation of a lagoon complex relies on the equilibrium between rates of sediment deposition and relative sea-level rise, in order to keep pace and avoid the overstepping of the lagoon (FitzGerald and Miner, 2013). Despite the number of papers focusing on modern inlets, little has been published on their fossil counterparts, especially on those evolved during the marine transgression occurred since the end of the last glaciation (cf. Lambeck et al., 2014). This absence of information can be mostly attributed to the lack of preservation of the tidal inlets and of lagoon deposits, in general due to the wave erosive effect of the rising sea (Belknap and Kraft, 1981; Cattaneo and Steel, 2003; Rieu et al., 2005; FitzGerald et al., 2012). Therefore, only few examples of such abandoned landforms have been detected in the stratigraphic record and they are usually only constituted by the lower portion of the tidal inlet filling. The few paleo tidal inlets identified on the Adriatic shelf are described in the works of Storms et al. (2008), Zecchin et al. (2009) and Ronchi et al. (2018).

This work offers a thoroughly analysis on the morphology and infilling of a transgressive tidal inlet and tries to infer some of the most notable characteristics of these features. On the basis of the analysis of this case study, we want to explore the possible use of these abandoned landforms as paleoenvironmental and paleogeographic proxies. Moreover, considering the ongoing sea-level rise, the study of these transgressive landforms may help to understand the evolutive pattern that will characterize the modern inlets and lagoons in the near future.
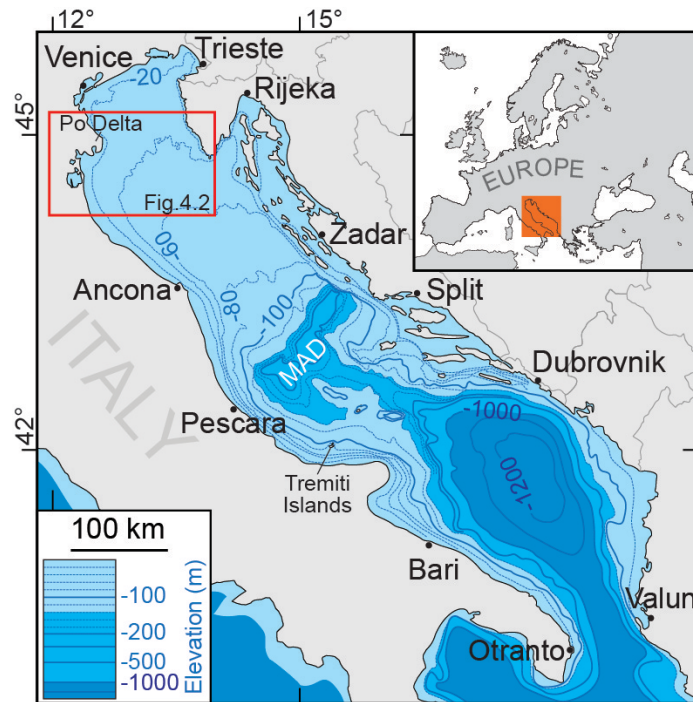
Figure 4.1: Location and bathymetry of the Adriatic Sea. The position of the area analysed in this work is indicated by the red rectangle.

4.2 REGIONAL SETTINGS

The Adriatic Sea is a narrow semi-enclosed epicontinental sea, approximately 200 km wide per 800 km long, which occupies the foreland basin between the Apennines and Dinaric thrust belts (Fig. 4.1; Doglioni, 1993; Scisciani and Calamita, 2009; Cuffaro et al. 2010).

Traditionally this basin is subdivided into three main sub-regions (northern, mid and southern Adriatic) on the basis of its morphological, structural and oceanographic characteristics. The study area is located in the northern Adriatic Sea, which occupies the entire continental shelf from the Gulf of Trieste to the shelf break, located approximately between Pescara and Zadar (Fig. 4.1). This sector extends for a total length of about 300 km and it is characterized by a peculiar low gradient (ca. 0.4‰), while an articulated micro topography, recognized by the bathymetric surveys carried-out in the area, can be locally observed (cf. Mosetti, 1966; Giorgietti and Mosetti, 1969; Gordini et al., 2003, 2004; Trincardi et al., 2014; Moscon et al., 2015; Trobec et al., 2017). The middle portion of the Adriatic basin is characterized by the Mid

Adriatic Deep (MAD), which is a depression that reaches a depth of 260 m below Mean Sea Level (MSL) and occupies the area between the shelf break and the Tremiti Islands structural high. The southern Adriatic occupies the rest of the basin down to the Otranto Strait, reaching a maximum depth of about -1 200 m MSL (Trincardi et al., 2014).

The present Po Delta and the area considered in this research are part of the foreland basin of the Northern Apennine. Although the front of the most external active thrusts runs from Ferrara to Comacchio to Rimini (Trincardi et al., 2001; Boccaletti et al., 2011), this area is characterized by a clear subsiding trend due to crustal deformation on regional scale and sediment compaction. An increasing downlift rate has been observed in the last century as a consequence of anthropic activity (Carminati et al., 2003; Ferranti et al., 2006; Amorosi et al., 2008; Antonioli et al., 2009; Perini et al., 2017). Along the coastal plain south of Po River, the average long-term subsidence rate is about ca. 1 mm/a, while in the offshore of Comacchio it is considerably lower (Antonioli et al., 2009; Vacchi et al., 2016).

Large portions of the western Adriatic shelf and of the contiguous coastal plains of the north-eastern Italy are mainly constituted by the outcropping alluvial sediments deposited during the Last Glacial Maximum (Correggiari et al., 1996; Fontana et al. 2014; Amorosi et al., 2017a; LGM, ca. $29 - 19$ ka BP, Clark et al., 2009). During this period the sea-level dropped below -120 m MSL (Lambeck et al., 2014; Amorosi et al., 2017a). The northern Adriatic shelf was thus exposed to subaerial condition, leading to the formation of an extensive alluvial plain crossed by the paleo-Po River, which was likely collecting the water and sediment discharges of a large part of the Alpine, Dinaric and Apennine fluvial systems (De Marchi, 1922; Kettner and Syvitski, 2009; Maselli et al., 2011; Amorosi et al., 2014; Pellegrini et al., 2017, 2018). With the end of the LGM, the northern Adriatic underwent a progressive submersion induced by the relative sea-level rise (Correggiari et al., 1996; Cattaneo and Trincardi, 1999). This condition lasted until ca. 5.5 ka BP, which marks the maximum marine transgression in the area and the beginning of the highstand period (Amorosi et al., 2017a).

The post-glacial transgression has been characterized by variable sea-level rise rates, which oscillated between the high values of the Melt Water Pulses (e.g. Bard et al., 1990; Siddall et al., 2003; Alley et al., 2005; Tanabe et al., 2015; Deschamps et al., 2012) to the null or even negative values of the Younger

Dryas (i.e. $12.8 - 11.7$ ka BP, Bard et al., 1990, 2010; Peltier and Fairbanks, 2006; Storms et al., 2008; Pellegrini et al., 2015). Another significant period of increased relative sea-level rise probably occurred between 9.5 and 9.2 ka BP (Liu et al., 2004) as also recently documented in the northern Adriatic Sea (Amorosi et al., 2017a; Ronchi et al., 2018a). The occurrence of periods characterized by low rates of sea-level rise is likely one of the factors that fostered the development of a series of transgressive barrier-lagoon system that were recognized by several authors at different bathymetries in the northern Adriatic Sea (Correggiari et al., 1996; Storms et al., 2008; Trincardi et al., 2011; Moscon et al., 2015; Zecchin et al., 2015).

The study area is located within the depth of -30 and -34 m MSL, about 30 km SSE of the main mouth of present Po river Delta and it extends for about 50 km^2 (Fig. 4.2). The evolution of this zone is strongly related to the post-LGM development of the Po River (Amorosi et al., 2017a). It is likely that during the Younger Dryas the main branches of Po used to flow rather close to the analysed area (Amorosi et al., 2017a), and the presence of submerged sand bodies on the Adriatic shelf testify the stabilisation of the coastline during this cold period around -70 and -50 m MSL (Correggiari et al., 1996; Trincardi et al., 2001; Storms et al., 2008). From ca. 10 ka BP the distributary channels of the Po outlet occupied almost entirely the analysed area, which was then submerged following the ongoing marine transgression (Amorosi et al., 2017a). From 7 ka BP the Po River main outlet fluctuated along more than 100 km of coastline, from the area of Ravenna to the southern margin of the Venice Lagoon (Bondesan et al., 1995; Stefani and Vincenzi, 2005; Zecchin et al., 2009; Piovan et al., 2012). The maximum marine ingression in this area was reached about 5.5 ka BP, when the coastline was placed up to 30 km landward of its present position (Stefani and Vincenzi, 2005). A decrease in the relative sea-level rise rate coupled with an increase in the sediment discharge promoted the transition to a marine normal regression phase (Bondesan et al. 1999; Stefani and Vincenzi, 2005) with the development of several wave-dominated cuspate highstand deltas (Correggiari et al., 2005a). The evolution and shifting of the Po River outlet during the last millennia is also evidenced by the presence of several prodelta lobes recognized in the offshore stratigraphy (Correggiari et al., 2005b; Maselli and Trincardi, 2013). The modern Po delta morphology and evolution markedly diverge from the previous trend, as it is the result of only 500 years evolution characterized both by anthropogenic
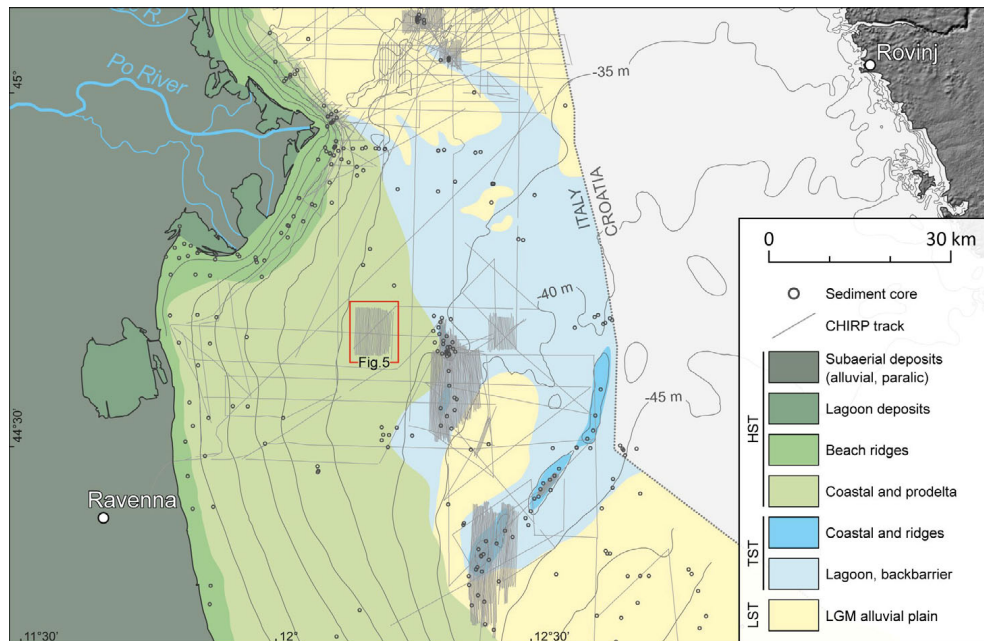
Figure 4.2: Geological map of the area considered in this work (location in Fig. 4.1) and available CHIRP dataset (Trincardi et al., 2001. The position of the area reconstructed in this work (Fig. 4.6) is reported.

activity and increasing in sediment runoff due to the onset of the Little Ice Age, which led to a seaward progradation of ca. 30 km (Correggiari et al., 2005a; Maselli and Trincardi, 2013).

The modern seafloor of the northern Adriatic Sea is mainly constituted by the remnants of the lowstand alluvial plain on which are resting bodies of transgressive material deposited in coastal or mixed water environments. On top of this unit, it is possible to recognize a thick muddy highstand wedge distributed along the modern Italian coast (Fig. 4.2; Trincardi et al., 2001, 2011; Cattaneto et al., 2007).

The Adriatic Sea is nowadays characterized by a counter-clockwise circulation of water (Amorosi et al., 2014), which was probably already active ca. 15 ka BP (Cattaneo and Trincardi, 1999). The model proposed by Storms et al. (2008) suggests a decreasing of the tidal amplitude and a slightly increase of the wave climate ratio during the post-LGM marine transgression. Their values can be however considered almost constant during the entire Holocene and, in particular, a mean tidal range of ca. 0.9 m can be estimated for the Comacchio and Po Delta area (Bondesan et al., 2001; Armaroli et al., 2012).

4.3 MATERIALS AND METHODS

CHIRP sonar profiles

The study area was investigated mainly through CHIRP profiles (Compressed High Intensity Radar Pulse). This technique is characterized by a high vertical resolution, ranging between 30 and 50 cm. In particular, 36 north-south oriented profiles, placed at evenly spaced intervals of about 200 m and covering a total length of ca. 270 km, were considered (Fig. 4.2, location marked by the red square). All these CHIRP profiles were collected during the ASCI14 oceanographic cruise organized by the CNR-ISMAR institute of Bologna on board of the R/V Urania. Other CHIRP profiles, collected with the same equipment during other oceanographic cruises, are here reported in order to provide a regional overview (cf. section 4.4).

All the seismic lines were acquired in water depths ranging from -30 and -33 m MSL. The obtained data have a good penetration, up to 8 m below seafloor but, in some cases, it was possible to reach depths up to 15 m. At higher depths the acoustic signal gradually fades and get blurry due to dispersion effects.

The CHIRP sonar profiles were collected with a Teledyne Benthos CHIRP-III SBP equipped with 16 low frequency transducers ($2 - 7$ kHz) mounted on the keel of R/V Urania. All the seismic data were recorded with SwanPRO 2.00 software as XTF files and converted to the open SEGY format. A D-GPS guaranteed the correct positioning of all the profiles. The collected data were analysed and processed through SeisPrho v.2.0 software (Gasperini and Stanghellini, 2009).

To provide the groundtruth for the interpretation of the seismic units, a series of already published cores, available for the northern Adriatic area, has been analysed (cf. for reference Correggiari et al., 1996; Trincardi et al., 2001; Moscon et al., 2015; Ronchi et al., 2018a).

DTM interpolation

The interpretation of the seismic facies recognized in the CHIRP profiles allowed to create the DTM of two main paleo surfaces. The digitalization of these reflectors was operated by manual picking, with the collection, on average, of one point every 7 m. The conversion of the profiles from two-way-time
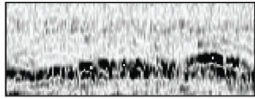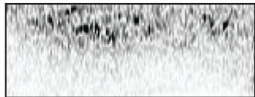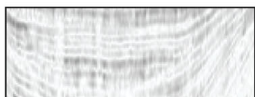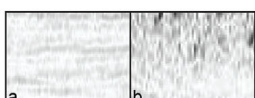
Unit	CHIRP	Characteristics	Interpretation
U3		Well stratified and prograding high-amplitude reflectors.	Muddy sediments. Po river prodelta deposits.
F5		Chaotic with rare horizontal layering.	Silty to very fine sand. Shallow marine environment.
F4		Semi-transparent bodies with chaotic internal geometry.	Sandy deposits. Remains of barrier complexes.
F3		Draping to lateral accreting reflectors. Low to high amplitude.	Silts to very-fine sands with brackish shell remains. Tidal inlet infilling.
F2		Irregular high-amplitude reflector, convex-upward cuspate shapes.	Muddy deposits with brackish shell remains. Brackish environment.
F1		Medium to high lateral continuity reflectors, subparallel and usually sub-horizontal.	Muddy deposits with brackish shell remains. Brackish environment.
U1		a: Sub-parallel horizontal reflectors with high lateral continuity. b: Chaotic facies with rare defined reflectors	Muddy (a) to sandy (b) sediments. Alluvial plain deposits and fluvial channel belts.

Figure 4.3: The main seismic units and facies recognized in this area along with their characteristic. The interpretation is based on published literature (cf. Correggiari et al., 2005b; Moscon et al., 2015; Ronchi et al., 2018a) and on core groundtruth.

(ms) to depth (m) was operated by considering a velocity of 1.5 m/ms (e.g. Goff et al., 2006; Nordfjord et al., 2005). The digitalized reflectors were then interpolated through ESRI ArcGis 10.5 software with the Topo to Raster interpolator tool. The obtained DTMs were then refined with a low-pass filter in order to smooth the artefacts produced by outliers in the hand-picked data. The resulting DTMs have a 5 m resolution.

4.4 RESULTS

Seismic units

The analysis of the CHIRP profiles led to the distinction of three main seismic units, in turn subdivided according to their different seismic facies, which

are summarized in Fig. 4.3 and described in detail below. All the identified facies are here reported together with their sedimentologic characteristics and paleontological content, if available, according to the already published data (Trincardi et al., 2001; Moscon et al., 2015).

UNIT 1 (U1)   This is the lowermost sedimentary unit and it is separated from the upper unit by the seismic reflector S1 (Fig. 4.4). This unit is present in all the analysed profiles at the bottom of the sequence. As partially lying outside the maximum depth of imaging permitted by the CHIRP method, this unit often appears almost transparent. The reflectors have usually high lateral continuity and are mostly sub-parallel and horizontal, but sometimes they are characterized by a more chaotic pattern (Figs. 4.3 and Fig. 4.4). Some convex-upward bodies can be distinguished at the top of this unit (Fig. 4.4, AS19). The groundtruth for the validation of the seismic interpretation was provided by a series of cores collected in the area (Fig. 4.2; cf. Trincardi et al., 2001). According to these data and the comparison with similar seismic facies described in the north Adriatic, the grain size of this unit spans from clay to sand, depending on the different depositional environments. The stratigraphy of the Po Plain (Bruno et al., 2017; Amorosi et al., 2017a,b) and of the northern Adriatic Sea (cf. section 4.4; Trincardi et al., 2001, 2011), coupled with the information provided by the topographic reconstruction of the area (cf. also paragraph 4.3.1), allowed to assess the alluvial genesis of Unit 1.

UNIT 2 (U2)   This unit is placed on top of Unit 1 and below the ravinement surface RS, as confirmed by the correlation to nearby areas (cf. paragraph 4.3; Fig. 4.5; Moscon et al., 2015). It has been sampled by several cores that allowed a detailed characterization of its deposits, which generally formed in a mixed fresh/brackish water environment, as also confirmed in studies carried out in nearby areas (Trincardi et al., 2001; Moscon et al., 2015). U2 has been further subdivided in a series of facies described below.

Facies 1 (U2F1).   This facies has low to medium amplitude in CHIRP profiles (Fig. 4.3) and it is constituted by reflectors with medium to high lateral continuity, subparallel and usually horizontal, but occasionally organized in sets of stacked inclined layers with a prograding geometry (Fig. 4.4, AS28). U2F1 is present only in few areas on top of S1 and it is often buried by U2F2, as described in the next paragraph. In the study area, the deposits
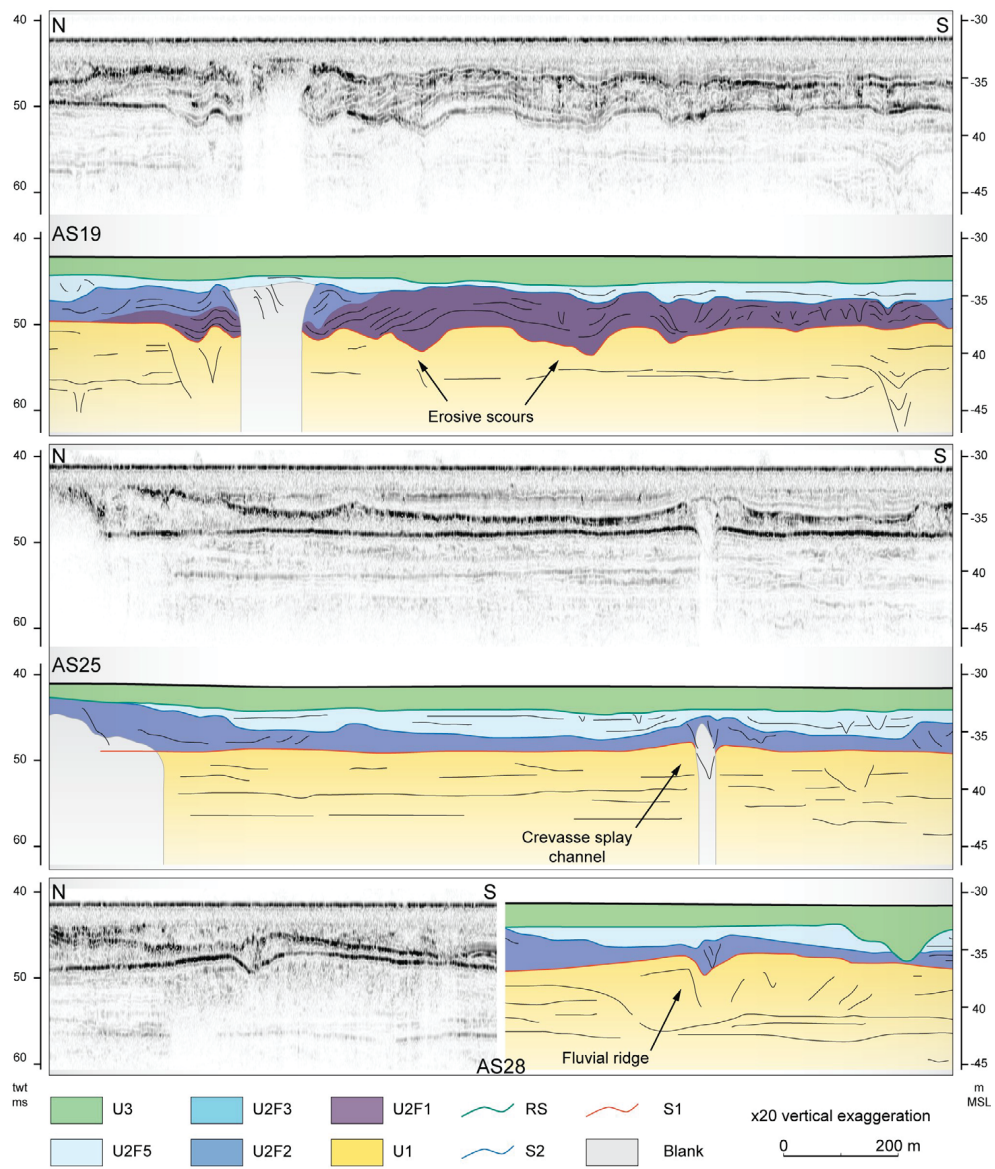
Figure 4.4: CHIRP profiles and related line drawing; position shown in Fig. 4.6. Details on the interpretation are provided in Chapter 4.

associated to this facies are often confined within shallow scours forming on top of S1 (Figs. 4.4 and Fig. 4.6). The lithologic information indicates a clayey composition with the occasional presence of laminations of organic material. The paleontological content of this facies, as provided by nearby cores (Fig. 4.5 for location), is characterized by an association of *Cerastoderma glaucum, Abra segmentum* and *Lentidium sp.*, that are generally representative of brackish water environment. It is likely that U2F1 formed in a partially-sheltered brackish environment that developed when the sea reached for the first time the area.

Facies 2 (U2F2). This facies is characterized by medium to low amplitude reflectors (Fig. 4.3), mostly arranged into a chaotic pattern with no recognizable geometries. The top of this unit has a high amplitude. Its upper boundary corresponds to an irregular high-amplitude reflector that delineates convex-upward cuspate shapes, spatially organized into elongated ridges (cf. paragraph 4.3). Similar reflectors are sometimes present also within this facies. U2F2 can be recognized in most of the studied area and a clear limit can be traced at the southern and eastern boundaries of the area (Fig. 4.5). The lithology and paleontological content of this facies are similar to those of U2F1, thus indicating a mixed brackish/fresh water environment. It is likely that the depositional environment corresponds to an estuarine/deltaic setting connected to the Po River outlet (cf. Amorosi et al., 2017a, Fig. 4.6).

Facies 3 (U2F3). This facies is constituted by stacked low to high-amplitude reflectors. This facies is always delimitated by a sharp erosive unconformity cut through the seismic facies described above. Its internal reflectors are typically arranged in a draping pattern that mimics the lower erosive boundary (Figs. 4.3 and Fig. 4.5). For a detailed description and interpretation of the infilling geometry of U2F3 see paragraph 4.4. The occurrence of deeply incised channels with similar internal geometries has been already described in several works from the Adriatic region, where these features have been univocally identified as paleo tidal inlets or main lagoon channels (cf. Trincardi et al., 2001, 2011; Storms et al., 2008; Ronchi et al., 2018a,b). Their infills are typically characterized by alternations of silts and very fine sands with a centimetric to millimetric lamination and the sporadic occurrence of organic-rich laminae. Considering the appearance of the seismic facies of the infilling of the incised

channel described in this work and its peculiar morphology (cf. section 4.4 and Fig. 4.6), U2F3 is interpreted as the infill deposit of a tidal inlet.

Facies 4 (U2F4).   This facies can be found in rare semi-transparent bodies with no clear internal geometry. Usually U2F4 is organized in convex-up, smoothed bodies resting on the top of the already described facies. Slightly east of the studied area, this seismic facies is represented by sandy deposits characterized by a Po River basin petrographic signature, as demonstrated by petrographic analyses (Moscon, 2016). This facies likely represent the remnants of the sandy barriers that delimitated the ancient lagoon environments connected to the described tidal inlets, as also recognized in other areas of the northern Adriatic (cf. Correggiari et al., 1996; Amorosi et al., 1999; Storms et al., 2008; Trincardi et al., 2011; Moscon et al., 2015).

Facies 5 (U2F5).   This facies fills the depressed areas defined by the ridge-shaped features visible on the S2 surface (cf. Fig. 4.6). This facies is characterized by low amplitude reflectors and is predominantly chaotic, at places showing a horizontal layering (Fig. 4.3). The top of U2F5 is bounded by the RS, as recognized through regional correlation (Moscon et al., 2015). This facies probably formed as the consequence of the generalized dismantlement of the landforms of the former lagoon promoted by the marine transgression. The available cores indicate a prevailing silty to very fine sand grain size, which become coarser and with abundant shell fragments in correspondence of the RS.

UNIT 3 (U3)   This unit is characterized by a well stratified, high amplitude wedge-shaped body shifting to a chaotic and transparent one moving seaward (Figs. 4.3 and Fig. 4.5) resting above the RS. This facies is constituted by the muddy sediments of the Po River prodelta, which correspond to the most recent deposits found in the area and that were produced by the marine highstand phase and the consequent progradation of the deltaic lobes (cf. Trincardi et al., 2001, 2011; Correggiari et al., 2005b).

Regional correlation

In order to provide a regional framework for this study, the CHIRP profiles NAD204 and ARP18 were merged, reaching a total length of 40 km (Fig. 4.5).

166

Lab code	Core	Lat N	Lon E	Seafloor (m MSL)	Depth (m)	Material	^{14}C age (a BP)	Calibrated 2σ age (a BP)	Mediane (a BP)	Unit	Source
-	CM95-12	44.78	12.65	-30.7	2.12 - 2.13	peat	8830 ± 60	9686 - 10166	9902	U2F2	Trincardi et al. (2001)
-	CM95-12	44.78	12.65	-30.7	3.26-3.34	peat	8960 ± 60	9910 - 10232	10070	U2F2	Trincardi et al. (2001)
-	CM95-13	44.75	12.71	-32.3	2.79 - 2.81	peat	9520 ± 60	10653 - 11099	10856	S1	Trincardi et al. (2001)
-	CM94-107	44.65	12.82	-34.2	3.63 - 3.65	peat	9600 ± 70	10731 - 11177	10944	S1	Trincardi et al. (2001)
ETH-57129	AR00-22	44.69	12.80	-34.2	0.67	Macrofossil	8828 ± 32	9312 - 9506	9452	S2	Moscon et al. (2015)
ETH-57130	AR00-22	44.69	12.80	-34.2	1.35	Macrofossil	8869 ± 23	9386 - 9594	9485	U2F2	Moscon et al. (2015)
ETH-57131	AR00-22	44.69	12.80	-34.2	3.39	Macrofossil	9307 ± 23	9907 - 10206	10089	U2F2	Moscon et al. (2015)

Table 4.1: List of radiocarbon dates used in this study. The position of the cores is indicated in Fig. 3.5.

This profile allows to correlate the study area with already published works (cf. Trincardi et al., 2001, Correggiari et al., 2005b; Moscon et al., 2015; Moscon, 2016; Amorosi et al., 2017a; Bruno et al., 2017) and selected cores (Fig. 4.5; Tab. 4.1) to support the stratigraphic interpretation.

As represented in Fig. 4.5, almost the entire area is covered by the highstand deposits of the Po River prodelta, here represented by U3. The smooth surface of the prodelta gently slopes toward east-southeast with a value of about 0.02°, which in landward direction increases up to 0.06°. The mixed-environment deposits of U2 are widespread all over the study area with a regular mean thickness of ca. 5 m, except in the case of the infilled paleo tidal inlets (U2F3), where the thickness can reach values up to 17 m. As shown in Fig. 4.5, the occurrence of the tidal inlet infilling facies (U2F3) is not limited to the area reconstructed in Fig. 4.6, as pieces of evidence of some smaller abandoned inlets are also present in landward direction.

The estuarine/deltaic facies U2F2 can be tracked on a wide and well-defined area through several seismic profiles. A clear boundary on the landward portion of the profile is also visible in Fig. 4.5, while the seaward limit lies outside the reported profile. Some radiocarbon dates, available from literature and performed on organic sediments from U2F2 indicate that this unit formed between ca. 10.0 ka and 9.5 ka cal BP during at least three main pulses of sediment input in the system (Tab. 4.1; Moscon et al., 2015). The lower unit, U1, is widespread below all the described younger deposits and it corresponds to the alluvial plain formed during the marine lowstand and early transgression phases. Several cores sampled in the coastal plain (Amorosi et al., 2017a; Bruno et al., 2017) and from the Adriatic shelf (Correggiari et al., 1996; Trincardi et al., 2001; Picone et al., 2008) document the continental environments and the LGM or Late Glacial age of the top portion of U1.
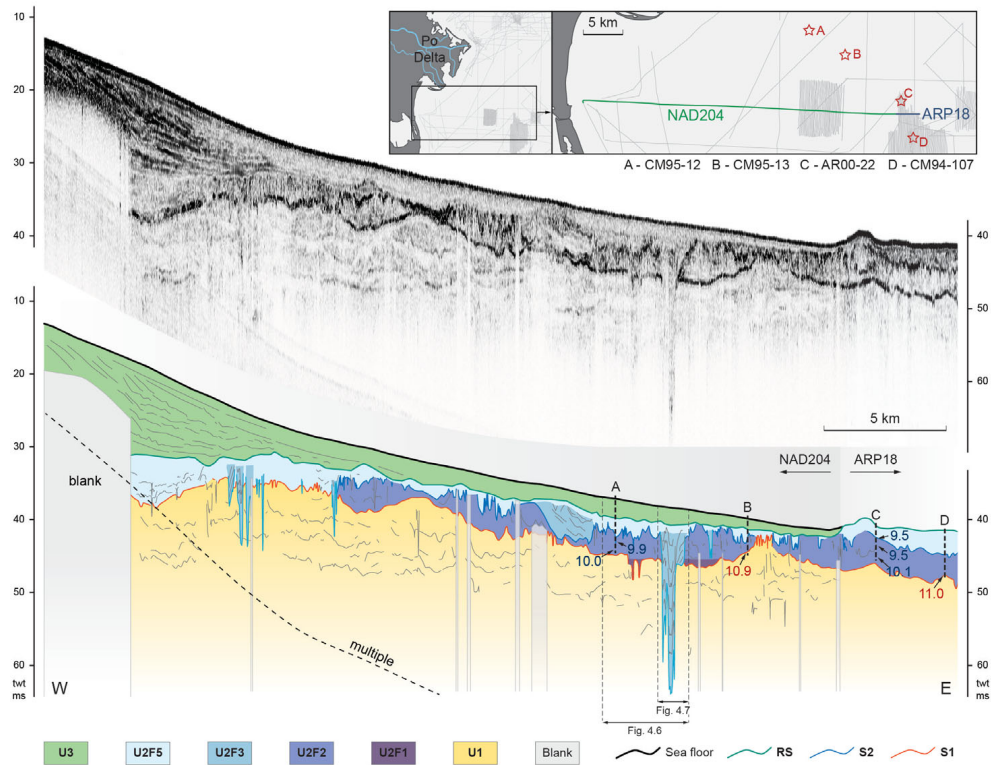
Figure 4.5: Longitudinal CHIRP profile showing the stratigraphy of the area. The location of the CHIRP profiles used for this reconstruction (profiles NAD204 and ARP18) is reported in Fig. 4.2. The ages reported on the cores (location in the inset) are expressed as ka cal BP.

Surface reconstruction and interpretation

A DTM reconstruction was carried out on the study area for the main surfaces S1 and S2 (Fig. 4.6). These reflectors are easily detectable because of their high acoustic impedance, which is a typical signature of the presence of organic-rich layers and peat deposits. The interpolation of these DTM was possible due to the availability of closely-spaced parallel CHIRP profiles (Figs. 4.2 and Fig. 4.6). The 3D reconstruction of these surfaces allowed to a detailed reconstruction of the paleogeographic evolution of the entire area.

SURFACE 1 (S1)   The DTM reconstructed through the interpolation of reflector S1 (Fig. 4.6) spans between -34 and -39 m MSL and separates U1 from U2, therefore it represents the boundary between the alluvial plain and the delta plain environments. The interpolation of this surface highlighted the presence

of some ridge-shaped structures that are elevated for about 2 m above the mean values of S1 (#A and B in Fig. 4.6). In particular, in the southern sector a ridge with a WSW-ENE direction is exceptionally well-preserved and it is possible to recognize a sinuous and slightly depressed feature that runs along almost the whole length of the ridge (#B in Fig. 4.6). This feature can be interpreted as the paleo channel which formed the recognized ridge and is characterized by a sinuosity index (Thorne et al., 1997) with an average value of 1.3. As also visible in the CHIRP profiles (AS19 in Fig. 4.4), this ridge is strongly asymmetric as the wider levee is always present at the inner portion of the meander. Another large ridge is documented by the DTM in the western sector (#A in Fig. 4.6), but in this case the paleochannel on top of the ridges is missing. A smaller ridge is also present in the central portion of the study area (#C in Fig. 4.6) and, considering its dimensions and morphology, it has been interpreted as the product of a crevasse splay stemming from the major fluvial ridge described above (#A in Fig. 4.6). The CHIRP profiles running through this deposit show that the lens of sediment associated to this crevasse has a thickness of about 2 m (AS25 in Fig. 4.4).

The presence of these fluvial ridges testifies that S1 mainly corresponds to the relief map of the alluvial plain existing in the area before that the brackish and coastal environments expanded over it. A slightly depressed area, characterized by an elevation up to 2 m lower than the mean value of S1, occurs in the central sector of the reconstructed DTM (#D in Fig. 4.6). This feature elongates from ENE to WSW and it occupies the region in between the fluvial ridges B and A/C of Fig. 4.6. The values get deeper towards ENE, where the depression is much wider, while in the WSW sector it is split in different branches that create a rather dendritic pattern. These minor channels seem to erode part of the ridges and, in several CHIRP profiles, the lower boundary of the depressed feature cuts some of the seismic reflector of U1, suggesting that it partly developed through the scouring of the pre-existing alluvial plain. This depression was likely produce by an early tidal channel system that would have developed over the older alluvial surface. This hypothesis is also supported by the typical occurrence of the brackish facies U2F1 within this scour.

The presence of an organic layer matching with S1, as recognized also in cores CM95-12 CM95-13 and AR00-22 (Fig. 4.5) documents that a depositional hiatus occurred between the deactivation of the alluvial surface of U1 and the deposition of the sediments over S1. This time interval in subaerial conditions

allowed the activation of pedogenetic processes and the accumulation of plant debris and organic sediments.

The age of S1 in the study area is constrained by two radiocarbon dates performed on peat samples (Tab. 4.1), which indicated an age of ca. 11.0 ka cal BP. Some dates performed on material sampled in the subsoil of the present coastal plain provided an age for the upper portion of U1 ranging from 20 to 30 ka cal BP (Bruno et al., 2017). It is reasonable to think that the alluvial processes that shaped the landscape here reconstructed were still active at least at 20 ka BP, therefore during the last period of the LGM and likely also in the Late Glacial (cf. Amorosi et al., 2017a). Therefore, the age of ca. 11.0 ka cal BP could be considered as a terrestrial limiting point for the area, documenting that the area was still in subaerial conditions at that time and relative sea-level was lower than -34 m MSL.

With the exception of the depression described above (#D in Fig. 4.6), the S1 surface has been probably left almost unscathed by the subsequent marine transgression, as it was covered by the deposits identified by facies U2F2 and, thus, it was not directly subjected to the pervasive erosion related to the wave action during the formation of the RS.

SURFACE 2 (S2) This DTM is the reconstruction of the S2 surface that caps the seismic facies U2F2 (Fig. 4.6). In this area it spans between -32 and -36 m MSL. The DTM depicts an intricate topography, characterized by several elongated and convex ridges that form an intersecting pattern. Two of these features enter in the area from NW and SW, respectively (Fig. 4.6, E and F), and they are up to 3 m higher than the surroundings. Several minor ridges branch out from the major ones and their connections isolate some small low-relief areas, interspersed among them. The seismic facies and stratigraphic data (U2F2, paragraph 4.1; Moscon et al., 2015) led to interpret these landforms as deltaic channel ridges that developed in an environment where fresh and brackish waters were mixing. Some minor ridges are superimposed on the older S1 ridges, as also visible in the CHIRP profiles (Figs. 4.4 and Fig. 4.6). The occasional presence of different overlapping reflectors within the body of U2F2 suggests that a temporary deactivation of some of the channels may have occurred (Fig. 4.4). Several radiocarbon dates carried out on shells of molluscs are available for these stacked bodies. The obtained ages span from 10.0 ka to 9.5 ka BP (Tab. 4.1).
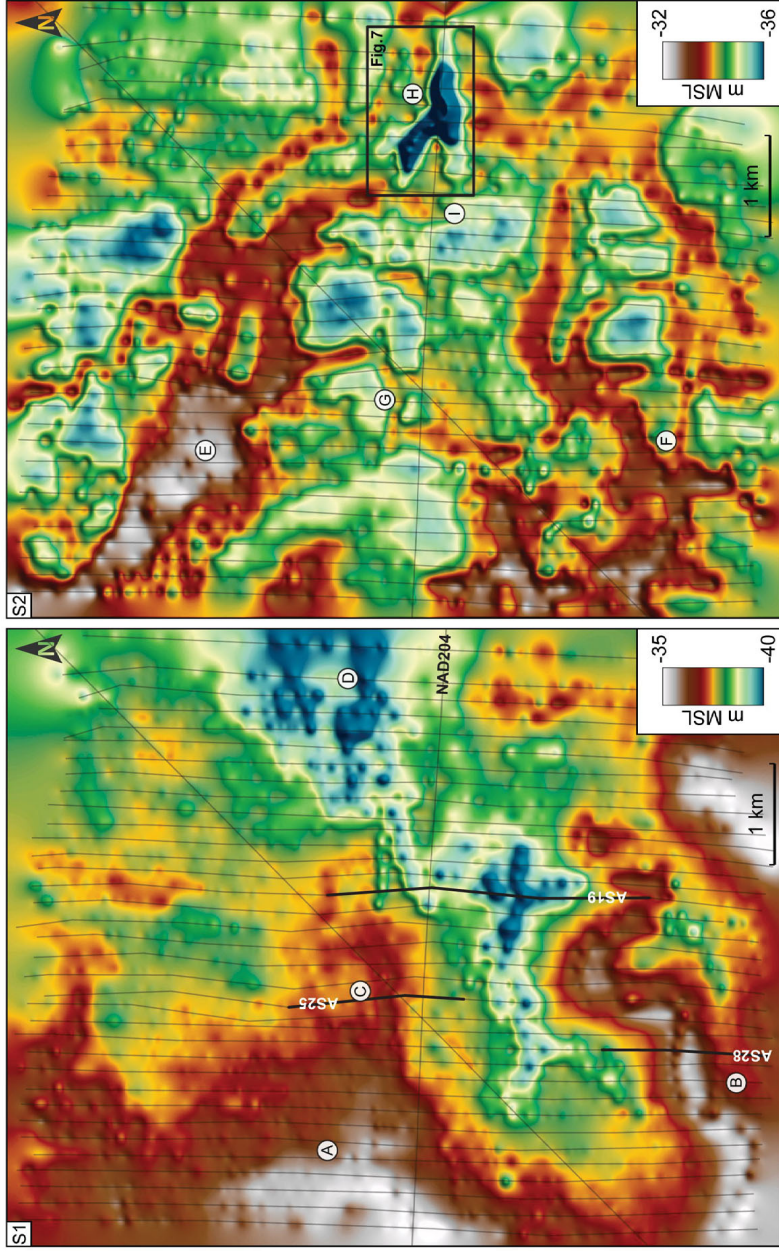
Figure 4.6: DTMs of S1, on the left, and S2, on the right. The labelled landforms (A to I) are described in section 4.4. The position of the CHIRP profiles used for this reconstruction is shown with grey lines. The labelled black lines on S1 represent the position of the CHIRPs reported in Fig. 4.4. The position of the tidal inlet shown in Fig. 4.7 is highlighted on S2.

In the central portion of the eastern sector of the DTM a deep erosive feature, corresponding to the tidal inlet mentioned above (#H in Fig. 4.6) and described in detail in the next paragraph, is visible. The erosive unconformity that delimitates the base of this tidal inlet cannot be properly considered as a part of the S2 as it was cut only after the evolution of the rest of the landforms described above. Nevertheless, this landform is only slightly younger than the rest of the reconstructed surface, as it evolved at the boundary between the terrestrial and the marine environments, just as the rest of the S2 surface. The erosive surface of this tidal inlet is therefore included in the reconstruction of S2 for sake of clarity.

Morphology and infilling geometry of the tidal inlet

This peculiar incised morphology strongly differs from the longitudinal profile of the bottom of a fluvial valley incised in soft sediments, where the scour generally develops over several kilometres and displays a downstream asymptotic shape (Blum et al., 2013). Some exceptions are documented in the regions where the river system crosses an area affected by tectonic deformations (cf. Schumm et al., 2000), but the study area corresponds to an undeformed foreland basin. Given these marked differences if compared to a fluvial-originated morphology, the similarities with other tidal inlets both in the Adriatic Sea (Ronchi et al., 2018,b and in other areas (Rieu et al., 2005; FitzGerald et al., 2012) and the brackish nature of the deposits recognized in the study area (Moscon et al., 2015), it can be assessed that the considered filled erosive channel represents a tidal inlet. The tidal inlet reconstructed in this research (#H in Fig. 4.6) is identified by a deep scour that cuts through U2F2 and U1. The infill of this erosive feature consists of U2F3. The upper portion of this landform was partly eroded by the formation of the RS. This tidal inlet has a maximum depth of 17 m below the mean surface of S2, a width of nearly 500 m and a total length up to 1.2 km (Figs. 4.7 and Fig. 4.8). In the westward portion (i.e. landward) the inlet split into two smaller channels which fade and disappear within few hundred of metres (Figs. 4.6 and Fig. 4.7). It can be speculated that the bifurcation observable in the western portion of the inlet was produce by the presence of a flood delta body, as observable in several modern features (cf. FitzGerald and Miner, 2013), but this hypothesis cannot be tested as only a slightly elevated body, tentatively identifiable as a remain of flood-tidal delta, is recognizable (#I in Fig. 4.6) The ebb channel of the tidal inlet is

markedly funnelled, and it can be recognized up to ca. 400 m from the inlet throat (Figs. 4.7 and Fig. 4.8). The terminations of the scour end abruptly both in landward and seaward directions, losing more than 10 m of depth in less than 100 m. The geometry of the infilling, as reconstructed through a longitudinal section and a series of cross sections (Fig. 4.8), is characterized by a set of draping reflectors which, in the lower portion, mimic the basal surface of the tidal inlet. Moving toward the upper portion of the infilling the curvature of these reflectors gradually decreases until they become almost horizontal. No evidence of lateral accretion is visible. Only in the funnelled channel in the eastern portion of the tidal inlet is actually possible to identify some downlapping layers, which suggest an initial backstepping deactivation in landward direction. Nevertheless, no evidences of migration of the inlet can be deduced from the internal configuration of the reflectors.

Stacking pattern

By comparing the reconstructed surfaces S1 and S2, some evolution trends of the area can be recognized. The position of the smaller ridges recognizable on S2 is often matching with that of the ridges form surface S1. This is the case, for instance of the ridges #C and #G in Fig. 4.6. This peculiar behaviour is also well recognizable in the corresponding CHIRP profiles (Fig. 4.4, AS25). The evidence suggests that, after a period of relative sedimentary stasis, the abandoned ridges of the former fluvial system were reactivated, at least for a short period. Nevertheless, the main features recognizable on S2 (#E and F in Fig. 4.6) are not related to any landform visible on S1. On the contrary, the overall evolution of the morphologies related to S2 appears to be controlled by a compensational stacking trend, as the thickness of the deposits between S1 and S2 (Fig. 4.4) is higher in correspondence of the lower reliefs of S1. The map shown in Fig. 4.9 furthermore indicates an aggradational trend on the entire area, with the accumulation of up to 4.5 m of sediments. The tidal inlet represents the only example of net erosion.
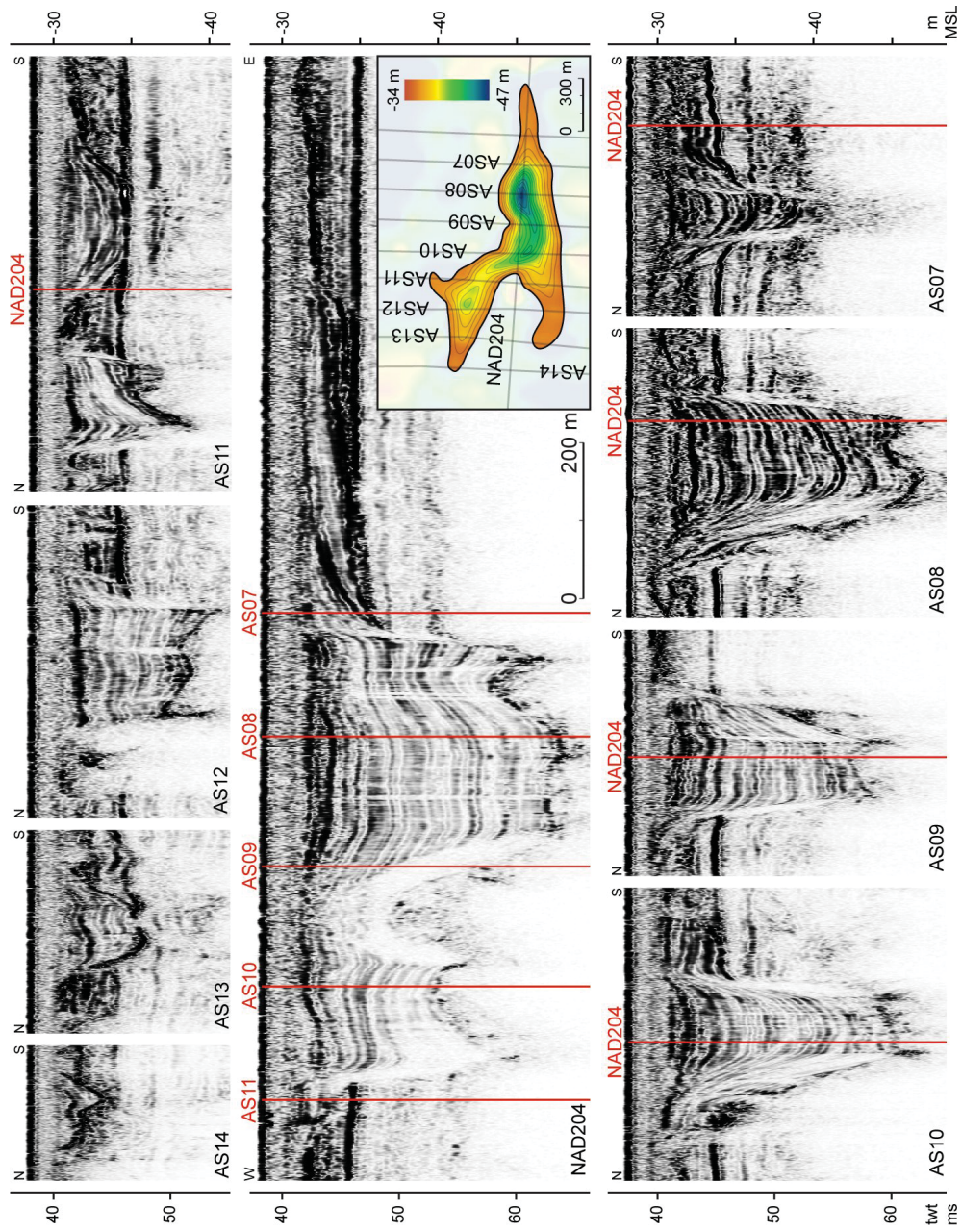
Figure 4.7: Compilation of the CHIRP profiles that intercepted the tidal inlet. The reconstruction of the erosive unconformity at the base of the inlet is reported in the inset.
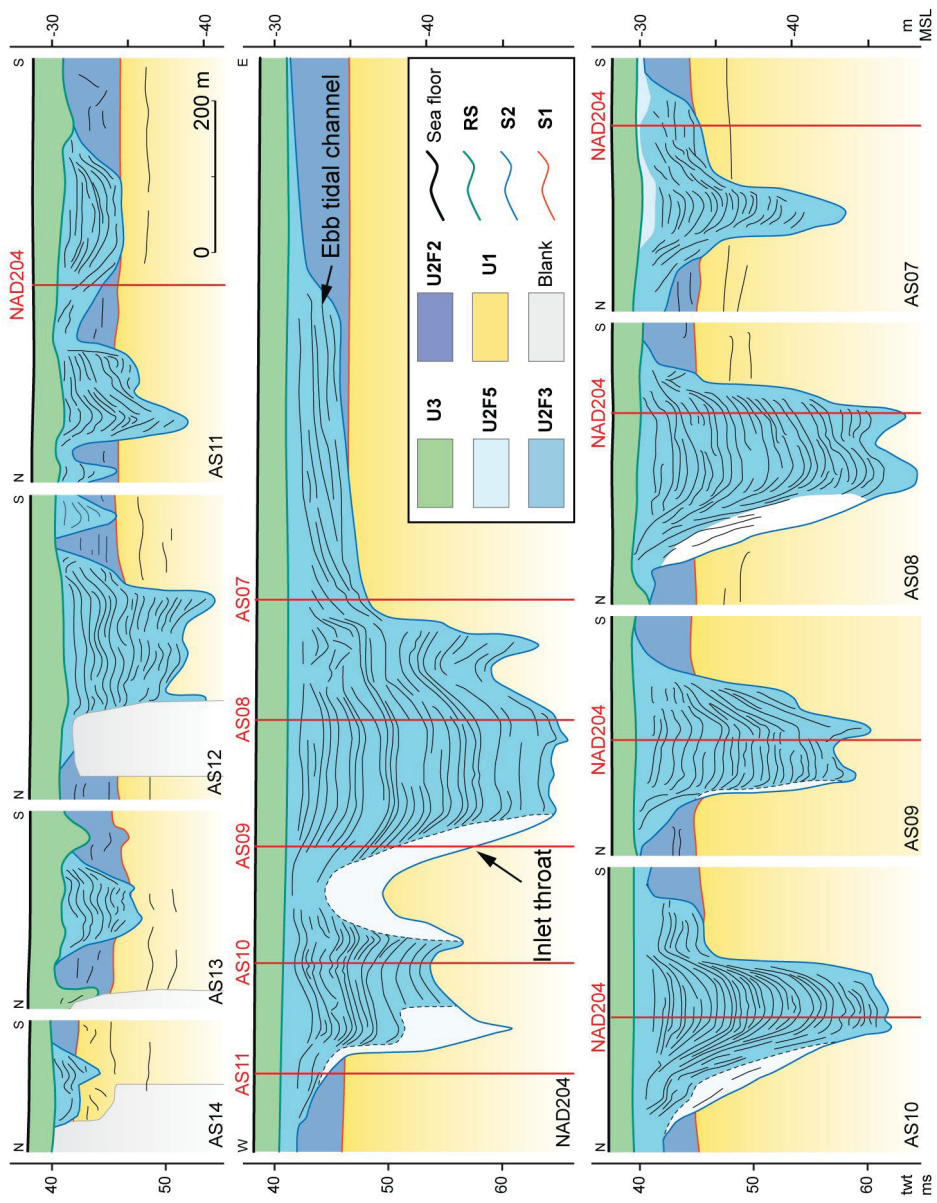
Figure 4.8: Line drawing of the CHIRPs reported in Fig. 4.7.

Preservation of the lagoon-related deposits

The preservation potential of transgressive deposits is strongly influenced by the pre-existing topography (Belknap and Kraft, 1981) and, typically, the conservation of relict barrier and lagoon systems and of tidal inlet remnants is associated to the presence of a morphological step (Cattaneo and Steel, 2003). In the case of unit U1, the topographic sill described by S1 and visible on the western sector of NAD204 (Fig. 4.5) probably fostered the preservation of the trangressive deposits in the area.

After the marine submersion, the action of wave and tides usually obliterate all the relieved landforms of a lagoon system (e.g. flood and ebb deltas, barriers) and even the shallow deposits and morphologies (e.g. tidal creeks, salt marsh deposits), while only the deposits of the deeper channels and inlets can be partly preserved (Cattaneo and Steel, 2003; FitzGerald et al., 2012). An estimation of the shoreface erosion occurred for an early Holocene microtidal environment (1 to 2 m tidal range) in the Southern Bight, offshore of the Netherlands coast, indicate that 3 to 6 m of the upper stratigraphy was removed (Rieu et al., 2005). In order to assess the total thickness of eroded sediments, we focused on the geometry of the infilling and on the presence of other lagoon deposits and landforms documented in the area.

In the investigated tidal inlet, the preservation of the horizontal layering of the top part of the infilling suggests that only a shallow layer of sediments was eroded during the marine transgression. The internal geometry of these kind of deposits gradually shift from a draping V-shape to sub-horizontal reflectors moving upward (Fig. 4.8), following the progressive deactivation of the inlet (cf. the Holocene tidal channel complexes reported in Zecchin et al., 2008). Moreover, the preserved funnelled ebb tidal channel described above (Fig. 4.8) has a maximum thickness of ca. 4 m and can be tracked for a length of nearly 400 m. These characteristics are well comparable to the values measured in modern highstand ebb channel analogues (cf. Fontolan et al., 2007; Pianca et al., 2014; Harrison et al., 2017) that, for similar tidal regimes, are not usually longer than 500 m and not deeper than $5 - 7$ m. Considering the morphological and stratigraphic evidence, we assume that in the study area the marine truncation associated with the formation of the RS reached maximum

values of ca. $2 - 4$ m.

Slightly in contrast with this hypothesis, in the study site no traces of a network of tidal channels, which was likely present on the lagoon side of the tidal inlet, had been detected. In the present lagoons of Venice (Carniello et al., 2009; Madricardo et al., 2017; Ghinassi et al., 2018) and Grado-Marano (Triches et al., 2011) these channel systems can reach depths up to $4 - 8$ m in the proximity of the tidal inlet and get shallower, up to < 1 m, moving away from the inlet throat. A possible solution to this apparently discrepancy may be provided by the shorter time generally available for the evolution of the transgressive lagoons, which would have fostered the formation of a slightly-incised network of creeks instead of the relatively deep channels that are commonly observable in the modern lagoons. Such a slightly entrenched network would have been completely erased after the submersion of the lagoon. This speculation is supported by the complete absence of any known channel network on the entire Adriatic shelf, but no further data is available to endorse this hypothesis. Tidal inlets within a marine transgressive context are subjected to a rapid evolution due to the continuous forcing exerted by the rising sea. In this context it is likely that the mobility of the inlet is limited, as the scouring and infilling of the channel have been consumed in the time frame of few centuries. As a matter of fact, the internal geometry of the analysed tidal inlet indicates the absence of any landward migration. Moreover, a progressive landward migration of the system would be possible only in the case of equilibrium between relative sea-level rise and sediment supply rates (cf. FitzGerald and Miner, 2013).

The deactivation of a tidal inlet may be the consequence of two main factors: 1) an internal dynamic of the lagoon; 2) an overstepping and deactivation of the entire lagoon complex. In the first hypothesis, the same lagoon complex may experience the formation and deactivation of several tidal inlets as consequence of the formation of new breaches in the barrier islands due to storm activity or simply due to the onset of a different sediment dispersion pattern in the area (Penland et al., 1988; FitzGerald et al., 2012). The formation of new tidal inlets can therefore force the deactivation of the older ones.

The second hypothesis suggests the deactivation of an entire lagoon complex, and of the related tidal inlets as a consequence of a rapid marine overstepping of the lagoon (cf. Hijma et al., 2010; Green et al., 2013). This process, as a result of the overextension of the backbarrier areas, could be particularly effective in low-gradient settings, where the abrupt increasing of the accommodation

space makes the sediment supply ineffective. This mechanism has been already suggested for another Adriatic paleo lagoon-barrier complex dating to the Early Holocene (Storms et al., 2008). In a first moment the widening of the lagoon area induced by the relative sea-level rise would lead to increase the tidal prism, leading to the consequent deepening of the inlet (cf. O'Brien, 1931). Nevertheless, a sudden overextension of the lagoon, if not coupled by the strengthening of the barriers protecting it, would have led to the abandonment and the progressive submersion of the lagoon. This lead to the decrease of the velocity of the water flux trough the tidal inlet and to its destabilization, followed by a gradual shrinking and, finally, to its completely filling (cf. Van De Kreeke, 2004). Eventually, the deactivation of the lagoon could be followed by the formation of a new one in a more landward location or, eventually, by the temporary drowning of a stretch of the former coastal plain and the expansion of estuarine environments along the final tract of the streams (cf. Vis et al., 2015).

At the moment, considering the available data presented in this work, it is not possible to link the deactivation of the analysed tidal inlet to one of the two deactivation mechanisms.

Evolution of a transgressive tidal inlet and implications for coastline and sea-level rise reconstruction

The modern lagoons of the northern Adriatic are the product of a fairly persistent setting that lasted for the entire highstand phase (i.e. last 5.5 ka). The tidal inlets thus experienced a rather complex and long development. On the contrary, the evolution of the lagoon environments during the post-LGM transgression was rapid and the lifespan of tidal inlets, from the scouring to the infilling phase, could have bene very fast. The dates available for other northern Adriatic transgressive tidal inlets reveal that the lifetime of such landforms is extremely short, as a window of less than five hundred years was recognized for the evolution of one of them, but the actual duration may be even smaller (Trincardi et al., 2011; Ronchi et al., 2018a). These landforms can therefore be seen as snapshots of a particular moments of the evolution of a transgressive lagoon. Thus, tidal inlets represent a good proxy for assessing the paleo coastline position at a basin scale.

The development of lagoon environments during a transgressive phase represents the outcome of the complex interplay between eustatic signals, physiog-
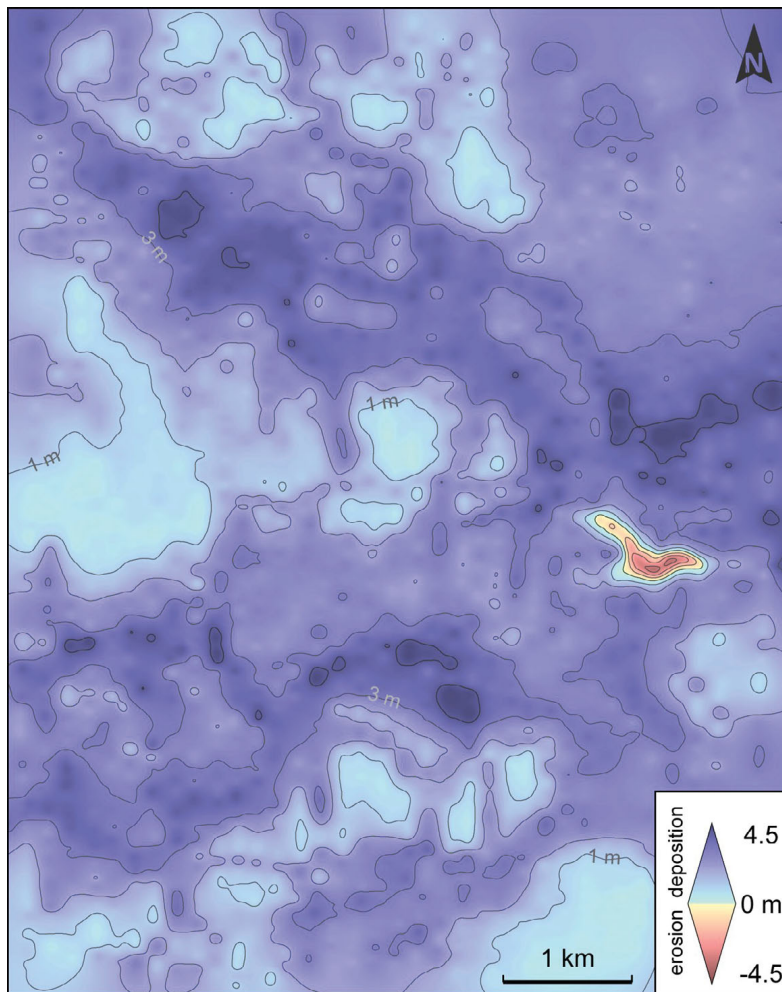
Figure 4.9: Map of the thickness of the deposits between S1 and S2 with 1 m-spaced isopachs.

raphy of the area and fluvial inputs (Cattaneo and Steel, 2003). Above all, the peculiar small gradient of the northern Adriatic Sea (ca. 0.04%) must be taken into account while trying to explain the evolution of these landforms, as this geometry favoured the drowning of large areas even for small increases of the sea level. This likely led to the formation of large plains directly influenced by the tidal activity and subjected to the development of mixed brackish-fresh marshes and ephemeral lagoon environments sheltered by temporary spits shaped by the longshore currents.

Even if all these factors are essential in determining the formation and evolution of a transgressive lagoon environment, here we want to stress the role of the

eustatic signal, as short periods of reduced rates of relative sea-level rise would have fostered the development of a series of lagoons along the paleo shoreline. We therefore suggest that a widespread presence of tidal inlets within a limited range of depths may constitute a proxy for the reconstruction of the paleo sea-level rise. Nevertheless, it must be notice that the presence of lagoons and tidal inlets may be the result of local condition rather than of a regional signal, and this latter scenario may constitute a more common situation. As a matter of fact, rather than considering a basin-scale sea-level rise variation, a change in the sediment discharge of a river or a switch of its position due to an upstream avulsion are the most readily identifiable conditions for the development or waning of a lagoon area. These lagoon complexes represent the result of a series of local factors rather than of an eustatic (i.e. climatic) signal. Nevertheless, the tidal inlets evolved within such lagoons can still provide important data for the paleogeographical and paleoenvironmental reconstructions of an area. The tidal inlet described in this work is likely representative for this second scenario, as the study area was characterized by the presence of the Po River outlet during the first millennia of the Holocene (Amorosi et al., 2017a). Nevertheless, a more in-depth analysis on the study area and on the whole northern Adriatic shelf is required for further consideration on the evolution of this system.

4.6 CONCLUSION

Through the interpolation of a series of seismic reflectors recognized on high-resolution CHIRP profiles, the DTMs of two paleo surfaces, now buried below the Po River prodelta deposits, were interpolated. This reconstruction allowed to identify the presence of a transgressive tidal inlet, formed during the post-LGM marine transgression. The morphology and infilling architecture of this landformwere thoroughly analysed. This landform is characterized by a width up to 500 m and a length of ca. 1.2 km. The maximum thickness was observed in its central portion, where it reaches a value of ca. 17 m, while in both landward and seaward direction it gradually gets thinner and finally disappear. The internal geometry of the infilling allowed to assess that the position of this inlet was stable through its entire life, suggesting a rapid evolution and deactivation, likely linked to the constant transgressive forcing exerted by the rising sea.

The repaired position of these incised landforms guarantees a high preservation

potential of both morphology and infilling, thus making them ideal indicators for the reconstruction of transgressive phases. We therefore suggest that the analysis on a wider scale of such features may provide important information for the paleogeographic and sea-level variation reconstruction.

REFERENCES

Alley, R.B., Clark, P.U., Huybrechts, P., Joughin, I., 2005. Ice-sheet and sea-level changes. Science, 310, 456-460.

Amorosi, A., Colalongo, M.L., Fusco, F., Pasini, G., Fiorini, F., 1999. Glacio-eustatic control of continental-shallow marine cyclicity from Late Quaternary deposits of the southeastern Po Plain, Northern Italy. Quaternary Research, 52, 1-13.

Amorosi, A., Fontana, A., Antonioli, F., Primon, S., Bondesan, A., 2008. Post-LGM sedimentation and Holocene shoreline evolution in the NW Adriatic coastal area. GeoActa, 7, 41-67.

Amorosi, A., Bruno, L., Rossi, V., Severi, P., Hajdas, I., 2014. Paleosol architecture of a late Quaternary basin margin sequence and its implications for high resolution, non-marine sequence stratigraphy. Glob. Planet. Change 112, 12-25.

Amorosi, A., Bruno, L., Campo, B., Morelli, A., Rossi, V., Scarponi, D., Drexler, T. M., 2017a. Global sea-level control on local parasequence architecture from the Holocene record of the Po Plain, Italy. Marine and Petroleum Geology, 87, 99-111.

Amorosi, A., Bruno, L., Cleveland D.M., Morelli, A., Hong, W., 2017b. Paleosols and associated channel-belt sand bodies from a continuously subsiding late Quaternary system (Po Basin, Italy): New insights into continental sequence stratigraphy Geological Society of America Bulletin, 129, B31575.1.

Antonioli, F., Ferranti, L., Fontana, A., Amorosi, A., Bondesan, A., Braitenberg, C., Fontolan, G., Furlani, S., Mastronuzzi, G., Monaco, C., Spada, G., Stocchi, P., 2009. Holocene relative sea-level changes and vertical movements along the Italian and Istrian coastlines. Quaternary International, 206, 102-133.

Armaroli, C., Ciavola, P., Perini, L., Calabrese, L., Lorito, S., Valentini, A., Masina, M., 2012. Critical storm thresholds for significant morphological changes and damage along the Emilia-Romagna coastline, Italy. Geomorphology, 143-144, 34-51.

Bard, E., Hamelin, B., Fairbanks, R.G., 1990. U-Th ages obtained by mass spectrometry in corals from Barbados: Sea level during the past 130,000 years. Nature, 346, 456-458.

Bard, E., Hamelin, B., Delanghe-Sabatier, D., 2010. Deglacial Meltwater Pulse 1B and Younger Dryas Sea Levels Revisited with Boreholes at Tahiti. Science, 327, 1235-1237.

Belknap, D.F., Kraft, J.C.,1981. Preservation potential of transgressive coastal lithosomes on the U S Atlantic shelf. Marine Geology, 42, 429-442.

Blum, M., Martin, J., Milliken, K., Garvin, M., 2013. Paleovalley systems: Insights from Quaternary analogs and experiments. Earth-Science Reviews, 116, 128-169.

Boccaletti, M., Corti, G., Martelli, L., 2011. Recent and active tectonics of the external zone of the Northern Apennines (Italy). Int. J. Earth Sci. 100, 1331-1348.

Bondesan, M., Calderoni, G., Cattani, L., Ferrari, M., Furini, A. L., Serandrei Barbero, R., Stefani, M. 1999. Nuovi dati stratigrafici, paleoambientali e di cronologia radiometrica sul ciclo trasgressivo-regressivo olocenico nell'area deltizia padana. Annali Dell'Università Di Ferrara, 8, 1-34.

Bondesan, M., Elmi, C., Marrocco, R., 2001. Landforms and deposits of lagoon and littoral origina. Castiglioni, G.B., 2001. Response of the fluvial system to environmental variations. In: Castiglioni, G.B., Pellegrini, G.B. (eds), Illustrative Notes of the Geomorphological Map of Po Plain (Italy). Geografia Fisica Dinamica Quaternaria (Suppl. 4), 105-118.

Bondesan, M., Favero, V., Viñals, M.J., 1995. New evidence on the evolution of the Po delta coastal plain during the Holocene. Quaternary International 29-30, 105-110.

Boothroyd, J.C., 1985. Tidal inlet and tidal deltas. In: Davis RA Jr(ed) Coastal sedimentary environments. Springer, New York.

Bruno, L., Bohacs, K.M., Campo, B., Drexler, T.M., Rossi, V., Sammartino, I., Scarponi, D., Hong, W., Amorosi, A., 2017. Early Holocene transgressive palaeogeography in the Po coastal plain (northern Italy). Sedimentology, 64, 1792-1816.

184

Carminati, E., Martinelli, G., Severi, P., 2003. Influence of glacial cycles and tectonics on natural subsidence in the Po Plain (Northern Italy): insights from 14C ages. Geochemistry, Geophysics, Geosystems 4, 1-14.

Carniello, L., Defina, A., D'Alpaos, L., 2009. Morphological evolution of the Venice Lagoon: Evidence from the past and trend for the future. J. Geophys. Res. 114, F04002.

Cattaneo, A., Steel, R.J., 2003. Transgressive deposits: A review of their variability. Earth-Science Reviews, 62, 187-228.

Cattaneo, A., Trincardi, F., 1999. The late Quaternary transgressive record in the Adriatic epicontinental sea: basin widening and facies partitioning. In K.M. Bergman J.W. Snedden, (eds), Isolated Shallow Marine Sand Bodies: Sequence Stratigraphic Analysis and sedimentologic Interpretation. Sequence Stratigraphic Analysis and Sedimentologic Interpretation. SEPM Special Publication, 64, 127-146.

Cattaneo, A., Trincardi, F., Asioli, A., Correggiari, A., 2007. The Western Adriatic shelf clinoform: energy-limited bottomset. Continental Shelf Research, 27, 506-525.

Chang, T.S., Flemming, B.W., Tilch, E., Bartholomae, A., Woestmann, R., 2006. Late Holocene stratigraphic evolution of a back-barrier tidal basin in the East Frisian Wadden Sea, southern North Sea: transgressive deposition and its preservation potential. Facies, 52, 329-340.

Clark, P., Dyke, A., Shakun, J., Carlson, A., Clark, J., Wohlfarth, B., Mitrovica, J., Hostetler, S., McCabe, A., 2009. The Last Glacial Maximum. Science, 325, 710-714.

Correggiari, A., Cattaneo, A., Trincardi, F., 2005. The modern Po Delta system: Lobe switching and asymmetric prodelta growth. Marine Geology, 222-223, 49-74.

Correggiari, A., Roveri, M. Trincardi, F., 1996b. Late Pleistocene and Holocene Evolution of the North Adriatic Sea. Il Quaternario-Italian Journal of Quaternary Sciences, 9, 697-704.

Correggiari, A., Cattaneo, A., Trincardi, F., 2005a. Depositional patterns in the Late-Holocene Po delta system. In: Bhattacharya, J.P., Giosan, L. (eds), Concepts, Models and Examples, SEPM Special Publication, 83, 365-392.

Cuffaro, M., Riguzzi, F., Scrocca, D., Antonioli, F., Carminati, E., Livani, M., Doglioni, C., 2010. On the geodynamics of the northern Adriatic plate. Rendiconti Lincei, 21, 253-279. D'Alpaos, A., Lanzoni, S., Marani, M., Rinaldo, A., 2009. On the O'Brien-Jarrett-Marchi law. Rendiconti Lincei, 20, 225-236.

De Marchi, L., 1922. Variazioni del livello dell'Adriatico in corrispondenza con le espansioni glaciali, Atti Accademia Scientifica Veneto-Trentino-Istriana 12-13, 1-15.

Deschamps, P., Durand, N., Bard, E., Hamelin, B., Camoin, G., Thomas, A.L., Henderson, G.M., Okuno, J., Yokoyama, Y., 2012. Ice-sheet collapse and sea-level rise at the B{o}lling warming 14,600 years ago. Nature, 483, 559-564.

Doglioni, C., 1993. Some remarks on the origin of foredeeps. Tectonophysics, 228, 1-20.

Escoffier, F.F., 1940. The stability of tidal inlets. Shore and Beach 8, 111-114.

Ferranti, L., Antonioli, F., Mauz, B., Amorosi, A., Dai Pra, G., Mastronuzzi, G., Monaco, C., Orrù, P., Pappalardo, M., Radtke, U., Renda, P., Romano, P., Sansò, P., Verrubbi, V., 2006. Markers of the last interglacial sea-level high stand along the coast of Italy: Tectonic implications. Quaternary International, 145-146, 30-54.

FitzGerald, D.M., Buynevich, I.V., Rosen, P.S., 2001. Geological evidence of former tidal inlets along a retrograding barrier: Duxbury Beach, Massachusetts, USA. Journal of Coastal Research, 34, 437-448.

FitzGerald, D.M., Miner, M.D., 2013. Tidal Inlets and Lagoons along Siliciclastic Barrier Coasts. Treatise on Geomorphology (Vol. 10). Elsevier Ltd.

FitzGerald, D.M., Buynevich, I.V., Hein, C.J., 2012. Morphodynamics and facies architecture of tidal inlets and tidal deltas. In: Davis, R.A., and Dalrymple, R.W. (eds), Principles of tidal sedimentology, Springer, New York. 12, 301-333.

Fontana, A., Monegato, G., Devoto, S., Zavagno, E., Burla, I., Cucchi, F., 2014. Evolution of an Alpine fluvioglacial system at the LGM decay: The Cormor megafan (NE Italy). Geomorphology, 204, 136-153.

Fontolan, G., Pillon, S., Delli Quadri, F., Bezzi, A., 2007. Sediment storage at tidal inlets in northern Adriatic lagoons: Ebb-tidal delta morphodynamics, conservation and sand use strategies. Estuarine, Coastal and Shelf Science, 75, 261-277.

Gasperini, L., Stanghellini, G., 2009. SeisPrho: An interactive computer program for processing and interpretation of high-resolution seismic reflection profiles. Computers and Geosciences, 35, 1497-1507.

Ghinassi, M., Brivio, L., D'Alpaos, A., Finotello, A., Carniello, L., Marani, M., Cantelli, A., 2018. Morphodynamic evolution and sedimentology of a microtidal meander bend of the Venice Lagoon (Italy). Marine and Petroleum Geology, 96, 391-404.

Giorgetti, G., Mosetti, F., 1969. General morphology of the Adriatic Sea. Bollettino di Geofisica Teorica ed Applicata, 11, 44-56.

Goff, J.A., Austin, J.A., Gulick, S., Nordfjord, S., Christensen, B., Sommerfield, C., Alexander, C., 2005. Recent and modern marine erosion on the New Jersey outer shelf. Marine Geology, 216, 275-296.

Gordini, E., Caressa, S., Marocco, R., 2003. New morpho-sedimentological map of the Trieste Gulf (from Punta Tagliamento to Isonzo mouth). Gortania-Atti Museo Friulano Storia Naturale, 25, 5-29.

Gordini, E., Marocco, R., Tunis, G., Ramella, R., 2004. The cemented deposits of the Trieste Gulf (Northern Adriatic Sea): areal distribution, geomorphologic characteristics and high resolution seismic survey. Il Quaternario,17, 555-563.

Green, A.N., Cooper, J.A.G., Leuci, R., Thackeray, Z., 2013. Formation and preservation of an overstepped segmented lagoon complex on a high-energy continental shelf. Sedimentology, 60, 1755-1768.

Harrison, S.R., Bryan, K.R., Mullarney, J.C., 2017. Observations of morphological change at an ebb-tidal delta. Marine Geology, 385, 131-145.

Hijma, M.P., van der Spek, A.J.F., van Heteren, S., 2010. Development of a mid-Holocene estuarine basin, Rhine-Meuse mouth area, offshore The Netherlands. Marine Geology, 271, 198-211.

Kettner, A.J., Syvitski, J.P.M.M., 2009. Fluvial responses to environmental perturbations in the Northern Mediterranean since the Last Glacial Maximum. Quaternary Science Reviews, 28, 2386-2397.

Kumar, R., Sanders, J.E., 1974. Inlet sequences: a vertical succession of sedimentary structures and textures created by the lateral migration of tidal inlets. Sedimentology 21, 291-323.

Lambeck, K., Roubya, H., Purcell, A., Sun, Y., Malcolm, S., 2014. Sea level and global ice volumes from the Last Glacial Maximum to the Holocene. PNAS, 111, 15296-15303.

Liu, J.P., Milliman, J.D., Gao, S., Cheng, P., 2004. Holocene development of the yellow River's subaqueous delta, north yellow sea. Mar. Geol. 209, 45-67

Madricardo, F., Foglini, F., Kruss, A., Ferrarin, C., Pizzeghello, N.M., Murri, C., Rossi, M., Bajo, M., Bellafiore, D., Campiani, E., Fogarin, S., Grande, V., Janowski, L., Keppel, E., Leidi, E., Lorenzetti, G., Maicu, F., Maselli, V., Mercorella, A., Montereale Gavazzi, G., Minuzzo, T., Pellegrini, C., Petrizzo, A., Prampolini, M., Remia, A., Rizzetto, F., Rovere, M., Sarretta, A., Sigovini, M., Sinapi, L., Umgiesser, G., Trincardi, F., 2017. High resolution multibeam and hydrodynamic datasets of tidal channels and inlets of the Venice Lagoon. Scientific Data, 4, 170121.

Maselli, V., Hutton, E.W., Kettner, A.J., Syvitski, J.P.M., Trincardi, F., 2011. High-frequency sea level and sediment supply fluctuations during Termination I: An integrated sequence-stratigraphy and modeling approach from the Adriatic Sea (Central Mediterranean). Marine Geology, 287, 54-70.

Maselli, V., Trincardi, F., 2013. Man made deltas. Scientific Reports, 3, 1-7.

Mehta, A.J., Joshi, P.B., 1988. Tidal Inlet Hydraulics. Journal of Hydraulic Engineering, 114, 1321-1338.

Moscon, G., Correggiari, A., Stefani, C., Fontana, A., Remia, A., 2015. Very-high resolution analysis of a transgressive deposit in the Northern Adriatic Sea (Italy). Alpine and Mediterranean Quaternary 28, 121-129.

Moscon, G., 2016. Variabilityo Late-Quaternary Transgressive Sedimentation in the Northern Adriatic Sea. PhD thesis: Padova, University of Padova.

Mosetti, F., 1966. Morfologia dell'Adriatico settentrionale, Bollettino di Geofisica Teorica ed Applicata, 8, 138-150.

Nordfjord, S., Goff, J.A., Austin, J.A., Sommerfield, C.K., 2005. Seismic geomorphology of buried channel systems on the New Jersey outer shelf: assessing past environmental conditions. Marine Geology, 214, 339-364.

O'Brien, M.P., 1931. Estuary tidal prisms related to entrance areas. Civil Engineering 1, 738-739.

Pellegrini, C., Asioli, A., Bohacs, K.M., Drexler, T.M., Feldman, H.R., Sweet, M.L., Maselli, V., Rovere, M., Gamberi, F., Dalla Valle, G., Trincardi, F., 2018. The late Pleistocene Po River lowstand wedge in the Adriatic Sea: Controls on architecture variability and sediment partitioning. Marine and Petroleum Geology, 96, 16-50.

Pellegrini, C., Maselli, V., Cattaneo, A., Piva, A., Ceregato, A., Trincardi, F., 2015. Anatomy of a compound delta from the post-glacial transgressive record in the Adriatic Sea. Marine Geology, 362, 43-59.

Pellegrini, C., Maselli, V., Gamberi, F., Asioli, A., Bohacs, K.M., Drexler, T.D., Trincardi, F., 2017. How to make a 350-m-thick lowstand systems tract in 17,000 years: The Late Pleistocene Po River (Italy) lowstand wedge. Geology, 45, 327-330.

Peltier, W.R., Fairbanks, R.G., 2006. Global glacial ice volume and Last Glacial Maximum duration from an extended Barbados sea level record. Quaternary Science Reviews 25, 3322-3337.

Penland, S., Boyd, R., Suter, J.R., 1988. Transgressive Depositional Systems of the Mississippi Delta Plain: A Model for Barrier Shoreline and Shelf Sand Development. SEPM Journal of Sedimentary Research, 58, 932-949.

Perini, L., Calabrese, L., Luciani, P., Olivieri, M., Galassi, G., Spada, G., 2017. Sea-level rise along the Emilia-Romagna coast (Northern Italy) in 2100: Scenarios and impacts. Natural Hazards and Earth System Sciences, 17, 2271-2287.

Pianca, C., Holman, R., Siegle, E., 2014. Mobility of meso-scale morphology on a microtidal ebb delta measured using remote sensing. Marine Geology, 357, 334-343.

Picone, S., Alvisi, F., Dinelli, E., Morigi, C., Negri, A., Ravaioli, M., Vaccaro, C., 2008. New insights on late Quaternary palaeogeographic setting in the Northern Adriatic Sea (Italy). Journal of Quaternary Science, 23, 489-501.

Piovan, S., Mozzi, P., Zecchin, M., 2012. The interplay between adjacent Adige and Po alluvial systems and deltas in the late Holocene (northern Italy). Geomorphologie 18, 427-440.

Price, W.A., 1947. Equilibrium of form and forces in tidal basins of coast of Texas and Louisiana. Bulletin of the American Association of Petroleum Geologists 31, 1619-1663.

Reimer, P.J., McCormac, F.G., 2002. Marine radiocarbon reservoir corrections for the Mediterranean and Aegean Seas. Radiocarbon 44, 159-166.

Reimer, P.J., Bard, E., Bayliss, A., Beck, J.W., Blackwell, P.G., Bronk Ramsey, C., Grootes, P.M., Guilderson, T.P., Haflidason, H., Hajdas, I., Hatté, C., Heaton, T.J., Hoffmann, D.L., Hogg, A.G., Hughen, K.A., Kaiser, K.F., Kromer, B., Manning, S.W., Niu, M., Reimer, R.W., Richards, D.A., Scott, E.M., Southon, J.R., Staff, R.A., Turney, C.S.M., van der Plicht, J., 2013. IntCal13 and Marine13 Radiocarbon Age Calibration Curves 0-50,000 Years cal BP. Radiocarbon 55, 1869-1887.

Rieu, R., van Heteren, S., Van der Spek, A.J.F., De Boer, P.L., 2005. Development and preservation of a Mid-Holocene tidal-channel network offshore the Western Netherlands. Journal of Sedimentary Research, 75, 409-419.

Ronchi, L., Fontana, A., Correggiari, A., Asioli, A., 2018a. Late Quaternary incised and infilled landforms in the shelf of the northern Adriatic Sea (Italy). Marine Geology, 405, 47-67.

Ronchi, L., Fontana, A., Correggiari, A., 2018b. Characteristics and potential application of Holocene Tidal Inlets in the Northern Adriatic Shelf (Italy). Alpine and Mediterranean Quaternary, 31.

Schumm, S.A., Dumont, J.F., Holbrook, J.M. 2000. Active Tectonics and Alluvial Rivers. 276 Cambridge, New York, Melbourne: Cambridge University Press.

Scisciani, V., Calamita, F., 2009. Active intraplate deformation within Adria: Examples from the Adriatic region. Tectonophysics, 476, 57-72.

Siddall, M., Rohling, E., Almogi-Labin, A., Hemleben, C., Meischner, D., Schmelzer, I., Smeed, D.A., 2003. Sea-level fluctuations during the last glacial cycle. Nature, 423, 853-858.

Stefani, M., Vincenzi, S., 2005. The interplay of eustasy, climate and human activity in the late Quaternary depositional evolution and sedimentary architecture of the Po Delta system. Marine Geology, 222-223, 19-48.

Storms, J.E.A., Weltje, G.J., Terra, G.J., Cattaneo, A., Trincardi, A., 2008. Coastal dynamics under conditions of rapid sea-level rise: Late Pleistocene to Early Holocene evolution of barrier-lagoon systems on the northern Adriatic shelf (Italy). Quaternary Science Reviews 27, 1107-1123.

Stuiver, M., Reimer, P.J., Reimer, R.W., 2017. CALIB 7.1 [WWW program]. http://calib.org.

Tanabe, S., Nakanishi, T., Ishihara, Y., Nakashima, R., 2015. Millennial-scale stratigraphy of a tide-dominated incised valley during the last 14 kyr: spatial and quantitative reconstruction in the Tokyo Lowland, central Japan. Sedimentology 62, 1837-1872.

Thorne, C.R., Hey, R.D., Newson, M.D., 1997. Applied Fluvial Geomorphology for River Engineering and Management, Wiley, Chichester.

Tran, T-T.T., van de Kreeke, J., Stive, M.J.F., Walstra, D.-J.J.R., 2012. Cross-sectional stability of tidal inlets: A comparison between numerical and empirical approaches. Coastal Engineering, 60, 21-29.

Triches, A., Pillon, S., Bezzi, A., Lipizer, M., Gordini, E., Villalta, R., Fontolan, G., Menchini, G., 2011. Carta batimetrica della Laguna di Marano e Grado. Arti Grafiche Friulane, Imoco spa (UD), 39.

Trincardi F., Argnani A. (eds), 2001. Note illustrative della Carta Geologica d'Italia alla scala 1:250,000-Foglio NL33-10 "Ravenna". ISPRA-Servizio Geologico d'Italia.

Trincardi, F., Argnani, A., Correggiari, A., 2011. Note illustrative della Carta Geologica d'Italia alla scala 1:250,000-Foglio NL33-7 "Venezia", ISPRA-Servizio Geologico d'Italia.

Trincardi, F., Campiani, E., Correggiari, A., Foglini, F., Maselli, V., Remia, A., 2014. Bathymetry of the Adriatic Sea: The legacy of the last eustatic cycle and the impact of modern sediment dispersal. Journal of Maps, 10, 151-158.

Trobec, A., Andrej, Š., Sašo, P., Marko, V., 2017. Submerged and Buried Pleistocene River Channels in the Gulf of Trieste (Northern Adriatic Sea): Geomorphic, Stratigraphic and Tectonic Inferences. Geomorphology, 286, 110-20.

Vacchi, M., Marriner, N., Morhange, C., Spada, G., Fontana, A., Rovere, A., 2016. Multiproxy assessment of Holocene relative sea-level changes in the western Mediterranean: variability in the sea-level histories and redefinition of the isostatic signal. Earth Science Reviews, 155, 172-197.

Van de Kreeke, J., 2004. Equilibrium and cross-sectional stability of tidal inlets: Application to the Frisian Inlet before and after basin reduction. Coastal Engineering, 51, 337-350.

Van Goor, M.A., Zitman, T.J., Wang, Z.B., Stive, M.J.F., 2003. Impact of sea-level rise on the morphological equilibrium state of tidal inlets. Marine Geology, 202, 211-227.

Vis, G., Cohen, K.M., Westerhoff, W.E., Ten Veen, J.H., Hijma, M.P., van der Spek, J.K., Vos, P.C., 2015. Paleogeography. In: Shennan J., Long A.J., Horton B.P. (eds), Handbook of Sea-Level Research. Wiley, 514-535.

Walton, T.L., Adams, W.D., 1976. Capacity of inlet outer bars to store sand. Proceedings of Fifteenth Coastal Engineering Conference. ASCE, Honolulu, Hawaii, 1919-1937.

Zecchin, M., Baradello, L., Brancolini, G., Donda, F., Rizzetto, F., Tosi, L., 2008. Sequence stratigraphy based on high-resolution seismic profiles in the late Pleistocene and Holocene deposits of the Venice area. Marine Geology, 253, 185-198.

Zecchin, M., Brancolini, G., Tosi, L., Rizzetto, F., Caffau, M., Baradello, L., 2009. Anatomy of the Holocene succession of the southern Venice lagoon revealed by very high resolution seismic data. Continental Shelf Research, 29, 1343-1359.

Zecchin, M., Gordini, E., Ramella, R., 2015. Recognition of a drowned delta in the northern Adriatic Sea, Italy: Stratigraphic characteristics and its significance in the frame of the early Holocene sea-level rise. The Holocene, 25, 1027-1038.

PALEO TIDAL INLETS OF THE NORTHERN ADRIATIC SHELF: AN OVERVIEW

Abstract

Several completely filled incised channels were identify in the subsurface of the northern Adriatic shelf via sub-bottom data. The analysis performed on some of the most notable examples of such features allowed to assess their tidal nature. These features often constitute the only widespread witnesses of the post-LGM marine transgression in the area. Paleo tidal inlets are therefore essential for the paleogeographic reconstruction and can provide new data to constrain the position of the paleo coastline. On the contrary, their application as paleo sea-level indicators is biased by the absence of a precise constrain on their vertical position in relation to the position of the paleo sea level, as the upper portion of the stratigraphy was removed by the wave action after the drowning of the lagoons. This work constitutes the first report of an extensive distribution of paleo tidal inlets on a Mediterranean scale.

5.1 INTRODUCTION

The reconstruction of the timing and modes of the last marine transgression, and in particular of the sea-level rise curve, is often hampered by the absence of available indicators. This is particularly true for the first period of the Holocene, between 7 ka and 11 ka cal BP, when the rate of transgression was high and the sea level was placed below ca. -20 m MSL (Vacchi et al., 2016). As a matter of fact, only few index points from this period are preserved, and they are usually difficult to access because of their depth (cf. Chapter 1).

The peculiar physiography of the Adriatic Sea, characterized by a gradient of ca. 0.4‰, offers the ideal settings for a high-resolution study of the post-LGM marine transgression, as even a small increase of the sea level would have caused the submersion of a large portion of the shelf. On the other hand, due to the rapid creation of new accomodation space, the low gradient promoted the formation of only a thin layer of transgressive deposits, (Cattaneo and Steel, 2003) that was reworked during the submersion of the shelf.

The only widespread and relatively well-preserved witnesses of the last marine transgression on the northern Adriatic shelf are represented by the paleo tidal inlets that punctuate the entire area. This chapter offers an overview on the
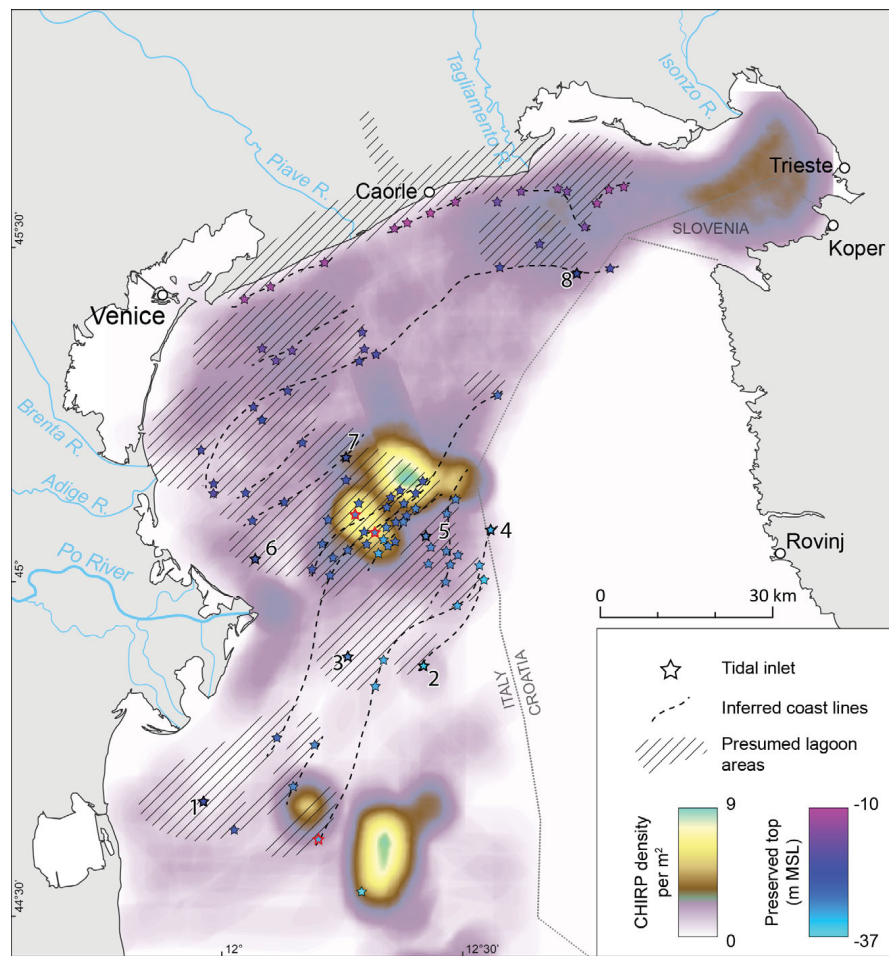
Figure 5.1: Position of the recognized tidal inlets on the northern Adriatic shelf. The CHIRP profiles and interpretation of the labelled tidal inlets are reported in Figs. 5.2 and 5.3. The tidal inlets marked with a red outline correspond to the landforms described in the chapters 3 and 4. The density map of the available CHIRP lines is reported to provide an indication on the reliability of the reconstruction.

paleo tidal inlets that have been recognized in the area and tries to infer some general characteristics of these landforms and to understand their possible implication in the paleogeographic and relative sea-level rise reconstruction.

5.2 METHODS AND RESULTS

More than 7 000 km of CHIRP profiles (Fig. 1) where analysed in order to recognize and classify the tidal inlets documented in the northern Adriatic

shelf.

The geometric characteristics of these paleo landforms where then stored into a GIS database. In contrast with those described in the previous chapters, most of the tidal inlets recognized on the whole Adriatic shelf were intercepted only by one or few CHIRP lines, therefore a thorough morphologic reconstruction has not been possible for most of them. The maximum depth and width values of these features can therefore be regarded only as relative values and cannot be used in the attempt of defining a regional trend. For the details on the acquisition of the CHIRP profiles the reader is referred to sections 3.3 and 4.3. The analysis of the CHIRP profiles allowed to recognized ca. 100 different tidal inlets rather homogeneously distributed on the entire surface of the northern Adriatic shelf (Fig. 5.1). It must be noticed that the position and density of the CHIRP lines strongly influenced the number and density of the recognized tidal inlets. For instance, the area south of Po Delta is characterized by a sparse network of seismic profiles if compared to other areas on the Adriatic shelf (Fig. 1), therefore it is likely that the number of recognized paleo tidal inlets can be strongly biased. Such a high concentration of transgressive tidal inlets was never reported before, as only few examples of them have been recognized and described in literature (cf. Rieu et al., 2005; Hijma et al., 2010).

5.3 DISCUSSION

A compilation of the most representative inlets is reported in Figs. 5.2 and 5.3. Similarly to the tidal inlets described in the previous chapters, the infilling geometry of most of the recognized incised channels is characterized by draping layers and the lack of lateral accreting reflectors, thus suggesting a rapid evolution of these landforms and the absence of lateral migration.

Moreover, the top portion of their infilling is always truncated due to the erosive action of the rising sea. This erosive unconformity, which often matches with the modern seafloor but can be also buried by highstand deposits, corresponds to the ravinement surface (cf. Catuneanu, 2006). These tidal inlets were identified between the depths of -10 and -37 m MSL, and a maximum thickness of ca. 20 m has been recognized among all the considered examples. In many cases, the tidal inlets recognized in this work constitute the only witnesses of transgressive lagoon environments which were completely erased by the wave action of the rising sea. The absence of any evidence of lateral
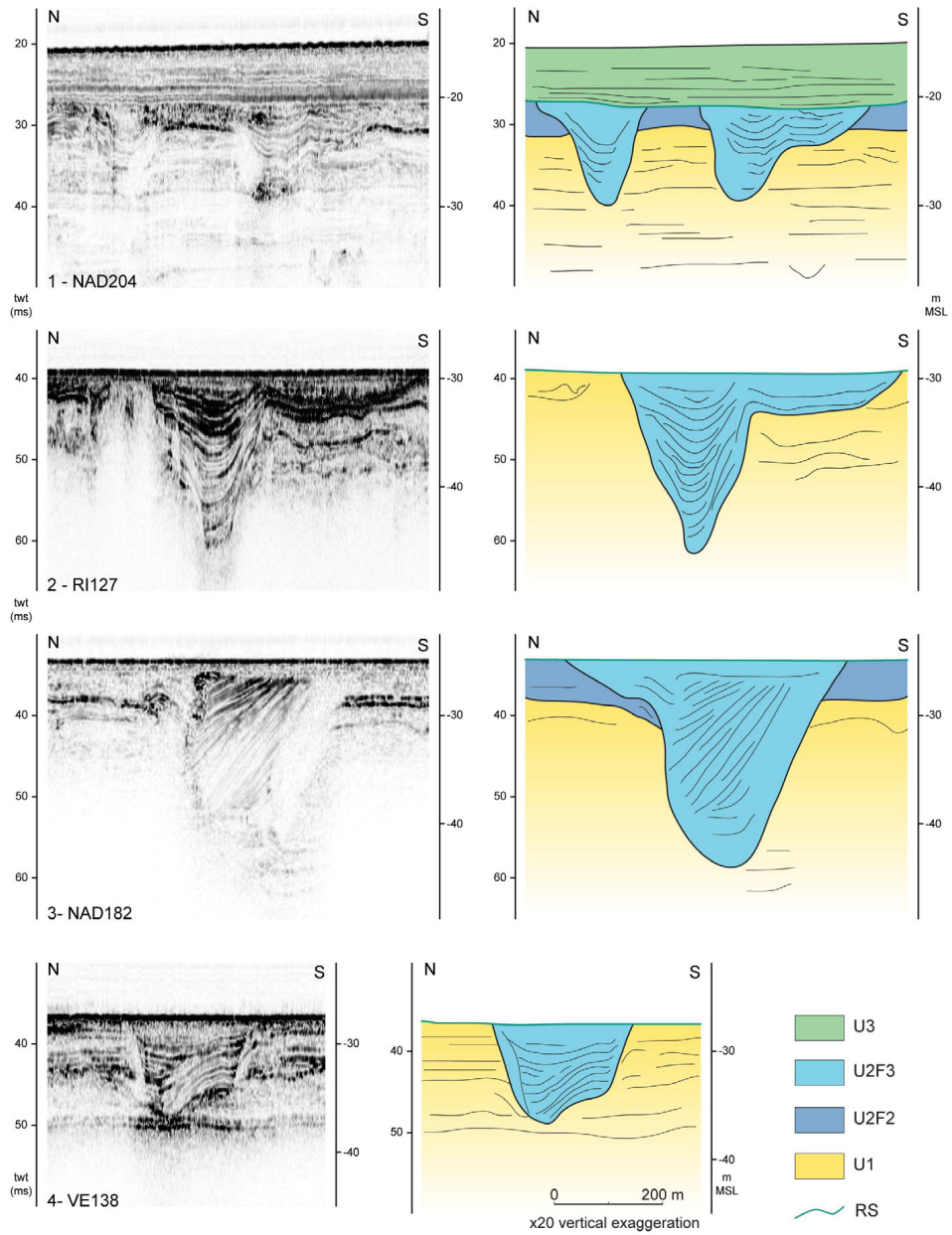
Figure 5.2: CHIRP profiles and interpretation of some of the tidal inlets recognized in the northern Adriatic Sea. See Chapter 4 for a complete description of the legend.

migration in all the recognized specimens indicates a rapid evolution and deactivation of these landforms. This is in line with the constant transgressive pressure exerted by the rising sea, which would have forced the lagoon environments into a rapid evolution path, probably often crowned by the overstepping of the entire system.

The formation of transgressive lagoons

The quantity of tidal inlets which form at comparable depths in the same region and during a transgressive phase is function of the number of coexisting lagoon, their extension (i.e. the presence of sub-basins within the same lagoon) and their lifespan. A high lagoon extension along a coast would result in a high number of tidal inlets. At the same time, the longer the life of a lagoon the higher the number of deactivated and newly formed tidal inlets as a consequence of internal dynamics of the lagoon itself. In turn, these parameters can be function of two main regional controls: 1) the occurrence of periods of relative slowdown of the relative sea-level (RSL) rise rate and 2) the onset of periods of enhanced sediment input in the system.

The first case, which represent the eustatic signal of the area, is an extensive process that would affected the entire considered area. A deceleration or stasis in the rate of relative sea-level rise would foster the formation of several lagoon environments along the coast.

In the second case, the sediment input in the system would match the high sediment demand of the inlets, allowing the establishment of a dynamic equilibrium which would grant the surviving of the lagoon and of the inlets (Van Goor et al., 2003). The amount of sediment supply is a fundamental parameter for tidal inlets, especially in a transgressive framework, as their preservation and evolution strongly depend on the littoral drift and riverine inflow sediments (cf. Chapter 1).

Considering the case of the northern Adriatic shelf, it is worth noting that during the Early Holocene the volume of sediment delivered by the Po River to the basin was greater than the modern value, as proposed by the *Hydrotrend* model (Kettner and Syvitski, 2008, 2009). This condition would have been fundamental for the maintenance of a barrier island-lagoon system during sea-level rise, as illustrated by the models of Van Goor et al., (2003). To assess this possibility the sediment dispersal routes and the position of the major river outlets during the Late Glacial and the Early Holocene should be
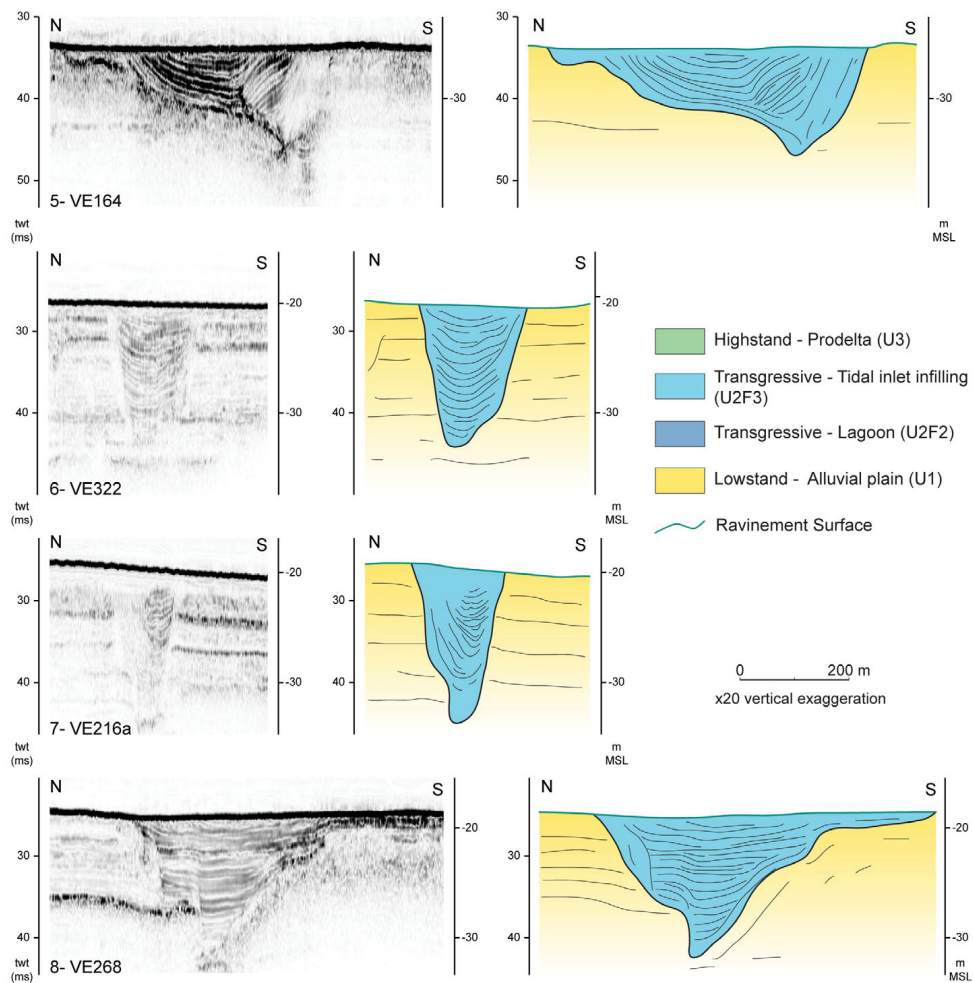
Figure 5.3: CHIRP profiles and interpretation of some of the tidal inlets recognized in the northern Adriatic Sea. See Chapter 4 for a complete description of the legend.

evaluated.

The hypothesis that the formation of tidal inlets can be the result of either one of these two scenarios is however too simplistic. The most likely condition contemplates a complex interplay between these two main factors. In order to evaluate the relative weight of the marine and riverine influence on the formation of the transgressive lagoon environments the recognized tidal inlets should be considered case by case, and other indicators should be integrated in this study.
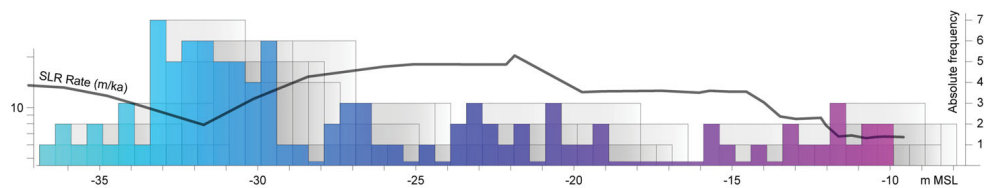
Figure 5.4: Histogram of the absolute frequency of the tidal inlets referred to the depth of the preserved top. The considered bin is 0.5 m. The grey shaded areas represent the 3 m-thick layer that is possibly missing from the top portion of the preserved inlets due to the marine erosion. The black line on top of the histogram represents the RSL variation rate according to the reconstruction of Lambeck et al., (2014). The RSL rise rate is here plotted in relation to the depth instead of the age. This was obtained via a transfer function in which was used the reconstructed RSL curve of the northern Adriatic (Lambeck et al., 2011). It is possible to notice a negative oscillation in correspondence of the maximum occurrence of tidal inlets.

Vertical distribution of the tidal inlets

By extrapolating from the GIS database the depths of the top of the infilling deposits of the recognized tidal inlets it was possible to reconstruct the vertical distribution of these landforms. As observable in Fig. 5.4, the recognized inlets are not homogeneously distributed in the considered range of depth. On the contrary, some depths are characterized by a higher occurrence of such landforms and some others have fewer or none. However, this representation is not completely reliable as it is affected by some uncertainties, which are described below.

Firstly, it must be noticed that the depth of the top of the infilling considered here probably does not match with the depth of the top of the active landform. This is due to the erosion of the upper portion of the stratigraphy operated by the wave action after the marine transgression. The thickness of the missing portion is matter of debate as the indicators are scarce. On the one hand, the conservation of a dendritic channel network in some cases (cf. Chapter 3) and the preservation of long reaches of the ebb or flood channels (cf. Chapter 4) apparently indicates a moderate truncation, probably not greater than $2 - 3$ m. On the other hand, the total absence of any tidal channel or other relatively shallow lagoon remains suggests the occurrence of a rather deeper erosion (cf. Chapter 4 for more insights). Moreover, it is not possible to assess if the portion of stratigraphy missing from the top of the tidal inlets

deposits is comparable among the different analysed examples. It is however reasonable to expect a similar thickness of the missing material at least for the specimens found at similar depths, as they would have been affected by similar hydrodynamic conditions. It is not possible to overcome this issues at the moment, as it is not possible to precisely determine the erosion in the different areas. Therefore, the clustering observable in Fig. 5.4 offers a relative information rather than an absolute one.

A second uncertainty is represented by the subsidence of the northern Adriatic Sea. These tidal inlets are distributed over a large surface which is probably affected by different rates of vertical displacement. The estimation on the long-term tectonic movements on the coastal areas indicates a general subsiding trend, with values going from $0.4 - 0.7$ mm/a in the area of the Venice Lagoon to 1 mm/a in the area of the Po Delta (Massari et al., 2004; Fontana et al., 2010; Vacchi et al., 2016). An estimation of the modern subsidence rates based on GPS data indicates values of roughly ca. 3 mm/a for the entire region (Serpelloni et al., 2013). The available data for the vertical displacement of the central Adriatic indicate a subsidence rate of ca. -0.3 mm/a (Maselli et al., 2010). The depths measured for these inlets can be therefore furthermore modified by differential rates of subsidence. For example, even considering an area with low rates of long term subsidence, as 0.3 mm/a, in 10 ka the top of a tidal inlet located there would had been downlifted for about 3 m. It should be notice though that while this can constitute an issue while considering the whole northern Adriatic Sea, by analysing groups of tidal inlets from a relatively small area the problem of the differential subsidence is negligible. The majority of the recognized tidal inlets are distributed between the depths of -36 and -29 m MSL (Fig. 5.4). It is worth noting that this range corresponds to a period of decreased RSL rise rate recorded at a global scale around 9.5 ka cal BP (Lambeck et al., 2014), probably related to a cooling event recognized in the Greenland ice cores by Rasmussen et al. (2007).

Paleogeographic reconstruction

The presence of groups of tidal inlets in the same area is a reliable indicator for the presence of a paleo lagoon system. The preservation of lagoon landforms (e.g. barrier systems) or of paleo shorelines is a rare occurrence in the northern Adriatic Sea area due to the limited thickness of such deposits induced by the extremely low gradient of the area (Cattaneo and Steel, 2003). This

is testified by the small number of recognized transgressive deposits in the northern Adriatic Sea (Correggiari et al., 1996; Storms et al., 2008; Moscon et al., 2015; Zecchin et al., 2015). By considering the spatial distribution of these landforms it is therefore possible to hypothesize which areas were occupied by lagoon environments during the post-LGM sea-level rise. Moreover, the presence of different tidal inlets at the same depth provides a precise indication for the position of the barrier islands that used to delimit the lagoons (Fig. 5.1). This method, if applied to small areas, can be considered highly reliable as the wave erosion and the vertical displacement caused by the subsidence would be comparable among the different inlets (cf. paragraph 5.3.2). A detailed spatial reconstruction is however biased by the quantity and distribution of the available seismic lines.

Tidal inlets as sea-level indicators

The paleo tidal inlets analysed in detail in this work (cf. Chapters 3 and 4) are characterized by a rapid evolution, which probably led to their formation and subsequent deactivation in a time span of few centuries. According with this limited time frame, a date obtained from the infilling of a tidal inlet would represent a high-resolution time indicator. Unfortunately, the use of paleo tidal inlets as relative sea-level indicators is biased by the absence of control on the relative position of the paleo sea level due to the erosion of the upper portion of the landform. Thus, the top of paleo tidal inlet can be used as a marine limiting point (Hijma et al., 2015; Vacchi et al., 2016). Any radiocarbon date obtained from the filling of an inlet must be accurately evaluated in order to understand its meaning and pertinence in the considered deposit, as the dated material could be exhumed during the lateral migration of an inlet and successively trapped within the infilling deposit. A similar case is reported in Ronchi et al. (2018). Most of the transgressive inlets documented on the northern Adriatic shelf underwent a rapid evolution and are typically filled by draping layers, as time and equilibrium conditions for their migration were usually lacking. In order to obtain an age for the peak of activity of these landforms the dated material should be recovered from the bottom of the infilling. This position would provide a limiting age (*terminus post quem*) for the start of the deactivation and blanketing of the inlet. In the absence of a precise indication on the vertical position of the real top of the considered landform, the top of the preserved infilling can be associated to the obtained

age, providing therefore a marine limiting point for the area.

5.4 CONCLUSIONS

The seismic survey performed on the northern Adriatic shelf allowed to recognized ca. 100 paleo tidal inlets. This is the first time that such a high number is recognized. The analysis carried out on these features provided important information on the paleogeography of the area, as they constitute the only witnesses of a series of lagoon environments that were completely erased by the wave action after the marine transgression. Moreover, it was possible to observe a non-homogeneous vertical distribution of the paleo tidal inlets on the shelf area. This distribution is function of the number of lagoons existing in a certain period and of their lifespan. These factors are regulated by the rate of relative sea-level rise and by the sediment input and dispersion in the system. Therefore, through an evaluation of the different cases, it would be possible to get information on the eustasy and sediment discharge to the considered areas. In particular, the high number of tidal inlets recognized between -36 and -29 m MSL was tentatively correlated with a period of decreased RSL rise rate recorded at a global scale. Nevertheless, this work is affected by some drawbacks, as the absence of a precise control on the paleobathymetric position of these landforms (i.e. before the erosion) and the lack of an indicator for the subsidence of the area hamper the use of tidal inlets as precise sea-level index points. Under average conditions, tidal inlets can be used as marine limiting points.

REFERENCES

Cattaneo, A., Steel, R.J., 2003. Transgressive deposits: A review of their variability. Earth-Science Reviews, 62, 187-228.

Catuneanu, O., 2006. Principles of Sequence Stratigraphy. Elsevier, Amsterdam, 386 pp.

Correggiari, A., Roveri, M. Trincardi, F., 1996b. Late Pleistocene and Holocene Evolution of the North Adriatic Sea. Il Quaternario-Italian Journal of Quaternary Sciences, 9, 697-704.

Hijma, M.P., van der Spek, A.J.F., van Heteren, S., 2010. Development of a mid-Holocene estuarine basin, Rhine-Meuse mouth area, offshore The Netherlands. Marine Geology, 271, pp.198-211.

Hijma, M., Engelhart, S.E., Tornqvist, T.E., Horton, B.P., Hu, P., Hill, D., 2015. A protocol for a Geological Sea-level Database. In: Shennan, I., Long, A., Horton, B.P. (eds), Handbook of Sea Level Research. Wiley, 536-553.

Kettner, A.J., Syvitski, J.P.M.M., 2008. Predicting Discharge and Sediment flux of the Po River, Italy since the Last Glacial Maximum. In Analogue and Numerical Modelling of Sedimentary Systems: From Understanding to Prediction (Vol. 40, 171-189). Oxford, UK: Wiley-Blackwell.

Kettner, A.J., Syvitski, J.P.M.M., 2009. Fluvial responses to environmental perturbations in the Northern Mediterranean since the Last Glacial Maximum. Quaternary Science Reviews, 28, 2386-2397.

Lambeck, K., Antonioli, F., Anzidei, M., Ferranti, L., Leoni, G., Scicchitano, G., Silenzi, S., 2011. Sea level change along the Italian coast during the Holocene and projections for the future. Quaternary International, 232, 250-257.

Lambeck, K., Roubya, H., Purcell, A., Sun, Y., Malcolm, S., 2014. Sea level and global ice volumes from the Last Glacial Maximum to the Holocene. PNAS, 111, 15296-15303.

Maselli, V., Trincardi, F., Cattaneo, A., Ridente, D., Asioli, A., 2010. Subsidence pattern in the central Adriatic and its influence on sediment architec-

ture during the last 400 kyr. Journal of Geophysical Research: Solid Earth, 115, 1-23.

Massari, F., Rio, D., Serandrei Barbero, R., Asioli, A., Capraro, L., Fornaciari, E., Vergerio, P.P., 2004. The environment of Venice area in the past two million years. Palaeogeography, Palaeoclimatology, Palaeoecology, 202, 273-308.

Moscon, G., Correggiari, A., Stefani, C., Fontana, A., Remia, A., 2015. Very-high resolution analysis of a transgressive deposit in the Northern Adriatic Sea (Italy). Alpine and Mediterranean Quaternary 28, 121-129.

Rasmussen, S.O., Vinther, B., Clausen, H.B., Andersen, K.K., 2007. Early Holocene climate oscillations recorded in three Greenland ice cores. Quaternary Science Reviews, 26, 1907-1914.

Rieu, R., van Heteren, S., Van der Spek, A.J.F., De Boer, P.L., 2005. Development and preservation of a Mid-Holocene tidal-channel network offshore the Western Netherlands. Journal of Sedimentary Research, 75, 409-419.

Ronchi, L., Fontana, A., Correggiari, A., Asioli, A., 2018. Late Quaternary incised and infilled landforms in the shelf of the northern Adriatic Sea (Italy). Marine Geology, 405, 47-67.

Serpelloni, E., Faccenna, C., Spada, G., Dong, D., Williams, S.D.P., 2013. Vertical GPS ground motion rates in the Euro-Mediterranean region: New evidence of velocity gradients at different spatial scales along the Nubia-Eurasia plate boundary. Journal of Geophysical Research: Solid Earth, 118(11), 6003-6024.

Storms, J.E.A., Weltje, G.J., Terra, G.J., Cattaneo, A., Trincardi, A., 2008. Coastal dynamics under conditions of rapid sea-level rise: Late Pleistocene to Early Holocene evolution of barrier-lagoon systems on the northern Adriatic shelf (Italy). Quaternary Science Reviews 27, 1107-1123.

Vacchi, M., Marriner, N., Morhange, C., Spada, G., Fontana, A., Rovere, A., 2016. Multiproxy assessment of Holocene relative sea-level changes in the western Mediterranean: variability in the sea-level histories and redefinition of the isostatic signal. Earth Science Reviews, 155, pp, 172-197.

Van Goor, M.A., Zitman, T.J., Wang, Z.B., Stive, M.J.F., 2003. Impact of sea-level rise on the morphological equilibrium state of tidal inlets. Marine Geology, 202, 211-227.

Zecchin, M., Gordini, E., Ramella, R., 2015. Recognition of a drowned delta in the northern Adriatic Sea, Italy: Stratigraphic characteristics and its significance in the frame of the early Holocene sea-level rise. The Holocene, 25, pp, 1027-1038.

The growing concern for the ongoing global warming and the consequent relative sea-level (RSL) rise dictates an ever-increasing effort in the development of climate change models, scenarios and projections. In order to be improved and refined, these models necessitate, among others, of a series of parameters that can be provided by the study of past indicators of sea-level rise, for instance the Glacio-Isostatic Adjustment and the long-term tectonic vertical movements (cf. Antonioli et al., 2017; Stocchi et al., 2018). Moreover, the study of the response of past natural systems to high rates of RSL rise can provided valuable information for the management and protection of the modern coastal areas. Through the analysis of a series of incised and infilled landform, notably incised valleys and paleo tidal inlets, this thesis aimed to search for new possible indicators to constrain and reconstruct the evolutionary history of the last marine transgression.

This research highlights the essential role played by the incised landforms as paleo-environmental, geographic and sea-level indicators, as these features often represent the only witnesses of complex landscapes now completely obliterated by the marine erosion.

The work presented in this thesis is focused on the northern Adriatic shelf and on the Venetian-Friulian Plain. This area has been chosen as it is characterized by a peculiar low-gradient of the continental shelf (ca. 0.4 ‰). This trait is fundamental for the production of a high-resolution reconstruction of the marine transgression, as even a small increase of the sea level would have produced the drowning of a large portion of the shelf. Moreover, the presence of some incised valleys and paleo tidal channels in the analysed area has been already reported (Fontana et al., 2008; Trincardi et al., 2011), but a specific study on the single features and on their significance in a regional view was never attempted. The analysis operated both on the modern coastal plain and on the northern portion of the Adriatic continental shelf allowed an extended characterization and cataloguing of all the incised and infilled features of the area. In particular, it has been possible to reconstruct their evolution in the framework of the post-LGM marine transgression and to test their aptitude to provide index points to constrain the mean relative sea-level rise.

6.1 THE VENETIAN-FRIULIAN PLAIN CASE

While the tidal inlets of the Adriatic shelf provided information on the early Holocene marine transgression, the analysis performed on an incised valley buried in the subsurface of the Venetian-Friulian Plain allowed to reconstruct the evolution of the upstream portion of the study area after the LGM period. The incised valley analysed in this work was carved by the Tagliamento River during the Late Glacial, probably as a consequence of the establishment of different hydraulic forcings promoted by a general sediment starvation of the system and by the different longitudinal grain size distribution of the sediments of the Tagliamento Megafan. While the shaping of the valley operated by the river was still ongoing, a first unit made of coarse gravels was being deposited (cf. Blum et al., 2013). This phase ended due to the disconnection of the Tagliamento from this valley, probably as a consequence of an upstream avulsion. This deactivation was followed by the formation of a swampy/lacustrine environment within the valley, as testified by the presence of extensive peat and gyttja deposits, dated ca. 9.5 ka cal BP at a depth of ca. -17 m MSL. The rising sea-level eventually led to the drowning of this low-energy freshwater environment, which was then substituted by a lagoon enclosed within the walls of the valley. This transition is recorded by a thick unit of lagoon muds, occasionally interrupted by the presence of extensive layers of peat formed in a temporary fresh-water environment. After their deposition, these organic-rich horizons have been prone to deformation because of the differential sedimentary load induced by the sedimentation of younger units.

6.2 THE NORTHERN ADRIATIC SHELF CASE

Through the analysis of a large dataset of high-resolution CHIRP profiles this research allowed to identify and compile a database of almost 100 incised and infilled channel-shaped features on the northern Adriatic shelf. These relict landforms were recognized as tidal channels and inlets through a morphologic, stratigraphic and paleontological analysis. The widespread presence of tidal inlets on the northern-western Adriatic shelf allows to delineate a complex transgressive history, made of frequent alternations between periods of relative stasis and of fast marine ingression. This peculiarity is highlighted by the inhomogeneous vertical distribution of the tidal inlets documented on the shelf
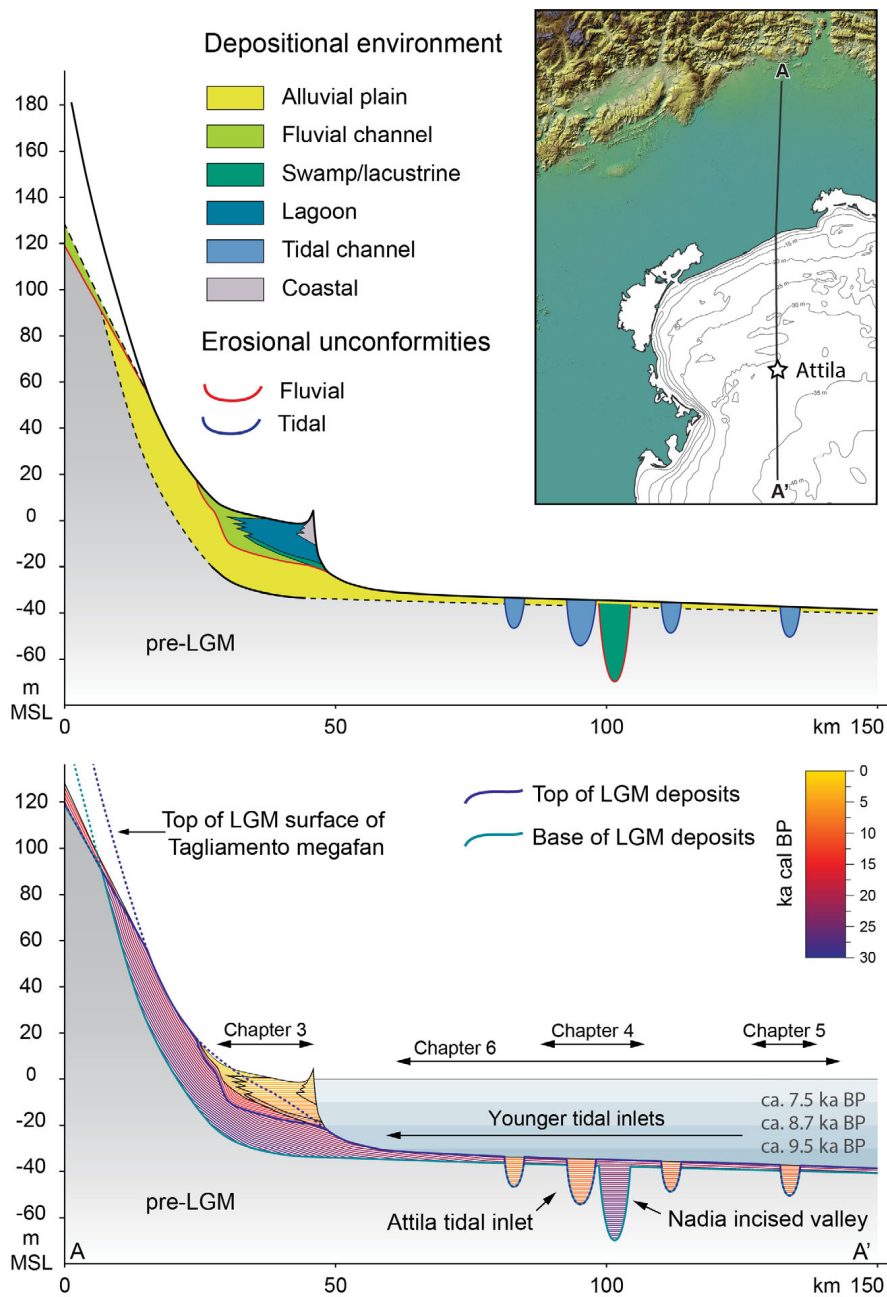
Figure 6.1: Simplified longitudinal profile of the entire northern Adriatic Sea (trace in Fig. 6.1). (A) Genetic subdivision of the different incised and infilled features. (B) Age of the deposits. In the mainland the profile starts from the apex of the alluvial megafan of Tagliamento and the trace passes over the incised valley of Concordia, while on the offshore tract the section intercepts the area of Nadia valley and Attila tidal inlet.

(Chapter 5). Most of the recognized tidal inlets can be found between the depth of -36 and -29 m MSL, thus indicating the possible occurrence of a period of lower rate of RSL rise. Though, it must be notice that this mechanism cannot univocally explain the formation of a lagoon and of the related tidal inlets in a transgressive context. Different factors, such as an increase in the sediment discharge to the basin or a change in its dispersion pattern, can strongly influence the evolution of a transgressive lagoon system.

Some of the most notable and well-preserved tidal inlets were analysed in detail in order to reconstruct their morphology, infilling architecture and age (Chapters 3 and 4). The radiocarbon dates obtained from the infilling of two tidal inlets found at a depth of ca. -30 m MSL confirm that by ca. 9.0 ka cal BP these landforms were already deactivated and that the infilling phase took no more than few centuries. The most notable cases can reach thicknesses of almost 25 m, with a maximum recognized length of 7 km and a width up to 300 m. The morphology of the analysed tidal inlets is exceptionally well-preserved, as our reconstruction allowed to recognize the main characteristic of an inlet throat, such as the occurrence of the maximum depth of the channel in its middle portion, the funnelling of the ebb channel and the presence of a channel dendritic pattern on the flood side of the inlet. The preservation of these features, along with the internal geometry of the infilling, allowed to speculate that only a relatively thin portion of the upper stratigraphy is missing due to the marine erosive processes, probably not greater than $2 - 4$ m.

Despite the great number of tidal inlets recognized through this extensive analysis, only one incised channel with fluvial origin was recognized (Chapter 3). This constitutes the only known example of incised valley on the entire northern Adriatic shelf. Two radiocarbon dates allowed to constrain the time range for the formation and infilling of this feature, which spans between ca. 28.0 ka and 23.0 ka cal BP, indicating that this landform evolved during the LGM, in a marine lowstand phase. Furthermore, the available CHIRP profiles indicate that this valley has no connection to any of the main riverine systems flowing from the Alpine region, therefore the entrenching that led to the formation of this channelized incision was probably caused by the capture of a minor stream flowing on the shelf along the Istrian Peninsula.

6.3 TOWARD A REGIONAL INTERPRETATION

The data collected on the entire northern Adriatic allowed a multiproxy assessment on the transgressive history of this area. In particular, the -34 and -29 m MSL depth range, which corresponds to the maximum occurrence of the recognized paleo tidal inlets, matches with a period of decreased RSL rise rate observable at a global scale at ca. 9.5 ka cal BP (Lambeck et al., 2014). This correspondence strengthens the hypothesis of an increased rate of lagoon formation and preservation during low RSL rise rates phases. Furthermore, this period can be approximately linked to a cooling event observed in the Greenland ice cores at ca. 9.3 ka cal BP (Rasmussen et al. 2007).

This phase would have been followed by a sudden increase of the RSL rise rate occurred after 9.3 ka cal BP, as suggested by the rapid deactivation and drowning of the tidal inlets described in Chapter 4. This hypothesis is supported by the occurrence of several other pieces of evidence widespread on the entire northern Adriatic area (Fig. 6.1). All the index points reported in Fig. 6.1 suggest a contemporaneous rapid drowning of a series of lagoon systems placed at similar depths both along the Italian coasts (Amorosi et al., 2017) and in the Trieste Gulf and within the Istrian rias (Covelli et al., 2006; Felja, 2017).

While the relative sea-level was rising at higher rates, the incised valley on the Venetian-Friulian Plain recorded the shift from a dynamic fluvial regime to a static swampy/lacustrine environment (Chapter 2). The available radiocarbon dates indicate for this environmental change an age spanning between 9.5 ka and 9.0 ka cal BP. The concomitance of this occurrence with the increase of the rate of RSL rise suggests a base level control for the interruption of the incising phase in the Venetian-Friulian Plain.

6.4 ON THE USE OF INCISED AND INFILLED LANDFORMS AS PALEOENVIRONMENTAL INDICATORS

The use of relict incised landforms proved to be a powerful tool for the reconstruction of the timing and modes of the post-LGM marine transgression in the northern Adriatic area. As illustrated in Fig. 6.2, these features provide information from different environments (e.g. fluvial, lacustrine, lagoon) and, regarding the case proposed in this thesis, potentially allow to cover a time interval that spans from the LGM almost to the present. As the morphology
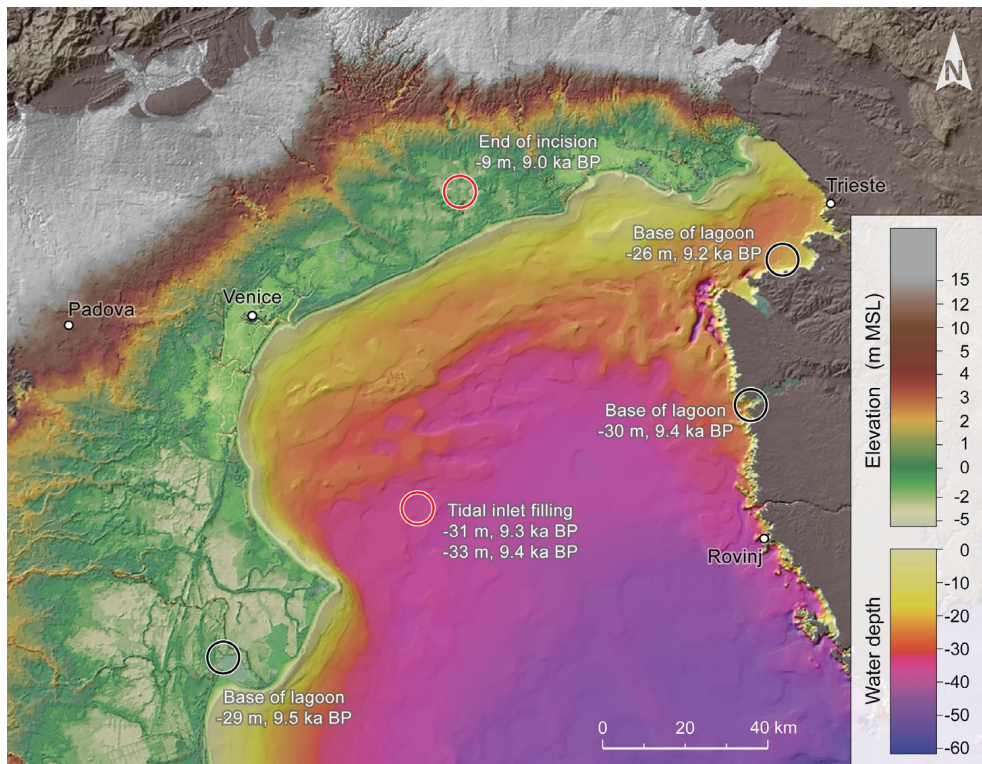
Figure 6.2: Location of the indicators available on the northern Adriatic Sea for the hypothesized 9.5 ka cal BP event.

and infilling stratigraphy of these incised landforms constitute one of the better-preserved witnesses of the post-LGM sea-level rise, we suggest that an extensive analysis on such features could provide new high-resolution proxies for the reconstruction of the last marine transgression. In particular, while the use of incised valley infilling for paleoenvironmental reconstructions is already well-known (e.g. Simms et al., 2010; Maselli and Trincardi, 2013), this PhD thesis highlighted the presence of a high number of preserved tidal inlets, which was never reported before. This suggests that, by extending this investigation to wider areas, a possible further evolution of this technique, and the production of more robust proxies, is likely.

The research for other "fields" of tidal inlets should concern similar low-gradient shelves. Considering the Mediterranean area, submerged landscapes comparable to the Adriatic case are rare, as only in the Gulf of Gabes (Tunis) an analogous physiography can be found (Morhange and Pirazzoli, 2005; Anzidei et al., 2011). Other smaller areas with similar characteristics are represented

by the Gulf of Lion (France) and the Gulf of Alexandretta (Turkey; cf. Benjamin et al., 2017).

Nevertheless, as reported in Chapter 5, several drawbacks still need to be addressed. In particular the paleo vertical position of the observed deposits and their relations with the paleo sea level constitute a major obstacle in this type of research. To overcome this issue, a feasible future development relies on the numerical modelling as a mean to provide new information on the evolution of such landforms in relation to the environmental forcing.

6.5 RECENT ANALOGUES AND ANCIENT FEATURES

The detailed reconstruction of tidal inlets and filled incised valley provided in this thesis, both for the internal sedimentary architecture and type and genesis of the infilling deposits, represent an excellent analogue for the interpretation of ancient features from outcrops and 3D seismic data. The new data presented in this work constitute therefore a benchmark for paleoenvironmental reconstructions and source-to-sink studies, providing new insights on the formation and evolution of incised valleys on the continental shelf and on the role of tidal inlets in the sediment storage and as gateways to the basin.

In particular, the work carried out on the tidal inlets offers a new perspective on the study of ancient features, as for the first time a high number of them was recognized, thus indicating a possible widespread presence also in the ancient geological record. This implies that some features, previously interpreted as incised valley, may now be revisited as tidal inlets/channels.

REFERENCES

Amorosi, A., Bruno, L., Cleveland D.M., Morelli, A., Hong, W., 2017b. Paleosols and associated channel-belt sand bodies from a continuously subsiding late Quaternary system (Po Basin, Italy): New insights into continental sequence stratigraphy Geological Society of America Bulletin, 129, B31575.1.

Antonioli, F., Anzidei, M., Amorosi, A., Lo Presti, V., Mastronuzzi, G., Deiana, G., De Falco, G., Fontana, A., Fontolan, G., Lisco, S., Marsico, A., Moretti, M., Orrú, P.E., Sannino, G.M., Serpelloni, E., Vecchio, A., 2017. Sea-level rise and potential drowning of the Italian coastal plains: Flooding risk scenarios for 2100. Quaternary Science Reviews, 158, 29-43.

Anzidei, M., Antonioli, F., Lambeck, K., Benini, A., Soussi, M., Lakhdar, R., 2011. New insights on the relative sea level change during Holocene along the coasts of Tunisia and western Libya from archaeological and geomorphological markers. Quaternary International, 232, 5-12.

Benjamin, J., Rovere, A., Fontana, A., Furlani, S., Vacchi, M., Inglis, R.H., Galili, E., Antonioli, F., Sivan, D., Miko, S., Mourtzas, N., Felja, I., Meredith-Williams, I., Goodman-Tchernov, B., Kolaiti, E., Anzidei, M., Gehrels, R., 2017. Late Quaternary sea-level changes and early human societies in the central and eastern Mediterranean Basin: An interdisciplinary review. Quaternary International, 449, 29-57.

Blum, M., Martin, J., Milliken, K., Garvin, M., 2013. Paleovalley systems: Insights from Quaternary analogs and experiments. Earth-Science Reviews, 116, 128-169.

Covelli, S., Fontolan, G., Faganeli, J., Ogrinc, N., 2006. Anthropogenic markers in the Holocene stratigraphic sequence of the Gulf of Trieste (northern Adriatic Sea). Marine Geology, 230(1-2), 29-51.

Felja I., 2017. Karstic estuaries along the eastern Adriatic coast: Late-Quaternary evolution of the Mirna and Neretva River mouths. Unpublished PhD thesis, Department of Geology, Faculty of Science, University of Zagreb, 169.

Fontana, A., Mozzi, P., Bondesan, A., 2008. Alluvial megafans in the Venetian-Friulian Plain (north-eastern Italy): Evidence of sedimentary and erosive

phases during Late Pleistocene and Holocene. Quaternary International, 189, 71-90.

Lambeck, K., Roubya, H., Purcell, A., Sun, Y., Malcolm, S., 2014. Sea level and global ice volumes from the Last Glacial Maximum to the Holocene. PNAS, 111, 15296-15303.

Maselli, V., Trincardi, F., 2013. Large-scale single incised valley from a small catchment basin on the western Adriatic margin (central Mediterranean Sea). Global and Planetary Change, 100, 245-262.

Morhange, C., Pirazzoli, P.A., 2005. Mid-Holocene of southern Tunisian coasts. Marine Geology, 220, 205-213.

Rasmussen, S.O., Vinther, B., Clausen, H.B., Andersen, K.K., 2007. Early Holocene climate oscillations recorded in three Greenland ice cores. Quaternary Science Reviews, 26, 1907-1914.

Simms, A.R., Aryal, N., Miller, L., Yokoyama, Y., 2010. The incised valley of Baffin Bay, Texas: a tale of two climates. Sedimentology 57, 642-669.

Stocchi, P., Vacchi, M., Lorscheid, T., de Boer, B., Simms, A. R., van de Wal, R.S.W., Vermeersen, B.L.A., Pappalardo, M., Rovere, A., 2018. MIS 5e relative sea-level changes in the Mediterranean Sea: Contribution of isostatic disequilibrium. Quaternary Science Reviews, 185, 122-134.

Trincardi, F., Argnani, A., Correggiari, A., 2011. Note illustrative della Carta Geologica d'Italia alla scala 1:250,000-Foglio NL33-7 "Venezia", ISPRA-Servizio Geologico d'Italia.

ACKNOWLEDGEMENTS